Climate Change and Microplastics: Their Impacts and Interactions with Corals and Coral Reefs

Jeremy B. Axworthy

A dissertation

submitted in partial fulfillment of the

requirements for the degree of

Doctor of Philosophy

University of Washington

2024

Reading Committee:

Jacqueline Padilla-Gamiño, Chair

Michelle DiBenedetto

Julie Masura

Program Authorized to Offer Degree:

School of Aquatic and Fishery Sciences

University of Washington

Abstract

Climate Change and Microplastics: Their Impacts and Interactions with Corals and Coral Reefs

Jeremy B. Axworthy

Chair of Supervisory Committee:

Jacqueline Padilla-Gamiño

School of Aquatic and Fishery Sciences

Coral reefs are some of the most important ecosystems worldwide, yet they are some of the most threatened by global change, including the effects of thermal stress and plastic pollution. Reef-building corals provide the architecture of these incredibly biodiverse habitats that millions of people who live in the tropics rely on for livelihood. Increased sea temperatures caused by climate change result in coral bleaching and the expulsion of algal symbionts that corals rely on for energy, leading to mass mortality and destruction of these ecosystems. The first chapter of this dissertation investigates how corals' outer layer (OL) tissue and inner core (IC) skeletal compartments respond to bleaching using shotgun proteomics. We identified 2631 proteins across both compartments of bleached and control corals and demonstrated that the proteomic signatures are different between the OL and IC and that these compartments respond in different ways to bleaching. Compared to control corals, the OL of bleached corals used the glyoxylate

cycle to derive carbon internally from lipids, had a high protein turnover rate, and shifted reliance on nitrogen from ammonia to nitrogen produced from the breakdown of urea and betaine. The IC of bleached corals compartmentalized the shunting of glucose to the pentose phosphate pathway. These results highlight contrasting strategies for responding to bleaching stress in different compartments of bleached corals and shed light on potential mechanisms behind bleaching resilience. Microplastics, plastic particles < 5 mm, are another threat to corals that have gained a lot of attention recently because they are increasing in marine ecosystems and have been shown to have a range of negative effects on corals. Corals can also sequester microplastics into their skeletons, serving as an important sink for microplastics. However, the factors influencing interactions between corals and microplastics remain poorly understood. The second chapter of this dissertation examines the role of thermal stress on microplastic ingestion by corals through controlled feeding experiments. Some coral species increase heterotrophy (heterotrophic plasticity) when they bleach, suggesting they might ingest more microplastics during this critical period. Moreover, some studies suggest that corals selectively ingest microplastics over prey, which could result in less feeding. The results of these experiments showed that increased temperatures did not result in increased microplastics ingestion and that microplastics exposure did not reduce corals' ability to feed on prey for the species studied but highlighted that we do not fully understand the role of bleaching on heterotrophic plasticity. In the third chapter of this dissertation, additional factors that could potentially influence coral and microplastic interactions were tested. Specifically, water flow, microplastic type, species, and coral condition were examined in laboratory experiments for their role in driving microplastic adhesion and ingestion in corals. Results of this chapter suggest that species and types of microplastic have a greater influence on both ingestion and adhesion than water flow in corals.

Micro-fibers interacted the most with corals and polyester fibers were the most likely microplastic type to be ingested. Moreover, microplastics adhered to dead parts of corals 3.7 times more than living sections. Collectively, the results of this dissertation chapter highlight which types of microplastics some corals are more likely to interact with. They also suggest that some corals may be capable of rejecting microplastics from their surface and that non-living structures on reefs could be important microplastic sinks. In the final chapter of this dissertation, field sampling was conducted in coral reefs in Kaneohe Bay, Hawaii, USA, to determine microplastic pollution levels in sediments, seawater, corals, and sea cucumbers. Overall, microplastic pollution was very low in these reefs compared to others, with very few sediment, coral, and sea cucumber samples having detectable levels of microplastics. Seawater was the only matrix that had quantifiable microplastic levels, ranging from 0.024 to 0.081 particles m^{-3}, and consisting of mostly larger, floating plastics. These results indicate that reef organisms in the bay are not under imminent threat of microplastics, but further monitoring is recommended to better understand temporal and future trends in microplastic pollution.

TABLE OF CONTENTS

LIST OF FIGURES

LIST OF TABLES

ACKNOWLEDGEMENTS

Obtaining a PhD has been an incredible journey that would not have been possible without the help of so many amazing people. Foremost, I would like to thank Dr. Jacqueline Padilla-Gamiño. Her confidence in me was a driving force when things were tough, and I always felt very well-supported throughout my graduate studies. I would also like to thank my committee members, Steven Roberts, Michelle DiBenedetto, Julie Masura, and Emily Carrington, who each helped me immensely with various aspects of my work. I would also like to thank a former committee member, Broon Nunn, who helped me considerably to learn proteomics.

My lab mates are an amazing group of people to share space and work with. Many thanks to Callum Backstromm for stimulating conversations about coral science and for being an amazing TA. Thanks to Lindsay Alma and Courtney Fiamengo for welcoming me so warmly into the lab. Thank you to Eileen Bates, Miranda Roethler, Corinne Klohmann, Sarah Tanja, Craig Norrie, Julietta Martinelli, Tanya Brown, Nuria Viladrich, and Xochitl Clare for of all of their support as well as great conversations and chances to rant.

I have been fortunate to collaborate with many amazing people on my dissertation work. Thank you to Emma Timmins-Schiffman, Beth Lenz, Lisa Rodrigues, and Ruth Sofield for assistance with manuscripts. Thank you to Julio Chávez-Dorado, Gavin Kreitman, Melissa Jaffe, Sean Frangos, and Brenner Wakayama for their support in the lab and field. Lab work was also made possible thanks to an army of undergraduate (and graduate) volunteers, including Sicheng Wang,

Romina Centurion, Malcolm Munsil, Abby Goudey, Kat Arnett, Alessia Simmen, Dylan Strauss, Aspen Katla, Jacki O'Maley, and Steve Flannigan.

Some staff and faculty in SAFS have also played important roles in my academic career for which I am very grateful. Samantha Scherer and Amy Fox were the best student advisors a person could hope for. Jon Wittouck helped me so much building experimental systems and supporting my teaching efforts. Tom Quinn was monumental in helping me become a better writer and getting my first manuscript published right after undergrad. José Guzmán and Greg Jensen were also excellent mentors during some of my TA-ships.

Finally, thank you to my family, Alanna and Rocky, who have put up with me during all of this. I love you both so dearly.

DEDICATION

This dissertation is dedicated to my grandmother, Diana Axworthy. I know you would be so proud of me. I love you and miss you so much, Gigi.

INTRODUCTION

Coral reefs are vital ecosystems that harbor immense biodiversity and sustain the livelihoods of millions of people in the tropics (Moberg and Folke, 1999). Reef-building corals play a central role by constructing intricate skeletal structures that form the foundation of coral reefs, offering a multitude of niches for thousands of organisms. These reefs support highly productive fisheries and are hotspots for ecotourism, providing essential income and nutrition for coastal communities (Bartelet et al., 2024). Reef structures also protect tropical coastlines by acting as a barrier to waves and storm surges, a service estimated globally to be worth 109 billion USD per decade (Burke and Spalding, 2022). The success of reef-building corals hinges on their relationship with symbiotic dinoflagellates in the family Symbiodiniaceae, which supply corals with critical energy and nutrients through the products of photosynthesis (Yonge, 1940). Unfortunately, coral reefs are threatened by global change, including the effects of climate change and pollution such as microplastics (Hoegh-Guldberg, 1999; Reichert et al., 2019). To conserve these precious ecosystems, we must understand how these stressors impact and interact with corals to help guide management in prioritizing conservation strategies and mitigating stress to these important organisms.

Anthropogenic climate change is accelerating rapidly, causing our planet to warm and adversely affecting ecosystems from the poles to the tropics (Doney et al., 2012). Rising sea temperatures are problematic for reef-building corals because it leads to coral bleaching. Under thermal stress, the symbiotic relationship between corals and Symbiodiniaceae breaks down, and the algae are

expelled from the corals, taking away their main energy source (Hoegh-Guldberg and Smith, 1989; Iglesias-Prieto et al., 1992). During this time, corals must rely on energy reserves or obtain energy through heterotrophy, or the corals will ultimately starve to death or succumb to disease or other stressors (Grottoli et al., 2006; Rodrigues and Grottoli, 2007). However, if conditions improve before the coral's energy is exhausted, Symbiodiniaceae can repopulate the corals, and they can recover. Coral's resilience to bleaching is greatly impacted by its ability to acquire energy and nutrients outside of symbiosis (Loya et al., 2001), and uncovering the mechanisms underlying these capabilities is critical for determining which corals will persist under global change.

Proteomics is a powerful tool for assessing cellular-level processes that are affected by environmental changes. Unlike genomics, which identifies specific genes and genetic variations that play key roles in environmental response, and transcriptomics, which describes the genes that are activated by environmental cues, proteomics is more representative of the cellular processes occurring in organisms at the time of interest (Gygi et al., 1999; Maier et al., 2009). Shotgun proteomics combines liquid chromatography with mass spectrometry to detect potentially thousands of proteins in a sample (Wu and MacCoss, 2002). Downstream analysis of identified proteins using gene ontology can elucidate the role the proteins play in physiological processes occurring in an organism's cells. To date, a few studies have used proteomics to determine how corals are affected by bleaching (Weston et al., 2015; Ricaurte et al., 2016; Mayfield et al., 2018, 2021; Hernández-Elizárraga et al., 2019; Mayfield, 2020; Petrou et al., 2021), and no studies have investigated changes in proteins across different parts of bleached coral colonies. Identifying the proteins impacted by environmental stressors and understanding

the cellular processes they are involved in can offer insights into how organisms are equipped to cope with stress. Additionally, it may uncover potential biomarkers of resilience that could be targeted for intervention.

Microplastic pollution is another stressor threatening corals and has gained much attention recently because of their ubiquity and impacts on marine life. Commonly defined as synthetic polymer-based particles between 1 μm and 5 mm in size (Frias and Nash, 2019), microplastics have been documented in nearly every corner of the planet, from polar sea ice to coral reefs (Hall et al., 2015; van Sebille et al., 2015; Peeken et al., 2018). In 2014, there were an estimated 15 – 51 trillion microplastics in the oceans (van Sebille et al., 2015), and that number is expected to increase as plastic waste is continually generated and mismanaged (Borrelle et al., 2020). Primary microplastics enter the oceans at an already micro-size and secondary microplastics result from the breakdown of larger plastic debris, further contributing to the abundance of these pollutants. The sources of microplastics include mismanaged municipal waste, litter, industry, and synthetic clothing (Auta et al., 2017; Kane and Clare, 2019). Their fate is less understood, but they are thought to accumulate on the sea surface, in seafloor and coastal sediments, in biogenic marine structures, and in organisms (Kane and Clare, 2019; Reichert et al., 2022; Soares et al., 2023). Their small size leads to them being ingested by planktivorous marine organisms (Wright et al., 2013), which have been shown to have various adverse effects (Guzzetti et al., 2018).

There is a great deal of literature on how corals interact with and are impacted by microplastics, but there are gaps in our understanding of what drives these processes. Corals interact with

microplastics in two ways: 1) actively through ingestion by polyps and 2) passively by adhesion to the coral's surface (Martin et al., 2019; Corona et al., 2020). Most microplastics that corals ingest are egested within a few hours, indicating that corals can actively reject them, but these processes are considered energetically costly (Hall et al., 2015; Chapron et al., 2018; Reichert et al., 2018). Recent experimental studies have shown that microplastics are 40 times more likely to adhere to a coral's surface than to be ingested (Martin et al., 2019; Corona et al., 2020). The surface mucus layer of corals may have a dual role in relation to microplastics. Mucus could trap microplastics and/or facilitate the removal of microplastics from the coral, akin to how corals expel sediment using mucus secretion (Stafford-Smith and Ormond, 1992; Martin et al., 2019; Hierl et al., 2021; Bejarano et al., 2022). Regardless of the type of interaction, exposure to microplastics has resulted in bleaching, tissue necrosis, reduced growth, reduced immune capacity, changes in gene expression, and altered photosynthesis in corals (Reichert et al., 2018, 2019; Hankins et al., 2021; Liao et al., 2021; Mendrik et al., 2021). Moreover, microplastics can be incorporated into coral skeletons, potentially securing them for many years (Hierl et al., 2021; Krishnakumar et al., 2021; Reichert et al., 2022).

To date, our understanding of factors influencing interactions between coral and microplastics is limited. The ingestion rates of microplastics by corals may be influenced by the size of the microplastics they encounter and the size of their corallites (skeletal depressions that house coral polyps) (Hankins et al., 2022). However, other characteristics of microplastics, corals, and the surrounding environment could potentially influence how likely a coral interacts with microplastics. For example, microplastics come in a variety of shapes and chemical compositions that could impact their bioavailability or preferential ingestion by corals (Allen et al., 2017;

Rotjan et al., 2019). Dynamic water flow conditions can affect the boundary layer and turbulent mixing around corals. Corals grow in various forms, affecting hydrodynamic processes and the chances for a microplastic to contact a coral (Sebens et al., 1997, 1998). Moreover, corals employ different feeding modes and have different rates of heterotrophy, which can also be affected by thermal stress (Grottoli et al., 2006; Hughes and Grottoli, 2013). Understanding the factors that influence interactions between corals and microplastics could help identify which corals and environments are vulnerable to specific types of microplastics.

Microplastics have been detected in the seawater and sediments associated with coral reefs, as well as in corals and other reef organisms. Some reefs appear to be highly polluted with microplastics, while others are low to moderately polluted. For example, some Asian reefs had seawater microplastic concentrations on the order of thousands of particles per cubic meter (Jeyasanta et al., 2020; Patterson et al., 2020, 2022), while reefs in the Maldives had concentrations ranging from 0.02 to 0.65 particles per cubic meter (Saliu et al., 2018, 2019), and microplastic concentrations reported in corals range from 0.9 to 5 particles per cm^2 (Tang et al., 2021; Zhou et al., 2022). Few studies utilize sampling strategies that incorporate both environmental and organismal samples, which could improve our understanding of the potential impacts of microplastics on critical reef organisms. Furthermore, numerous reefs remained unexamined for the presence of microplastics.

Climate change and microplastic pollution are two of the most pressing issues in coral reef conservation today. They are inextricably linked in their roles in the global carbon cycle: the production of plastic from fossil fuels contributes to climate change, and the disposal and

incineration of plastic release carbon back into the earth's system (Stubbins et al., 2021). Rising ocean temperatures are already devastating coral reefs across the tropics, and mitigating climate change will be the only way to ensure that coral reefs will persist into the future (Hoegh-Guldberg, 1999). However, understanding and mitigating microplastic pollution could reduce some additional pressure on these highly stressed ecosystems.

My four dissertation chapters aim to:

1) **Investigate how proteins are affected by bleaching in tissue and intraskeletal compartments of reef-building corals.**
2) **Examine the role of bleaching in microplastic ingestion and heterotrophy in corals.**
3) **Explore how water flow microplastic type affect microplastic ingestion and adhesion in different coral species.**
4) **Determine the amount of microplastic pollution and how it is distributed in coral reefs in Kaneohe Bay, Hawaii.**

References

Allen, A. S., Seymour, A. C., and Rittschof, D. (2017). Chemoreception drives plastic consumption in a hard coral. *Mar. Pollut. Bull.* 124, 198–205. doi: 10.1016/j.marpolbul.2017.07.030

Auta, H. S., Emenike, C. U., and Fauziah, S. H. (2017). Distribution and importance of microplastics in the marine environment: A review of the sources, fate, effects, and potential solutions. *Environ. Int.* 102, 165–176. doi: 10.1016/j.envint.2017.02.013

Bartelet, H. A., Barnes, M. L., and Cumming, G. S. (2024). Estimating and comparing the direct economic contributions of reef fisheries and tourism in the Asia-Pacific. *Mar. Policy* 159, 105939. doi: 10.1016/j.marpol.2023.105939

Bejarano, S., Diemel, V., Feuring, A., Ghilardi, M., and Harder, T. (2022). No short-term effect of sinking microplastics on heterotrophy or sediment clearing in the tropical coral *Stylophora pistillata*. *Sci. Rep.* 12, 1468. doi: 10.1038/s41598-022-05420-7

Borrelle, S. B., Ringma, J., Law, K. L., Monnahan, C. C., Lebreton, L., McGivern, A., et al. (2020). Predicted growth in plastic waste exceeds efforts to mitigate plastic pollution. *Science* 369, 1515–1518. doi: 10.1126/science.aba3656

Burke, L., and Spalding, M. (2022). Shoreline protection by the world's coral reefs: Mapping the benefits to people, assets, and infrastructure. *Mar. Policy* 146, 105311. doi: 10.1016/j.marpol.2022.105311

Chapron, L., Peru, E., Engler, A., Ghiglione, J. F., Meistertzheim, A. L., Pruski, A. M., et al. (2018). Macro- and microplastics affect cold-water corals growth, feeding and behaviour. *Sci. Rep.* 8, 15299. doi: 10.1038/s41598-018-33683-6

Corona, E., Martin, C., Marasco, R., and Duarte, C. M. (2020). Passive and Active Removal of Marine Microplastics by a Mushroom Coral (*Danafungia scruposa*). *Front. Mar. Sci.* 7, 128. doi: 10.3389/fmars.2020.00128

Doney, S. C., Ruckelshaus, M., Duffy, J. E., Barry, J. P., Chan, F., English, C. A., et al. (2012). Climate Change Impacts on Marine Ecosystems. *Annu. Rev. Mar. Sci.* 4, 11–37. doi: 10.1146/annurev-marine-041911-111611

Frias, J. P. G. L., and Nash, R. (2019). Microplastics: Finding a consensus on the definition. *Mar. Poll.* 138, 145–147. doi: 10.1016/j.marpolbul.2018.11.022

Grottoli, A. G., Rodrigues, L. J., and Palardy, J. E. (2006). Heterotrophic plasticity and resilience in bleached corals. *Nature* 440, 1186–1189. doi: 10.1038/nature04565

Guzzetti, E., Sureda, A., Tejada, S., and Faggio, C. (2018). Microplastic in marine organism: Environmental and toxicological effects. *Environ. Toxicol. Pharma.* 64, 164–171. doi: 10.1016/j.etap.2018.10.009

Gygi, S. P., Rochon, Y., Franza, B. R., and Aebersold, R. (1999). Correlation between Protein and mRNA Abundance in Yeast. *Mol. Cell Biol.* 19, 1720–1730. doi: 10.1128/MCB.19.3.1720

Hall, N. M., Berry, K. L. E., Rintoul, L., and Hoogenboom, M. O. (2015). Microplastic ingestion by scleractinian corals. *Mar. Biol.* 162, 725–732. doi: 10.1007/s00227-015-2619-7

Hankins, C., Moso, E., and Lasseigne, D. (2021). Microplastics impair growth in two Atlantic scleractinian coral species, *Pseudodiploria clivosa* and *Acropora cervicornis*. *Environ. Pollut.* 275, 116649. doi: 10.1016/j.envpol.2021.116649

Hankins, C., Raimondo, S., and Lasseigne, D. (2022). Microplastic ingestion by coral as a function of the interaction between calyx and microplastic size. *Sci. Total Environ.* 810, 152333. doi: 10.1016/j.scitotenv.2021.152333

Hernández-Elizárraga, V. H., Olguín-López, N., Hernández-Matehuala, R., Ocharán-Mercado, A., Cruz-Hernández, A., Guevara-González, R. G., et al. (2019). Comparative Analysis of the Soluble Proteome and the Cytolytic Activity of Unbleached and Bleached *Millepora complanata* ("Fire Coral") from the Mexican Caribbean. *Marine Drugs* 17, 393. doi: 10.3390/md17070393

Hierl, F., Wu, H. C., and Westphal, H. (2021). Scleractinian corals incorporate microplastic particles: identification from a laboratory study. *Environ. Sci. Pollut. Res.* 28, 37882–37893. doi: 10.1007/s11356-021-13240-x

Hoegh-Guldberg, O. (1999). Climate change, coral bleaching and the future of the world's coral reefs. *Mar. Freshwater Res.* 50, 839–866. doi: 10.1071/mf99078

Hoegh-Guldberg, O., and Smith, G. J. (1989). The effect of sudden changes in temperature, light and salinity on the population density and export of zooxanthellae from the reef corals *Stylophora pistillata* Esper and *Seriatopora* hystrix Dana. *J. Exp. Mar. Biol. Ecol.* 129, 279–303. doi: 10.1016/0022-0981(89)90109-3

Hughes, A. D., and Grottoli, A. G. (2013). Heterotrophic Compensation: A Possible Mechanism for Resilience of Coral Reefs to Global Warming or a Sign of Prolonged Stress? *PLoS ONE* 8, e81172. doi: 10.1371/journal.pone.0081172

Iglesias-Prieto, R., Matta, J. L., Robins, W. A., and Trench, R. K. (1992). Photosynthetic response to elevated temperature in the symbiotic dinoflagellate *Symbiodinium microadriaticum* in culture. *Proc. Natl. Acad. Sci.* 89, 10302–10305. doi: 10.1073/pnas.89.21.10302

Jeyasanta, K. I., Patterson, J., Grimsditch, G., and Edward, J. K. P. (2020). Occurrence and characteristics of microplastics in the coral reef, sea grass and near shore habitats of Rameswaram Island, India. *Mar. Pollut. Bull.* 160, 111674. doi: 10.1016/j.marpolbul.2020.111674

Kane, I. A., and Clare, M. A. (2019). Dispersion, Accumulation, and the Ultimate Fate of Microplastics in Deep-Marine Environments: A Review and Future Directions. *Front. Earth Sci.* 7. doi: 10.3389/feart.2019.00080

Krishnakumar, S., Anbalagan, S., Hussain, S. M., Bharani, R., Godson, P. S., and Srinivasalu, S. (2021). Coral annual growth band impregnated microplastics (Porites sp.): a first investigation report. *Wetlands Ecol. Manage* 29, 677–687. doi: 10.1007/s11273-021-09786-9

Liao, B., Wang, J., Xiao, B., Yang, X., Xie, Z., Li, D., et al. (2021). Effects of acute microplastic exposure on physiological parameters in *Tubastrea aurea* corals. *Mar. Pollut. Bull.* 165, 112173. doi: 10.1016/j.marpolbul.2021.112173

Loya, Y., Sakai, K., Yamazato, K., Nakano, Y., Sambali, H., and van Woesik, R. (2001). Coral bleaching: the winners and the losers. *Ecol. Letters* 4, 122–131. doi: 10.1046/j.1461-0248.2001.00203.x

Maier, T., Güell, M., and Serrano, L. (2009). Correlation of mRNA and protein in complex biological samples. *FEBS Letters* 583, 3966–3973. doi: 10.1016/j.febslet.2009.10.036

Martin, C., Corona, E., Mahadik, G. A., and Duarte, C. M. (2019). Adhesion to coral surface as a potential sink for marine microplastics. *Environ. Pollut.* 255, 113281. doi: 10.1016/j.envpol.2019.113281

Mayfield, A. B. (2020). Proteomic Signatures of Corals from Thermodynamic Reefs. *Microorganisms* 8, 1171. doi: 10.3390/microorganisms8081171

Mayfield, A. B., Aguilar, C., Kolodziej, G., Enochs, I. C., and Manzello, D. P. (2021). Shotgun Proteomic Analysis of Thermally Challenged Reef Corals. *Front. Mar. Sci.* 8, 547. doi: 10.3389/fmars.2021.660153

Mayfield, A. B., Chen, Y.-J., Lu, C.-Y., and Chen, C.-S. (2018). The proteomic response of the reef coral *Pocillopora acuta* to experimentally elevated temperatures. *PLoS ONE* 13, e0192001. doi: 10.1371/journal.pone.0192001

Mendrik, F. M., Henry, T. B., Burdett, H., Hackney, C. R., Waller, C., Parsons, D. R., et al. (2021). Species-specific impact of microplastics on coral physiology. *Environ. Pollut.* 269, 116238. doi: 10.1016/j.envpol.2020.116238

Moberg, F., and Folke, C. (1999). Ecological goods and services of coral reef ecosystems. *Ecol. Econ.* 29, 215–233. doi: 10.1016/S0921-8009(99)00009-9

Patterson, J., Jeyasanta, K. I., Laju, R. L., Booth, A. M., Sathish, N., and Edward, J. K. P. (2022). Microplastic in the coral reef environments of the Gulf of Mannar, India - Characteristics, distributions, sources and ecological risks. *Environ. Pollut.* 298, 118848. doi: 10.1016/j.envpol.2022.118848

Patterson, J., Jeyasanta, K. I., Sathish, N., Edward, J. K. P., and Booth, A. M. (2020). Microplastic and heavy metal distributions in an Indian coral reef ecosystem. *Sci. Total Environ.* 744, 140706. doi: 10.1016/j.scitotenv.2020.140706

Peeken, I., Primpke, S., Beyer, B., Gütermann, J., Katlein, C., Krumpen, T., et al. (2018). Arctic sea ice is an important temporal sink and means of transport for microplastic. *Nat. Commun.* 9, 1505. doi: 10.1038/s41467-018-03825-5

Petrou, K., Nunn, B. L., Padula, M. P., Miller, D. J., and Nielsen, D. A. (2021). Broad scale proteomic analysis of heat-destabilised symbiosis in the hard coral *Acropora millepora*. *Sci. Rep.* 11, 19061. doi: 10.1038/s41598-021-98548-x

Reichert, J., Arnold, A. L., Hammer, N., Miller, I. B., Rades, M., Schubert, P., et al. (2022). Reef-building corals act as long-term sink for microplastic. *Glob. Change Biol.* 28, 33–45. doi: 10.1111/gcb.15920

Reichert, J., Arnold, A. L., Hoogenboom, M. O., Schubert, P., and Wilke, T. (2019). Impacts of microplastics on growth and health of hermatypic corals are species-specific. *Environ. Pollut.* 254, 113074. doi: 10.1016/j.envpol.2019.113074

Reichert, J., Schellenberg, J., Schubert, P., and Wilke, T. (2018). Responses of reef building corals to microplastic exposure. *Environ. Pollut.* 237, 955–960. doi: 10.1016/j.envpol.2017.11.006

Ricaurte, M., Schizas, N. V., Ciborowski, P., and Boukli, N. M. (2016). Proteomic analysis of bleached and unbleached *Acropora palmata*, a threatened coral species of the Caribbean. *Mar. Pollut. Bullet.* 107, 224–232. doi: 10.1016/j.marpolbul.2016.03.068

Rodrigues, L. J., and Grottoli, G. (2007). Energy reserves and metabolism as indicators of coral recovery from bleaching. *Limnol. and Oceanogr.* 52, 1874–1882.

Rotjan, R. D., Sharp, K. H., Gauthier, A. E., Yelton, R., Lopez, E. M. B., Carilli, J., et al. (2019). Patterns, dynamics and consequences of microplastic ingestion by the temperate coral, *Astrangia poculata*. *Proc. R. Soc. B.* 286, 20190726. doi: 10.1098/rspb.2019.0726

Saliu, F., Montano, S., Garavaglia, M. G., Lasagni, M., Seveso, D., and Galli, P. (2018). Microplastic and charred microplastic in the Faafu Atoll, Maldives. *Mar. Pollut. Bull.* 136, 464–471. doi: 10.1016/j.marpolbul.2018.09.023

Saliu, F., Montano, S., Leoni, B., Lasagni, M., and Galli, P. (2019). Microplastics as a threat to coral reef environments: Detection of phthalate esters in neuston and scleractinian corals from the Faafu Atoll, Maldives. *Mar. Pollut. Bull.* 142, 234–241. doi: 10.1016/j.marpolbul.2019.03.043

Sebens, K. P., Grace, S. P., Helmuth, B., Maney Jr., E. J., and Miles, J. S. (1998). Water flow and prey capture by three scleractinian corals, *Madracis mirabilis*, *Montastrea cavernosa* and *Porites porites*, in a field enclosure. *Mar. Biol.* 131, 347–360. doi: 10.1007/s002270050328

Sebens, K. P., Witting, J., and Helmuth, B. (1997). Effects of water flow and branch spacing on particle capture by the reef coral *Madracis mirabilis* (Duchassaing and Michelotti). *J. Exp. Mar. Biol. Ecol.* 211, 1–28. doi: 10.1016/S0022-0981(96)02636-6

Soares, M. O., Rizzo, L., Ximenes Neto, A. R., Barros, Y., Martinelli Filho, J. E., Giarrizzo, T., et al. (2023). Do coral reefs act as sinks for microplastics? *Environ. Pollut.* 337, 122509. doi: 10.1016/j.envpol.2023.122509

Stafford-Smith, M., and Ormond, R. (1992). Sediment-rejection mechanisms of 42 species of Australian scleractinian corals. *Mar. Freshwater Res.* 43, 683. doi: 10.1071/MF9920683

Stubbins, A., Law, K. L., Muñoz, S. E., Bianchi, T. S., and Zhu, L. (2021). Plastics in the Earth system. *Science* 373, 51–55. doi: 10.1126/science.abb0354

Tang, J., Wu, Z., Wan, L., Cai, W., Chen, S., Wang, X., et al. (2021). Differential enrichment and physiological impacts of ingested microplastics in scleractinian corals in situ. *J. Hazard Mater.* 404, 124205. doi: 10.1016/j.jhazmat.2020.124205

van Sebille, E., Wilcox, C., Lebreton, L., Maximenko, N., Hardesty, B. D., van Franeker, J. A., et al. (2015). A global inventory of small floating plastic debris. *Environ. Res. Lett.* 10, 124006. doi: 10.1088/1748-9326/10/12/124006

Weston, A. J., Dunlap, W. C., Beltran, V. H., Starcevic, A., Hranueli, D., Ward, M., et al. (2015). Proteomics Links the Redox State to Calcium Signaling During Bleaching of the Scleractinian Coral *Acropora microphthalma* on Exposure to High Solar Irradiance and Thermal Stress. *Mol. Cell. Proteomics* 14, 585–595. doi: 10.1074/mcp.M114.043125

Wright, S. L., Thompson, R. C., and Galloway, T. S. (2013). The physical impacts of microplastics on marine organisms: A review. *Environ. Pollut.* 178, 483–492. doi: 10.1016/j.envpol.2013.02.031

Wu, C. C., and MacCoss, M. J. (2002). Shotgun proteomics: Tools for the analysis of complex biological systems. *Curr. Opin. Mol. Ther.* 4, 242–250.

Yonge, C. M. (1940). THE BIOLOGY OF REEF-BUILDING CORALS. *Scientific Reports / Great Barrier Reef Expedition 1928-29* 1, 353–391.

Zhou, Z., Wan, L., Cai, W., Tang, J., Wu, Z., and Zhang, K. (2022). Species-specific microplastic enrichment characteristics of scleractinian corals from reef environment: Insights from an in-situ study at the Xisha Islands. *Sci. Tot. Environ.* 815, 152845. doi: 10.1016/j.scitotenv.2021.152845

Chapter 1. SHOTGUN PROTEOMICS IDENTIFIES ACTIVE METABOLIC PATHWAYS IN BLEACHED CORAL TISSUE AND INTRASKELETAL COMPARTMENTS

Publication history: This study was co-authored with Emma Timmins-Schiffman, Tanya Brown, Lisa J. Rodrigues, Brook L. Nunn, and Jacqueline L. Padilla-Gamiño. At the time this dissertation was published, a version of this chapter was published in Frontiers in Marine Science.

1.1 ABSTRACT

Coral bleaching events are increasing with such frequency and intensity that many of the world's reef-building corals are in peril. Some corals appear to be more resilient after bleaching but the mechanisms underlying their ability to recover from bleaching and persist are not fully understood. We used shotgun proteomics to compare the proteomes of the outer layer (OL) tissue and inner core (IC) tissue and skeleton compartments of experimentally bleached and control (i.e., non-bleached) colonies of *Montipora capitata*, a perforate Hawaiian species noted for its resilience after bleaching. We identified 2361 proteins in the OL and IC compartments for both bleached and non-bleached individuals. In the OL of bleached corals, 63 proteins were significantly more abundant and 28 were significantly less abundant compared to the OL of non-bleached corals. In the IC of bleached corals, 22 proteins were significantly more abundant and 17 were significantly less abundant compared to the IC of non-bleached corals. Gene ontology (GO) and pathway analyses revealed metabolic processes that were occurring in bleached corals but not in non-bleached corals. The OL of bleached corals used the glyoxylate cycle to derive carbon from internal storage compounds such as lipids, had a high protein turnover rate, and shifted reliance on nitrogen from ammonia to nitrogen produced from the breakdown of urea and

betaine. The IC of bleached corals compartmentalized the shunting of glucose to the pentose phosphate pathway. Bleached corals increased abundances of several antioxidant proteins in both the OL and IC compartments compared to non-bleached corals. These results highlight contrasting strategies for responding to bleaching stress in different compartments of bleached *M. capitata* and shed light on some potential mechanisms behind bleaching resilience.

1.2 INTRODUCTION

Rising seawater temperatures threaten the future of coral reefs and the ecosystem services they provide. Increased temperatures can result in the breakdown of mutualistic symbiosis between corals and Symbiodiniaceae (i.e., coral bleaching), causing a severe energy deficit to the coral that impairs critical physiological functions and can lead to mortality. However, if temperature stress abates before the coral's energy stores are consumed, symbiosis can be restored, and the coral can recover. To survive and recover from bleaching, corals must rely on internal energy and nutrient stores and/or employ alternative strategies to sustain themselves until the stressor abates and their Symbiodiniaceae population can recover (Rodrigues and Grottoli, 2007; Grottoli et al. 2006). For example, some corals exploit energy from stored lipids following bleaching, and some corals increase feeding on zooplankton to make up the energy deficit (Grottoli et al., 2006; Rodrigues and Grottoli 2007; Ferrier-Pagès et al., 2010; Hughes and Grottoli, 2013). Bleaching comes with physiological costs and important consequences for coral fitness, such as decreased fecundity and skeletal growth, shifts in metabolic activity, increased antioxidant response and susceptibility to diseases and mortality (Lesser et al., 1990; Ward et al., 2000; Rodrigues and Grottoli, 2007; Cantin et al., 2010; Muller et al., 2018). While these processes are well

documented, and we are beginning to understand their underlying cellular mechanisms, many knowledge gaps remain, including how a coral's proteome responds to bleaching stress and how variable the response is in different parts of the colony. Identifying such proteins and patterns can help to develop physiological biomarkers of coral resilience and improve our mechanistic understanding of recovery from bleaching.

The coral host has two distinct compartments: the tissue, where cellular functions involved in the overall maintenance and fitness of the coral occur; and the skeleton, which provides structural foundation for individual corals and entire reef ecosystems. The coral's polyps and interconnecting tissue or coenosarc between polyps make up the tissue fraction where physiological functions such as feeding, nutrient acquisition and reproduction occur, and it is in this compartment where the majority of Symbiodiniaceae reside (Yost et al., 2013). The coral's skeleton consists of an inorganic aragonitic calcium carbonate structure deposited by the coral tissue and an intra-skeletal organic matrix, including sugars, lipids and proteins (Isa and Okazaki, 1987; Dauphin, 2001; Puverel et al., 2005). The interface between coral tissue and skeleton depends on a coral's skeletal architecture. In corals with a perforate (porous) skeleton, tissue penetrates the cavities of the skeletal matrix. In contrast, tissue does not typically penetrate imperforate coral skeletons. It has been suggested that perforate corals are more resistant to external stressors than imperforate corals because they provide refuge for coral tissue and Symbiodiniaceae (Brown et al., 1994; Santos et al., 2009; Yost et al., 2013). Furthermore, tissue that penetrates perforate coral skeletons can host Symbiodiniaceae which may enhance calcification (Pearse and Muscatine, 1971; Gladfelter, 1983; Yost et al., 2013). These benefits of having a perforate skeleton suggest that there may be differences in cellular functions and biological processes that occur between a corals outer tissue layer and intra-skeletal tissue.

However, to our knowledge, no studies have attempted to uncover these potential differences. Nor has there been a comparison of how these different compartments respond to bleaching stress.

Proteomics is a powerful tool that has advantages over other "omics" technologies for exploring how an organism responds to stress. While genomics and epigenomics provide the blueprint for all potential proteins, revealing the metabolic flexibility of an organism, they do not reveal metabolic pathways that are actively responding to the environment at a time of interest. In contrast, transcriptomics reveals which genes are transcribed in response to a specific stress, yet it has been demonstrated to be a magnified response that does not often correlate to protein translation (Gygi et al., 1999; Maier et al., 2009; Mayfield et al., 2016; Mayfield, 2020). As a result, there are challenges with relating how genes and transcripts equate to biological processes occurring in cells at the time of collection. High-throughput discovery-based proteomics circumvents these challenges by directly identifying and quantifying proteins in the cells at the time of collection, which are closer to the realized function of mRNA and have been shown to be environmentally sensitive (Pandey and Mann, 2000; Tomanek, 2014; Stuhr et al., 2018). Recent advances in proteomics allow for the identification of potentially thousands of proteins by coupling liquid chromatography with tandem mass spectrometry, i.e., "shotgun" proteomics.

In this study, we used shotgun proteomics to explore how a reef-building perforate coral, *Montipora capitata*, responds at the proteomic level to experimental bleaching and to investigate whether the outer layer (OL) tissue and inner core (IC) intra-skeletal tissue and skeleton compartments respond to bleaching differently. By examining proteins from these two distinct compartments, we aimed to uncover connections between metabolic functions of the OL that

support overall maintenance of the coral, and of the IC that support skeletal processes. Specifically, we aimed to address these questions: 1) Are there differential abundances of metabolic proteins in the OL and IC? and 2) Which metabolic pathways differ between these different coral compartments in response to bleaching? We hypothesized that the proteomes of coral OL and IC reflect different functions specific to these two compartments, and that the proteomes and metabolic pathways of coral's OL and IC respond differently to bleaching.

1.3 Materials and Methods

1.3.1 *Species and experimental design*

Montipora capitata is locally abundant, dominant reef-building coral in Hawai‘i, USA. It is a small-polyp species (ca. 0.8 mm) that grows in branching and plating forms, or it can exhibit both morphologies in a single colony. Only the branching form was collected for this study. *M. capitata* was chosen because it has a highly perforate skeleton, and because it is often noted for its resilience (Ritson-Williams and Gates, 2020) indicated by its shift from auto- to heterotrophy (Grottoli et al., 2006) and its ability to reproduce following thermally induced bleaching (Cox, 2007).

Between August 22 – 25, 2017, 10 colonies of *Montipora capitata* with a diameter of ~ 24 cm were collected from the inner lagoon of Kāne‘ohe Bay, surrounding the Hawai‘i Institute of Marine Biology (HIMB, 21.428° N, 157.792° W). Individual colonies were collected more than 3 m apart and although no genetic analyses were conducted, they were considered to be different genets. Upon collection, each colony was halved using a hammer and chisel to produce two genetically identical colonies (ramets). The two halves from each colony were randomly assigned to one of three outdoor flow-through tanks for the ambient temperature control group or

one of three tanks for the bleaching treatment group. Colonies were allowed to acclimate for 7 – 10 days prior to temperature adjustments. The thermal stress treatment started in September during the period when coral bleaching events may occur. Maximum monthly mean temperature for the main Hawaiian Islands is 27ºC and occurs between August – September (NOAA Coral Reef Watch, 2018). On September 1, the temperature in the bleaching treatment tanks was elevated (600 W Titanium Aquarium Heater, Bulk Reef Supply, USA) 0.6ºC day^{-1} over four days, reaching a mean (± SD) temperature of 30.4 ± 0.5ºC (range: 29.4 – 31ºC). The control tanks had a temperature of 28 ± 0.9ºC. On September 26, the heat in the bleaching treatment tanks was gradually decreased to ambient levels by September 29. Twenty-four hours later, two small fragments (ca. 2 cm) were sampled from each colony, one to quantify chlorophyll *a* and Symbiodiniaceae density, and one for proteomics. Samples were cut from the colonies using toe-nail clippers (Revlon Inc., USA) and were immediately frozen in liquid nitrogen. They were stored at -80ºC at HIMB until they were shipped on dry ice to the University of Washington, WA, USA.

All tanks were maintained with a volume of 400 L of ambient sand-filtered seawater from Kāneʻohe Bay. Throughout the experiment, corals were randomly rotated among tanks weekly to minimize any tank effects. Water was circulated using 100 W submersible pumps (Rio® 26HF HyperFlow Water Pump 6019 LPH, TAAM, USA). Mean daytime photosynthetic active radiation (PAR) levels in the tanks were 584 µmol photons m^{-2} s^{-1}, and mean PAR at 12:00 was 1249 µmol photons m^{-2} s^{-1}, measured using a waterproof PAR logger (Odyssey®, Dataflow Systems Limited, NZ). Corals were not given any supplemental food during the experiment.

1.3.2 *Bleaching status*

Bleaching was measured by quantifying chlorophyll *a* and Symbiodiniaceae densities. Chlorophyll *a* was extracted by first grinding each sample in separate glass mortar and pestle. Extractions were then conducted for two consecutive 24 hour-periods with fresh 100% acetone used at the start of each period. The two-part extraction allowed us to extract total chlorophyll per coral fragment. At the end of each 24-hour period absorbances were measured at 630 nm, 663 nm, and 750 nm. Equations from Jeffrey and Humphrey (1975) were used to calculate chlorophyll concentration for each period and summed to determine total chlorophyll per sample. Symbiodiniaceae were separated from ground coral tissue by centrifugation (two times for 5 min at 4000 rpm). Symbiodiniaceae pellets were resuspended in filtered seawater with 1% formalin and 2 – 3 drops of Lugol's iodine, then homogenized using a Tissue Tearer™ (Model# 985-370). Three subsamples were counted using a hemocytometer and the mean was determined. Chlorophyll *a* and Symbiodiniaceae densities were standardized to grams of ash-free dry weight (gdw) of coral tissue.

1.3.3 *Proteomics*

Coral branches for proteomics were sub-sectioned into two sample types: an outer layer (OL) of coral tissue and an inner core (IC) consisting of intra-skeletal tissue and skeleton (Fig 1.1). Samples were collected at least 1 cm from the tip of the fragment. A cross-section, about 5 mm thick, was cut from the fragment, then the OL and IC were separated using a razor blade. An effort was made to collect OL samples of tissue from the oral surface of the coral to the base of the polyps where tissue meets the surface of the skeleton. The remaining skeleton and intra-skeletal tissue material made up the IC samples. All samples were crushed with a metal spatula, placed in 1.5 ml microcentrifuge tubes and frozen at -80°C until proteomic analyses.

To lyse cells, coral samples were sonicated in a 100 µl solution of 50 mM sodium bicarbonate (NH_4HCO_3) with 6 M urea three times (for 15 s then placed on ice for 20 – 30 s each time), using a titanium micro-probe sonicator (Branson 250 Sonifier; 20 kHz), then flash frozen in a dry ice bath for 30 s and stored at -80°C. Samples were thawed on ice and centrifuged at 4°C at 5000 rpm for 10 min to separate and remove solid skeletal material to prevent particles from clogging the chromatography system and from disrupting pH balance during the digestion step. Protein concentrations were quantified from the supernatant in triplicate using a BCA assay (Pierce™), following the manufacturer's instructions for limited sample size (microplate procedure). Samples from one coral colony yielded extremely low protein concentration and were removed from further analyses. For each sample, 50 µg of protein were aliquoted into a new microcentrifuge tube, then brought to a total volume of 100 µl using a solution of 50 mM NH_4HCO_3 with 6 M urea. Samples were frozen at -80°C until further processing.

Enzymatic digestions of the 50 µg protein lysate aliquots were performed following Nunn et al. (2015). Briefly, samples were reduced with T tris(2-carboxyethyl)phosphine, alkylated with iodoacetamide, and diluted with a 4:1 ratio of ammonium bicarbonate to methanol prior to enzymatic digestion with Promega Trypsin (1:20; enzyme : protein) overnight at 37°C. To stop the digestion, each sample's pH was modified with 10% formic acid to a pH $\leq$ 2. Samples were evaporated to near dryness (< 20 µl) in a speed vacuum (CentriVap ® Refrigerated Centrifugal Concentrator Model 7310021) prior to desalting. To remove buffer salts, urea and other non-peptide molecules prior to mass spectrometry analysis, samples were desalted with MicroSpin™ Columns (Nest Group) following the manufacturer's instructions. The resulting peptide samples were evaporated to near dryness, then reconstituted in 5% acetonitrile (ACN) with 0.1% formic acid to final concentration of 0.5 µg μl^{-1} and stored at -80°C prior to analysis.

Liquid chromatography tandem mass spectrometry was performed on Thermo Fisher QExactive according to Nunn et al. (2015). Liquid chromatography was performed using a 28 cm, 75 μm i.d., fused silica capillary column (Magic C18AQ, 100 Å, 5; Michrom, Bioresources, CA) with a 4 cm, 100 mm i.d., precolumn (Magic C18AQ, 100 Å, 5; Michrom). Peptide samples were randomized in the autosampler and loaded on the precolumn for 10 min with 5% ACN, followed by elution onto the analytical column using a 90 min gradient of 5 – 35% ACN with 0.1% formic acid. Top 20 data dependent acquisition (DDA) was used to collect tandem mass spectrometry data. MS1 data was collected on the mass range of 400 – 1400 *m/z* and collision energy was set to 25. The 20 most intense ions with +2 to +4 charge states were selected for collision induced fragmentation and subsequent data acquisition in the MS2 using a dynamic exclusion of 10 seconds. The column was then washed for 10 minutes with 80% ACN and 0.1% formic acid and equilibrated for 10 minutes in 5% ACN and 0.1% formic acid prior to the next sample. Quality control standards were introduced every five runs to monitor chromatography and MS performance and visualized using Skyline (MacLean et al., 2010).

To generate a high quality protein database, the transcriptome of *M. capitata* [(Frazier et al., 2017); GSE97888_Montiporacapitata_transcriptome.fasta] was translated using Transdecoder v 2.0.1 (Haas et al., 2013). Peptide tandem mass spectra were searched against the resulting protein database of *M. capitata* concatenated with 50 common contaminant proteins (Mellacheruvu et al., 2013). Spectra were searched using Comet version 2017.01 rev. 4 (Eng et al., 2013). Search parameters included a concatenated decoy search, peptide mass tolerance of 10 ppm, trypsin as the search enzyme, oxidized methionine as a variable modification (+15.9949 Da), alkylated cysteine (57.021464 Da), and up to three missed cleavages. PeptideProphet (Keller et al., 2002) and ProteinProphet (Nesvizhskii et al., 2003) were used to assign probabilities to peptide and

protein identifications. Adjusted normalized spectral abundance factor (ADJNSAF) for each sample was determined using Abacus (Fermin et al., 2011). Abacus parameters included minimum PeptideProphet score “maxIniProbTH” = 0.99 and “miniProbTH” = 0.50, and a combined ProteinProphet score > 0.88 (FDR of 0.01) (Supplemental file 1). For all downstream analyses, the dataset included only proteins with at least 2 unique peptides across all samples and proteins identified at FDR < 0.01. The mass spectrometry proteomics data have been deposited to the ProteomeXchange Consortium via the PRIDE [1] partner repository with the dataset identifier PXD021243 (Reviewer access- Username: reviewer06494@ebi.ac.uk; Password: aV8SgAO3).

1.3.4 *Data analysis*

To investigate the role of proteins identified by the proteomics experiments we used Gene Ontology (GO) and Kyoto Encyclopedia of Genes and Genomes (KEGG) (Kanehisa and Goto, 2000) pathway analyses. To recover GO terms for each protein, protein sequences were BLASTed against the UniProtKB Swiss-Prot non-redundant protein database (downloaded 10.15.2018). Top results are reported with cutoff E-value <1E-10. Due to a low annotation rate retrieved from the UniProtKB database (~49%), a second BLAST analysis was performed against the National Center for Biotechnology Information (NCBI) nr database on proteins that lacked detailed UniProt annotations. KEGG ID numbers were retrieved from BlastKoala (Kanehisa et al., 2016) using *M. capitata* predicted protein sequence data. GO terms and KEGG data were used to organize proteins into functional categories (e.g., carbon metabolism, response to oxidative stress, etc.; Supplemental file 2).

Proteomics differences among all sample types were visualized using non-metric multidimensional scaling (NMDS) plots based on log (base 10) transformed adjusted normalized spectral abundance factor (ADJNSAF) values. NMDS was performed with distance = “bray”, trymax = 100 and autotransform = FALSE, using the vegan package in R (Oksanen et al., 2020). Bray-Curtis dissimilarity was used to account for a high amount of zero values in the dataset. Analysis of similarity (ANOSIM) was used to test for significant differences among all sample types and between the following comparisons: bleached outer layer (BOL) vs. non-bleached outer layer (NBOL), bleached inner core (BIC) vs non-bleached inner core (NBIC), and NBOL vs NBIC. Statistical differences of protein abundances between sample types were determined using Qspec, a program that computes differential protein abundance (Choi et al., 2015). Analyses were performed on (n = 9) paired samples (ramets) using the qspec-paired command (burn-in = 2000, iterations = 10000, normalized = 1) for the following comparisons: BOL vs. NBOL, BIC vs NBIC, and NBOL vs NBIC. Qspec was performed using raw spectral counts with a sum of at least two unique peptides for each protein in each comparison. Qspec output included a protein-length corrected log-fold change analysis (base 2) and a false discovery rate (FDR)-corrected z-score based on the posterior distribution of the LFC parameter, guided by the FDR estimated by a well-known Empirical Bayes method. Differential expression was reported using a LFC $\geq |0.5|$ and z-score $\geq |2|$ (Supplemental file 3). Enrichment analysis of biological processes were compared between NBOL and NBIC using MetaGOmics ver. 0.1.1 (Riffle et al., 2017). MetaGOmics quantifies functional differences among treatments based on peptide, not protein, abundance using GO. The *M. capitata* proteome identified in this study was set as the background reference. Then, for each treatment group spectral counts were pooled across all samples (n=9) and compared against the reference. GO terms were considered significant when

Laplace corrected LFC > |0.5| and when Laplace corrected and Bonferroni corrected p-value < 0.01. The Laplace correction adds one to every spectral count for each GO term to account for spectral counts that equal zero when calculating log fold ratios, while the Bonferroni correction controls for type I errors due to multiple hypothesis testing (Riffle et al., 2017). As above, GO term data were used to organize proteins into functional categories.

1.4 RESULTS

1.4.1 *Bleaching status.*

Photobiological data confirmed that the bleaching treatment corals were bleached (Fig 1.2). Symbiodiniaceae density (number of cells gdw^{-1}) decreased ~71% in bleached corals compared to non-bleached control corals (Wilcoxon rank sum test, W = 8, p-value = 0.002756). Chlorophyll *a* concentration (µg gdw^{-1}) decreased ~78% in bleached corals compared to non-bleached corals (T-test, t = -8.0304, df = 13.91, p-value = 1.368e-06).

1.4.2 *Proteomic results across all sample types*

Proteomic analyses revealed a total of 2361 proteins that were identified across all treatments and sample types. Overall, ~90% (2128) of the proteins identified in this study were annotated with either National Center for Biotechnology Information (NCBI) (n=2082) or UniProtKB IDs (n=1167) and ~81% (1918) were associated with GO terms. Of all 2361 proteins, ~71% (1687) had associated KEGG terms. This high percentage of annotated proteins allowed for more detailed analysis of active metabolic pathways utilized in each sample type across both treatments. About 70% (1660 proteins) of all proteins were found in every sample group and the number of unique proteins per treatment or sample type ranged from 0.5% – 2%, with the highest number of unique proteins observed in the OL of bleached corals (Fig 1.3A). NMDS ordination

of protein profiles of all sample types show a distinction between the OL and IC compartments but not between bleached and non-bleached samples for either OL or IC. ANOSIM revealed that there was a significant difference of protein profiles among all sample types (R = 0.5701; p = 9.999e-05).

1.4.3 *Comparison of protein profiles from the OL and IC of non-bleached corals*

To gain a general understanding of the overall protein differences between *M. capitata* OL and IC, we compared the proteomes of the OL and IC of non-bleached corals. Across the two sample types, we identified 2242 proteins. ANOSIM revealed that there was a significant difference of protein profiles between the OL and IC of non-bleached samples (R = 0.5936; p = 0.001). Further analysis revealed that 187 proteins were significantly more abundant in the OL and 132 proteins were more abundant in the IC (Supplemental file 3). Based on enrichment analysis, the OL of non-bleached *M. capitata* was enriched in biological processes involved in anatomical development, carbohydrate metabolism, cell differentiation, endocytosis, lipid metabolism, protein metabolism, RNA processing and small molecule processing (Fig 1.4A and Supplemental file 4). Peroxidasin (PER2; m.25079; LFC - 3.7) was detected at the highest abundance in the OL and is part of cellular response to oxidative stress. Several other proteins related to carbon and nitrogen metabolism were also present in high abundances such as GDP-mannose 4,6 dehydratase (GMD; m.26053; LFC - 1.2), pyruvate dehydrogenase (PDH; m.4559; LFC - 1.1), aconitate hydratase (ACN; m.20259; LFC - 0.7), and isocitrate dehydrogenase (IDH; m.11767; LFC - 0.7) (Fig 1.4B). The IC was characterized by an enrichment in GO biological processes involved in cellular structure and adhesion, carbohydrate metabolism, immune response, lipid metabolism, oxidoreductase activity and response to stimulus (Fig 1.4A and Supplemental file 4). The protein identified in the OL to have the highest fold change difference

compared to the IC was a lipase-related protein (LIP1; m.21324, LFC +2.1) that is involved in lipid metabolism (Fig 1.4B). Von Willebrand factor type A (VWA; m.31548, LFC +1.5), an important adhesion structural protein, was also present at significantly high concentration in the IC (Fig 1.4B).

1.4.4 *Comparison of bleaching effects on the OL proteome*

In the OL of bleached and non-bleached *M. capitata*, 2281 proteins were identified. ANOSIM did not reveal a significant difference of protein profiles between OL of bleached and non-bleached corals ($R = 0.05316$; $p = 0.159$). Qspec analysis of differential abundances between the OL of bleached and non-bleached corals revealed 63 significant proteins at higher, and 28 at lower, abundance in bleached corals compared to non-bleached corals (Supplemental file 3). Biological enrichment analysis of GO terms identified that the OL of bleached corals have a higher abundance of proteins involved in carbon metabolism, lipid metabolism, nitrogen metabolism, protein metabolism, response to oxidative stress, RNA processing and cellular signaling and transport than non-bleached corals (Figs 1.5A and 1.6). Proteins with the highest log-fold change included calumenin (CALU; m.10914, LFC +1.8), betaine-homocysteine S-methyltransferase (BHMT; m.1453, LFC +1.6), peroxidasin (PER1; m.28022, LFC +1.5), urease (URE; m.24102, LFC +1.4), and catalase (CAT; m.4762, LFC +1) (Figs 1.5A and 1.6). Key cellular pathways that increased in the OL of bleached corals include the glyoxylate cycle, fatty acid beta oxidation, beta alanine metabolism, protein degradation and synthesis, betaine degradation and urea degradation. GO terms associated with less abundant proteins in the OL of bleached corals are associated with biological processes involved in lipid metabolism, amino acid synthesis, protein metabolism, RNA processing, cellular signaling and transport, and cellular structure (Figs 1.5A and 1.6). Proteins that were significantly lower in abundance in the

OL of bleached corals included cholesterol transporter (CHLT; m.15955, LFC -1.8), glutamine synthetase (GS; m.30399, LFC -1.6), phospholipase B (PLIP; m.27749, LFC -1.1), and mucin protein (MUC; m.29491, LFC -1) (Figs 1.5A and 1.6).

1.4.5 *Comparison of bleaching effects on the IC proteome*

In the IC of bleached and non-bleached *M. capitata*, 2181 proteins were identified. ANOSIM did not reveal a significant difference of protein profiles between the IC of bleached and non-bleached corals ($R = -0.04287$; $p = 0.636$). Qspec analysis of relative abundances of the proteins detected in the IC revealed 22 proteins at significantly higher abundance and 17 at lower abundance in the IC of bleached corals compared to non-bleached corals. Associated GO terms indicate that proteins at higher abundance in the IC of bleached corals are involved in biological functions including carbon metabolism, protein metabolism, response to oxidative stress and RNA processing (Figs 1.5B and 1.6). The top 5 proteins with the highest positive log-fold change in the IC of bleached corals included peroxidasin (PER2; m.25079, LFC 1.9), ependymin (EPDR; m.10937, LFC 1), aldehyde dehydrogenase (ALDH; m.27710, LFC 1), calumenin (CALU; m.10914, LFC 0.9), and stomatin (STOM; m.21902, LFC 0.8) (Figs 1.5B and 1.6). Additionally, a protein involved in the pentose phosphate pathway was also represented in this dataset with significantly increased abundance (Figs 1.5B and 1.6). Biologically enriched GO terms associated with the IC of non-bleached corals were involved in nitrogen metabolism, cellular signaling and cellular structure (Figs 1.5B and 1.6). The proteins that were lower in abundance in the IC of bleached corals compared to the IC of non-bleached corals included glutamine synthetase (GS; m.30399, LFC -1.9), peroxidasin (PER3; m.6107, LFC -1.2), and mucin (MUC; m.29491, LFC -0.8) (Figs 1.5B and 1.6).

1.5 DISCUSSION

Proteomics has proven to be a valuable tool for uncovering active cellular processes and elucidating the response of different biological compartments of symbiotic cnidarians in response to stress (Weston et al., 2015; Ricaurte et al., 2016; Cziesielski et al., 2018; Hernández-Elizárraga et al., 2019; Mayfield, 2020; Mayfield et al., 2021; Petrou et al., 2021). Our high-throughput discovery-based proteomic analyses of the OL and IC of bleached and non-bleached corals support our hypothesis that proteomic signatures differ between *M. capitata* OL and IC, reflecting different biological functions associated with these two compartments. Additionally, comparisons of bleached and non-bleached proteomes support our hypothesis that *M. capitata* OL and IC respond in different metabolic ways to bleaching stress. We observed bleaching induced differences in carbon metabolism, response to oxidative stress, protein turnover and nitrogen metabolism between corals' OL and IC compartments. Our results corroborate several previous transcriptomics studies (DeSalvo et al., 2010, 2012; Barshis et al., 2013; Kenkel et al., 2013; Polato et al., 2013; Aguilar et al., 2019) by providing direct evidence of protein translation in response to bleaching stress. To our knowledge, our analysis was the first to compare the simultaneous bleaching proteomic response in both OL and IC. Our results highlight the differential metabolic response between OL and IC in *M. capitata* that may reflect the compartmentalization of specific physiological functions and energy acquisition and allocation in each compartment.

1.5.1 *Biological functions of (non-bleached) OL and IC*

Among our four sample types, the most significant proteomic difference was found when comparing the OL and IC (see Fig 1.3B). Biological enrichment analysis of GO terms using

MetaGOmics highlight how the coral OL is characterized by routine cellular activities such as metabolic processes, cellular maintenance, and growth, while the IC was significantly enriched in proteins related to structural maintenance, cell adhesion, immune and stimulus response, as well as carbon and lipid metabolism. These differences in biological processes suggest that there are compartmentalized pathways between the OL and IC, with IC proteins playing a larger role in skeletal formation than OL proteins. Previous proteomic studies of coral skeleton report the presence of structural and cell adhesion proteins that were also found in this study in the *M. capitata* IC compartment, including von Willebrand factor type A (VWA), hemicentin (HMCN), and collagens (COL) (Drake et al., 2013; Ramos-Silva et al., 2013). The von Willebrand factor type A containing proteins have been suggested to play a role in connecting the layer of cells at the interface of the skeleton organic matrix to the skeleton, and collagen has been suggested to serve as a site for proteins to bind where minerals, such as calcium carbonate, can nucleate (Drake et al., 2013).

A considerable amount of redundancy was revealed between the OL and IC of *M. capitata* as ~2000 proteins were detected with similar abundances between the two compartments, which is likely due in part to our sampling method of a perforate coral. In corals with a perforate skeleton, tissue penetrates the complex matrix of crevices and cavities and can host Symbiodiniaceae that can drive biological activity (Pearse and Muscatine, 1971; Gladfelter, 1983; Yost et al., 2013). In contrast, the skeleton of imperforate corals is more dense and typically does not contain coral tissue. Evidence suggests that perforate corals are more robust to stressful events than imperforate corals (Krupp et al., 1992; Jokiel et al., 1993; Santos et al., 2009), which may be due to higher protein and Symbiodiniaceae densities in their deep tissue compared to imperforate corals (Schlöder and D'Croz, 2004). It has also been suggested that perforate skeletons can

provide refuge for deep coral tissue and Symbiodiniaceae that reside deep in the skeleton during stressful conditions (Santos et al., 2009). Given that the IC samples collected here contain both coral tissue and skeleton, it is likely that there is some overlap in metabolic processes and pathways that occur between the OL and IC compartments, which would explain some of the similarity in proteins between them. Furthermore, proteins from tissue within the skeleton that do not play a role in calcification may have been at a higher abundance and were more likely to be sampled with our mass spectrometry methods than proteins that are directly involved in calcification, such as carbonic anhydrase, calcium ion pumps or the coral acid rich proteins identified by other studies (Drake et al., 2013; Ramos-Silva et al., 2013).

1.5.2 *Molecular responses to bleaching*

Carbon metabolism. Carbon is a critical nutrient for corals that is primarily provided in the form of glucose-based photosynthate that is passed to the host from Symbiodiniaceae (Muscatine et al., 1981). As corals bleach and the association with Symbiodiniaceae is weakened and carbon-based photosynthate decreases, it has been proposed that corals maintain their energetic needs through the degradation of stored lipids (Grottoli and Rodrigues, 2011). Here, we provide direct evidence of modifications to carbon metabolic pathways through quantitative analyses of proteins that are differentially abundant in bleached corals compared to non-bleached corals. Our results reveal mitigation strategies for bleached corals to generate the required energy needed to persist after bleaching stress.

In the OL of bleached *M. capitata* , increased abundance of isocitrate lyase (ISL) suggests an increased capacity to produce glyoxylate. Typically produced in the glyoxylate cycle, glyoxylate is a two-carbon metabolite and a precursor to glucose and many other C-storage molecules. The

glyoxylate cycle, a variation of the Krebs cycle, uses acetyl-CoA as a source of carbon and conserves carbon by bypassing two decarboxylation steps of the Krebs Cycle (Kornberg and Krebs, 1957). Although it was once thought to only occur in plants and bacteria, recent transcriptomics studies have shown that glyoxylate cycle enzymes also occur in corals (DeSalvo et al., 2010; Kenkel et al., 2013; Polato et al., 2013). Bleached corals may upregulate the glyoxylate cycle, or the production of glyoxylate, to metabolize energy in stored lipids, breaking down triacylglycerol into their component fatty acids for release of acetyl-CoA, when carbohydrate supply is low (Polato et al., 2013; Wright et al., 2015; Petrou et al., 2021). Malate synthetase (MS), the other key enzyme of the glyoxylate cycle that converts glyoxylate and acetyl-CoA to malate, was present in the proteomes identified in this study, but no significant difference was detected between bleached and non-bleached corals. The same trend of increased ISL abundance and no increase in MS abundance has been reported for *Porites asteroides* (Kenkel et al., 2013) and *Acropora millepora* (Petrou et al., 2021). We also detected three key enzymes involved in lipid metabolism in higher abundance in the OL of bleached corals compared to the OL of non-bleached corals: very long-chain specific acyl-CoA dehydrogenase (ACADVL), medium chain specific acyl-CoA dehydrogenase (ACADM) and acetyl-CoA acetyltransferase (ACAT1). The presence of these enzymes further supports the hypothesis that bleached corals utilize the glyoxylate cycle to extract energy from lipids when Symbiodiniaceae-derived photosynthate is decreased (Fig 1.7).

Malonate-semialdehyde dehydrogenase (ALDH) was another enzyme that was significantly increased in bleached corals and can provide an additional source of acetyl-CoA that could be used in the glyoxylate cycle. ALDH is involved in several metabolic pathways including carbon metabolism, beta-alanine metabolism and propanoate metabolism where it catalyzes the

conversion of malonate semialdehyde (3-oxopropanoate) to acetyl-CoA. Enzymes associated with the glyoxylate cycle and fatty acid beta-oxidation were higher in the OL of bleached corals than the OL of non-bleached corals. However, ALDH was more abundant in both the OL and IC of bleached corals compared to these compartments in non-bleached corals (Fig 1.5).

An enzyme involved in the pentose phosphate pathway (PPP), transketolase (TKT), was lower in the IC of non-bleached corals compared to the OL of non-bleached corals, but higher in the IC of bleached corals than the IC of non-bleached corals, suggesting that this pathway is initially prioritized in the OL but becomes more essential in the IC during bleaching. The PPP helps maintain carbon homeostasis, generates precursors to nucleotides, and produces reducing molecules (e.g., NADPH) to fight oxidative stress. This pathway has been elevated in stressed cnidarians suffering from disease (Wright et al., 2015; Garcia et al., 2016) as well as thermal stress (Oakley et al., 2017; Fonseca et al., 2019). Hernández-Elizárraga et al. (2019) found proteomic evidence that bleached fire coral, *Millepora complanata*, redirected carbohydrate flux from glycolysis to the PPP, which would help the coral alleviate oxidative stress through the production of NADPH. Additionally, the generation of nucleotides could assist with multiple other cellular processes. Future research should investigate potential links between the pentose phosphate pathway and coral calcification.

Response to oxidative stress. Oxidative stress, due to production of excess reactive oxygen species (ROS), has been implicated as a key underlying mechanism in the breakdown of coral-algal symbiosis leading to bleaching (Lesser et al., 1990; Lesser, 1997; Downs et al., 2002). Under environments favoring physiological homeostasis, ROS produced during metabolic processes of the coral host, Symbiodiniaceae, and in the chloroplasts of Symbiodiniaceae, are

kept in check by cellular antioxidants. Under environmental stress, however, this tightly regulated process can become unbalanced resulting in excess ROS, leading to cellular damage and bleaching (Lesser et al., 1990; Downs et al., 2002). One possible mechanism for a coral's resilience to bleaching may be explained by the timing, magnitude, and types of antioxidants regulated during stress (Gardner et al., 2017).

Several enzymes involved in oxidative stress response were at higher abundance in both the OL and IC of bleached *M. capitata* compared to samples from non-bleached corals. This observation is consistent with proteomics (e.g., Weston et al., 2015; Cziesielski et al., 2018; Petrou et al., 2021) and transcriptomics (e.g., DeSalvo et al., 2008; Voolstra et al., 2009; DeSalvo et al., 2010) studies that have demonstrated increased antioxidant activity in response to thermal stress in cnidarians. Multiple catalases (CAT) were elevated in the OL and IC of bleached corals. This antioxidant enzyme is an efficient scavenger of hydrogen peroxide and is commonly observed in high quantities in bleached corals (Lesser et al., 1990; Seneca et al., 2010; Krueger et al., 2015; Gardner et al., 2017). Peroxidasins (PER1, PER2, PER3) that also neutralize hydrogen peroxide were detected at significantly higher abundances in both compartments from bleached corals. In coral embryos, significant upregulation of peroxidasin genes, a multi-domain peroxidase, has been observed after 48 h of thermal stress (Voolstra et al., 2009), while in adult corals it was downregulated after 11 days of thermal stress exposure (Desalvo et al., 2008). Here we report that peroxidases are present in an adult coral following nearly one month of thermal stress. Peroxidasin has been proposed as a biomarker for heat stress in coral embryos and adults (Voolstra et al., 2009) and may be important for resilience to high temperatures (Barshis et al., 2013).

Another enzyme higher in the OL of bleached corals, gamma-glutamyltranspeptidase 1 (GGT1), likely plays an indirect role in oxidative stress response through its role in the glutathione cycle. Glutathione, in its reduced form, is important for various metabolic processes where it can neutralize ROS and help break down toxins (Mailloux et al., 2013; Bachhawat and Yadav, 2018). GGTs break down oxidized glutathione that has been transported out of the cell into glutamate and cysteine-glycine. Cysteine-glycine can then be transported back into the cell to produce more glutathione in its reduced form, ready to neutralize ROS (Mailloux et al., 2013; Bachhawat and Yadav, 2018).

Protein turnover. Environmental stressors that have the potential to induce cellular damage, or significantly alter homeostatic metabolisms, drive high protein turnover rates (Downs et al., 2002; Oakley et al., 2017). Several pathways, including protein degradation, translation, and protein folding, play key roles in the turnover of proteins and maintaining proteostasis. Significantly higher abundances of proteins involved in each of those pathways were quantified in bleached corals compared to non-bleached controls, indicating a significantly higher level of protein turnover. In the OL of bleached corals, protein degradation was indicated by higher abundance of two proteins associated with proteasomes, the protein complexes responsible for degrading extraneous or damaged proteins: 26S proteasome regulatory subunit 6A-B (PSMC6A-B) and proteasome subunit beta type-7-like (PSMB7). The observed increase in proteasome components in this study is consistent with transcriptomic (Traylor-Knowles et al., 2017) and proteomic (Petrou et al., 2021) research investigating short term heat stress in corals.

Multiple chaperone subunits of the T-complex protein Ring Complex (TRiC: TCPE, TCPEt, TCPZ), as well as calnexin (CANX) were in high abundance in the OL of bleached corals,

suggesting that bleached corals were undergoing endoplasmic reticulum (ER) stress. ER stress occurs due to accumulation of unfolded or misfolded proteins and initiates the unfolded protein response which, under prolonged or severe stress, can lead to cell death (Xu et al., 2005). The TRiC assists the folding of up to 10% of eukaryotic cytosolic proteins involved in a broad range of functions (Yam et al., 2008). It is suggested to be well-equipped for folding complex, slow-folding proteins that are prone to aggregation (Yam et al., 2008; Gestaut et al., 2019), making it critical for maintaining proteostasis and reducing ER stress. Calnexin is recognized for its role in processing glycoproteins in the ER where it binds to unfolded or misfolded proteins and prohibits their release (Ou et al., 1993). Eight different calumenins (CALU) were in higher abundance in bleached corals, including five in the OL (CALU1-5) and three in the IC (CALU2, CALU3, CALU4). Although its role as a chaperone in the ER has not been directly confirmed, increased abundance of calumenin resulted in down-regulation of proteins involved in ER stress reduction, suggesting it functions similarly to chaperones (Lee et al., 2013). Chaperones, most notably heat shock proteins, are commonly detected in heat-stressed and bleached corals (Black et al., 1995; Brown et al., 2002; Barshis et al., 2013; Weston et al., 2015; Ricaurte et al., 2016; Traylor-Knowles et al., 2017; Seveso et al., 2020) because of their role in stress response. However, no heat shock proteins were identified at significant levels in this study. Few coral bleaching studies have reported the presence of the chaperone proteins detected in the current study (Bellantuono et al., 2012; Maor-Landaw et al., 2014; Chakravarti et al., 2020).

The increased abundances of proteins related to high protein turnover in our bleached samples, one day after the heat stress was removed, may be the result of a rapid adjustment to a change in the coral's environment (e.g., a recovery phase) via alteration of its proteome. High rates of protein turnover have been associated with an organism's ability to acclimatize (Hawkins, 1991).

For corals it has been suggested that slow growth rates and high metabolic rates correlate to high protein turnover and acclimatization potential (Gates and Edmunds, 1999). An analysis of protein turnover rates in bleached and healthy states between *M. capitata* and other species would allow more direct testing of the hypothesis that protein turnover is directly linked to thermal acclimation.

Nitrogen metabolism. Nitrogen (N) is a critical element used for synthesizing nucleotides, amino acids, proteins and other molecules in both the coral host and Symbiodiniaceae. Living in oligotrophic, tropical waters, the coral holobiont has adapted to efficiently acquire N from the surrounding environment via heterotrophy, or assimilation of dissolved organic and inorganic N by the host and the Symbiodiniaceae (Grover et al., 2006, 2008; Pernice et al., 2012). Although ammonia is the primary N-based metabolite (Grover et al., 2008), corals also have the enzymatic capacity for transport and assimilation of nitrate, dissolved free amino acids and, to a much lesser degree, urea from the surrounding water, providing them with a range of mechanisms to adapt to changing nutrient conditions (Grover et al., 2008). Nitrogen is transferred between the host and Symbiodiniaceae (Rahav et al., 1989; Atkinson et al., 1994; Hoegh-Guldberg and Williamson, 1999), however, when symbiosis breaks down due to prolonged thermal stress, mutualistic N-exchange decreases, demanding the coral host independently acquire N from the environment or intracellularly recycle it. Here we show that bleached *M. capitata* switches its dominant N- acquisition strategy from ammonia uptake to the degradation of urea and betaine (Fig 1.8).

Enzymes involved in the typical pathway of ammonia assimilation decreased in bleached corals. Both the coral host and Symbiodiniaceae are able to assimilate ammonia via catalysis by

glutamine synthetase (GS) or glutamine dehydrogenase in the host (Yellowlees et al., 1994; Wang and Douglas, 1998; Su et al., 2018) and via the glutamine synthetase/glutamine:2-oxoglutarate aminotransferase (GS/GOGAT) cycle in Symbiodiniaceae (D'Elia et al., 1983; Roberts et al., 2001). In bleached corals, GS was present at significantly lower abundances in both the OL and the IC compared to non-bleached corals, suggesting an alternate route for N acquisition must be utilized (Figs 1.5 and 1.6). This result is consistent with recent studies in corals (Petrou et al., 2021; Rädecker et al., 2021), however, increased GS activity has been reported for other cnidarians (Oakley et al., 2016; Wang and Douglas, 1998; Lipschultz and Cook, 2002). Both Petrou et al. (2021) and Rädecker et al. (2021) also observed concurrent increases in glutamate dehydrogenase (GDH) in bleached corals, which catabolizes glutamate to α-ketoglutarate, an intermediate of the Krebs Cycle. Thus, GDH indicates the degradation of amino acids for use as energy while producing ammonia as a byproduct. While we did not observe any change in GDH in bleached corals in this study, we propose two alternative nitrogen sources in bleached corals.

Urease (URE), an enzyme that catalyzes the conversion of urea to ammonia and carbon dioxide, provides another metabolic pathway for acquiring nitrogen and was significantly more abundant in the OL of bleached corals than non-bleached corals. Urea is thought to be an important source of nitrogen for corals (Grover et al., 2006; Crandall and Teece, 2012) because they can easily assimilate it from the surrounding environment where it accumulates from anthropogenic runoff and is a naturally produced metabolite from a variety of biological sources (Conover and Gustavson, 1999; Lomas et al., 2002; Glibert et al., 2006; McDonald et al., 2006). Grover et al. (2008), however, calculated that urea only constitutes about three percent of nitrogen uptake in *Stylophora pistillata*. Corals may also produce urea on their own, but the mechanism remains

unclear because the complete enzymatic toolkit of the urea cycle has yet to be observed in corals (Streamer, 1980). Genes encoding four of the five enzymes of the urea cycle are present in the *M. capitata* genome, including: carbamoyl phosphate synthetase I (CPS1), ornithine transcarbamylase (OTC), argininosuccinate synthase (ASS) and argininosuccinate lyase (ASL), but the fifth enzyme, arginase (ARG1), has not been identified. Three of those enzymes, OTC, ASS and ASL, were detected in the proteome identified in this study. Regardless, the elevated level of urease provides direct evidence that bleached corals rely on urea as a source of nitrogen, which may help to counteract the effects of decreased GS activity described above.

Here, we reveal that a critical source of nitrogen in bleached corals likely comes from the intracellular degradation of glycine betaine. Two enzymes involved in betaine degradation pathway, betaine-homocysteine S-methyltransferase (BHMT) and dimethylglycine dehydrogenase (DMGDH), were significantly more abundant in the OL of bleached corals than non-bleached corals. Enzymatic components of this pathway have been observed in multiple marine organisms, including marine invertebrates and corals (DeSalvo et al., 2012; Aguilar et al., 2019; Sproles et al., 2019). Glycine betaine is an important osmolyte because of its role in counteracting osmotic and other abiotic stressors (Rathinasabapathi, 2000; Jahn et al., 2006) and may have been produced in abundance in response to bleaching (DeSalvo et al., 2012). Recently, however, betaine has been proposed as a major source of nitrogen in reef-building corals where it can account for up to 16% of total nitrogen biomass (Ngugi et al., 2020). A recent metabolomics study on the bleaching history of *M. capitata* demonstrates that betaine-lipids are depleted in bleached samples, whereas historically non-bleached *M. capitata* is enriched in this metabolite (Roach et al., 2021). These proteomic profiles on the same coral species complement the metabolomic profiles of bleached versus non-bleached *M. capitata* and provide direct evidence

of active molecular pathways utilized by bleached corals to acquire N from stored betaine-lipids, potentially leading to its long-term persistence on reefs.

1.5.3 *Conclusion*

Through analyzing the proteomes of the OL and IC of bleached and non-bleached *M. capitata*, we investigated 1) whether there were differential abundances of metabolic proteins in the OL and IC compartments, and 2) if metabolic pathways differ between these two compartments in response to bleaching. We identified several metabolic pathways and biological processes that are used in specific compartments or shared across compartments following bleaching stress. These included different strategies for metabolizing carbon, lipids and nitrogen by each compartment and high oxidative stress response and protein turnover in both compartments following bleaching. Our findings suggest that some molecular responses to bleaching are compartmentalized, which may be the most efficient way to continue functions specific to each compartment following bleaching. Future research should assess whether these compartmentalized responses to bleaching are linked to compartment-specific physiological functions. For example, does energy produced from lipids via the glyoxylate cycle help fuel reproductive output in the coral OL compartment? Or are there links between the products of the pentose phosphate pathway, such as NADPH and nucleotide generation, and calcification? Additionally, employing these compartmentalized strategies may convey resilience to bleaching and studies targeting these pathways, such as the glyoxylate cycle, the pentose phosphate pathway, protein turnover, urea assimilation and betaine degradation, should be undertaken to better understand their influence on coral resilience. Answers to questions like these will further our understanding of how and where distinct physiological functions in corals are affected by thermal stress and bleaching. Furthermore, elucidating the precise role of these metabolic

pathways and cellular responses to bleaching could provide management with molecular-based tools, such as biomarkers, for conservation and restoration.

1.6 ACKNOWLEDGEMENTS

We offer our warmest gratitude to the Gates Coral Lab for hosting and supporting us during this experiment at the Hawai‘i Institute of Marine Biology. We thank Brenner Wakayama, Gavin Kreitman, Melissa Jaffe and Sean Frangos for help with collecting and culturing the experimental corals. We thank Callum Backstrom for assistance with processing Symbiodiniaceae and chlorophyll data. We thank Hyungwon Choi for assistance with statistical software.

1.7 FIGURES

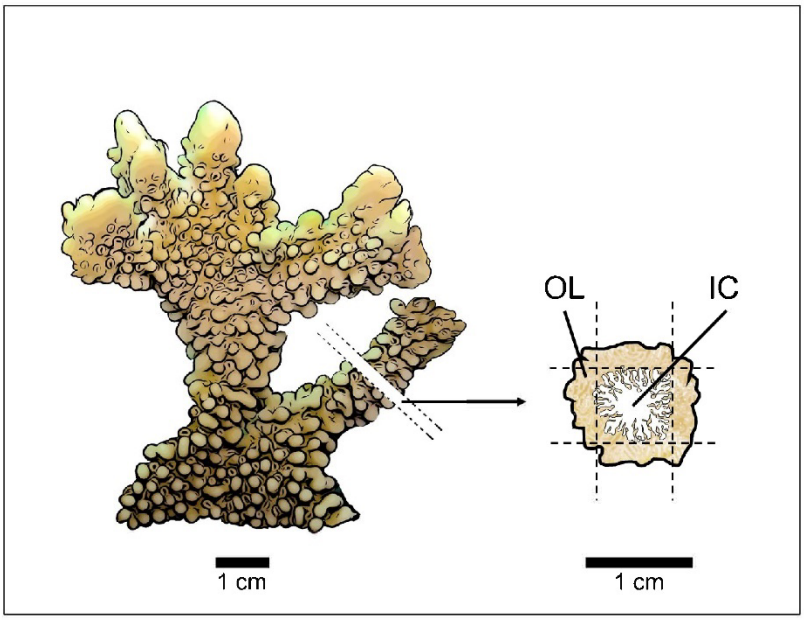

Figure 1.1 Sampling method for protein extractions from bleached and non-bleached *Montipora capitata* colonies. A small cross-section (~5 mm thick) was removed from one branch of each coral fragment at least 1 cm from the tip. The cross-section was laid flat, and a thin layer of tissue (~1 – 2 mm) was removed from four sides using a sterilized razor blade producing an outer layer (OL) of tissue and an inner core (IC) of intra-skeletal tissue and skeleton. The cross-section diagram shows the composition of our two sample types as the tissue of *M. capitata* penetrates the perforate skeleton (coral tissue indicated in brown and skeleton indicated in white).

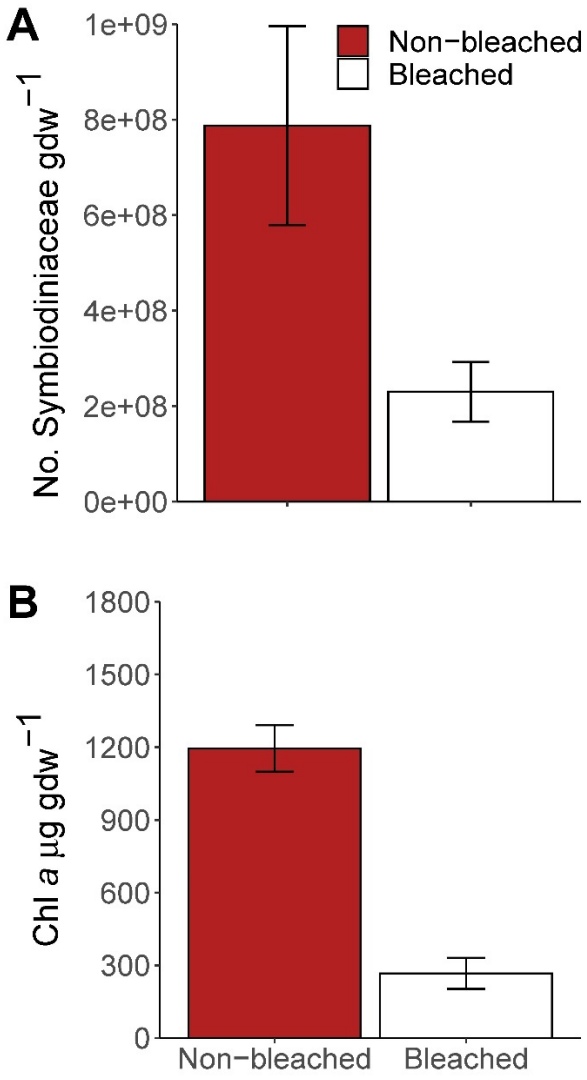

Figure 1.2 Photobiological measurements of experimental corals. Bars indicate the mean and error bars indicate 1 standard error, for (A) Symbiodiniaceae density (number of cells gdw-1) and (B) chlorophyll a concentration (µg gdw-1).

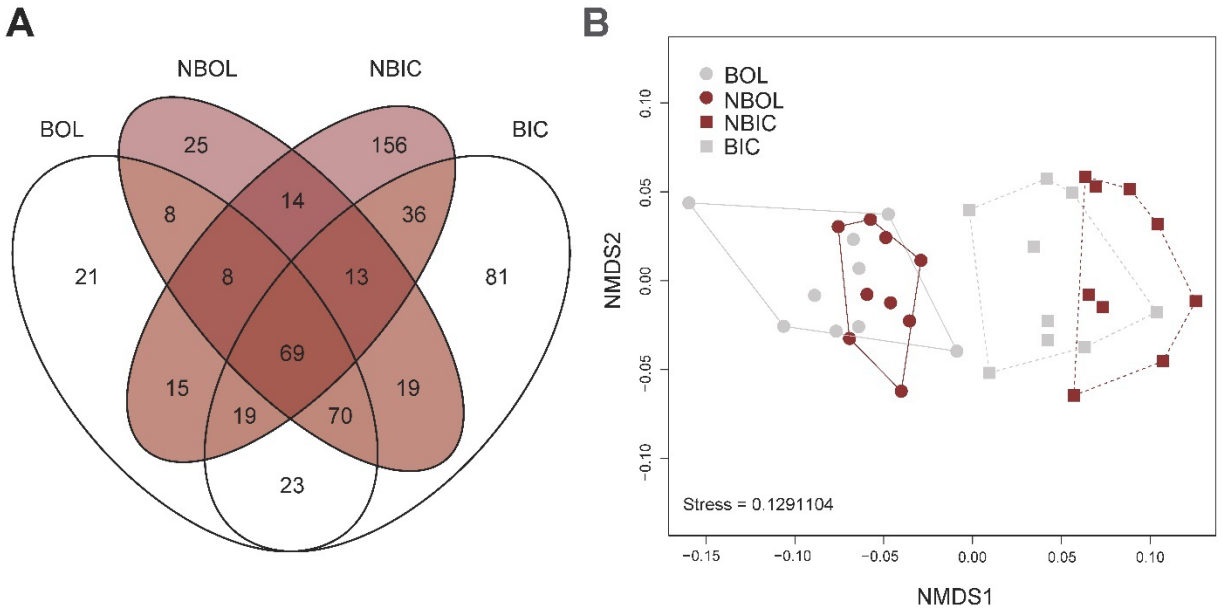

Figure 1.3 Global results of proteomics analysis of bleached and non-bleached *Montipora capitata* outer layer (OL) tissue and inner core (IC) intra-skeletal tissue and skeleton. (A) Venn diagram depicts number of proteins identified in each sample type, and (B) Non-metric dimensional scaling (NMDS) plot of all treatments. BOL = bleached outer layer; NBOL = non-bleached outer layer; NBIC = bleached inner core; BIC = bleached inner core.

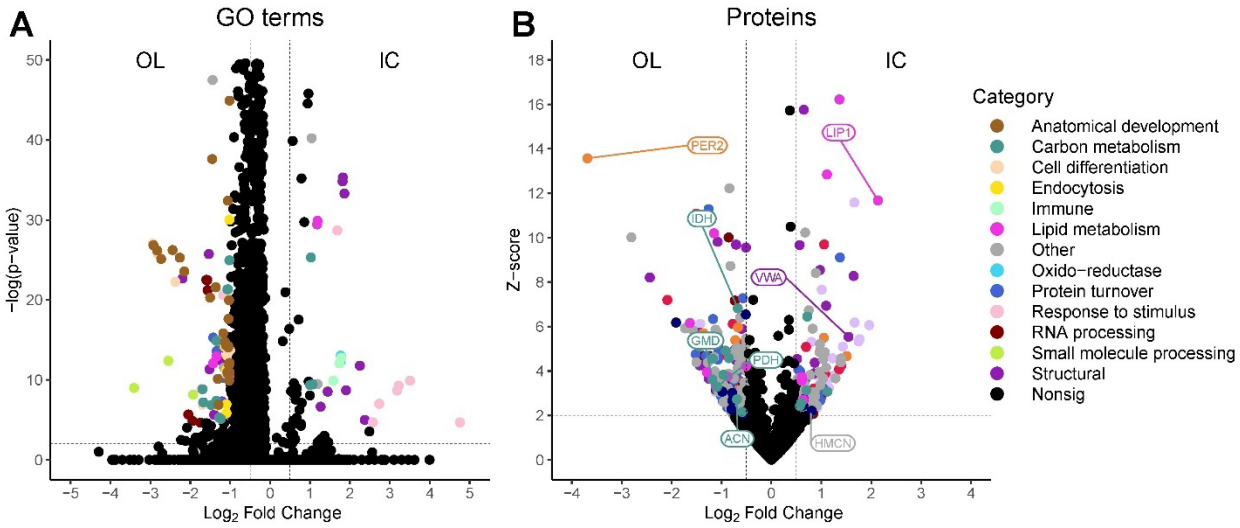

Figure 1.4 Volcano plots of (A) associated gene ontology (GO) terms derived from MetaGOmics and (B) proteins identified in non-bleached outer layer (OL) tissue and inner core (IC) intra-skeletal tissue and skeleton of *Montipora capitata*. Points represent the magnitude of the log_2 fold change and the -log(p-value) or z-score for each GO term or protein, respectively. Dashed lines indicate significance thresholds. Select proteins that are discussed in the text are indicated by their abbreviated protein name.

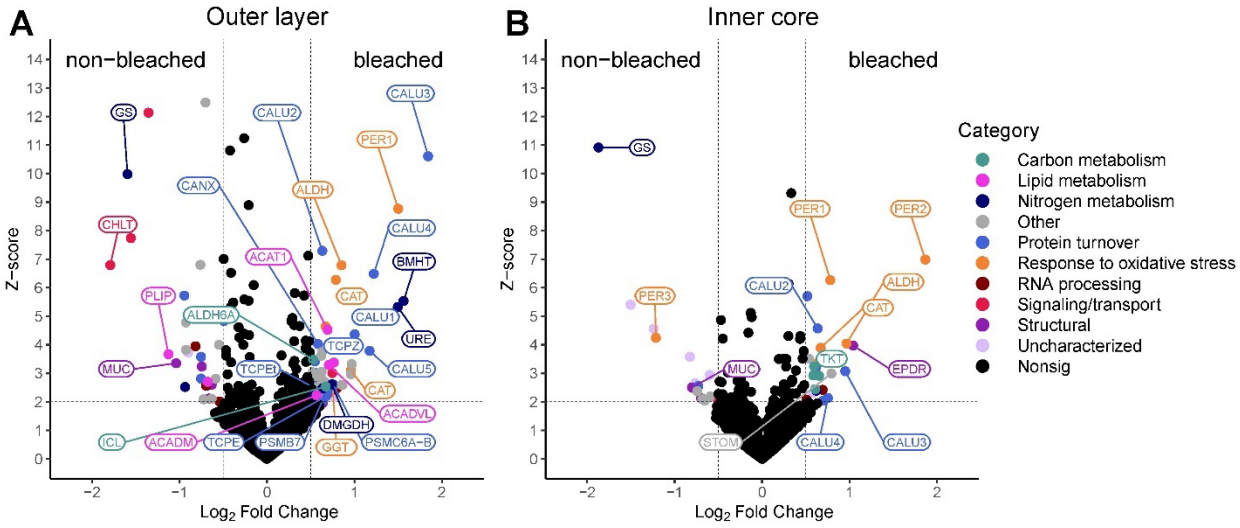

Figure 1.5 Volcano plots of proteins identified in non-bleached and bleached (A) outer layer (OL) tissue and (B) inner core (IC) intra-skeletal tissue and skeleton of *Montipora capitata*. Points represent the magnitude of the log2 fold change and the z-score for each protein. Dashed lines indicate significance thresholds. Select proteins that are discussed in the text are indicated by their abbreviated protein name.

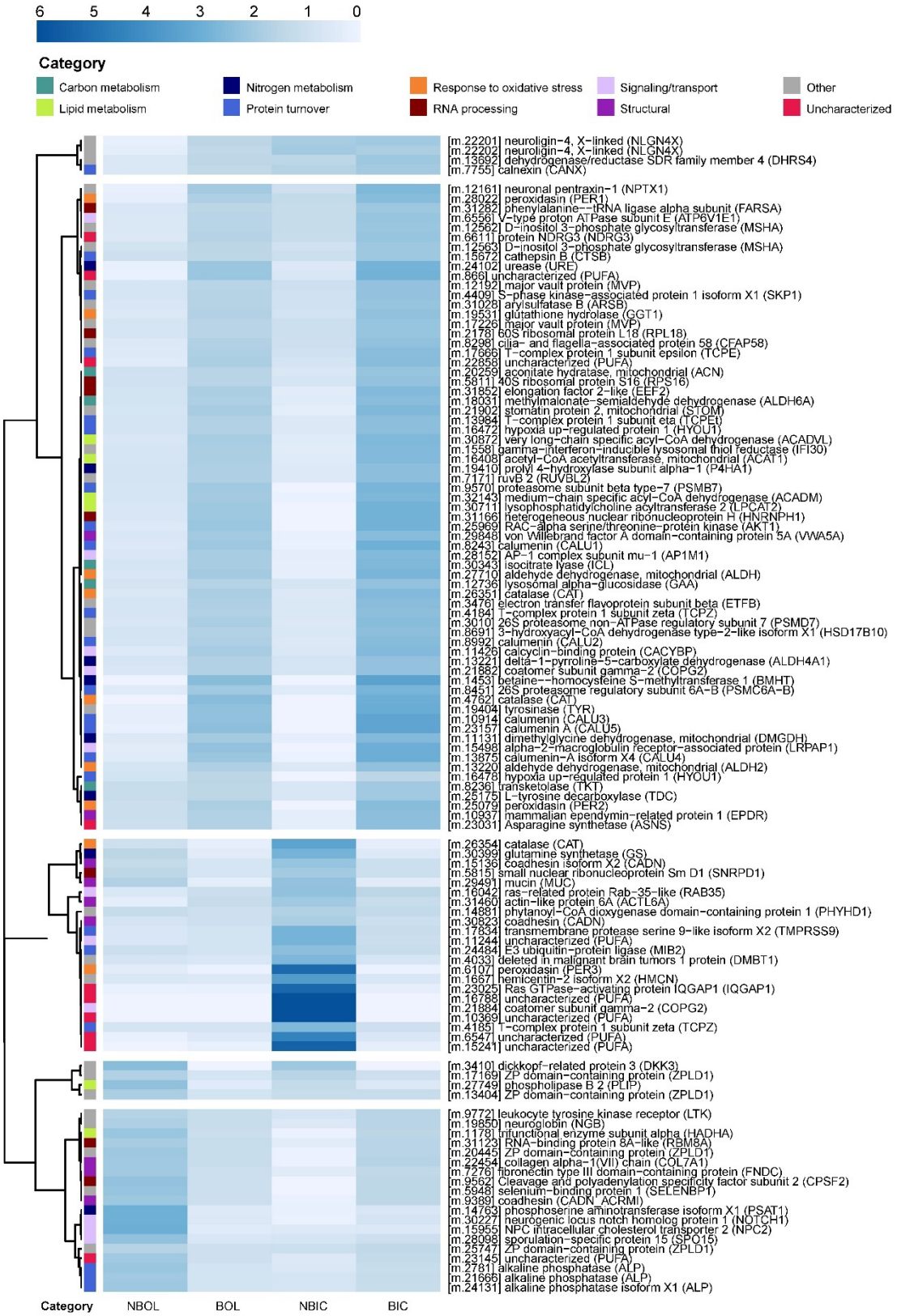
6 5 4 3 2 1 0
Category
Carbon metabolism
Nitrogen metabolism
Response to oxidative stress
Signaling/transport
Other
Lipid metabolism
Protein turnover
RNA processing
Structural
Uncharacterized
[m.22201] neuroligin−4, X−linked (NLGN4X)
[m.22202] neuroligin−4, X−linked (NLGN4X)
[m.13692] dehydrogenase/reductase SDR family member 4 (DHRS4)
[m.7755] calnexin (CANX)
[m.12161] neuronal pentraxin−1 (NPTX1)
[m.28022] peroxidasin (PER1)
[m.31282] phenylalanine−−tRNA ligase alpha subunit (FARSA)
[m.6556] V−type proton ATPase subunit E (ATP6V1E1)
[m.12562] D−inositol 3−phosphate glycosyltransferase (MSHA)
[m.6611] protein NDRG3 (NDRG3)
[m.12563] D−inositol 3−phosphate glycosyltransferase (MSHA)
[m.15672] cathepsin B (CTSB)
[m.24102] urease (URE)
[m.866] uncharacterized (PUFA)
[m.12192] major vault protein (MVP)
[m.4409] S−phase kinase−associated protein 1 isoform X1 (SKP1)
[m.31028] arylsulfatase B (ARSB)
[m.19531] glutathione hydrolase (GGT1)
[m.17226] major vault protein (MVP)
[m.2178] 60S ribosomal protein L18 (RPL18)
[m.8298] cilia− and flagella−associated protein 58 (CFAP58)
[m.17666] T−complex protein 1 subunit epsilon (TCPE)
[m.22858] uncharacterized (PUFA)
[m.20259] aconitate hydratase, mitochondrial (ACN)
[m.5811] 40S ribosomal protein S16 (RPS16)
[m.31852] elongation factor 2−like (EEF2)
[m.18031] methylmalonate−semialdehyde dehydrogenase (ALDH6A)
[m.21902] stomatin protein 2, mitochondrial (STOM)
[m.13954] T−complex protein 1 subunit eta (TCPE1)
[m.16472] hypoxia up−regulated protein 1 (HYOU1)
[m.30872] very long−chain specific acyl−CoA dehydrogenase (ACADVL)
[m.1558] gamma−interferon−inducible lysosomal thiol reductase (IFI30)
[m.16408] acetyl−CoA acetyltransferase, mitochondrial (ACAT1)
[m.19410] prolyl 4−hydroxylase subunit alpha−1 (P4HA1)
[m.7171] ruvB 2 (RUVBL2)
[m.9570] proteasome subunit beta type−7 (PSMB7)
[m.32143] medium−chain specific acyl−CoA dehydrogenase (ACADM)
[m.30711] lysophosphatidylcholine acyltransferase 2 (LPCAT2)
[m.31166] heterogeneous nuclear ribonucleoprotein H (HNRNPH1)
[m.25969] RAC−alpha serine/threonine−protein kinase (AKT1)
[m.29848] von Willebrand factor A domain−containing protein 5A (VWA5A)
[m.8243] calumenin (CALU1)
[m.28152] AP−1 complex subunit mu−1 (AP1M1)
[m.30343] isocitrate lyase (ICL)
[m.27710] aldehyde dehydrogenase, mitochondrial (ALDH)
[m.12736] lysosomal alpha−glucosidase (GAA)
[m.26351] catalase (CAT)
[m.3476] electron transfer flavoprotein subunit beta (ETFB)
[m.4184] T−complex protein 1 subunit zeta (TCPZ)
[m.3010] 26S proteasome non−ATPase regulatory subunit 7 (PSMD7)
[m.8691] 3−hydroxyacyl−CoA dehydrogenase type−2−like isoform X1 (HSD17B10)
[m.8992] calumenin (CALU2)
[m.11426] calcyclin−binding protein (CACYBP)
[m.13221] delta−1−pyrroline−5−carboxylate dehydrogenase (ALDH4A1)
[m.21882] coatomer subunit gamma−2 (COPG2)
[m.1453] betaine−−homocysteine S−methyltransferase 1 (BMHT)
[m.8451] 26S proteasome regulatory subunit 6A−B (PSMC6A−B)
[m.4762] catalase (CAT)
[m.19404] tyrosinase (TYR)
[m.10914] calumenin (CALU3)
[m.23157] calumenin A (CALU5)
[m.11131] dimethylglycine dehydrogenase, mitochondrial (DMGDH)
[m.15498] alpha−2−macroglobulin receptor−associated protein (LRPAP1)
[m.13875] calumenin−A isoform X4 (CALU4)
[m.13220] aldehyde dehydrogenase, mitochondrial (ALDH2)
[m.16478] hypoxia up−regulated protein 1 (HYOU1)
[m.8236] transketolase (TKT)
[m.25175] L−tyrosine decarboxylase (TDC)
[m.25079] peroxidasin (PER2)
[m.10937] mammalian ependymin−related protein 1 (EPDR)
[m.23031] Asparagine synthetase (ASNS)
[m.26354] catalase (CAT)
[m.30399] glutamine synthetase (GS)
[m.15136] coadhesin isoform X2 (CADN)
[m.5815] small nuclear ribonucleoprotein Sm D1 (SNRPD1)
[m.29491] mucin (MUC)
[m.16042] ras−related protein Rab−35−like (RAB35)
[m.31460] actin−like protein 6A (ACTL6A)
[m.14881] phytanoyl−CoA dioxygenase domain−containing protein 1 (PHYHD1)
[m.30823] coadhesin (CADN)
[m.17834] transmembrane protease serine 9−like isoform X2 (TMPRSS9)
[m.11244] uncharacterized (PUFA)
[m.24484] E3 ubiquitin−protein ligase (MIB2)
[m.4033] deleted in malignant brain tumors 1 protein (DMBT1)
[m.6107] peroxidasin (PER3)
[m.1657] hemicentin−2 isoform X2 (HMCN)
[m.23025] Ras GTPase−activating protein IQGAP1 (IQGAP1)
[m.1678] uncharacterized (PUFA)
[m.21884] coatomer subunit gamma−2 (COPG2)
[m.10369] uncharacterized (PUFA)
[m.4185] T−complex protein 1 subunit zeta (TCPZ)
[m.6547] uncharacterized (PUFA)
[m.15241] uncharacterized (PUFA)
[m.3410] dickkopf−related protein 3 (DKK3)
[m.17169] ZP domain−containing protein (ZPLD1)
[m.27749] phospholipase B 2 (PLIP)
[m.13404] ZP domain−containing protein (ZPLD1)
[m.9772] leukocyte tyrosine kinase receptor (LTK)
[m.19850] neuroglobin (NGB)
[m.1178] trifunctional enzyme subunit alpha (HADHA)
[m.31123] RNA−binding protein 8A−like (RBM8A)
[m.20445] ZP domain−containing protein (ZPLD1)
[m.22454] collagen alpha−1(VII) chain (COL7A1)
[m.7276] fibronectin type III domain−containing protein (FNDC)
[m.9562] Cleavage and polyadenylation specificity factor subunit 2 (CPSF2)
[m.5948] selenium−binding protein 1 (SELENBP1)
[m.9389] coadhesin (CADN_ACRMI)
[m.14763] phosphoserine aminotransferase isoform X1 (PSAT1)
[m.30227] neurogenic locus notch homolog protein 1 (NOTCH1)
[m.15955] NPC intracellular cholesterol transporter 2 (NPC2)
[m.28098] sporulation−specific protein 15 (SPO15)
[m.25747] ZP domain−containing protein (ZPLD1)
[m.23145] uncharacterized (PUFA)
[m.2781] alkaline phosphatase (ALP)
[m.21666] alkaline phosphatase (ALP)
[m.24131] alkaline phosphatase isoform X1 (ALP)
Category
NBOL
BOL
NBIC
BIC

Figure 1.6 Heatmap of differentially abundant proteins in non-bleached and bleached *Montipora capitata* outer layer (OL) tissue and inner core (IC) intra-skeletal tissue and skeleton. Cell shading represents the mean NSAF value for each treatment normalized by the row mean. Rows are clustered using the "correlation" method of the pheatmap function in R. The dendrogram was set to cut 5 distinct clusters. The row annotations (categories) represent broad biological function categories based on GO and KEGG terms associated with each protein. NBOL = non-bleached outer layer; BOL = bleached outer layer; NBIC = non-bleached inner core; BIC = bleached inner core.

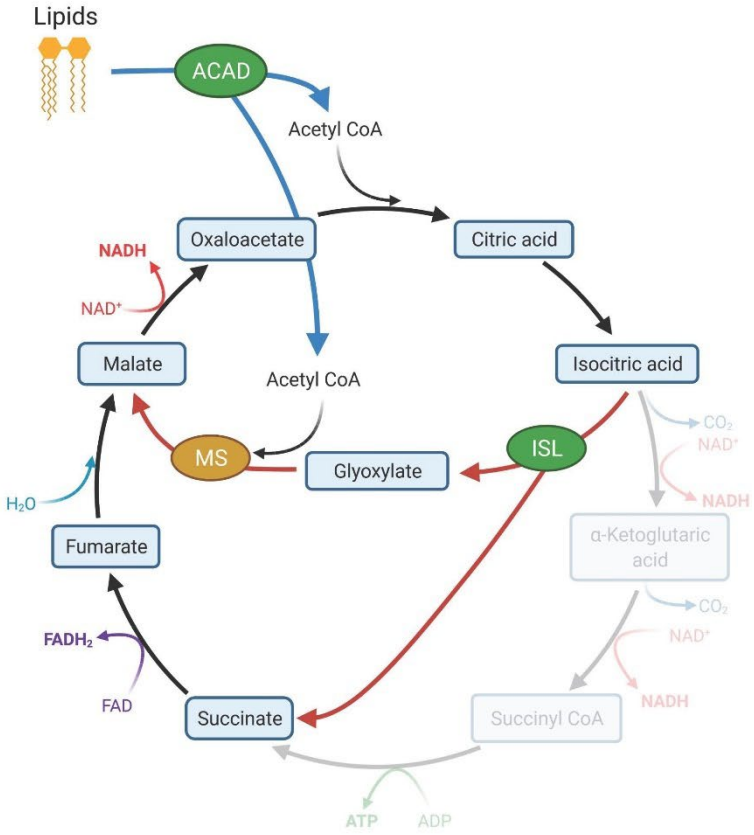

Figure 1.7 Lipid degradation and the glyoxylate cycle. Increased abundance of acyl-CoA dehydrogenases (ACAD) in the outer layer (OL) tissue of bleached coral indicated the breakdown of lipids that produce acetyl CoA (blue arrows). Acetyl CoA is the primary source of carbon in the glyoxylate cycle (red arrows). The glyoxylate cycle, a modified version of the Kreb's cycle (black arrows), utilizes isocitrate lyase (ISL) and malate synthetase (MS) and can produce additional intermediate molecules of the Krebs cycle that can be used to generate glucose. ISL was significantly elevated in the OL of bleached corals while MS was elevated but not significantly. Created with BioRender.com

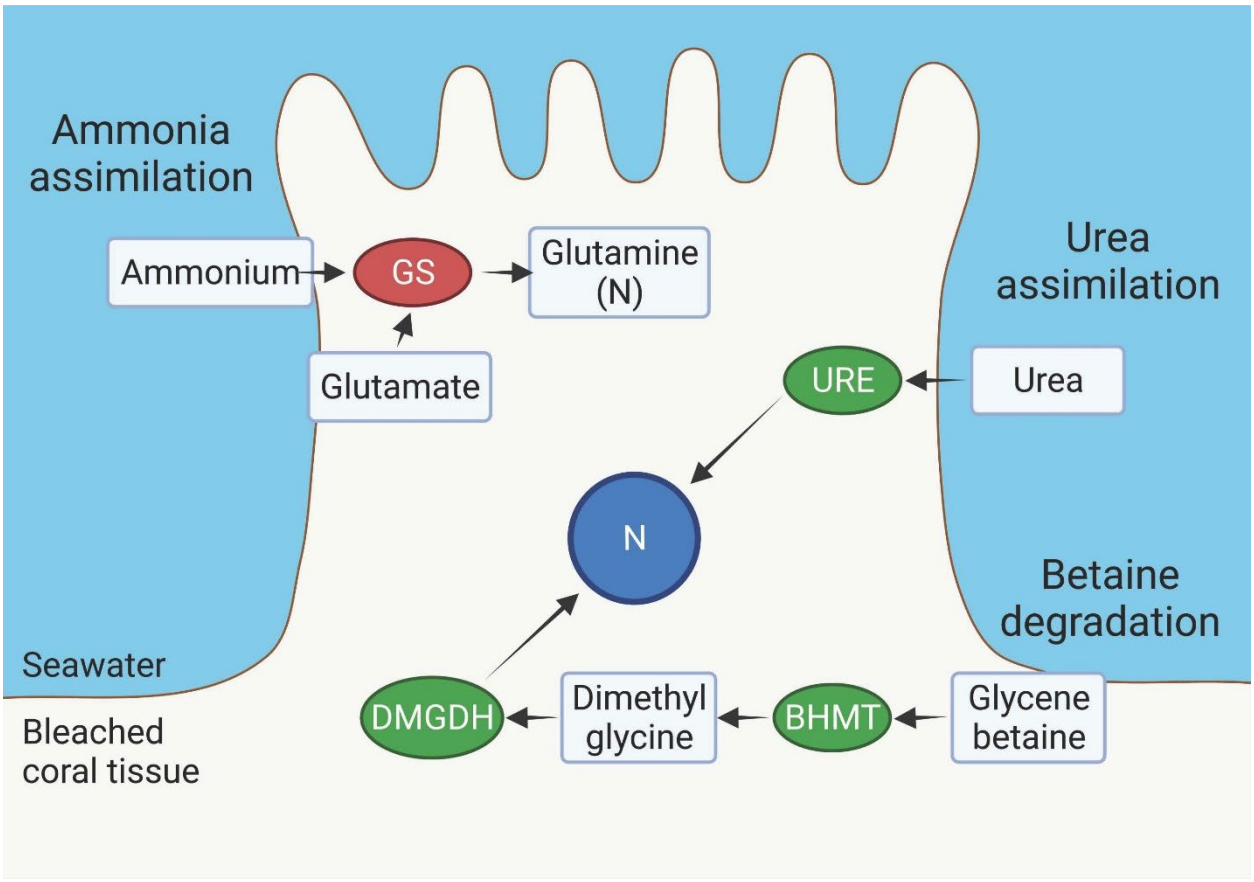

Figure 1.8 Nitrogen (N) source pathways in the outer layer (OL) tissue of bleached *Montipora capitata*. Decreased abundance of glutamine synthetase (GS) suggests a decrease in ammonium assimilation from surrounding seawater. An increased abundance of urease (URE) suggests an increase in assimilation of urea from surrounding seawater that is broken down by URE to ammonia and carbon dioxide. Increased abundances of dimethylglycine dehydrogenase (DMGDH) and betaine--homocysteine S-methyltransferase (BHMT) indicate an increase in the betaine degradation pathway. Created with BioRender.com

1.8 REFERENCES

Aguilar, C., Raina, J.-B., Fôret, S., Hayward, D. C., Lapeyre, B., Bourne, D. G., et al. (2019). Transcriptomic analysis reveals protein homeostasis breakdown in the coral *Acropora millepora* during hypo-saline stress. *BMC Genomics* 20, 148. doi:10.1186/s12864-019-5527-2.

Atkinson, M. J., Kotler, E., and Newton, P. (1994). Effects of Water Velocity on Respiration, Calcification, and Ammonium Uptake of a *Porites compressa* Community. *Pac. Sci.* 48, 296–303.

Bachhawat, A. K., and Yadav, S. (2018). The glutathione cycle: Glutathione metabolism beyond the γ-glutamyl cycle. *IUBMB Life* 70, 585–592. doi:10.1002/iub.1756.

Baird, A. H., and Marshall, P. A. (2002). Mortality, growth and reproduction in scleractinian corals following bleaching on the Great Barrier Reef. *Mar. Ecol. Prog. Ser.* 237, 133–141. doi:10.3354/meps237133.

Barshis, D. J., Ladner, J. T., Oliver, T. A., Seneca, F. O., Traylor-Knowles, N., and Palumbi, S. R. (2013). Genomic basis for coral resilience to climate change. *Proc. Natl. Acad. Sci.* 110, 1387–1392. doi:10.1073/pnas.1210224110.

Bellantuono, A. J., Granados-Cifuentes, C., Miller, D. J., Hoegh-Guldberg, O., and Rodriguez-Lanetty, M. (2012). Coral Thermal Tolerance: Tuning Gene Expression to Resist Thermal Stress. *PLOS ONE* 7, e50685. doi:10.1371/journal.pone.0050685.

Black, N. A., Voellmy, R., and Szmant, A. M. (1995). Heat Shock Protein Induction in *Montastraea faveolata* and *Aiptasia pallida* Exposed to Elevated Temperatures. *Biol. Bull.* 188, 234–240. doi:10.2307/1542301.

Brown, B., Downs, C., Dunne, R., and Gibb, S. (2002). Exploring the basis of thermotolerance in the reef coral *Goniastrea aspera*. *Mar. Ecol. Prog. Ser.* 242, 119–129. doi:10.3354/meps242119.

Brown, B. E., Le Tissier, M. D. A., and Dunne, R. P. (1994). Tissue retraction in the scleractinian coral *Coeloseris mayeri*, its effect upon coral pigmentation, and preliminary implications for heat balance. *Mar. Ecol. Prog. Ser.* 105, 209–218.

Cantin, N. E., Cohen, A. L., Karnauskas, K. B., Tarrant, A. M., and McCorkle, D. C. (2010). Ocean Warming Slows Coral Growth in the Central Red Sea. *Science* 329, 322–325. doi:10.1126/science.1190182.

Chakravarti, L. J., Buerger, P., Levin, R. A., and van Oppen, M. J. H. (2020). Gene regulation underpinning increased thermal tolerance in a laboratory-evolved coral photosymbiont. *Mol. Ecol.* 29, 1684–1703. doi:10.1111/mec.15432.

Choi, H., Kim, S., Fermin, D., Tsou, C.-C., and Nesvizhskii, A. I. (2015). QPROT: Statistical method for testing differential expression using protein-level intensity data in label-free quantitative proteomics. *J. Proteomics* 129, 121–126. doi:10.1016/j.jprot.2015.07.036.

Conover, R., and Gustavson, K. (1999). Sources of urea in arctic seas: zooplankton metabolism. *Mar. Ecol. Prog. Ser.* 179, 41–54. doi:10.3354/meps179041.

Cox, E. F. (2007). Continuation of sexual reproduction in *Montipora capitata* following bleaching. *Coral Reefs* 26, 721–724. doi:10.1007/s00338-007-0251-9.

Crandall, J. B., and Teece, M. A. (2012). Urea is a dynamic pool of bioavailable nitrogen in coral reefs. *Coral Reefs* 31, 207–214. doi:10.1007/s00338-011-0836-1.

Cziesielski, M. J., Schmidt-Roach, S., and Aranda, M. (2019). The past, present, and future of coral heat stress studies. *Ecol. Evol.* 9, 10055–10066. doi:10.1002/ece3.5576.

Cziesielski, M. J., Liew, Y. J., Cui, G., Schmidt-Roach, S., Campana, S., Marondedze, C., et al. (2018). Multi-omics analysis of thermal stress response in a zooxanthellate cnidarian reveals the importance of associating with thermotolerant symbionts. *Proc. R. Soc. B Biol. Sci.* 285, 20172654. doi:10.1098/rspb.2017.2654.

Dauphin, Y. (2001). Comparative studies of skeletal soluble matrices from some Scleractinian corals and Molluscs. *Int. J. Biol. Macromol.* 28, 293–304. doi:10.1016/S0141-8130(01)00124-6.

D'Elia, C. F., Domotor, S. L., and Webb, K. L. (1983). Nutrient uptake kinetics of freshly isolated zooxanthellae. *Mar. Biol.* 75, 157–167. doi:10.1007/BF00405998.

DeSalvo, M. K., Estrada, A., Sunagawa, S., and Medina, M. (2012). Transcriptomic responses to darkness stress point to common coral bleaching mechanisms. *Coral Reefs* 31, 215–228. doi:10.1007/s00338-011-0833-4.

DeSalvo, M. K., Voolstra, C. R., Sunagawa, S., Schwarz, J. A., Stillman, J. H., Coffroth, M. A., et al. (2008). Differential gene expression during thermal stress and bleaching in the Caribbean coral *Montastraea faveolata*. *Mol. Ecol.* 17, 3952–3971. doi:10.1111/j.1365-294X.2008.03879.x.

DeSalvo, M., Sunagawa, S., Voolstra, C., and Medina, M. (2010). Transcriptomic responses to heat stress and bleaching in the elkhorn coral *Acropora palmata*. *Mar. Ecol. Prog. Ser.* 402, 97–113. doi:10.3354/meps08372.

Downs, C. A., Fauth, J. E., Halas, J. C., Dustan, P., Bemiss, J., and Woodley, C. M. (2002). Oxidative stress and seasonal coral bleaching. *Free Radic. Biol. Med.* 33, 533–543. doi:10.1016/S0891-5849(02)00907-3.

Drake, J. L., Mass, T., Haramaty, L., Zelzion, E., Bhattacharya, D., and Falkowski, P. G. (2013). Proteomic analysis of skeletal organic matrix from the stony coral *Stylophora pistillata*. *Proc. Natl. Acad. Sci.* 110, 3788–3793. doi:10.1073/pnas.1301419110.

Eng, J. K., Jahan, T. A., and Hoopmann, M. R. (2013). Comet: An open-source MS/MS sequence database search tool. *Proteomics* 13, 22–24. doi:10.1002/pmic.201200439.

Fermin, D., Basrur, V., Yocum, A. K., and Nesvizhskii, A. I. (2011). Abacus: A computational tool for extracting and pre-processing spectral count data for label-free quantitative proteomic analysis. *Proteomics* 11, 1340–1345. doi:10.1002/pmic.201000650.

Ferrier-Pagès, C., Rottier, C., Beraud, E., and Levy, O. (2010). Experimental assessment of the feeding effort of three scleractinian coral species during a thermal stress: Effect on the rates of photosynthesis. *J. Exp. Mar. Biol. Ecol.* 390, 118–124. doi:10.1016/j.jembe.2010.05.007.

Fonseca, da S. J., Marangoni, de B. L. F., Marques, J. A., and Bianchini, A. (2019). Energy metabolism enzymes inhibition by the combined effects of increasing temperature and copper exposure in the coral *Mussismilia harttii*. *Chemosphere* 236, 124420. doi:10.1016/j.chemosphere.2019.124420.

Frazier, M., Helmkampf, M., Bellinger, M. R., Geib, S. M., and Takabayashi, M. (2017). De novo metatranscriptome assembly and coral gene expression profile of *Montipora capitata* with growth anomaly. *BMC Genomics* 18, 710. doi:10.1186/s12864-017-4090-y.

Garcia, G. D., Santos, E. de O., Sousa, G. V., Zingali, R. B., Thompson, C. C., and Thompson, F. L. (2016). Metaproteomics reveals metabolic transitions between healthy and diseased stony coral *Mussismilia braziliensis*. *Mol. Ecol.* 25, 4632–4644. doi:10.1111/mec.13775.

Gardner, S. G., Raina, J.-B., Nitschke, M. R., Nielsen, D. A., Stat, M., Motti, C. A., et al. (2017). A multi-trait systems approach reveals a response cascade to bleaching in corals. *BMC Biol.* 15, 117. doi:10.1186/s12915-017-0459-2.

Gates, R. D., and Edmunds, P. J. (1999). The Physiological Mechanisms of Acclimatization in Tropical Reef Corals. *Am. Zool.* 39, 30–43. doi:10.1093/icb/39.1.30.

Gestaut, D., Limatola, A., Joachimiak, L., and Frydman, J. (2019). The ATP-powered gymnastics of TRiC/CCT: an asymmetric protein folding machine with a symmetric origin story. *Curr. Opin. Struct. Biol.* 55, 50–58. doi:10.1016/j.sbi.2019.03.002.

Gladfelter, E. H. (1983). Circulation of fluids in the gastrovascular system of the reef coral *Acropora cervicornis*. *Biol. Bull.* 165, 619–636. doi:10.2307/1541469.

Glibert, P. M., Harrison, J., Heil, C., and Seitzinger, S. (2006). Escalating Worldwide use of Urea – A Global Change Contributing to Coastal Eutrophication. *Biogeochemistry* 77, 441–463. doi:10.1007/s10533-005-3070-5.

Grottoli, A. G., and Rodrigues, L. J. (2011). Bleached *Porites compressa* and *Montipora capitata* corals catabolize δ13C-enriched lipids. *Coral Reefs* 30, 687. doi:10.1007/s00338-011-0756-0.

Grottoli, A. G., Rodrigues, L. J., and Palardy, J. E. (2006). Heterotrophic plasticity and resilience in bleached corals. *Nature* 440, 1186–1189. doi:10.1038/nature04565.

Grover, R., Maguer, J.-F., Allemand, D., and Ferrier-Pagès, C. (2006). Urea uptake by the scleractinian coral *Stylophora pistillata*. *J. Exp. Mar. Biol. Ecol.* 332, 216–225. doi:10.1016/j.jembe.2005.11.020.

Grover, R., Maguer, J.-F., Allemand, D., and Ferrier-Pages, C. (2008). Uptake of dissolved free amino acids by the scleractinian coral *Stylophora pistillata*. *J. Exp. Biol.* 211, 860–865. doi:10.1242/jeb.012807.

Gygi, S. P., Rochon, Y., Franza, B. R., and Aebersold, R. (1999). Correlation between Protein and mRNA Abundance in Yeast. *Mol. Cell. Biol.* 19, 1720–1730. doi:10.1128/MCB.19.3.1720.

Haas, B. J., Papanicolaou, A., Yassour, M., Grabherr, M., Blood, P. D., Bowden, J., et al. (2013). De novo transcript sequence reconstruction from RNA-Seq: reference generation and analysis with Trinity. *Nat. Protoc.* 8, 10.1038/nprot.2013.084. doi:10.1038/nprot.2013.084.

Hawkins, A. J. S. (1991). Protein Turnover: A Functional Appraisal. *Funct. Ecol.* 5, 222. doi:10.2307/2389260.

Hernández-Elizárraga, V. H., Olguín-López, N., Hernández-Matehuala, R., Ocharán-Mercado, A., Cruz-Hernández, A., Guevara-González, R. G., et al. (2019). Comparative Analysis of the Soluble Proteome and the Cytolytic Activity of Unbleached and Bleached *Millepora complanata* ("Fire Coral") from the Mexican Caribbean. *Mar. Drugs* 17, 393. doi:10.3390/md17070393.

Hoegh-Guldberg, O., and Williamson, J. (1999). Availability of two forms of dissolved nitrogen to the coral *Pocillopora damicornis* and its symbiotic zooxanthellae. *Mar. Biol.* 133, 561–570. doi:10.1007/s002270050496.

Hughes, A. D., and Grottoli, A. G. (2013). Heterotrophic Compensation: A Possible Mechanism for Resilience of Coral Reefs to Global Warming or a Sign of Prolonged Stress? *PLoS ONE* 8, e81172. doi:10.1371/journal.pone.0081172.

Isa, Y., and Okazaki, M. (1987). Some observations on the Ca2+-binding phospholipid from scleractinian coral skeletons. *Comp. Biochem. Physiol. Part B Comp. Biochem.* 87, 507–512. doi:https://doi.org/10.1016/0305-0491(87)90045-9.

Jahn, M. P., Cavagni, G. M., Kaiser, D., and Kucharski, L. C. (2006). Osmotic effect of choline and glycine betaine on the gills and hepatopancreas of the *Chasmagnathus granulata* crab submitted to hyperosmotic stress. *J. Exp. Mar. Biol. Ecol.* 334, 1–9. doi:10.1016/j.jembe.2006.01.006.

Jeffrey, S. W., and Humphrey, G. F. (1975). New spectrophotometric equations for determining chlorophylls *a*, *b*, *c1* and *c2* in higher plants, algae and natural phytoplankton. *Biochem. Physiol. Pflanz.* 167, 191–194. doi:10.1016/S0015-3796(17)30778-3.

Jokiel, P. L., Hunter, C. L., Taguchi, S., and Watarai, L. (1993). Ecological impact of a fresh-water "reef kill" in Kaneohe Bay, Oahu, Hawaii. *Coral Reefs* 12, 177–184. doi:10.1007/BF00334477.

Jones, A. M., Berkelmans, R., van Oppen, M. J. H., Mieog, J. C., and Sinclair, W. (2008). A community change in the algal endosymbionts of a scleractinian coral following a natural bleaching event: field evidence of acclimatization. *Proc. R. Soc. B Biol. Sci.* 275, 1359–1365. doi:10.1098/rspb.2008.0069.

Kanehisa, M., and Goto, S. (2000). KEGG: Kyoto Encyclopedia of Genes and Genomes. *Nucleic Acids Res.* 28, 27–30. doi:10.1093/nar/28.1.27.

Kanehisa, M., Sato, Y., and Morishima, K. (2016). BlastKOALA and GhostKOALA: KEGG Tools for Functional Characterization of Genome and Metagenome Sequences. *J. Mol. Biol.* 428, 726–731. doi:10.1016/j.jmb.2015.11.006.

Keller, A., Nesvizhskii, A. I., Kolker, E., and Aebersold, R. (2002). Empirical Statistical Model To Estimate the Accuracy of Peptide Identifications Made by MS/MS and Database Search. *Anal. Chem.* 74, 5383–5392. doi:10.1021/ac025747h.

Kenkel, C. D., Meyer, E., and Matz, M. V. (2013). Gene expression under chronic heat stress in populations of the mustard hill coral (*Porites astreoides*) from different thermal environments. *Mol. Ecol.* 22, 4322–4334. doi:10.1111/mec.12390.

Kornberg, H. L., and Krebs, H. A. (1957). Synthesis of Cell Constituents from C_2-Units by a Modified Tricarboxylic Acid Cycle. *Nature* 179, 988–991. doi:10.1038/179988a0.

Krueger, T., Hawkins, T. D., Becker, S., Pontasch, S., Dove, S., Hoegh-Guldberg, O., et al. (2015). Differential coral bleaching—Contrasting the activity and response of enzymatic antioxidants in symbiotic partners under thermal stress. *Comp. Biochem. Physiol. A. Mol. Integr. Physiol.* 190, 15–25. doi:10.1016/j.cbpa.2015.08.012.

Krupp, D. A., Jokiel, P. L., and Chartrand, T. S. (1992). Asexual reproduction by the solitary scleractinian coral *Fungia scutaria* on dead parent coralla in Kaneohe Bay, Oahu, Hawaiian Islands. *7th Int. Coral Reef Guam Univ. Guam Press RH Richmond* 1, 527–534.

Ladd, M. C., Shantz, A. A., Bartels, E., and Burkepile, D. E. (2017). Thermal stress reveals a genotype-specific tradeoff between growth and tissue loss in restored *Acropora cervicornis*. *Mar. Ecol. Prog. Ser.* 572, 129–139. doi:10.3354/meps12169.

Lee, J. H., Kwon, E. J., and Kim, D. H. (2013). Calumenin has a role in the alleviation of ER stress in neonatal rat cardiomyocytes. *Biochem. Biophys. Res. Commun.* 439, 327–332. doi:10.1016/j.bbrc.2013.08.087.

Lesser, M. P. (1997). Oxidative stress causes coral bleaching during exposure to elevated temperatures. *Coral Reefs* 16, 187–192. doi:10.1007/s003380050073.

Lesser, M. P., Stochaj, W. R., Tapley, D. W., and Shick, J. M. (1990). Bleaching in coral reef anthozoans: effects of irradiance, ultraviolet radiation, and temperature on the activities of protective enzymes against active oxygen. *Coral Reefs* 8, 225–232. doi:10.1007/BF00265015.

Lipschultz, F., and Cook, C. (2002). Uptake and assimilation of 15N-ammonium by the symbiotic sea anemones *Bartholomea annulata* and *Aiptasia pallida*: conservation versus recycling of nitrogen. *Mar. Biol.* 140, 489–502. doi:10.1007/s00227-001-0717-1.

Lomas, M. W., Mark Trice, T., Glibert, P. M., Bronk, D. A., and McCarthy, J. J. (2002). Temporal and spatial dynamics of urea uptake and regeneration rates and concentrations in Chesapeake Bay. *Estuaries* 25, 469–482. doi:10.1007/BF02695988.

MacLean, B., Tomazela, D. M., Shulman, N., Chambers, M., Finney, G. L., Frewen, B., et al. (2010). Skyline: an open source document editor for creating and analyzing targeted proteomics experiments. *Bioinforma. Oxf. Engl.* 26, 966–968. doi:10.1093/bioinformatics/btq054.

Maier, T., Güell, M., and Serrano, L. (2009). Correlation of mRNA and protein in complex biological samples. *FEBS Lett.* 583, 3966–3973. doi:10.1016/j.febslet.2009.10.036.

Mailloux, R. J., McBride, S. L., and Harper, M.-E. (2013). Unearthing the secrets of mitochondrial ROS and glutathione in bioenergetics. *Trends Biochem. Sci.* 38, 592–602. doi:10.1016/j.tibs.2013.09.001.

Maor-Landaw, K., Karako-Lampert, S., Ben-Asher, H. W., Goffredo, S., Falini, G., Dubinsky, Z., et al. (2014). Gene expression profiles during short-term heat stress in the red sea coral *Stylophora pistillata*. *Glob. Change Biol.* 20, 3026–3035. doi:10.1111/gcb.12592.

Mayfield, A. B., Aguilar, C., Kolodziej, G., Enochs, I. C., and Manzello, D. P. (2021). Shotgun Proteomic Analysis of Thermally Challenged Reef Corals. *Front. Mar. Sci.* 8, 547. doi:10.3389/fmars.2021.660153.

Mayfield, A. B. (2020). Proteomic Signatures of Corals from Thermodynamic Reefs. *Microorganisms* 8, 1171. doi:10.3390/microorganisms8081171.

Mayfield, A. B., Chen, Y.-J., Lu, C.-Y., and Chen, C.-S. (2018). The proteomic response of the reef coral *Pocillopora acuta* to experimentally elevated temperatures. *PLOS ONE* 13, e0192001. doi:10.1371/journal.pone.0192001.

Mayfield, A. B., Wang, Y., Chen, C., Chen, S., and Lin, C. (2016). Dual-compartmental transcriptomic + proteomic analysis of a marine endosymbiosis exposed to environmental change. *Mol. Ecol.* 25, 5944–5958. doi:10.1111/mec.13896.

McDonald, M. D., Smith, C. P., and Walsh, P. J. (2006). The Physiology and Evolution of Urea Transport in Fishes. *J. Membr. Biol.* 212, 93–107. doi:10.1007/s00232-006-0869-5.

Mellacheruvu, D., Wright, Z., Couzens, A. L., Lambert, J.-P., St-Denis, N. A., Li, T., et al. (2013). The CRAPome: a contaminant repository for affinity purification–mass spectrometry data. *Nat. Methods* 10, 730–736. doi:10.1038/nmeth.2557.

Mendes, J., and Woodley, J. (2002). Effect of the 1995-1996 bleaching event on polyp tissue depth, growth, reproduction and skeletal band formation in *Montastraea annularis*. *Mar. Ecol. Prog. Ser.* 235, 93–102. doi:10.3354/meps235093.

Muller, E. M., Bartels, E., and Baums, I. B. (2018). Bleaching causes loss of disease resistance within the threatened coral species *Acropora cervicornis*. *eLife* 7, e35066. doi:10.7554/eLife.35066.

Muscatine, L., R. McCloskey, L., and E. Marian, R. (1981). Estimating the daily contribution of carbon from zooxanthellae to coral animal respiration. *Limnol. Oceanogr.* 26, 601–611. doi:10.4319/lo.1981.26.4.0601.

Nesvizhskii, A. I., Keller, A., Kolker, E., and Aebersold, R. (2003). A Statistical Model for Identifying Proteins by Tandem Mass Spectrometry. *Anal. Chem.* 75, 4646–4658. doi:10.1021/ac0341261.

Ngugi, D. K., Ziegler, M., Duarte, C. M., and Voolstra, C. R. (2020). Genomic Blueprint of Glycine Betaine Metabolism in Coral Metaorganisms and Their Contribution to Reef Nitrogen Budgets. *iScience* 23, 101120. doi:10.1016/j.isci.2020.101120.

NOAA Coral Reef Watch (2018). NOAA Coral Reef Watch Virtual Station for the Main Hawaiian Islands, Jan. 1, 2007-Dec. 31, 2017. College Park, Maryland, USA.

Nunn, B. L., Slattery, K. V., Cameron, K. A., Timmins-Schiffman, E., and Junge, K. (2015). Proteomics of *Colwellia psychrerythraea* at subzero temperatures - a life with limited movement, flexible membranes and vital DNA repair: Proteomics of microbes at subzero temperatures. *Environ. Microbiol.* 17, 2319–2335. doi:10.1111/1462-2920.12691.

Oakley, C. A., Durand, E., Wilkinson, S. P., Peng, L., Weis, V. M., Grossman, A. R., et al. (2017). Thermal Shock Induces Host Proteostasis Disruption and Endoplasmic Reticulum Stress in the Model Symbiotic Cnidarian *Aiptasia*. *J. Proteome Res.* 16, 2121–2134. doi:10.1021/acs.jproteome.6b00797.

Oakley, C. A., Ameismeier, M. F., Peng, L., Weis, V. M., Grossman, A. R., and Davy, S. K. (2016). Symbiosis induces widespread changes in the proteome of the model cnidarian *Aiptasia*. *Cell. Microbiol.* 18, 1009–1023. doi:10.1111/cmi.12564.

Oksanen, J., Blanchet, F. G., Friendly, M., Kindt, R., Legendre, P., McGlinn, D., et al. (2020). *vegan: Community Ecology Package*. Available at: https://CRAN.R-project.org/package=vegan [Accessed February 11, 2021].

Ou, W.-J., Cameron, P. H., Thomas, D. Y., and Bergeron, J. J. M. (1993). Association of folding intermediates of glycoproteins with calnexin during protein maturation. *Nature* 364, 771–776. doi:10.1038/364771a0.

Pandey, A., and Mann, M. (2000). Proteomics to study genes and genomes. *Nature* 405, 837–846. doi:10.1038/35015709.

Pearse, V. B., and Muscatine, L. (1971). Role of symbiotic algae (zooxanthellae) in coral calcification. *Biol. Bull.* 141, 350–363. doi:10.2307/1540123.

Pernice, M., Meibom, A., Van Den Heuvel, A., Kopp, C., Domart-Coulon, I., Hoegh-Guldberg, O., et al. (2012). A single-cell view of ammonium assimilation in coral–dinoflagellate symbiosis. *ISME J.* 6, 1314–1324. doi:10.1038/ismej.2011.196.

Petrou, K., Nunn, B. L., Padula, M. P., Miller, D. J., and Nielsen, D. A. (2021). Broad scale proteomic analysis of heat-destabilised symbiosis in the hard coral *Acropora millepora*. *Sci. Rep.* 11, 19061. doi:10.1038/s41598-021-98548-x.

Polato, N. R., Altman, N. S., and Baums, I. B. (2013). Variation in the transcriptional response of threatened coral larvae to elevated temperatures. *Mol. Ecol.* 22, 1366–1382. doi:10.1111/mec.12163.

Puverel, S., Tambutté, E., Pereira-Mouriès, L., Zoccola, D., Allemand, D., and Tambutté, S. (2005). Soluble organic matrix of two Scleractinian corals: Partial and comparative analysis. *Comp. Biochem. Physiol. B Biochem. Mol. Biol.* 141, 480–487. doi:10.1016/j.cbpc.2005.05.013.

Rädecker, N., Pogoreutz, C., Gegner, H. M., Cárdenas, A., Roth, F., Bougoure, J., et al. (2021). Heat stress destabilizes symbiotic nutrient cycling in corals. *Proc. Natl. Acad. Sci.* 118. doi:10.1073/pnas.2022653118.

Rahav, O., Dubinsky, Z., Achituv, Y., and Falkowski, P. G. (1989). Ammonium metabolism in the zooxanthellate coral, *Stylophora pistillata*. *Proc. R. Soc. Lond. B Biol. Sci.* 236, 325–337. doi:10.1098/rspb.1989.0026.

Ramos-Silva, P., Kaandorp, J., Huisman, L., Marie, B., Zanella-Cléon, I., Guichard, N., et al. (2013). The Skeletal Proteome of the Coral *Acropora millepora*: The Evolution of Calcification by Co-Option and Domain Shuffling. *Mol. Biol. Evol.* 30, 2099–2112. doi:10.1093/molbev/mst109.

Rathinasabapathi, B. (2000). Metabolic Engineering for Stress Tolerance: Installing Osmoprotectant Synthesis Pathways. *Ann. Bot.* 86, 709–716. doi:10.1006/anbo.2000.1254.

Ricaurte, M., Schizas, N. V., Ciborowski, P., and Boukli, N. M. (2016). Proteomic analysis of bleached and unbleached *Acropora palmata*, a threatened coral species of the Caribbean. *Mar. Pollut. Bull.* 107, 224–232. doi:10.1016/j.marpolbul.2016.03.068.

Riffle, M., May, D., Timmins-Schiffman, E., Mikan, M., Jaschob, D., Noble, W., et al. (2017). MetaGOmics: A Web-Based Tool for Peptide-Centric Functional and Taxonomic Analysis of Metaproteomics Data. *Proteomes* 6, 2. doi:10.3390/proteomes6010002.

Ritson-Williams, R., and Gates, R. D. (2020). Coral community resilience to successive years of bleaching in Kāneʻohe Bay, Hawaiʻi. *Coral Reefs* 39, 757–769. doi:10.1007/s00338-020-01944-4.

Roach, T. N. F., Dilworth, J., H., C. M., Jones, A. D., Quinn, R. A., and Drury, C. (2021). Metabolomic signatures of coral bleaching history. *Nat. Ecol. Evol.* 5, 495–503. doi:10.1038/s41559-020-01388-7.

Roberts, J. M., Fixter, L. M., and Davies, P. S. (2001). Ammonium metabolism in the symbiotic sea anemone *Anemonia viridis*. *Hydrobiologia* 461, 25–35. doi:10.1023/A:1012752828587.

Santos, S. R., Toyoshima, J., and Kinzie Iii, R. A. (2009). Spatial and temporal dynamics of symbiotic dinoflagellates (*Symbiodinium*: Dinophyta) in the perforate coral *Montipora capitata*. *Galaxea J. Coral Reef Stud.* 11, 139–147. doi:10.3755/galaxea.11.139.

Schlöder, C., and D'Croz, L. (2004). Responses of massive and branching coral species to the combined effects of water temperature and nitrate enrichment. *J. Exp. Mar. Biol. Ecol.* 313, 255–268. doi:10.1016/j.jembe.2004.08.012.

Seneca, F. O., Forêt, S., Ball, E. E., Smith-Keune, C., Miller, D. J., and van Oppen, M. J. H. (2010). Patterns of Gene Expression in a Scleractinian Coral Undergoing Natural Bleaching. *Mar. Biotechnol.* 12, 594–604. doi:10.1007/s10126-009-9247-5.

Seveso, D., Arrigoni, R., Montano, S., Maggioni, D., Orlandi, I., Berumen, M. L., et al. (2020). Investigating the heat shock protein response involved in coral bleaching across scleractinian species in the central Red Sea. *Coral Reefs* 39, 85–98. doi:10.1007/s00338-019-01878-6.

Sproles, A. E., Oakley, C. A., Matthews, J. L., Peng, L., Owen, J. G., Grossman, A. R., et al. (2019). Proteomics quantifies protein expression changes in a model cnidarian colonised by a thermally tolerant but suboptimal symbiont. *ISME J.* 13, 2334–2345. doi:10.1038/s41396-019-0437-5.

Streamer, M. (1980). Urea and arginine metabolism in the hard coral, *Acropora acuminata*. *Comp. Biochem. Physiol. Part B Comp. Biochem.* 65, 669–674. doi:10.1016/0305-0491(80)90177-7.

Stuhr, M., Blank-Landeshammer, B., Reymond, C. E., Kollipara, L., Sickmann, A., Kucera, M., et al. (2018). Disentangling thermal stress responses in a reef-calcifier and its photosymbionts by shotgun proteomics. *Sci. Rep.* 8, 3524. doi:10.1038/s41598-018-21875-z.

Su, Y., Zhou, Z., and Yu, X. (2018). Possible roles of glutamine synthetase in responding to environmental changes in a scleractinian coral. *Mol. Biol. Rep.* 45, 2115–2124. doi:10.1007/s11033-018-4369-3.

Takeuchi, T., Yamada, L., Shinzato, C., Sawada, H., and Satoh, N. (2016). Stepwise Evolution of Coral Biomineralization Revealed with Genome-Wide Proteomics and Transcriptomics. *PLOS ONE* 11, e0156424. doi:10.1371/journal.pone.0156424.

Tomanek, L. (2014). Proteomics to study adaptations in marine organisms to environmental stress. *J. Proteomics* 105, 92–106. doi:10.1016/j.jprot.2014.04.009.

Traylor-Knowles, N., Rose, N. H., Sheets, E. A., and Palumbi, S. R. (2017). Early Transcriptional Responses during Heat Stress in the Coral *Acropora hyacinthus*. *Biol. Bull.* 232, 91–100. doi:10.1086/692717.

Voolstra, C. R., Schnetzer, J., Peshkin, L., Randall, C. J., Szmant, A. M., and Medina, M. (2009). Effects of temperature on gene expression in embryos of the coral *Montastraea faveolata*. *BMC Genomics* 10, 627. doi:10.1186/1471-2164-10-627.

Wang, J., and Douglas, A. E. (1998). Nitrogen recycling or nitrogen conservation in an alga-invertebrate symbiosis? *J. Exp. Biol.* 201, 2445–2453.

Ward, S., Harrison, P., and Hoegh-Guldberg, O. (2000). Coral bleaching reduces reproduction of scleractinian corals and increases susceptibility to future stress. *Proc. 9th Int. Coral Reef Symp. Bali Indones. 23-27 Oct. 2000*, 7.

Weston, L. A., Bauer, K. M., and Hummon, A. B. (2013). Comparison of bottom-up proteomic approaches for LC-MS analysis of complex proteomes. *Anal. Methods* 5, 4615. doi:10.1039/c3ay40853a.

Wright, R. M., Aglyamova, G. V., Meyer, E., and Matz, M. V. (2015). Gene expression associated with white syndromes in a reef building coral, *Acropora hyacinthus*. *BMC Genomics* 16, 371. doi:10.1186/s12864-015-1540-2.

Wu, C. C., and MacCoss, M. J. (2002). Shotgun proteomics: Tools for the analysis of complex biological systems. *Curr. Opin. Mol. Ther.* 4, 242–250.

Xu, C., Bailly-Maitre, B., and Reed, J. C. (2005). Endoplasmic reticulum stress: cell life and death decisions. *J. Clin. Invest.* 115, 2656–2664. doi:10.1172/JCI26373.

Yam, A. Y., Xia, Y., Lin, H.-T. J., Burlingame, A., Gerstein, M., and Frydman, J. (2008). Defining the TRiC/CCT interactome links chaperonin function to stabilization of newly made proteins with complex topologies. *Nat. Struct. Mol. Biol.* 15, 1255–1262. doi:10.1038/nsmb.1515.

Yellowlees, D., Rees, T. A. V., and Fiti, W. K. (1994). Effect of Ammonium-supplemented Seawater on Glutamine Synthetase and Glutamate Dehydrogenase Activities in Host

Tissue and Zooxanthellae of *Pocillopora damicornis* and on Ammonium Uptake Rates of the Zooxanthellae. *Pac. Sci.* 48, 6.

Yost, D. M., Wang, L.-H., Fan, T.-Y., Chen, C.-S., Lee, R. W., Sogin, E., et al. (2013). Diversity in skeletal architecture influences biological heterogeneity and *Symbiodinium* habitat in corals. *Zoology* 116, 262–269. doi:10.1016/j.zool.2013.06.001.

1.9 SUPPLEMENTARY MATERIALS

The supplementary files associated with this chapter can be found in the Proquest repository associated with this dissertation.

Chapter 2. MICROPLASTICS INGESTION AND HETEROTROPHY IN THERMALLY STRESSED CORALS

Publication history: This study was co-authored with Jacqueline Padilla-Gamiño. At the time this dissertation was published, a version of this chapter was published in Scientific Reports

2.1 ABSTRACT

Rising sea temperatures and increasing pollution threaten the fate of coral reefs and millions of people who depend on them. Some reef-building corals respond to thermal stress and subsequent bleaching with increases in heterotrophy, which may increase the risk of ingesting microplastics. Whether this heterotrophic plasticity affects microplastics ingestion or whether ingesting microplastics affects heterotrophic feeding in corals is unknown. To determine this, two coral species, *Montipora capitata* and *Pocillopora damicornis*, were exposed to ambient (~27 °C) and increased (~30 °C) temperature and then fed microplastics, *Artemia* nauplii, or both. Following thermal stress, both species significantly reduced feeding on *Artemia* but no significant decrease in microplastics ingestion was observed. Interestingly, *P. damicornis* only ingested microplastics when *Artemia* were also present, providing evidence that microplastics are not selectively ingested by this species and are only incidentally ingested when food is available. As the first study to examine microplastics ingestion following thermal stress in corals, our results highlight the variability in the risk of microplastics ingestion among species and the importance of considering multiple drivers to project how corals will be affected by global change.

2.2 INTRODUCTION

Reef building corals (Scleractinia) are increasingly challenged by a suite of anthropogenic stressors including pollution and rising sea temperatures due to climate change (Hoegh-Guldberg et al., 2007; U.S. Global Change Research Program, 2018). These stressors threaten the fate of coral reefs and the ecosystem services they provide which support the livelihoods of tens of millions of people worldwide (Moberg and Folke, 1999). Model projections forecast that more than 75% of coral reefs will be subjected to annual severe bleaching before 2070 due to thermal stress alone (Van Hooidonk et al., 2016), but the fate of corals may be worsened when they face additional stressors (Hughes and Connell, 1999; Ban et al., 2014). Recent evidence suggests that microplastics (plastic particles or fibers < 5 mm), may negatively affect corals (Hall et al., 2015; Chapron et al., 2018; Reichert et al., 2018, 2019). To date, however, no studies have looked at the potential for thermal stress to affect microplastics ingestion by reef-building corals.

Under normal conditions, most reef-building corals acquire the majority of their energy from a symbiotic partnership with photosynthetic dinoflagellates in the family Symbiodiniaceae (LaJeunesse et al., 2018), while less energy is generally derived from heterotrophic feeding on zooplankton (Muscatine and Porter, 1977; Muscatine, 1990; Grottoli et al., 2006). When thermally stressed, Symbiodiniaceae are expelled from corals (bleaching) leading to a net decrease in autotrophic energy acquisition (Hoegh-Guldberg and Smith, 1989; Iglesias-Prieto et al., 1992). If elevated temperatures persist, corals deplete their energy reserves and can starve, but if the temperature reduces before the corals' energy reserves are exhausted, Symbiodiniaceae can be reacquired and the coral may recover (Hayes and Bush, 1990; Loya et al., 2001; Jones et al., 2008).

Some corals respond to thermal stress and subsequent bleaching by increased heterotrophy which shifts the corals' reliance from energy derived from photosynthesis to energy derived from zooplankton prey, an adaptation termed heterotrophic plasticity (Grottoli et al., 2006; Palardy et al., 2008; Ferrier-pagès et al., 2010; Hughes and Grottoli, 2013; Bessell-Browne et al., 2014). While the underlying mechanisms and timing of this response are still unclear, increased carbon acquisition from heterotrophy can help corals maintain daily metabolic costs until Symbiodiniaceae can be reacquired. In contrast, other corals decrease their feeding rate during, or following, thermal stress (Palardy et al., 2008; Ferrier-pagès et al., 2010; Courtial et al., 2017) which may negatively impact their resilience. For corals that display heterotrophic plasticity, increased feeding of zooplankton prey could potentially increase their risk of ingesting unwanted particles in the water, such as microplastics.

Microplastics are considered ubiquitous in aquatic ecosystems worldwide and are negatively impacting marine life (Gideon and Faggio, 2019). By 2014, there was an estimated 15 to 51 trillion microplastic particles in the oceans (Sebille et al., 2015), which are derived from direct manufacturing or break down from larger plastic debris due to abrasion, wave action, and UV radiation. Plastic waste entering the oceans is expected to increase 10-fold by 2025 (Jambeck et al., 2015) leading to growing concerns about the potential for these pollutants to negatively affect marine organisms. Their similarity in shape and size to zooplankton make microplastics particularly problematic for planktivorous animals such as corals that can ingest them while feeding (Hall et al., 2015). In some organisms, ingesting microplastics can lead to decreased feeding efficiency, growth and fecundity (Besseling et al., 2013; Sussarellu et al., 2016; Chapron et al., 2018) but for corals these effects are still not fully understood. Further, there is increasing

concern about the role of plastics, large and small, to act as vectors for diseases and contaminants (Goldstein et al., 2014; Lamb et al., 2018; Rotjan et al., 2019).

Previous studies have demonstrated that ingesting, and exposure to, microplastics can have negative effects on corals. Corals that ingested microplastics tended to egest most of them within 48 h which limited the time microplastics could cause internal damage but is still thought to be energetically costly (Hall et al., 2015; Chapron et al., 2018; Reichert et al., 2018). For some coral species, exposure to microplastics resulted in increased mucous production, bleaching, necrosis, changes in photosynthetic performance, and decreased growth and feeding rates (Chapron et al., 2018; Reichert et al., 2018, 2019). One coral species, *Astrangia poculata*, appeared to selectively feed on clean microplastics when also offered bio-fouled particles, leading researchers to suggest that chemical cues released by plastics (i.e., chemoreception) drove ingestion (Allen et al., 2017). Additional research also showed that *A. poculata* preferred to feed on microplastics over similar sized brine shrimp eggs, and that ingesting microplastics can inhibit later feeding on nutritious prey (Rotjan et al., 2019). While we are beginning to understand the responses and mechanisms of microplastics ingestion by corals, we still do not know how this pervasive pollutant interacts with other stressors, such as rising sea temperatures.

The objective of this study was to examine whether prior exposure to thermal stress affects microplastics ingestion and if microplastics exposure and ingestion affects the amount of prey ingested by reef-building corals. To determine this, we compared ingestion rates of corals, exposed to microplastics (MP) only, *Artemia* only, or MP and *Artemia* following ambient and increased temperature treatments. We hypothesized that if *Artemia* ingestion changed due to thermal stress, we would also see a similar trend in MP ingestion rates. Additionally, if a

chemical in microplastics makes them more appealing to corals (Allen et al., 2017), then we hypothesized that corals exposed to microplastics would ingest less prey in favor of microplastics. As thermal stress events are predicted to occur with greater frequency and intensity, and microplastics continue to accumulate in the oceans, it is critical that we understand how corals respond to these stressors to better manage coral resilience in our changing world.

2.3 Materials and Methods

2.3.1 *Location and species*

This study was conducted from June 21 to August 20, 2018, at the Hawai‘i Institute of Marine Biology (HIMB), located in Kane‘ohe Bay, O‘ahu, Hawai‘i (21.4282° N, 157.7919° W). We performed our experiments on two locally common reef-building coral species. *Montipora capitata* (rice coral) is a dominant reef-builder in Hawai‘i. It was chosen for this experiment because it displays heterotrophic plasticity (increased feeding) following bleaching due to thermal stress (Grottoli et al., 2006; Palardy et al., 2008). This species occurs in plating and branching forms though only the branching form was used in this experiment. *M. capitata* is a small polyp species (ca. 0.8 mm diameter), has a perforate skeleton and has a plocoid coralite arrangement. *Pocillopora damicornis* (cauliflower coral) is a less-dominant branching coral species on Hawaiian reefs but is locally abundant (Jokiel, 1991). To our knowledge, heterotrophic plasticity following thermal stress had not been reported for this species, which allowed us to investigate whether it also employs this strategy. *P. damicornis* has small polyps (ca. 1 mm diameter), a plocoid coralite arrangement and an imperforate skeleton.

2.3.2 *Experimental set-up*

Ten colonies of *M. capitata* and *P. damicornis* (ca. 14 cm in diameter) were collected from 1-2 m depth in the inner lagoon surrounding HIMB on June 21 and July 12, 2018, respectively (DAR Special Activities Permit No. 2019-21). Colonies were collected at least 5 m apart to reduce the likelihood of getting genetically identical clones. From each colony, eight fragments (ca. 5 cm) were removed, attached to ceramic tiles and allowed to acclimate in an outdoor flow-through tank for 6-7 days. All tanks, one for acclimation and three for each temperature, were maintained with a volume of 400 L of sand-filtered seawater from Kane'ohe Bay and shaded to mimic photosynthetically active radiation (PAR) on the reef. Mean daytime PAR was 235 µmol photons m^{-2} s^{-1} and mean PAR at 12:00 was 522 µmol photons m^{-2} s^{-1} (Odyssey Submersible PAR Logger, Dataflow Systems LTD.). The average temperature of ambient seawater supplied during the acclimation period was 27.3 ± 0.5 °C, measured hourly (HOBO pendant temperature loggers #UA-002-64, Onset Computer Corporation).

After the acclimation period, four fragments from each colony were moved to ambient temperature treatments (27.2 ± 0.5 °C) and the other four were moved to increased temperature treatments (see below). The coral fragments were randomly assigned to one of the three tanks for each temperature treatment, and rotated weekly between tanks to minimize potential tank effects. For *M. capitata*, the temperature was increased slowly over five days to 30.8 ± 0.8 °C, similar to Palardy et al.(Palardy et al., 2008). In a preliminary experiment, *P. damicornis* experienced ca. 50% mortality under 30.8 °C so the water temperature was increased to only 29.2 ± 0.4 ˚C over five days. For both species, the increased temperature treatments lasted for 20 days and noticeable bleaching was observed, although not quantified. After the temperature treatment, the

heaters were turned off and feeding trials began the following day, based on the assumption that *M. capitata* would increase feeding following thermal stress and bleaching(Grottoli et al., 2006; Palardy et al., 2008).

2.3.3 *Feeding trials*

Feeding chambers were constructed of rectangular polycarbonate 3.7 L food pans fit with an adjustable circulation pump (Hydor pico 70, Hydor USA Inc.) on the lowest flow setting (49 L h^{-1}) and an air-stone. The circulation pump was glued to the floor of one end of the chamber and the nozzle was pointed up at a 45° angle towards the middle of the chamber to break the water's surface tension. It was necessary to supply air bubbles in the chamber to facilitate microplastics suspension in the water. Thirty minutes prior to adding the coral fragments, the chambers were filled with 2 L of 1 µm filtered seawater (FSW) and placed in water baths at ambient seawater temperature.

Each night, for ten consecutive nights, feeding trials were performed with all eight fragments from each colony (four fragments previously exposed to ambient temperature and four fragments previously exposed to increased temperature). The experiments started on July 20 for *M. capitata* and Aug. 11 for *P. damicornis*. The fragments from each temperature treatment were given one of four feeding treatments: (i) microplastics (2 particles mL^{-1}) only, (ii) *Artemia* nauplii (2 individuals mL^{-1}) only, (iii) microplastics (2 particles mL^{-1}) and *Artemia* nauplii (2 individuals mL^{-1}), and (iv) 1 µm FSW control. The concentration of microplastics used in this study was higher than what has been reported for coral reefs(Connors, 2017; Saliu et al., 2018) but was lower than most previous experiments that studied microplastics ingestion by corals(Hall et al., 2015; Allen et al., 2017; Reichert et al., 2018; Tang et al., 2018). A high concentration of

Artemia was also used because, as noted in previous studies(Palardy et al., 2008; Ferrier-pagès et al., 2010), it allowed for smaller sample sizes, minimized dissection time and increased statistical power. Green fluorescent polyethylene (confirmed by Fourier Transform Infrared Spectroscopy, see Supplementary Fig. S2.1) microbeads (Cospheric LLC.) with a diameter of 150 – 180 µm and a density of 1.025 g mL^{-1} were used for the microplastics treatment because they had similar mass (2.4 µg per particle) to the *Artemia* used and the same density as sea water. The microbeads were served clean (not bio-fouled) to allow for potential chemical cues to influence the corals' feeding behavior(Allen et al., 2017). Freshly hatched *Artemia* nauplii (Grade A, SLU strain, Brine Shrimp Direct, Ogden, UT; dry weight = 2.42 µg per individual(Vanhaecke and Sorgeloos, 1980)) were used because they fall within the prey size range for *P damicornis* and *M, capitata*(Palardy et al., 2006, 2008), and to facilitate the quantification of treatment concentrations and ingestion rates. FSW controls were used to account for the potential ingestion of residual microplastics that stuck to chamber components despite rigorous cleaning between trials. No microplastics were found in dissected control corals, thus control data were left out of further analyses.

Coral fragments were placed in the feeding chambers each day at 12:00 h to give them ample time to acclimate to the chamber and digest any previously ingested prey(Palardy et al., 2008). At 20:00 h, microplastics and *Artemia* nauplii were added to the feeding chambers and the coral fragments were allowed to feed for one hour before being removed from their chambers and fixed immediately in 10% formalin. Though both species used in this study presumably feed throughout the night, previous research has shown that they feed heavily enough within the first hour of dusk to draw meaningful biological conclusions(Palardy et al., 2005, 2008), thus a one hour feeding duration was used. The next day, the number of microplastics and *Artemia* ingested

by 200 polyps were counted by dissecting 200 polyps from each fragment under a stereo microscope (10-40 x) using fine dissection probes, forceps and a UV light. An ingestion was defined as a microplastic or *Artemia* nauplii found in the coral polyp and did not include any information on egested particles. Microplastics counted in the polyps were nudged sufficiently to be certain that we were counting the green fluorescent microbeads and not autofluorescence of the coral or symbionts. Microplastics and *Artemia* ingestion rates are reported as the mean number of ingestions per 200 polyps h^{-1} ± one standard error.

2.3.4 *Statistics*

Microplastic and *Artemia* ingestion were compared separately for each species (n = 10) following a fully factorial 2 x 3 (2 temperatures x 3 feeding treatments) mixed effects permutation analysis of variance, using the aovp function(Wheeler and Torchiano, 2016) in R (Rstudio v.1.1.463). This randomization procedure was used because most of the data did not meet the normality nor the equal variance assumptions of a typical ANOVA, due to high occurrences of zeros in the data (no ingestions by corals in some treatments). Temperature and feeding treatments were treated as main effects and colony as a random effect. The aovp function was ran with 10,000 iterations and results were considered significant when $p < 0.05$.

2.4 RESULTS

2.4.1 *Microplastics ingestion*

Both species, *Montipora capitata* and *Pocillopora damicornis*, ingested microplastics (Fig. 2.1). The number of microplastics ingested by individual polyps ranged from zero to one in *M.*

capitata, and from zero to seven in *P. damicornis*. Overall, *P. damicornis* ingested over 520% more microplastics than *M. capitata*.

Compared to ambient temperature controls, corals exposed to three weeks of thermal stress were visibly pale (bleached). This did not, however, result in significantly different microplastics ingestion rates (Fig. 2.2A and 2.2B). *M. capitata*, ingested very few microplastics overall, ingesting only 0.2 ± 0.2 (mean ± 1 SEM) microplastics per 200 polyps h^{-1} in the MP only treatment after thermal stress, and 0.3 ± 0.2 microplastics per 200 polyps h^{-1} in the MP & *Artemia* treatment at ambient temperature (Fig. 2.2A). *M. capitata* did not ingest any microplastics in the MP only treatment at ambient temperature or in the MP & *Artemia* treatment after thermal stress (Fig. 2.2A).

Though thermal stress was not a significant factor, *P. damicornis* ingested significantly more microplastics in the MP & *Artemia* treatments than in the MP only treatments after both temperature treatments (Permutation ANOVA [aovp], df = 1, F = 20.16, p = 0.00012, Fig. 2.2B). In the MP & *Artemia* treatments *P. damicornis* ingested 15.7 ± 5.2 microplastics per 200 polyps h^{-1} at ambient temperature and 9.6 ± 3.1 microplastics per 200 polyps h^{-1} after thermal stress (Fig. 2.2B). When *P. damicornis* was exposed to microplastics only, particle ingestion was absent or negligible after both ambient and increased temperature treatments (Fig. 2.2B).

2.4.2 *Artemia ingestion*

Artemia were ingested by both species in all treatments (Fig. 2.2C and 2.2D). The number of *Artemia* ingested by individual polyps ranged from zero to one in *M. capitata* and zero to twelve in *P. damicornis*.

Following thermal stress, *Artemia* ingestion was significantly decreased in both *M. capitata* (aovp, df = 1, F = 11.65, p = 0.002, Fig. 2.2C) and *P. damicornis* (aovp, df = 1, F = 6.658, p = 0.0156, Fig. 2.2D) compared to ambient temperature controls. For both species, there was no significant difference in *Artemia* ingestion between MP only and MP & *Artemia* treatments after either temperature treatment. *M. capitata* in the *Artemia* only treatments ingested 12.3 ± 5.4 *Artemia* per 200 polyps h^{-1} at ambient temperature and 3.7 ± 1.6 *Artemia* per 200 polyps h^{-1} after thermal stress. In the MP & *Artemia* treatments, *M. capitata* ingested 12.1 ± 5.4 *Artemia* per 200 polyps h^{-1} at ambient temperature and 4.3 ± 1.6 *Artemia* per 200 polyps h^{-1} after thermal stress (Fig. 2.2C). *P. damicornis* in the *Artemia* only treatments ingested 120.6 ± 17.5 *Artemia* per 200 polyps h^{-1} at ambient temperature and 73.3 ± 17.3 *Artemia* per 200 polyps h^{-1} after thermal stress. In the MP & *Artemia* treatments, *P. damicornis* ingested 134.2 ± 11.9 *Artemia* per 200 polyps h^{-1} at ambient temperature and 111.3 ± 17.7 *Artemia* per 200 polyps h^{-1} after thermal stress (Fig. 2.2D).

2.5 Discussion

In this study we investigated how microplastics ingestion and heterotrophy are impacted after thermal stress in two reef-building corals, *Montipora capitata* and *Pocillopora damicornis*. Our results revealed that prior exposure to thermal stress did not affect microplastics ingestion but can lead to decreased feeding on prey. We also found that ingesting microplastics did not affect the amount of prey ingested, and that these corals did not selectively ingest microplastics as has been observed in another species (Allen et al., 2017). Additionally, we observed considerable variability in microplastics and *Artemia* ingestion rates under different scenarios between the two

studied species. Our results suggest that coral species will respond differently to microplastics pollution following thermal stress events.

In contrast to previous studies (Grottoli et al., 2006; Palardy et al., 2008), we did not observe higher feeding rates in corals following thermal stress and subsequent bleaching. On the contrary, *Artemia* feeding rates significantly decreased for both species, and microplastics ingestion rates decreased slightly in *P. damicornis*. This may be due to the corals being stressed, which has been suggested to cause decreased tentacle activity and/or nematocyst function (Johannes and Tepley, 1974; Ferrier-pagès et al., 2010; Courtial et al., 2017). The fact that feeding did not increase may be due to not reaching a "bleaching threshold" needed to see an increased feeding response. In the present study, we followed a similar thermal stress regime to that of Grottoli et al. (2006) and, though we did not quantify bleaching (symbiont counts, pigment concentrations, photophysiology), most coral fragments were completely white, and the rest were very pale. Alternatively, it may be that energy reserve status is the mechanism controlling heterotrophic plasticity. In our study we measured ingestion immediately after thermal stress, whereas Grottoli et al. (2006) measured it two weeks after thermal stress exposure. Thus it may be that these corals needed to spend more time bleached in order to reach such critical energy levels and increase heterotrophy. Two corals, *Turbinaria reniformis* and *Galaxea fascicularis*, display increased feeding rates in as little as five days of exposure to thermal stress (Ferrier-pagès et al., 2010) suggesting that such critical thresholds can be met rapidly, and supporting that this response is considerably variable among species. Furthermore, heterotrophic plasticity can also be driven by other environmental factors such as ultraviolet radiation and seasonal weather patterns (Courtial et al., 2017; Mies et al., 2018). With the increasing threat of thermal stress events and microplastics accumulation in the oceans, further

research should compare feeding rates of prey (and microplastics), as well as assimilation and allocation of heterotrophic carbon to the corals' energy reserves (e.g. lipids, carbohydrates). Feeding rates (prey/microplastics) and carbon transfer should be evaluated at several periods over the entire bleaching cycle, from the initiation of thermal stress to the full recovery of the coral.

Even though exposure to microplastics led to them being ingested by both species, it did not affect *Artemia* ingestion rates as expected. A similar behavior was observed in *A. poculata* which, following exposure to microplastics, did not change the amount it fed on live *Artemia* and copepods (Rotjan et al., 2019). While this suggests that ingesting microplastics may not have a large effect on heterotrophic energy acquisition for these species, more information is needed to draw such a conclusion. First, this study was limited by the short duration (1 h) of feeding trials. For many corals that generally feed all night, constant exposure could allow microplastics to accumulate in the polyps and prevent further ingestion of prey. However, the amount of accumulation that occurs depends on retention time and egestion rates, which were not measured in this study. To our knowledge, there is currently no published information on accumulation rates (e.g. mass balance) in coral polyps constantly exposed to microplastics and should be a priority for future research. Additionally, we lack data on the assimilation rate of carbon and nutrients from the *Artemia* prey in corals exposed to microplastics. Though microplastics did not appear to act as a barrier to prey ingestion, at least in the short-term, they may act as a barrier to digestion and nutrient assimilation. In the oyster, *Pinctada margaritifera*, microplastics exposure did not affect ingestion rate but did significantly decrease macroalgae assimilation efficiency (Gardon et al., 2018).

Chemoreception did not appear to drive microplastics ingestion for either species studied here. In contrast, the presence of *Artemia* prey appeared to strongly influence whether microplastics were ingested for *P. damicornis*, which did not selectivity ingest microplastics. Allen et al. (2017) found that *A. poculata* ingested clean weathered plastics over bio-fouled ones and suggested that microplastics ingestion by corals was driven by phagostimulant (feeding cue) release by the plastics. However, in the present study, microplastics ingestion by *P. damicornis* was absent or negligible when exposed only to clean microplastics. In a similar study, symbiotic sea anemones, *Aiptasia pallida*, were also reluctant to ingest any microplastics, including nylon, polyester and polypropylene fibers, in the absence of prey tissue (Romano de Orte et al., 2019). Differences among studies could be due to species specific responses to phagostimulants in plastics, and/or the use of different types of microplastics. The microplastics used in our study were all polyethylene, whereas Allen et al. (2017) used a mixture of plastic particles consisting of two-thirds polyethylene and one-third polystyrene, and it might be that only polystyrene released a phagostimulant. Further research should focus on the potential of phagostimulant release by different types of plastic. Our results suggest that chemicals released by certain plastics may drive selectivity in some corals, such as *A. poculata*, but not so in other corals, such as *P. damicornis*, that are simply at risk of inadvertently ingesting microplastics during times when they are feeding.

The fact that acute thermal stress led to decreased microplastics ingestion in this study does not eliminate corals' risk of exposure, as microplastics were still ingested. The act of ingesting and then egesting microplastics is assumed to be energetically costly (Hall et al., 2015; Chapron et al., 2018; Reichert et al., 2018), although further research is needed to determine how costly those behaviors are (Hankins et al., 2018). Additionally, exposure to microplastics can trigger

rejection mechanisms, similar to how corals handle sediment exposure (Stafford-Smith and Ormond, 1992; Riegl and Branch, 1995), that also consume the coral's energy reserves(Reichert et al., 2018). In other benthic marine invertebrates, microplastics ingestion has also led to weight loss (Besseling et al., 2013) and decreased fitness (Sussarellu et al., 2016) which were attributed to decreased prey ingestion or assimilation efficiency due to the presence of microplastics in the gut. In corals, chronic exposure to microplastics resulted in species-specific stress responses, including decreased growth, supporting the notion of depleted energy reserves (Reichert et al., 2019). Future research should focus on examining how and to what degree microplastics exposure and ingestion can affect a coral's energetic status in the long-term, especially during bleaching when energy reserves are critical for the coral's survival (Rodrigues and Grottoli, 2007). Furthermore, the ability of some corals to increase feeding due to bleaching or other factors could exacerbate these effects if microplastics ingestion increases accordingly, but this still needs to be determined. For future corals that will have to endure increasingly prolonged and intense thermal stress, and numerous other stressors (Van Hooidonk et al., 2016), any amount of energy wasted could be significant.

Results from this study, and from other studies that investigated microplastics ingestion by corals, support that some corals are likely more at risk of microplastics exposure than others (Reichert et al., 2019). For example, in agreement with Reichert et al. (2018), this study observed variable microplastics ingestion rates among coral species, and challenging Allen et al. (2017), our work showed that plastics are not so "tasty" to all corals. Furthermore, coral feeding rates can vary depending on a variety of factors (Grottoli et al., 2006; Palardy et al., 2008; Ferrier-pagès et al., 2010; Courtial et al., 2017; Mies et al., 2018) and may potentially effect microplastics ingestion. Given the various responses to microplastics and feeding behaviors of

corals, future research should focus on how, and which, corals are likely to be affected by microplastics under future scenarios.

Here we present the first study to examine the roles of thermal stress on microplastic ingestion and of microplastics exposure on heterotrophy in two reef-building corals. Overall, *P. damicornis* ingested more microplastics and fed more heavily on *Artemia* than *M. capitata*, while both species displayed decreased feeding on *Artemia* under thermal stress. When offered *Artemia*, *P. damicornis* readily ingested microplastics, but without live prey it ingested virtually no microplastics, indicating that chemoreception does not drive microplastics ingestion in all corals. Collectively, these results suggest that some coral species may be at greater risk of microplastics exposure than others. Further research should focus on the physiological effects of microplastics, how a corals' feeding behavior influences its potential to ingest microplastics, how ingesting microplastics affect nutrient assimilation, which plastics release phagostimulants, and which coral species are affected by these phagostimulants. When used in the context of global change, these data will be critical for predicting the potential impact of microplastics on future corals and coral reefs.

2.6 ACKNOWLEDGEMENTS

We offer our warmest gratitude to the Gates Coral Lab for hosting and supporting us during this experiment at the Hawaii Institute of Marine Biology. We thank Lisa Rodrigues for advice about the experimental design and manuscript. We thank Tanya Brown, Brenner Wakayama, Gavin Kreitman, Melissa Jaffe and Sean Frangos for help with collecting and culturing the experimental corals. We thank Samantha Pham for validating the polymer composition of our experimental microplastics. We would also like to especially thank Yanbo Ge and the

Biostatistics Consulting group from the University of Washington Department of Statistics for guidance on the statistical tests used in our analyses. Work was supported by NSF IOS (1655682) awarded to J.L.P.G. This material is based upon work supported by the National Science Foundation Graduate Research Fellowship Program under Grant No. (DGE1762114). Any opinions, findings, and conclusions or recommendations expressed in this material are those of the author(s) and do not necessarily reflect the views of the National Science Foundation.

2.7 FIGURES

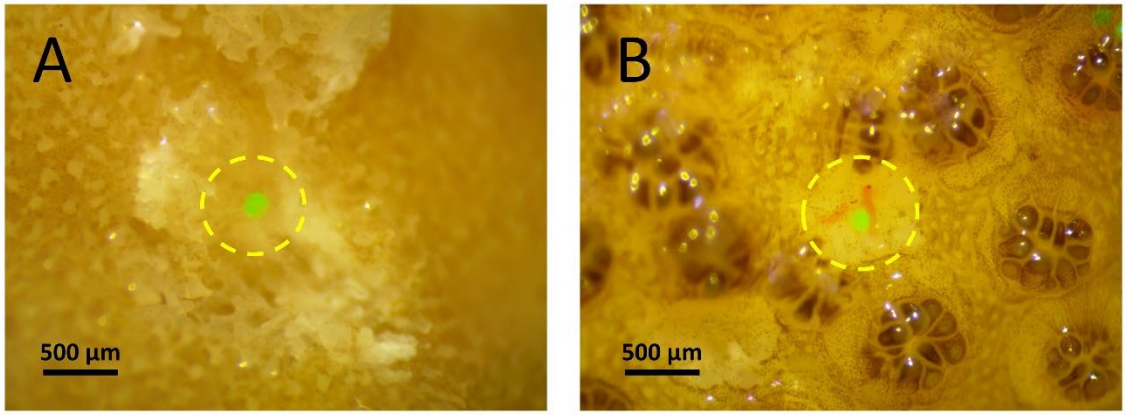

Figure 2.1 Microplastics ingested in the polyps of (A) *Montipora capitata*, and (B) *Pocillopora damicornis*. The yellow dotted circles show where the polyp was dissected exposing the contents of the gut.

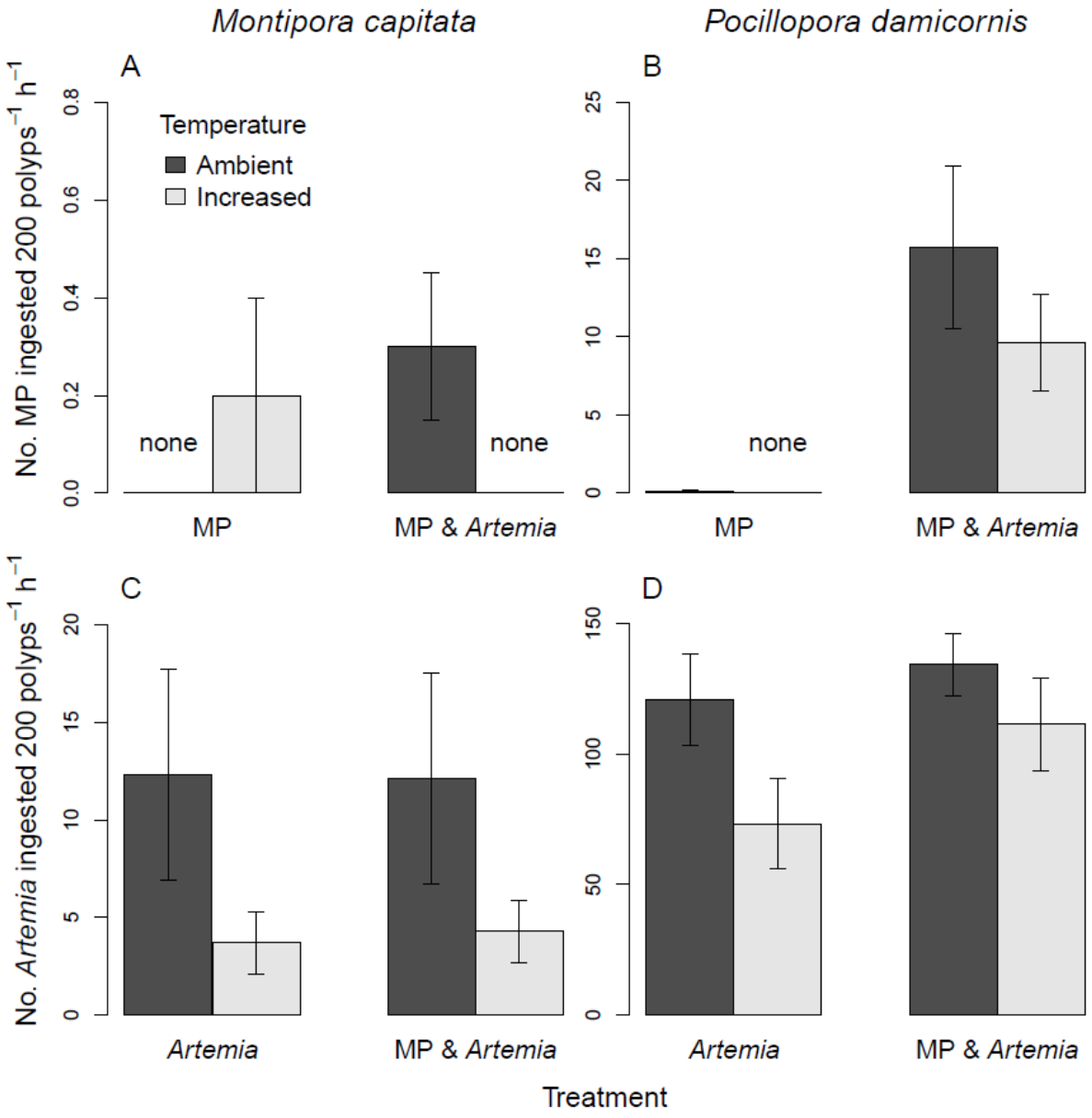

Figure 2.2 Mean (± SEM) microplastics ([MP], A and B) and *Artemia* nauplii (C and D) ingestion rates of corals exposed to ambient (dark bars) and increased (light bars) temperature. Note the difference in scales of the y-axes.

2.8 REFERENCES

Allen, A. S., Seymour, A. C., and Rittschof, D. (2017). Chemoreception drives plastic consumption in a hard coral. *Mar. Pollut. Bull.* 124, 198–205. doi: 10.1016/j.marpolbul.2017.07.030

Ban, S. S., Graham, N. A. J., and Connolly, S. R. (2014). Evidence for multiple stressor interactions and effects on coral reefs. *Glob. Change Biol.* 20, 681–697. doi: 10.1111/gcb.12453

Besseling, E., Wegner, A., Foekema, E. M., Van Den Heuvel-Greve, M. J., and Koelmans, A. A. (2013). Effects of microplastic on fitness and PCB bioaccumulation by the lugworm *Arenicola marina* (L.). *Environ. Sci. Technol.* 47, 593–600. doi: 10.1021/es302763x

Bessell-Browne, P., Stat, M., Thomson, D., and Clode, P. L. (2014). *Coscinaraea marshae* corals that have survived prolonged bleaching exhibit signs of increased heterotrophic feeding. *Coral Reefs* 33, 795–804. doi: 10.1007/s00338-014-1156-z

Chapron, L., Peru, E., Engler, A., Ghiglione, J. F., Meistertzheim, A. L., Pruski, A. M., et al. (2018). Macro- and microplastics affect cold-water corals growth, feeding and behaviour. *Sci. Rep.* 8, 1–8. doi: 10.1038/s41598-018-33683-6

Connors, E. J. (2017). Distribution and biological implications of plastic pollution on the fringing reef of Mo'orea, French Polynesia. *PeerJ* 5:e3733 doi: 10.7717/peerj.3733

Courtial, L., Roberty, S., Shick, J. M., Houlbreque, F., and Ferrier-pages, C. (2017). Interactive effects of ultraviolet radiation and thermal stress on two reef-building corals. *Limnol. Oceanogr.* 62, 1000–1013. doi: 10.1002/lno.10481

Ferrier-pagès, C., Rottier, C., Beraud, E., and Levy, O. (2010). Experimental assessment of the feeding effort of three scleractinian coral species during a thermal stress: Effect on the rates of photosynthesis. *J. Exp. Mar. Biol. Ecol.* 390, 118–124. doi: 10.1016/j.jembe.2010.05.007

Gardon, T., Reisser, C., Soyez, C., Quillien, V., and Le Moullac, G. (2018). Microplastics affect energy balance and gametogenesis in the pearl oyster *Pinctada margaritifera*. *Environ. Sci. Technol.* 52, 5277–5286. doi: 10.1021/acs.est.8b00168

Gideon, C., and Faggio, C. (2019). Microplastics in the marine environment: Current trends in environmental pollution and mechanisms of toxicological profile. *Environ. Toxicol. Pharma.* 68, 61–74. doi: 10.1016/j.etap.2019.03.001

Goldstein, M. C., Carson, H. S., and Eriksen, M. (2014). Relationship of diversity and habitat area in North Pacific plastic-associated rafting communities. *Mar. Biol.* 161, 1441–1453. doi: 10.1007/s00227-014-2432-8

Grottoli, A. G., Rodrigues, L. J., and Palardy, J. E. (2006). Heterotrophic plasticity and resilience in bleached corals. *Nature* 440, 1186–1189. doi: 10.1038/nature04565

Hall, N. M., Berry, L. E., Rintoul, L., and Hoogenboom, M. O. (2015). Microplastic ingestion by scleractinian corals. *Mar. Biol.* 162, 725–732. doi: 10.1007/s00227-015-2619-7

Hankins, C., Duffy, A., and Drisco, K. (2018). Scleractinian coral microplastic ingestion: Potential calcification effects, size limits, and retention. *Mar. Pollut. Bull.* 135, 587–593. doi: 10.1016/j.marpolbul.2018.07.067

Hayes, R. L., and Bush, P. G. (1990). Microscopic observations of recovery in the reef-building scleractinian coral, *Montastrea annularis*, after bleaching on a Cayman reef. *Coral Reefs* 8, 203–209. doi: 10.1007/BF00265012

Hoegh-Guldberg, O., Mumby, P. J., Hooten, A., Steneck, R. S., Greenfield, P., Gomez, E., et al. (2007). Coral reefs under rapid climate change and ocean acidification. *Science* 318, 1737–1742. doi: 10.1126/science.1152509

Hoegh-Guldberg, O., and Smith, G. J. (1989). The effect of sudden changes in temperature, light and salinity on the population density and export of zooxanthellae from the reef corals *Stylophora pistillata* Esper and *Seriatopora histrix* Dana. *J. Exp. Mar. Biol. Ecol.* 129, 279–303. doi: 10.1016/0022-0981(89)90109-3

Hughes, A. D., and Grottoli, A. G. (2013). Heterotrophic compensation: A possible mechanism for resilience of coral reefs to global warming or a sign of prolonged stress? *PLoS ONE* 8, 1–10. doi: 10.1371/journal.pone.0081172

Hughes, T. P., and Connell, J. H. (1999). Multiple stressors on coral reefs: A long -term perspective. *Limnol. Oceanogr.* 44, 932–940. doi: 10.4319/lo.1999.44.3_part_2.0932

Iglesias-Prieto, R., Matta, J. L., Robins, W. A., and Trench, R. K. (1992). Photosynthetic response to elevated temperature in the symbiotic dinoflagellate *Symbiodinium microadriaticum* in culture. *Proc. Nat. Acad. Sci.* 89, 10302–10305. doi: 10.1073/pnas.89.21.10302

Jambeck, J. R., Geyer, R., Wilcox, C., Siegler, T. R., Perryman, M., Andrady, A., et al. (2015). Plastic waste inputs from land into the ocean. *Science* 347, 768–771. doi: 10.1126/science.1260352

Johannes, R. E., and Tepley, L. (1974). Examination of feeding of the reef coral *Porties lobata in situ* using time lapse photography., in *Proc. 2nd Int. Coral Reef Symp*. (Brisbane), 1:127-131.

Jokiel, P. L. (1991). Jokiel's Illustrated Scientific Guide to Kaneohe Bay, Oahu. Kaneohe, HI.

Jones, A. M., Berkelmans, R., Van Oppen, M. J. H., Mieog, J. C., and Sinclair, W. (2008). A community change in the algal endosymbionts of a scleractinian coral following a natural

bleaching event: Field evidence of acclimatization. *Proc. R. Soc. B: Biol. Sci.* 275, 1359–1365. doi: 10.1098/rspb.2008.0069

LaJeunesse, T. C., Parkinson, J. E., Gabrielson, P. W., Jeong, H. J., Reimer, J. D., Voolstra, C. R., et al. (2018). Systematic Revision of Symbiodiniaceae Highlights the Antiquity and Diversity of Coral Endosymbionts. *Curr. Biol.* 28, 2570-2580.e6. doi: 10.1016/j.cub.2018.07.008

Lamb, J. B., Willis, B. L., Fiorenza, E. A., Couch, C. S., Howard, R., Rader, D. N., et al. (2018). Plastic waste associated with disease on coral reefs. *Science* 359, 460–462. doi: 10.4081/aiol.2017.7211

Loya, Y., Sakai, K., Yamazato, K., Nakano, Y., Sambali, H., and van Woesik, R. (2001). Coral bleaching: the winners and the losers. *Ecol. Lett.* 4, 122–131. doi: 10.1046/j.1461-0248.2001.00203.x

Mies, M., Guth, A. Z., Tenorio, A. A., Banha, T. N. S., Waters, L. G., Polito, P. S., et al. (2018). In situ shifts of predominance between autotrophic and heterotrophic feeding in the reef-building coral *Mussismilia hispida*: an approach using fatty acid trophic markers. *Coral Reefs* 37, 677–689. doi: 10.1007/s00338-018-1692-z

Moberg, F., and Folke, C. (1999). Ecological goods and services of coral reef ecosystems. *Ecol. Econ.* 29, 215–233. doi: 10.1016/S0921-8009(99)00009-9

Muscatine, L. (1990). "The role of symbiotic algae in carbon and energy flux in reef corals," in *Ecosystems of the world, Vol. 25. Coral reefs*, ed. Z. Dubinsky (Amsterdam: Elsevier), 75–87.

Muscatine, L., and Porter, J. W. (1977). Reef Corals: Mutualistic Symbioses Adapted to Nutrient-Poor Environments. *BioScience* 27, 454–460. doi: 10.2307/1297526

Palardy, J. E., Grottoli, A. G., and Matthews, K. (2005). The effect of morphology, polyp size, depth, and temperature on feeding in three species of Panamanian corals. *Mar. Ecol. Prog. Ser.* 300, 79–85. doi: 10.3354/meps300079

Palardy, J. E., Grottoli, A. G., and Matthews, K. A. (2006). Effect of naturally changing zooplankton concentrations on feeding rates of two coral species in the Eastern Pacific. *J. Exp. Mar. Biol. Ecol.* 331, 99–107. doi: 10.1016/j.jembe.2005.10.001

Palardy, J. E., Rodrigues, L. J., and Grottoli, A. G. (2008). The importance of zooplankton to the daily metabolic carbon requirements of healthy and bleached corals at two depths. *J. Exp. Mar. Biol. Ecol.* 367, 180–188. doi: 10.1016/j.jembe.2008.09.015

Reichert, J., Arnold, A. L., Hoogenboom, M. O., Schubert, P., and Wilke, T. (2019). Impacts of microplastics on growth and health of hermatypic corals are species-specific. *Environ. Pollut.* 254, 113074. doi: 10.1016/j.envpol.2019.113074

Reichert, J., Schellenberg, J., Schubert, P., and Wilke, T. (2018). Responses of reef building corals to microplastic exposure. *Environ. Pollut.* 237, 955–960. doi: 10.1016/j.envpol.2017.11.006

Riegl, B., and Branch, G. M. (1995). Effects of sediment on the energy budgets of four scleractinian (Bourne 1900) and five alcyonacean (Lamouroux 1816) corals. *J. Exp. Mar. Biol. Ecol.* 186, 259–275. doi: 10.1016/0022-0981(94)00164-9

Rodrigues, L. J., and Grottoli, A. G. (2007). Energy reserves and metabolism as indicators of coral recovery from bleaching. *Limnol. Oceanogr.* 52, 1874–1882. doi: 10.4319/lo.2007.52.5.1874

Romano de Orte, M., Clowez, S., and Caldeira, K. (2019). Response of bleached and symbiotic sea anemones to plastic microfiber exposure. *Environ. Pollut.* 249, 512–517. doi: 10.1016/j.envpol.2019.02.100

Rotjan, R. D., Sharp, K. H., Gauthier, A. E., Yelton, R., Lopez, E. M. B., Carilli, J., et al. (2019). Patterns, dynamics and consequences of microplastic ingestion by the temperate coral, *Astrangia poculata*. *Proc. R. Soc. B* 286. doi: 10.1098/rspb.2019.0726

Saliu, F., Montano, S., Seveso, D., Galli, P., Garavaglia, M. G., and Lasagni, M. (2018). Microplastic and charred microplastic in the Faafu Atoll, Maldives. *Mar. Pollut. Bull.* 136, 464–471. doi: 10.1016/j.marpolbul.2018.09.023

Sebille, E. van, Wilcox, C., Lebreton, L., Maximenko, N., Hardesty, B. D., Franeker, J. A. van, et al. (2015). A global inventory of small floating plastic debris. *Environ. Res. Lett.* 10.

Stafford-Smith, M. G., and Ormond, R. F. G. (1992). Sediment-rejection mechanisms of 42 species of Australian scleractinian corals. *Mar. Freshw. Res.* 43, 683–705. doi: 10.1071/MF9920683

Sussarellu, R., Suquet, M., Thomas, Y., Lambert, C., Fabioux, C., Eve, M., et al. (2016). Oyster reproduction is affected by exposure to polystyrene microplastics. *Proc. Nat. Acad. Sci.* 113, 2430–2435. doi: 10.1073/pnas.1519019113

Tang, J., Ni, X., Zhou, Z., Wang, L., and Lin, S. (2018). Acute microplastic exposure raises stress response and suppresses detoxi fi cation and immune capacities in the scleractinian coral. *Environ. Pollut.* 243, 66–74. doi: 10.1016/j.envpol.2018.08.045

U.S. Global Change Research Program (2018). Fourth National Climate Assessment. II, 1–470. doi: 10.1016/j.pbb.2008.09.016

Van Hooidonk, R., Maynard, J., Tamelander, J., Gove, J., Ahmadia, G., Raymundo, L., et al. (2016). Local-scale projections of coral reef futures and implications of the Paris Agreement. *Sci. Rep.* 6, 1–8. doi: 10.1038/srep39666

Vanhaecke, P., and Sorgeloos, P. (1980). “International Study on Artemia IV. The biometrics of Artemia strains from different geographical origin,” in *The Brine Shrimp Artemia Vol. 3*

Ecology, Culturing, Use in Aquaculture, eds. G. Persoone, P. Sorgeloos, O. Roels, and E. Jaspers (Wettern, Belgium: Universa Press), 456.

Wheeler, R. E., and Torchiano, M. (2016). lmPerm: Permutation tests for linear models. *http://CRAN.R-project.org/package=lmPerm.*, 24 p.

2.9 SUPPLEMENTARY MATERIALS

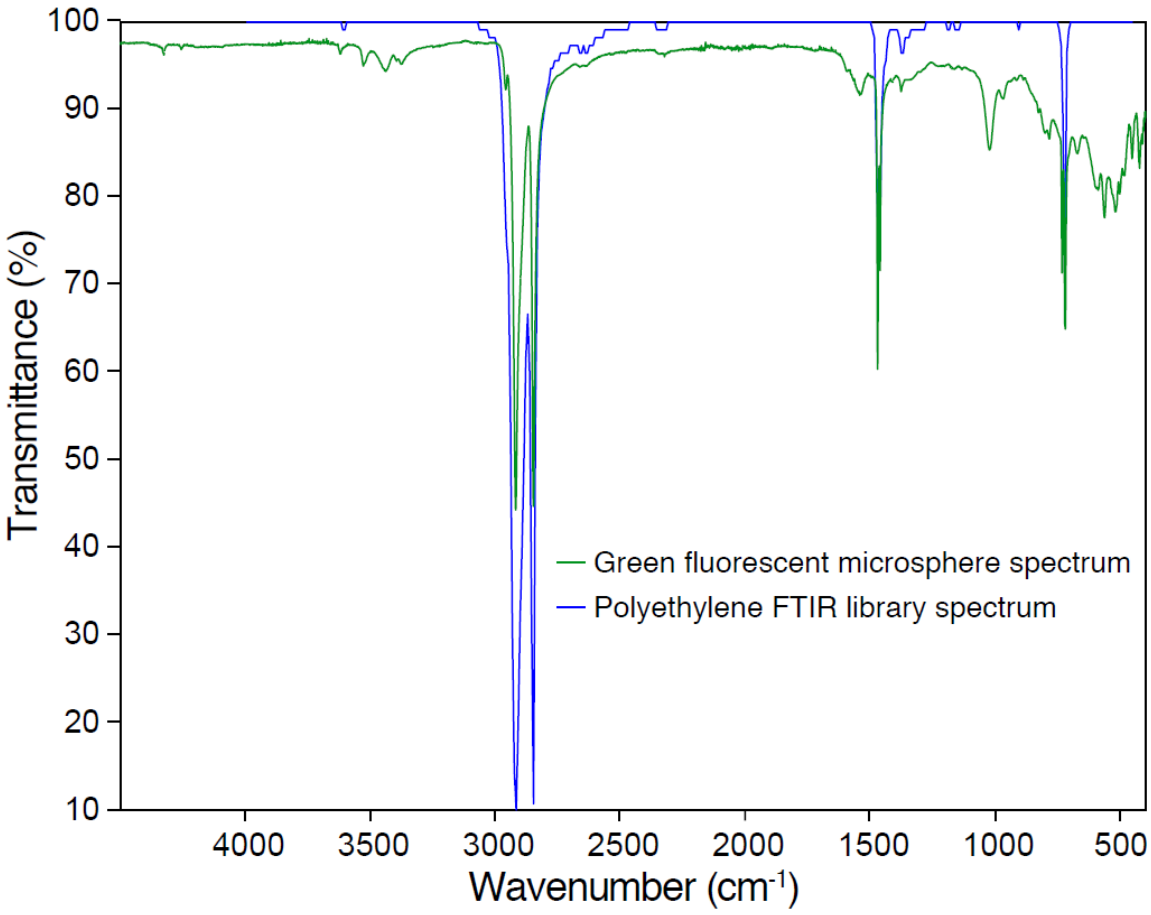

Figure S2.1 Polymer confirmation of experimental microplastics by Fourier Transform Infrared Spectroscopy (FTIR).

Chapter 3. EXPLORING MICROPLASTIC INTERACTIONS WITH REEF-BUILDING CORALS ACROSS FLOW CONDITIONS

Publication history: This study was co-authored with Sicheng Wang, Ruth M. Sofield, Julio E. Chávez-Dorado, Michelle H. DiBenedetto, and Jacqueline L. Padilla-Gamiño. At the time this dissertation was published, this chapter was not in review with a journal.

3.1 ABSTRACT

Microplastics are increasing in marine environments worldwide, but their fate is not fully understood. Reef-building corals are suggested to serve as sinks for microplastics via active removal through ingestion and passive removal by adhesion. However, it is unknown which type of plastics are more likely to be ingested or adhered to corals and whether water flow or coral morphology affects these processes. We exposed the corals, *Leptoseris sp*., *Montipora capitata*, *Montipora digitata*, and *Pocillopora acuta* to weathered polyester fibers, acrylic fibers, and polystyrene fragments under three unidirectional flow regimes (2.6, 5.0 and 7.5 cm s^{-1}). Adhesion rates were 3.9 times higher than ingestion rates and fibers were the dominant type of microplastics for both ingestion and adhesion. Flow significantly affected adhesion but not ingestion. Species was a significant factor for both ingestion and adhesion, but we did not find a significant correlation to morphological traits for either process. Moreover, on *M. capitata*, we observed higher adhesion rates on exposed skeleton than live tissue, suggesting that *M. capitata* actively removes microplastics from its surface and that non-living sections of reefs may also serve as an important sink for microplastic pollution. Our data revealed that processes that influence coral and microplastic interactions are complex but appear to be species-specific and

are likely influenced by feeding strategies and other characteristics of corals. We also highlight the potential for non-living structures on reefs to serve as microplastic sinks.

3.2 INTRODUCTION

Plastic pollution is increasing globally and has been documented in nearly every corner of the planet, from polar ice to tropical coral reefs (Hall et al., 2015; van Sebille et al., 2015; Peeken et al., 2018). Microplastics, synthetic polymers between 1 μm and 5 mm, constitute the vast abundance of plastic waste, resulting from the breakdown of larger plastic debris or entering water bodies at an already micro size. An estimated 19 – 23 million metric tons of plastic waste entered aquatic ecosystems in 2016 and may reach 53 million metric tons by 2030, even under ambitious mitigation efforts (Borrelle et al., 2020). Sources of plastic and microplastic pollution include mismanaged municipal waste, litter, industry, and synthetic clothing; the fate of microplastics are less understood (Auta et al., 2017; Kane and Clare, 2019). Sea surface microplastics are thought to account for about 1% of microplastics predicted to be in the oceans (van Sebille et al., 2015). It has been proposed that a large fraction of microplastics in the oceans sink to the seafloor and accumulate in sediments and organisms (Kane and Clare, 2019; Reichert et al., 2022). As plastic waste continues to increase, plastic debris and associated microplastics accumulate in oceans raising concern about their impact on marine life and ecosystems.

Coral reefs support highly diverse ecosystems, protect coastlines, and support the livelihoods of millions of people worldwide through productive fisheries, subsistence, and ecotourism (Moberg and Folke, 1999). However, the fate of coral reefs is under threat from a suite of stressors, including microplastics. Field studies have shown that coral reefs are polluted with microplastics which are found in seawater, sediments, and in the tissues and skeletons of corals and other reef

organisms (Hall et al., 2015; Ding et al., 2019; Krishnakumar et al., 2021; Tang et al., 2021; Zhou et al., 2022). Laboratory studies have demonstrated a range of negative effects on corals exposed to microplastics, including increased immune response, increased mucus, bleaching, tissue necrosis, altered photosynthetic performance of symbionts, decreased prey capture and decreased growth rates (Reichert et al., 2018, 2019; Hankins et al., 2021; Liao et al., 2021; Mendrik et al., 2021). Additionally, it has been proposed that interactions between corals and microplastics, such as ingestion and egestion, reduce energy in corals (Hall et al., 2015; Chapron et al., 2018; Rotjan et al., 2019). Recently, however, corals have been proposed as being a significant sink for microplastics, removing and storing an estimated 0.09%–2.82% of microplastics from tropical coral reefs (Reichert et al., 2022). In this role, corals may be providing yet another ecosystem service by removing microplastics from the oceans.

Corals may remove microplastics from seawater passively through adhesion to their tissue and actively through ingestion by polyps (Martin et al., 2019; Corona et al., 2020). Their role as a sink for microplastics may be temporary when adhered microplastics are shed from coral tissue or when they are ingested and then egested from polyps, or permanent when microplastics are incorporated into the coral skeleton (Ding et al., 2019; Hierl et al., 2021; Krishnakumar et al., 2021; Reichert et al., 2022). Corals may be able to shed microplastics from themselves similar to the way they deal with sediment (Stafford-Smith and Ormond, 1992; Martin et al., 2019). However, the mechanisms have yet to be revealed empirically, and some corals appear to not display acclimatory coping mechanisms (Rades et al., 2022). Regardless, very little is known about the factors that influence how corals and microplastics interact.

In the current study, we considered three factors that could potentially affect interactions between corals and microplastics: water flow, microplastics type, and coral morphology, and we identified coral condition as another potential factor while performing the experiments. Depending on their location within reefs, corals experience different water flow regimes, from calm lagoons to highly dynamic areas of the forereef. Prior studies have shown that water velocity influences the feeding rate and interactions with zooplankton prey in corals (McFadden, 1986; Patterson, 1991; Johnson and Sebens, 1993; Sebens et al., 1997, 1998). Water velocity also affects the hydrodynamic environment around the coral, e.g. controlling the boundary layer thickness over the coral and the local turbulent mixing, which in turn affects both the likelihood that particles, such as zooplankton or microplastics, encounter a coral polyp and the coral's overall particle capture efficiency.

Microplastics are considerably variable in their physical and chemical properties, which could impact how corals interact with them. They occur in diverse forms, such as fragments, fibers, films, beads, and nurdles, which could influence their bioavailability to corals. In addition, the chemical composition varies between different types of plastics depending on the type of polymer and its chemical additives, such as plasticizers, flame retardants, etc. Chemicals in microplastics have been suggested to provide a cue that results in the preferential ingestion of microplastics over food (Allen et al., 2017; Rotjan et al., 2019). However, our previous work showed that at least one coral species does not preferentially ingest microplastics over prey (Axworthy and Padilla-Gamiño, 2019), suggesting that not all corals are stimulated to feed on plastics, or that corals may respond differently to different types of microplastics. Moreover, experiments investigating coral and microfiber interactions have not been reported despite them

being the most common type of microplastics recovered from coral reefs (Ding et al., 2019; Lei et al., 2021; Tang et al., 2021; Lim et al., 2022; Zhou et al., 2022).

At both the inter- and intra-specific levels, corals display different morphologies. Coral growth forms can be dependent on extrinsic physical factors such as light, water velocity, and sedimentation (Chappell, 1980). In contrast, a coral's morphology can impact intrinsic factors such as susceptibility to stressors and feeding efficiency (Helmuth and Sebens, 1993; Loya et al., 2001; Palardy et al., 2005; Mizerek et al., 2018). In addition, a coral colony's orientation to water flow and proximity to other corals can affect coral's feeding dynamics across the colony (McFadden, 1986; Helmuth and Sebens, 1993; Sebens et al., 1998). Morphological characteristics, such as a coral's growth form or surface ornamentation, affect the fluid flow around them, potentially influencing the patterns observed in coral feeding studies.

Another potential factor that could affect coral and microplastics interactions is the condition (tissue presence) of the coral fragment. As some corals grow upward, or transition to a different growth form, older coral tissue can die off leaving exposed skeleton on lower parts of the colony. We observed this in *Montipora capitata* colonies, which were collected from the wild in their branching form, but transitioned to a plating morphology in our aquaria, leaving areas of non-living, exposed skeleton on the coral fragments (Fig. 3.1). During preliminary experiments, we observed microplastics adhered to the non-living skeletal parts of these fragments, raising the question of whether coral skeletons or other non-living, biologically produced reef structures could be a sink for microplastics in addition to living corals. We considered that the non-living skeleton of *M. capitata* would be suitable for microplastics adhesion because it has a rough surface texture and can grow a potentially sticky biofilm.

In this study, we experimentally tested the effects of flow velocity, microplastic type, and coral species on microplastic ingestion and adhesion rates. Experiments were performed under three different average water velocities with a concoction of three different types of microplastics on four different coral species with differing morphologies. Additionally, we investigated differences in microplastic adhesion rates between living and non-living parts of *M. capitata*. Our aim is to better understand which environments, what types of microplastics, and which coral species or parts of coral reefs are more likely to interact with microplastics and what this may indicate regarding their role as a sink for microplastic and the potential risk of damage resulting from exposure to these pollutants.

3.3 Materials and Methods

3.3.1 *Species*

To test the effect of morphology on microplastics ingestion and adhesion, we used four different coral species, ordered here by their apparent increasing morphological complexity: *Leptoseris sp*. (encrusting/plating), *Montipora capitata* (plating/branching), *Montipora digitata* (simple branching), and *Pocillopora acuta* (formerly *P. damicornis*; complex branching). In June 2019, fragments of *M. capitata* and *P. acuta* were collected from the lagoon surrounding the Hawai‘i Institute of Marine Biology (HIMB), Kāne‘ohe Bay, Oahu, Hawai‘i while snorkeling (DAR Special Activities Permit No. 2020-44). Fragments were removed from colonies using toenail clippers (Revlon, USA), and maintained in outdoor, flow-through seawater tanks at HIMB for 2 – 3 days until they were packed and shipped overnight to the University of Washington (UW). *M. capitata* were packed in Whirl packs with seawater and *P. acuta* were wrapped in bubble wrap and wetted with seawater for shipping.

At UW, the coral fragments were glued to ceramic base and maintained in 150 L aquariums filled with artificial seawater (Instant Ocean, 34.5 ppt salinity). Corals were fed twice a week with Benereef coral food (Benepets, USA) according to the manufacturer's instructions. The tanks were illuminated using Aqua Illumination Hydra 26 LED lights. Initially, daytime photosynthetic active radiation (PAR) was ~80 μmol m^{-2} s^{-1}, but this resulted in paling of coral tissue and some mortality, so the lights were reduced to PAR of 40 μmol m^{-2} s^{-1}. The light regime was adjusted so sunrise occurred at 0300, ramping up in intensity for 2 hours, maintained for 8 hours, then ramping down for two hours to darkness at 1500. The temperature of the tanks was maintained at 26.1º C. *M. capitata* and *P. acuta* were maintained under these conditions for over two years. During this time, *M. capitata* changed growth form from branching to plating morphology, presumably due to lower PAR levels than it experienced in Hawai'i (Padilla-Gamiño et al., 2014). It should also be mentioned that after its morphological change, plating *M. capitata* did not regrow prominent verrucae, and patches of tissue, mainly towards the bottom of the branching fragments, died, leaving bare skeleton remaining (Fig. 3.1). In August 2020, the saltwater used in the tanks was changed from artificial to natural seawater. The natural seawater was filtered to 1 μm and UV sterilized. The salinity of the natural seawater was considerably lower than the artificial seawater, so the corals were acclimated from 34.5 ppt to 32 ppt salinity over two months, during water changes. In the Spring of 2022, fragments of *Leptoseris sp*. and *M. digitata* were purchased from a local aquarist and maintained in the same aquariums described above until experiments were performed in Autumn, 2022.

3.3.2 *Microplastics treatment*

To test the effect of microplastic type on ingestion and adhesion, three types of microplastics were used: polyester fibers, acrylic fibers, and polystyrene fragments. These microplastics were

weathered in Bellingham Bay, Washington, as part of an experiment that assessed weathering on the physical and chemical properties of microplastics (Johnson, 2021). In brief, green polyester felt and red acrylic yarn were cut into ~1 cm^2 and 1cm pieces, respectively, and frozen in Ultrapure water. These cubes were then blended to further reduce the fiber size. Black polystyrene forks were first ground into smaller pieces before being frozen in Ultrapure water and blended into micro-sized fragments. The ground fibers and fragments were sieved to 1,000 and 63 µm. The fibers and fragments remaining on the 63 µm sieve were then deployed in Bellingham Bay, WA, in 10 µm nylon mesh bags in Autumn 2019 and left in the field for approximately 2.5 months. Upon removal, the nylon bags containing microplastics were squeezed to remove excess seawater, wrapped in foil, and stored at -20º C. A subset of each microplastic type was sent to the University of Washington for the current study. The polyester and acrylic fibers were cut further with scissors and measured using a microscope camera and software (Amscope, MU503B, USA), resulting in mean (± SD) fiber lengths of 174.0 ± 123.8 µm and 154.2 ± 11.4 µm, respectively. The black polystyrene fragments were measured using particle analysis (Image J) and had a mean ferret diameter of 24.8 ± 16.4 µm. Density of each microplastic type was estimated using dilutions of sodium iodide in deionized water according to Li et al. (2018), resulting in density ranges of 1.3 – 1.4 mg ml^{-1}, 1.1 – 1.2 mg ml^{-1}, and 1.1 – 1.2 mg ml^{-1}, for polyester fibers, acrylic fibers and polystyrene fragments, respectively. Polymer composition was confirmed using µ-FTIR (Nicolet iN10, Thermo Fisher; Fig. S3.1).

Stock solutions of each microplastic type were prepared by suspending the particles in filtered (1.2 µm) seawater in clear plastic containers stored in a glass lab cabinet. It is possible that the microplastics grew some biofilm, but potential microbial and algal colonization was not assessed. Prior to each experiment, a mixture of equal parts of each plastic type (250 particles L^{-}

^{1}) was prepared to a total treatment concentration of 750 particles L^{-1}. Based on a prior experiment where *P. acuta* did not ingest microplastics unless food was available (Axworthy and Padilla-Gamiño, 2019), the supernatant of a coral food solution (1/4 tsp Benereef in 50 ml of filtered seawater) was filtered and added to each experimental treatment.

3.3.3 *Experimental system*

Experiments were conducted in a custom-designed, oval-shaped flume (Fig. 3.2, Fig. S3.2). The flume was designed to produce low flows within a closed, recirculating system to test microplastic exposure in relevant conditions for corals. The flume was 91 cm long, 61 cm wide, and 30.5 cm deep, and the test area had a length of 30.5 cm. During experiments the flume was filled to a depth of 29 cm. The flume was fitted with a heater, thermometer, and variable speed circulation pump (Nero 3, Aqua Illumination). A laminar flow apparatus was constructed using plastic straws to reduce and straighten the flow. To measure the flow velocity, we used particle tracking velocimetry (PTV), through a sidewall of the test section. Time-averaged velocity profiles over depth in the center of the tank were measured over a range of pump speeds, and the depth-averaged velocity was used to construct a calibration curve (Fig. S3.3). The fluid velocity was relatively two-dimensional and uniform, with a relatively small boundary layer at the bottom (Fig. S3.4). A stage for the coral fragments was constructed out of egg crate and PVC pipe so that the corals sat 6.5 cm above the floor inside the flume. The flume was illuminated during the day using the same light regime and PAR levels as the holding tanks. During experiments, the system was illuminated with a separate red LED light to not disrupt feeding behavior. A viewing window allowed us to observe the corals during the experiments.

At 0800, seawater was added to the system, and the pump and heater were turned on. Experiments were performed at three different water velocities that corals from Kāneʻohe Bay experience naturally: 2.6, 5.0, and 7.5 cm s^{-1} (Jokiel, 1991). The water temperature was maintained at 26.1º C and salinity at 32 ppt. At 0830, two coral fragments of the same species were placed on the stage to acclimate them to the experimental settings. Corals were placed with one in front of the other, separated by 6.5 cm. At 1500, the feeding trials began by adding one dose of the microplastics mixture to the system. For all corals except *Leptoseris sp*., which did not expand its tentacles, we observed expanded tentacles before each experiment. One hour later, the corals were removed from the system and immediately put under a microscope to quantify adhesion. The system was drained, and all its components were rinsed heavily at least three times with freshwater to remove salt and microplastics.

3.3.4 *Quantifying adhesion*

Adhesion was quantified visually under a stereo microscope (Amscope). Black polystyrene fragments and red acrylic fibers were visible under the microscope light. The green polyester fibers were nearly transparent under the microscope light, so UV light was used to identify them. In contrast to Martin et al. (2019), we were unable to differentiate adhered and strongly adhered particles, so any microplastics that were attached to the coral tissue that were not fully or partially in the mouth of a polyp were considered adhered. Each particle type was counted on the front and back side of each fragment, and then removed from the fragment so that they would not be counted again later when quantifying ingestion. Coral fragments were then wrapped in aluminum foil, placed in plastic bags, and frozen at - 20º C until they were analyzed for morphological measurements.

3.3.5 *Quantifying ingestion*

Microplastics ingestion was quantified by dissection under a dissecting microscope following 3D scanning (see below). An ingested particle was defined as a fragment or fiber observed partially or fully in the mouth or gut of a polyp. Prior to dissection, the frozen coral fragments were thawed at room temperature for approximately one hour. Using dissection probes, coral polyps were splayed open and investigated for microplastics. For *Leptoseris sp*. and *M. capitiata*, every polyp on each fragment was investigated for microplastics. For *M. digitata* and *P. acuta*, 100 randomly selected polyps on the front and 100 polyps on the back side of each fragment were dissected. Microplastic type and the side of the coral they were observed on were recorded.

3.3.6 *Morphological traits*

3D meshes of the coral fragments were obtained using the Artec Spider 3D scanner and Artec Studio 13 software, according to Reichert et al. (2016) and exported as .obj files. The surface area and volume of the whole coral fragments, as well as the surface area of the up and downstream sides, were obtained from the 3D mesh .obj files using the "compute geometric measures" function in Meshlab (ver. 2022.02).

Morphological traits, including two metrics for volume compactness: sphericity and convexity, and one metric for surface complexity: packing, were calculated based on the equations in Zawada et al. (2019b). Another metric for surface complexity, fractal dimension, was calculated using the Bouligand–Minkowski 3D Toolbox developed by (Reichert et al., 2017; https://www.facom.ufu.br/~backes/mink3d.html). For a more detailed description of 3D scanning, processing, and morphological traits calculations, see the Supplementary Materials.

3.3.7 *Normalization and Corrections*

All microplastic ingestion and adhesion counts were normalized to the surface area (cm^2) of coral fragment or the surface area of the side (up or downstream) of the fragment.

Although the microplastic treatments consisted of equal concentrations of each particle type, they did not remain equally suspended during the experimental trials because they naturally settled out over time at a settling speed controlled by the particle characteristics (i.e., size, shape, and density) and the flow conditions. To account for this, experiments were performed as described above, without corals, to determine correction factors used to standardize ingestion and adhesion rates based on the mean concentration of each microplastic type available to interact with the corals under each flow velocity. For each experiment, one dose of the microplastic treatment was added to the system and allowed to disperse for 1 min, then 25 ml of water was sampled three times every 10 minutes for one hour (sampled at 1, 11, 21, 31, 41, 51, and 61 min.). Separate experiments were performed at each water velocity so that microplastic concentrations could be determined for each experimental condition. The procedure was repeated five times to increase sample size (n = 105 for each flow velocity). The water samples were filtered onto 1.2 µm glass fiber filters, and each microplastic type was counted. To determine correction factors, first the counts of each microplastic type from all samples under each flow velocity were averaged to find the mean concentration (C) of each microplastic type under each condition:

$$C_{t,f} = \overline{MP_{t,f}}$$

Where MP equals the particle count, t equals the microplastic type, and f equals the flow velocity. Next, the average proportion (P) of each microplastic type under each flow velocity was determined by dividing C by the sum of C for the relevant microplastic type and flow velocity:

$$P_{t,f} = \frac{C_{t,f}}{\sum_{t,f=1}^{3} C_{t,f}}$$

Finally, to correct ingestion and adhesion rates across all microplastic types and flow conditions for comparison of the observed values, P for each microplastic type under each flow velocity was divided by the median P value (acrylic fibers, 2.6 cm s^{-1}), giving the correction factor (F), for each microplastic type under each flow velocity:

$$F_{t,f} = \frac{P_{t,f}}{median(P_{t,f})}$$

Corrections were made to microplastic ingestion and adhesion rates by diving the normalized particle count from each coral (per cm^2) by the respective F. The mean concentrations and correction factors for each microplastic type under each flow velocity are reported in Table 3.1.

Although these corrections altered the actual ingestion and adhesion rates observed, they were performed to allow for relative comparisons across microplastic types and flow conditions on these processes. Accordingly, the ingestion and adhesion rates reported can be interpreted as if the concentration of each microplastic type remained equal throughout the experiments.

One more correction was made to be able to test for the effects of the variables while accounting for particle flux, i.e., the increased chance of particle encounter as flow increases. For these corrections, microplastic ingestion and adhesion rates (per cm^2, and corrected as described

above), were divided by their respective flow treatment velocity divided by the minimum flow velocity (2.6 cm s^{-1}). Considering both corrections, the reported values for ingestion and adhesion rates for polyester fibers at 2.6 cm $^{-1}$ are the actual values observed in the experiments, while reported data from all other microplastic type and flow combinations are either higher or lower than observed values depending on their correction factors.

3.3.8 *Statistics*

Effects of experimental variables on the corrected ingestion and adhesion rates of microplastics in corals were tested using the "aovperm" function in the R package 'permuco' (Frossard and Renaud, 2022) in R Studio (ver. 2023.09.1). This randomization procedure was used because the data did not meet the normality nor the equal variance assumptions of a typical ANOVA due to the high occurrences of zeros in the data (no microplastic ingestion or adhesion by corals in some treatments). Models were fit for either ingestion or adhesion rate, with effects of flow velocity, species, microplastic type and the interactions between them, and the effect of side (up or downstream) treated as main effects. The aovp function was run with 10,000 iterations and results were considered significant when $p < 0.05$.

Analysis of variance and Tukey's post hoc tests were used to test for differences in morphological traits between species. A Pearson's correlation test was performed using the base R function "cor" to test for correlations between microplastic ingestion and adhesion rates, and morphological traits.

3.4 RESULTS

3.4.1 *Morphology*

Morphological traits of the experimental coral fragments were quantified using surface area and volume data calculated from 3D meshes obtained for each fragment. Four traits were determined, including two metrics for volume compactness, sphericity and packing, and two metrics for surface complexity, convexity and fractal dimension (Fig. 3.3, Table S3.1). We aimed to capture increasing morphological complexity from the different growth patterns of the corals (*Leptoseris sp*. (mounding/plating), *Montipora capitata* (plating), *Montipora digitata* (simple branching), and *Pocillopora acuta/acuta* (complex branching). The morphological trait most aligned with morphological complexity among the coral species tested was sphericity, which decreased as morphological complexity increased. Results from ANOVA and post-hoc Tukey pairwise test show that there is a significant effect of species ($R^2 = 0.72$, $F = 77.09$, $p < 0.001$) and a significant difference between each pairwise comparison in sphericity between species. Correlation analysis showed that there was a weak negative correlation between microplastic adhesion and packing (Pearson's correlation, -0.312) but there were no other significant correlations between microplastic ingestion and adhesion and any other morphological traits (Table S3.2).

3.4.2 *Microplastic ingestion rates*

A total of 395 microplastics were ingested by 54 (out of 96) coral fragments. Of those, 83% were polyester fibers, 12% were acrylic fibers, and 5% were polystyrene fragments. Microplastics were ingested by all coral species but not by every coral fragment. Specifically, microplastics were ingested by 25% of *Leptoseris sp*., 71% of *M. capitata*, 54% of *M. digitata*, and 75% of *P.*

acuta fragments. Total microplastic ingestion rates per coral fragment (corrected for microplastic concentrations) ranged from 0 to 11.3 particles cm^{-2}. Average total microplastics ingestion by species was highest for *P. acuta* (1.11 ± 2.39, mean ± sd particles cm^{-2}), followed by *M. digitata* (0.48 ± 0.98), *M. capitata* (0.17 ± 0.23), and *Leptoseris sp*. (0.10 ± 0.26).

To test the effects of species, water flow, microplastic type, and side of the coral fragments (up or downstream) on corrected microplastic ingestion rates, we ran a permutation ANOVA. When microplastic ingestion was corrected only for microplastic concentrations and not for flow velocity, the model showed a significant effect of species ($F = 5.93$, $df = 3$, $p = 0.0003$), microplastic type ($F = 15.40$, $df = 2$, $p = 0.0001$), and the interaction between species ~ microplastic type ($p < 0.01$), but no significant effect of flow, side of the fragment, or any other interactions (Figs. 3.4A and S3.5, Table S3.3). Similarly, when microplastic ingestion was corrected for both microplastic concentrations and flow velocity, the model showed a significant effect of species ($F = 7.17$, $df = 3$, $p = 0.0001$), microplastic type ($F = 15.81$, $df = 2$, $p = 0.0001$), and the interaction between species ~ microplastic type ($p < 0.01$), but no significant effect of flow, side of the fragment, or any other interactions on microplastic ingestion rates (Figs. 3.4B and S3.6, Table S3.4).

3.4.3 *Microplastic adhesion rates*

A total of 1694 microplastics adhered to 93 (out of 96) coral fragments. Of those, 56% were acrylic fibers, 34% were polyester fibers, and 10% were polystyrene fragments. Microplastics adhered to all coral species but not to every fragment, including 96% of *Leptoseris sp*., 100% of *M. capitata*, 96% of *M. digitata*, and 96% of *P. acuta* fragments. Total microplastic adhesion rates per coral fragment (corrected for microplastic concentrations) ranged from 0 to 11.2

particles cm^{-2}. Average total microplastic adhesion by species was highest for *M. digitata* (3.40 ± 3.62, mean ± sd particles cm^{-2}), followed by *Leptoseris sp.* (1.86 ± 1.40), *P. acuta* (0.99 ± 1.27), and *M. capitata* (0.98 ± 0.93). Overall, adhesion rates were 3.9 times greater than ingestion rates.

The effects of species, water velocity, microplastic type, and side of the coral fragment was tested using a permutation ANOVA. When microplastic adhesion was corrected only for microplastic concentrations and not for flow velocity, the model showed a significant effect for all variables: species ($F = 22.69$, $df = 3$, $p < 0.0001$), flow ($F = 20.53$, $df = 2$, $p < 0.0001$), microplastic type ($F = 28.19$, $df = 2$, $p < 0.0001$), side of the fragment ($F = 17.95$, $df = 1$, $p < 0.0001$), and every interaction combination ($p < 0.01$) except for species ~ flow ~ microplastic type (Figs. 3.5A and S3.7, Table S3.5). When microplastic adhesion was corrected for both microplastic concentrations and flow velocity, there was a significant effect of species ($F = 17.37$, $df = 3$, $p = 0.0001$), microplastic type ($F = 28.53$, $df = 2$, $p = 0.0001$), side of the fragment ($F = 17.51$, $df = 1$, $p = 0.0002$), and the interactions between species ~ flow and species ~ microplastic type ($p < 0.01$), but not flow, or the interactions between flow ~ microplastic type or species ~ flow ~ microplastic type, on adhesion rates (Figs. 3.5B and S3.8, Table S3.6).

3.4.4 *Microplastic adhesion on living and dead parts of coral fragments*

To test whether microplastics adhered more to living or dead parts of coral fragments, we quantified adhesion on *M. capitata* because it was the only species that had both living and dead areas on each fragment. Total adhesion rates, corrected for microplastic concentrations, of all microplastic types were 3.6 times higher in the dead areas (3.6 ± 2.7 particles cm^{-2}) than in living areas (1.0 ± 0.9 particles cm^{-2}) of the fragments. Polyester and acrylic fibers were 4.4 and 3.9

times, respectively, more likely to adhere to the dead parts of *M. capitata* than polystyrene fragments.

When microplastic adhesion rate was corrected only for microplastic concentrations, and not for flow velocity, permutation ANOVA showed that flow ($F = 12.59$, $df = 2$, $p = 0.0001$), condition (live vs dead; $F = 52.24$, $df = 1$, $p = 0.0001$), and microplastic type ($F = 17.76$, $df = 2$, $p = 0.0001$), and the interactions flow ~ condition, condition ~ microplastic type, and flow ~ condition ~ microplastic type ($p < 0.01$), significantly affected microplastic adhesion rates (Fig. 3.6A, Table S3.7). When adhesion rates were corrected for both microplastic type and flow velocity, flow ($F = 3.61$, $df = 2$, $p = 0.0243$), condition ($F = 47.95$, $df = 1$, $p = 0.0001$), microplastic type ($F = 19.45$, $df = 2$, $p = 0.0001$), and the interaction between condition and microplastic type significantly affected adhesion rates ($p < 0.01$) (Fig. 3.6B, Table S3.8).

3.5 Discussion

In this study, we investigated the effects of water flow, microplastic type, and coral morphology on microplastic ingestion and adhesion rates for four species of reef-building corals. Additionally, we compared microplastic adhesion rates between living and dead parts of coral fragments. Our results show that (1) adhesion rates (per cm^2) are nearly four times greater than ingestion rates, (2) ingestion rates are affected by coral species and microplastic type but not water velocity, (3) adhesion rates are affected by species, water velocity, microplastic type and orientation to water flow, and (4) microplastics adhere more to dead than living parts of coral fragments. Collectively, these findings highlight some of the factors that impact how corals interact with microplastic pollution.

3.5.1 *Patterns of ingestion and adhesion rates under different flow*

Water velocity and orientation to the flow significantly affected microplastic adhesion rates but not ingestion rates. This was surprising since flow velocity had been shown to be an important factor affecting zooplankton and particle capture rates in scleractinian corals (Sebens and Johnson, 1991; Sebens et al., 1997, 1998; Piniak, 2002; Purser et al., 2010; Orejas et al., 2016) and other aquatic suspension feeders (Labarbera, 1984; Shimeta and Jumars, 1991; Espinosa-Gayosso et al., 2021). Theoretically, the chance for particles to encounter a stationary organism increases with water velocity because it brings a higher flux of particles to the organism. However, this is not always reflected in coral prey capture rates. For example, prey capture rate increased with water velocity in *Madracis mirabilis* and *Montastraea cavernosa* but not in *Porites porites* (Sebens et al., 1998) and decreased with flow in the cold water coral, *Lophelia pertusa* (Purser et al., 2010; Orejas et al., 2016). At very high water velocities (40 – 50 cm s^{-1}), prey capture rate decreased in *Madracis mirabilis* (Sebens et al., 1997). These discrepancies between studies and species were likely due to factors that affect the ability of a coral's tentacles to handle prey or particles, such as tentacle deformation under high flow, increased momentum of prey or particle items, or dislodgment of prey or particles from tentacles under high flow (Purser et al., 2010). In the present study, although not significant, there were notable differences in microplastic ingestion rates for *M. digitata* and *P. acuta*. For *M. digitata*, microplastic ingestion rates were small under low and moderate flow velocities; however, at high velocity, the ingestion rate increased by over 4-fold. For *P. acuta*, microplastic ingestion rates under low flow were two to three times higher than for all other species, increasing nearly three-fold under intermediate flow and decreasing again by nearly fifty percent under high flow.

Adhesion, on the other hand, was significantly affected by water velocity and orientation to the flow. This was most notable in the patterns of increasing microplastic adhesion rates with increasing water velocity in *M. digitata* and *P. acuta*, and aligns with the theory of higher particle encounter rates as flow increases (Labarbera, 1984; Shimeta and Jumars, 1991; Espinosa-Gayosso et al., 2021). Similarly, the effect of orientation to the flow was most notable for *M. digitata* and, to some extent in *M. capitata* and *P. acuta*, where for all flow conditions, adhesion rates were higher on the upstream side of coral fragments. An opposite pattern, in regards to flow orientation, was observed in *Madracis mirabilis* and *Agaricia agaricites,* where under low flow, prey ingestion was higher on the upstream side of the corals but under high flow became greater on the downstream side (Helmuth and Sebens, 1993; Sebens et al., 1997). They attributed these shifts to tentacle flattening of upstream-orientated polyps, an increase in turbulent eddies in the wake on the downstream side of coral fragments under high flow, and asymmetrical particle concentrations on either side of the coral colonies due to the flow's boundary layer around the coral.

A possible explanation for the different patterns observed in the current study, with regards to adhesion and orientation to flow, is the mechanism by which suspension feeders encounter particles. Several mechanisms of particle capture by suspension feeding organisms have been proposed. Among these, the most important for seemingly passive suspension-feeding organisms are direct interception, inertial compaction, and gravitational deposition (Labarbera, 1984). Direct particle interception occurs when a particle moving along a streamline is large enough to penetrate the boundary layer and then adheres to (or is ingested by) an object it encounters (Rubenstein and Koehl, 1977; Labarbera, 1984). When the particle is relatively small, and the boundary layer is relatively thick, as would be the case under low flow, particles are more likely

to follow the streamline and pass by the object. This mechanism is thought to be the most prevalent for suspension-feeding planktivores like corals since most biological particles are neutrally buoyant and small (Strathmann, 1971; Koehl, 1977; Rubenstein and Koehl, 1977; Labarbera, 1984; Helmuth and Sebens, 1993). However, for particles that are denser than seawater, like the microplastics used in this study (density range: 1.1 – 1.4 mg ml^{-1}), inertial compaction is more likely the dominant process. When particles are denser than seawater, their inertia can cause them to deflect from the streamlines, penetrate the boundary layer more easily, and encounter an object. Consequently, more particles are likely to adhere to the upstream side of corals, whereas, on the downstream side, adhesion might be reduced where particle encounter is primarily driven by wake turbulence and direct interception. This was particularly evident in *M. digitata* which is characterized by relatively thin branches spaced widely apart. As a result, the flow around it would have a lower Reynolds number, leading to a smaller wake and, thus, less turbulence and eddies on its downstream side. It is also possible that gravitational deposition could play a role in microplastic adhesion, but this process becomes less important with increasing flow.

3.5.2 *Species affected microplastic ingestion and adhesion rates*

Species was a significant factor for both ingestion and adhesion rates. We chose four coral species that display a gradient of morphological complexity to investigate whether morphology impacts coral and microplastics interactions. Ordered from lowest to highest complexity, we used *Leptoseris sp*. (encrusting/plating), *M. capitata* (plating/branching), *M. digitata* (simple branching), and *P. acuta* (complex branching). The morphological traits that best fit this order of complexity were two measures of volume compactness: sphericity and convexity (Zawada et al., 2019a). Sphericity showed differences among all species and convexity followed a similar

pattern, except for the inability to distinguish between the two branching species, *M. digitata* and *P. acuta*. This demonstrates a strong alignment with the overall gross morphologies described for the corals (Zawada et al., 2019a, 2019b). However, neither of these metrics correlated with microplastic ingestion or adhesion rates. Likewise, surface complexity metrics, packing and fractal dimension did not correlate to microplastic ingestion and adhesion. Surface complexity metrics capture the gradient from smooth to roughness, and we hypothesized that interactions between corals and microplastics would correlate positively along this gradient. However, these metrics also did not align with the complexity gradient of corals in this study, nor did they correlate with microplastic ingestion and adhesion rates.

Microplastics were ingested by all species tested, but ingestion rates were relatively low for all species except *P. acuta*. This aligns with our previous work, where *P. acuta* ingested significantly more microplastics than *M. capitata* (Axworthy and Padilla-Gamiño, 2019) and other studies that demonstrate species-specific differences in microplastic ingestion rates (Hankins et al., 2018, 2021, 2022; Reichert et al., 2018; Martin et al., 2019). Differential microplastic ingestion rates have been linked to coral's calyx diameter or polyp size and microplastic size (Martin et al., 2019; Hankins et al., 2022). In the current study, the coral species tested had similar polyp sizes (~ 0.8 – 1 mm), and no significant correlation between fragment morphology and microplastic ingestion was observed, suggesting that other processes might be at play.

Differences in heterotrophic feeding rates and feeding strategies likely explain some differences in microplastic ingestion patterns between species. Corals can feed actively via tentacles and the use of nematocysts, passively via suspension using mucus with the aid of cilia, or employ some

degree of both methods (Lewis and Price, 1975). Corals of the genus *Leptoseris* have been described as being suspension feeders (Schlichter, 1991; Backstrom et al., 2024), while corals in the family Acroporidae, which includes the genus *Montipora*, have been described as employing both methods, and *P. acuta* has been shown to be mainly a tentacle feeder (Lewis and Price, 1975; Anthony, 1999). If these feeding strategies remain consistent within coral families, then the gradient from suspension to tentacle feeding might provide insight into the species-specific differences in microplastic ingestion. Specifically, a higher ratio of tentacle to suspension feeding may correspond to increased capture rates. This could also explain why only 25% of *Leptoseris sp*. fragments ingested any microplastics.

Furthermore, polyp orientation could influence microplastic ingestion rates. The *Leptoseris sp*. and *M. capitata* fragments used had upward-facing polyps orientated parallel to flow and lower relative ingestion rates, whereas *M. digitata* and *P. acuta* had laterally orientated polyps orientated perpendicular to flow and ingested more microplastics overall. This hypothesis relies partially on gravitational deposition being negligible and emphasizes that the likelihood of polyps encountering microplastics is more influenced by direct interception or inertial compaction. In this scenario, particles are more likely to flow right past horizontal surfaces than vertical ones. This is supported by the work of Helmuth and Sebens (1993) where they observed higher capture rates by polyps of *A. agaracites* orientated into the flow than polyps orientated parallel to the flow.

Microplastics adhesion was relatively low and similar for *M. capitata* and *P. acuta* but increased for *Leptoseris sp*. and was highest for *M. digitata*. Martin et al. (2019) attributed microplastic adhesion in corals to skeletal characteristics and suggested that mucus was responsible for

species-specific differences in adhesion rates. Although not quantified, we did observe mucus on some of the coral fragments during the exposure trials. In these cases, mucus was observed as strands originating on the coral tissue and trailing into the water column. Mucus as a defense mechanism varies significantly between coral species (Stafford-Smith and Ormond, 1992) and some corals use mucus as a defense against sedimentation. When sediment levels increase in the field, these corals produce mucus, which entraps particles and then is sloughed off, effectively removing the sediment and other particles from the surface of the coral (Stafford-Smith and Ormond, 1992). Several studies have reported an acute increase in mucus production by corals under microplastic exposure (Reichert et al., 2018; Martin et al., 2019; Mouchi et al., 2019; Hierl et al., 2021; Jiang et al., 2021; Bejarano et al., 2022). Martin et al. (2019) suggested that corals use mucus as a defense mechanism by trapping microplastics in it and then releasing it and used that to explain the relatively low adhesion rate on *Acropora hemprichii*. Conversely, Hierl et al. (2021) speculated that high levels of mucus enhanced microplastics trapping, resulting in higher incorporation of microplastics into the corals' tissue and, ultimately, their skeleton. Bejarano et al. (2022) also observed increased mucus and particle entrapment in corals exposed to microplastics and sediment and noted that in some cases, the mucus entrenched with particles was sloughed off quickly, while at other times, the mucus remained on the corals for more than 12 hours. Indeed, it appears that coral mucus serves as a trap for microplastics, but whether or for how long the microplastics are incorporated into the coral (either via ingestion or adhesion) depends on how efficiently the coral can slough away the mucus.

3.5.3 *Microplastic type affected ingestion and adhesion rates*

Microplastics type was a significant factor affecting both ingestion and adhesion. We hypothesized that corals would ingest more polystyrene fragments than either fiber type because

the fragments were smaller and could fit more easily into the coral polyps. However, neither *Leptoseris* sp. nor *M. capitata* appeared to discriminate against any plastic type, although there was some variation between different flows. In contrast, *M. digitata* and *P. acuta* ingested considerably more polyester fibers than either acrylic fibers or polystyrene fragments, regardless of flow. It has been proposed that plastics release phagostimulants, driving microplastics ingestion by corals (Allen et al., 2017). In their analysis, Allen et al. (2017) reported that seven chemically different types of pristine (not fouled or weathered) plastics were ingested by ≥ 80% of corals that were offered to them. The only plastic type consistent between Allen et al. (2017) and the present study was polystyrene, which was scarcely ingested here by any species, especially *M. digitata* and *P. acuta*. Moreover, our previous work with polyethylene microbeads suggested that some corals, such as *P. acuta*, only ingest microplastics when stimulated by prey (Axworthy and Padilla-Gamiño, 2019). To our knowledge, no studies have investigated interactions between corals and polyester or acrylic microplastics. However, polyester microfibers have been recovered from the tissues of wild corals (Ding et al., 2019; Krishnakumar et al., 2021; Lei et al., 2021; Tang et al., 2021; Lim et al., 2022; Zhou et al., 2022). Although, it is possible that polyester and other microplastics, as proposed by Allen et al. (2017), leach chemicals that stimulate feeding this should be further investigated. The weathering of the microplastics in our treatments addresses the question of how environmentally relevant microplastics would interact with corals. During the weathering process, chemicals can leach out of plastics, with the leaching rate depending on factors such as polymer type and plastic additives (Gewert et al., 2015). Johnson (2021) used high-resolution mass spectrometry to characterize the leachates from the weathered microplastics used in this work; compared to unweathered microplastics they found differences in the chemical composition. This could

impact the potential for phagostimulant release from different plastics, thus affecting the ingestion rates observed here. Moreover, micro-fibers may be easier for corals to capture from the water column than micro-fragments. Or, polyester fibers, which are denser than acrylic fibers and polystyrene fragments, may be less likely to be swept from a coral's feeding structures after they come in contact since they are heavier than the other particle types. Future work could investigate whether weathering, or the chemical and physical properties of plastics influence their likelihood of interacting with corals.

Both polyester and acrylic fibers adhered to all coral species at much higher rates than polystyrene fragments. We hypothesized this to be the case because their fibrous shape could cause them to behave less tracer-like making them deviate from the fluid streamlines greater than the more compact-shaped fragments. Moreover, their length and flexibility could make fibers more likely to become entangled on the corals' surface structures. To our knowledge, there have not been any experimental studies investigating interactions between corals and micro-fibers, but they have been observed on the surface of corals collected from the wild (Lim et al., 2022). As discussed above, mucus entrapment appears to be a mechanism for microplastics adhesion on corals (Reichert et al., 2018; Martin et al., 2019; Mouchi et al., 2019; Hierl et al., 2021; Jiang et al., 2021; Bejarano et al., 2022). However, it is unclear whether there is a relationship between mucus and adhesion of different microplastic types, which could be an area for future study.

3.5.4 *Microplastics adhered more to dead than living parts of corals*

Microplastic adhesion was significantly greater on dead parts of *M. capitata* than on living parts of the fragments, suggesting that either 1) the living parts of *M. capitata* are less capable of trapping microplastics than its exposed skeleton, or 2) that the living tissue has some sort of

mechanism for reducing adhesion. We propose that the latter case is what occurred. A higher proportion of the microplastic fibers adhered to *M. capitata* were observed at the margin where tissue meets the skeleton (Fig. 3.7), compared to the living surface. This observation potentially indicates that the coral transported microplastics to this location. Alternatively, this could also be due to the tissue–skeleton interface being a "stickier" place for microplastics to adhere to. However, during an experimental trial, we observed a mucus strand on *M. capitata*, at the margin of where living tissue meets the exposed skeleton, which contained microplastics (Figure 3.8). After a few minutes, the mucus strand was sloughed from the coral, carrying away the microplastics. This observation suggests that *M. capitata* was actively removing the particles. This aligns with Martin et al. (2019) and Bejarano et al. (2022) who suggest that mucus acts as a defense against microplastics. In addition to mucus, corals may use other sediment defense mechanisms to remove microplastics, such as ciliary currents, tissue expansion, tentacle manipulation, polyp contraction, or some combination of these and mucus entrapment (Stafford-Smith and Ormond, 1992). An interesting area of future research could investigate how sediment rejection mechanisms are used by corals to remove microplastics (Rades et al., 2022).

3.5.5 *Implications for corals and reefs*

Coral reefs are highly dynamic environments where the different reef zones experience different flow regimes, and corals are subjected to various degrees of water movement. For example, corals on the fore reef may experience a gradient of tidal-influenced unidirectional flow, whereas corals on the reef crest may experience bidirectional, fluctuating flow due to waves. Our results indicate that under unidirectional flow, water velocity has a greater effect on microplastic adhesion than ingestion rates and that there are species-specific differences in how corals interact with microplastics. From a coral's standpoint, individual characteristics, growth patterns, and

geographic location play significant roles in determining the risk of microplastic exposure and the ability to remove these particles from the environment (Reichert et al., 2018, 2019; Martin et al., 2019; Corona et al., 2020; Hankins et al., 2021; Liao et al., 2021; Soares et al., 2023). For example, *M. digitata*, an Indo-Pacific species that occupies depths between 0 – 33 (Babcock et al., 2003; Sealifebase, n.d.), could experience few interactions with microplastics if it inhabits a shallow calm lagoon but has a high chance of interacting with microplastics if it grows several meters down in a high current area of the fore reef, assuming microplastics concentrations are similar in these areas.

Our objective was to assign or rank the likelihood of corals interacting with microplastics based on the flow conditions they experience, their morphology, and the type of microplastics in their environment. Based on our findings, it appears that fibers are the most likely type of microplastics to interact with corals, regardless of species or flow, which is important to consider given that fibers are the dominant type of microplastics found in reefs (Ding et al., 2019; Lei et al., 2021; Tang et al., 2021; Lim et al., 2022; Zhou et al., 2022). However, due to the diverse ingestion and adhesion rates observed among and within species under different flow conditions and the fact that many coral fragments did not ingest any microplastics and a few experienced no adhesion, it is difficult to make such broad generalizations based on our experimental variables. It is likely that intrinsic factors, such as feeding strategy and heterotrophic plasticity, play an important role in whether and how corals interact with microplastics. Regardless, our results highlight that factors that influence coral and microplastic interactions are complex, and to gain a better understanding of the mechanisms underlying these processes, more studies are needed.

As reported previously, adhesion appears to be a more important process than ingestion in the context of coral and microplastic interactions (Martin et al., 2019; Corona et al., 2020). However, we observed a much smaller ratio of adhesion to ingestion, 3.9:1, than the 40:1 ratio observed in those studies. This is likely due to experimental methods, where we counted adhesion looking at corals directly under a microscope, and our exposure time was one hour, while in those studies, adhesion was estimated by rinsing corals and counting particles in the resulting solution, and experiments lasted 28 hours. Regardless, the adhesion of microplastics on the coral's surface can lead to necrosis, bleaching, and overgrowth, which can lead to deposition into the skeleton (Reichert et al., 2018, 2022; Hierl et al., 2021). Multiple field studies have reported microplastics contamination in wild corals, yet to our knowledge, none have discriminated between ingestion and adhesion (Lei et al., 2021; Oldenburg et al., 2021; Tang et al., 2021; Raguso et al., 2022; Sabdono et al., 2022; Zhou et al., 2022). However, some studies allude to the possibility that the microplastics they recovered from corals are likely due to adhesion (Ding et al., 2019; Lim et al., 2022). Making the distinction between microplastic ingestion and adhesion by corals should be considered in future field studies.

The fact that microplastic adhesion was lower on living parts of coral than on exposed dead skeletons is promising because it indicates that (at least some) corals may be defending themselves from these pollutants. Yet, it also highlights that previously un-studied areas of coral reefs, i.e., non-living biogenic structures, might also be a significant sink for microplastics (Soares et al., 2023). Sediments have been extensively explored for microplastics (see review by Huang et al., 2021), and in giant clams, *Tridacna maxima*, passive adhesion on the surface of their shells was the dominant microplastic removal mechanism compared to ingestion (Arossa et al., 2019). Other potential unexplored sinks for microplastics in coral reefs could include

tubeworm casings, bivalve and mollusk shells, calcareous algae, and other bafflers that live in reef cavities and trap loose sediment. Moreover, particles that adhere to these structures could become trapped indefinitely in the reef by cementers that consolidate sediments into rock, serving as another mechanism for microplastic sequestration into coral reefs. An interesting area for future research could be to determine if microplastics affect lithification and what that would imply for reef accretion and dissolution processes. How permanent these potential sinks for microplastics are would depend on accretion and dissolution processes such as bioerosion, ocean acidification, and the growth and mortality of reef-building corals. This implies that, under global change, the role of coral reefs serving as long-term sinks for microplastics remains uncertain. There is still much we do not understand regarding the fate of microplastics pollution, however, when wondering where all the microplastics go in our oceans (van Sebille et al., 2015; Auta et al., 2017; Kane and Clare, 2019; Reichert et al., 2022), perhaps we need to broaden our search.

3.6 ACKNOWLEDGEMENTS

We would like to thank the Gates Coral Lab for hosting and supporting us during field work at the Hawaii Institute of Marine Biology. We thank Abby Goudy, Kat Arnett and Dylan Strauss for dissecting coral fragments. We are grateful to Jorden Allie Johnson for help acquiring weathered microplastics. We thank Jon Wittouck for technical assistance with aquariums and other laboratory materials. We are thankful to Kristin Privitera-Johnson and Mark Schurell for guidance with statistical analyses. We thank Katie Anderson, Michael Holland and the Burke Museum for their assistance with 3D modelling. This research was supported by the National Science Foundation's Division of Biological Oceanography (NSF CAREER, BIO-OCE, 2044840) and the Sloan Foundation Fellowship to JPG. This material is based upon work

supported by the National Science Foundation Graduate Research Fellowship Program (DGE1762114) awarded to JBA.

3.7 TABLES AND FIGURES

Table 3.1 Mean concentrations (C, particles per 25 ml), proportion (P) of the sum of all concentrations, and correction factors (F) for all microplastic (MP) types and flow velocities. Bolded values represent the median P which was used to standardize C.

	Flow (s^{-1})	*C*	*P*	*F*
Acrylic fibers	2.6	4.302	0.123	**1.000**
	5.0	5.544	0.159	1.289
	7.5	5.650	0.162	1.313
PET fibers	2.6	1.857	0.053	0.432
	5.0	2.649	0.076	0.616
	7.5	4.267	0.122	0.992
PS fragments	2.6	3.460	0.099	0.804
	5.0	3.526	0.101	0.820
	7.5	3.708	0.106	0.862

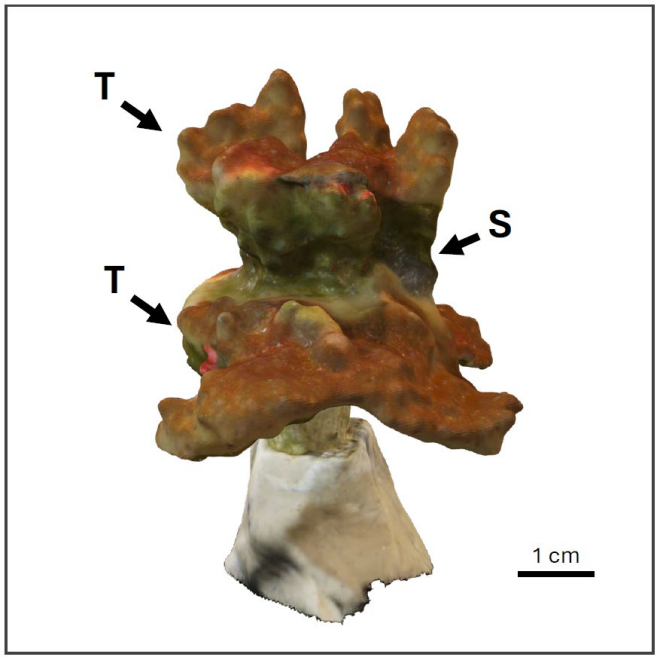

Figure 3.1 Fragment of Montipora capitata displaying portions of living tissue (T) and exposed skeleton (S).

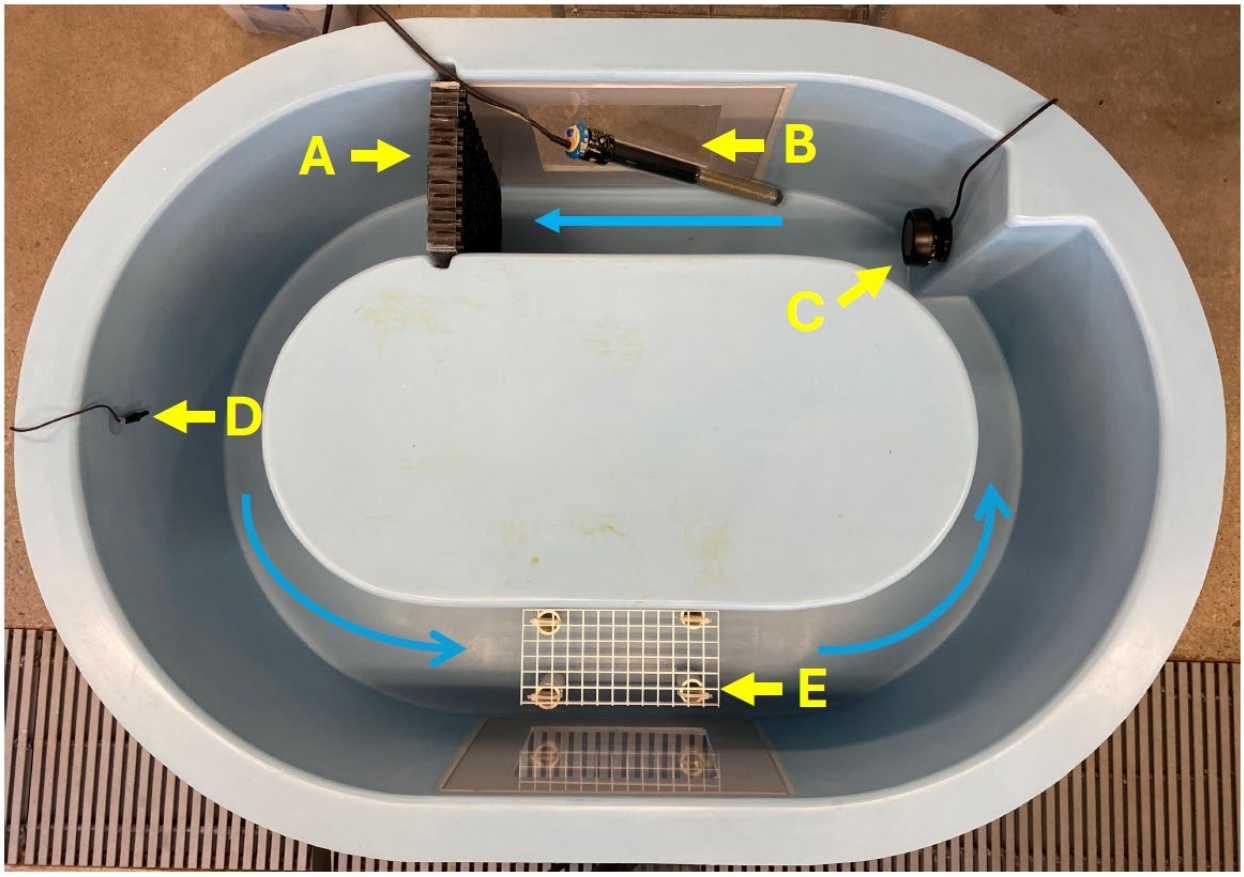

Figure 3.2 Experimental flume. Blue arrows indicate water flow direction. A = laminar flow apparatus, B = heater, C = circulation pump, D = thermometer probe, E = stage.

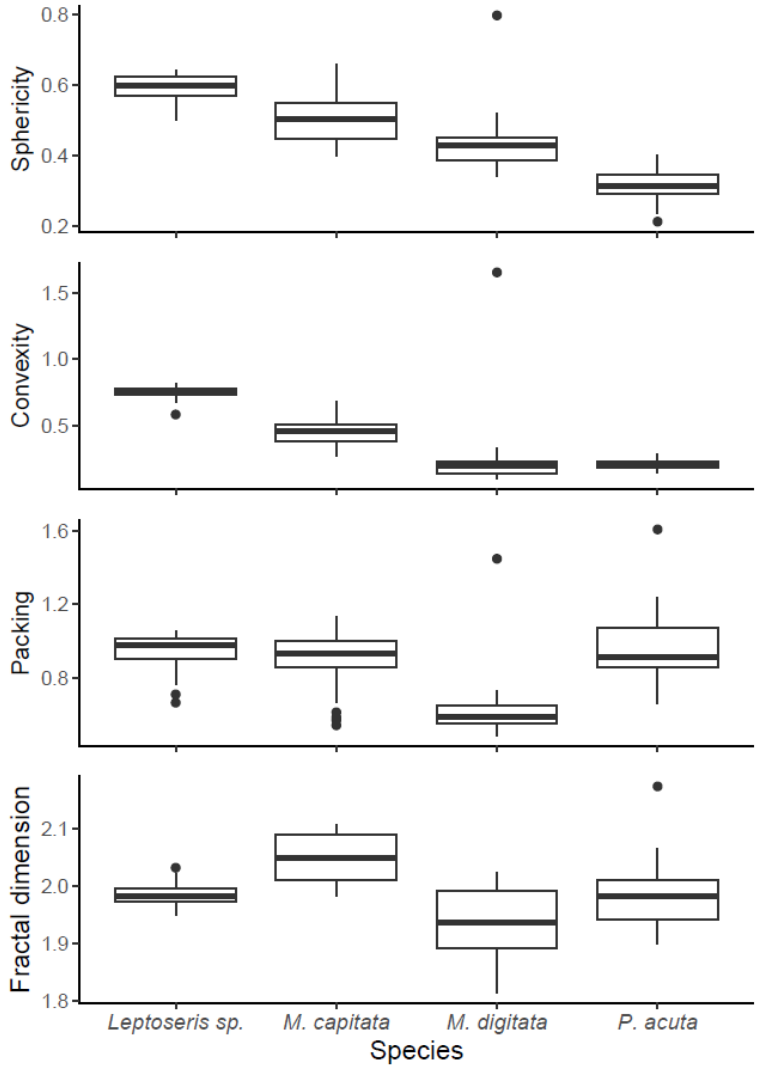

Figure 3.3 Median, quartiles and range of morphological traits data for experimental corals by species.

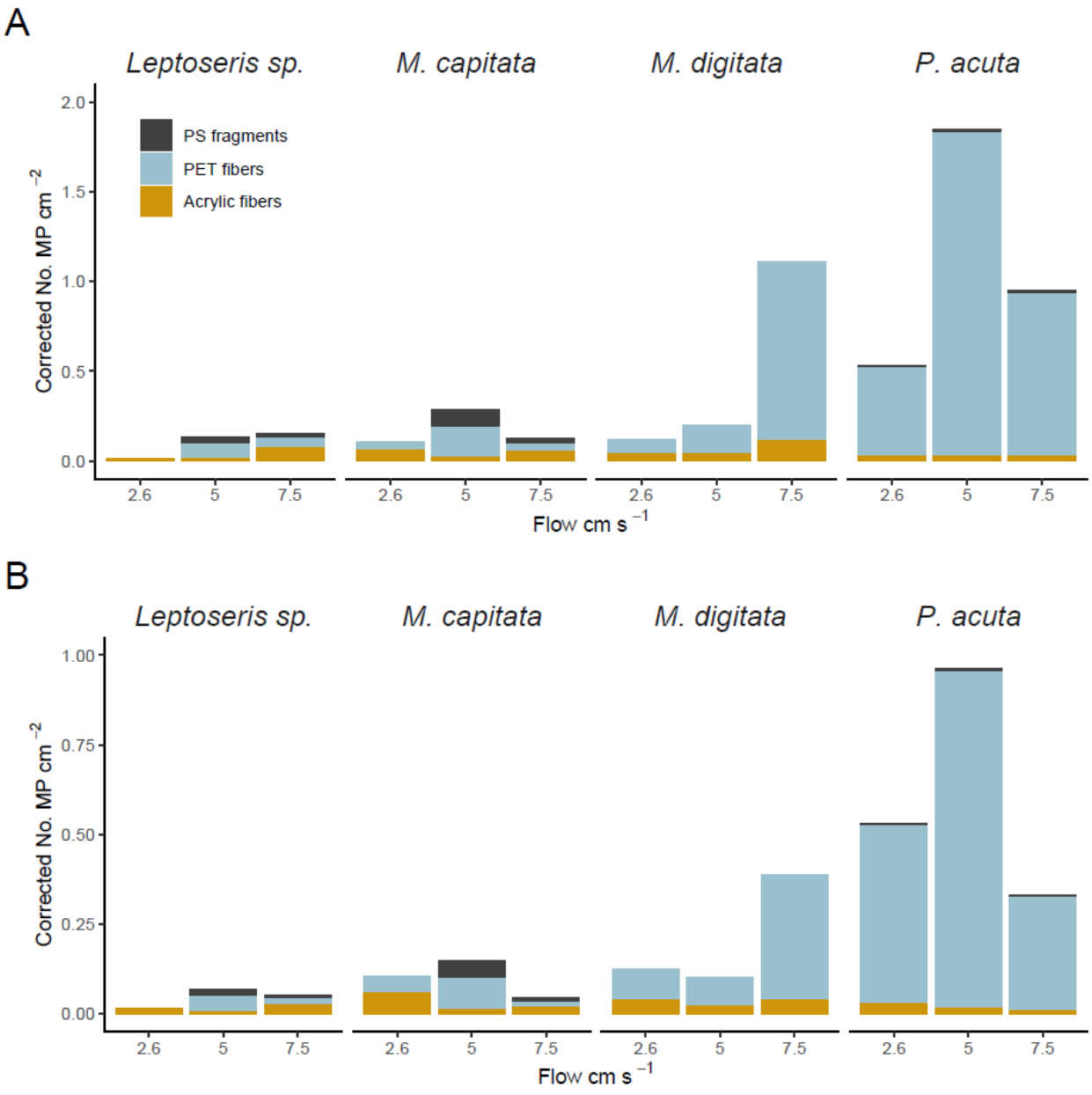

Figure 3.4 Mean corrected microplastics ingestion rates for each coral species under different flow velocities. A) corrected for different concentrations of each microplastics type. B) corrected for different concentrations of each microplastics type and particle flux under different flow velocities. PS = polystyrene, PET = polyester.

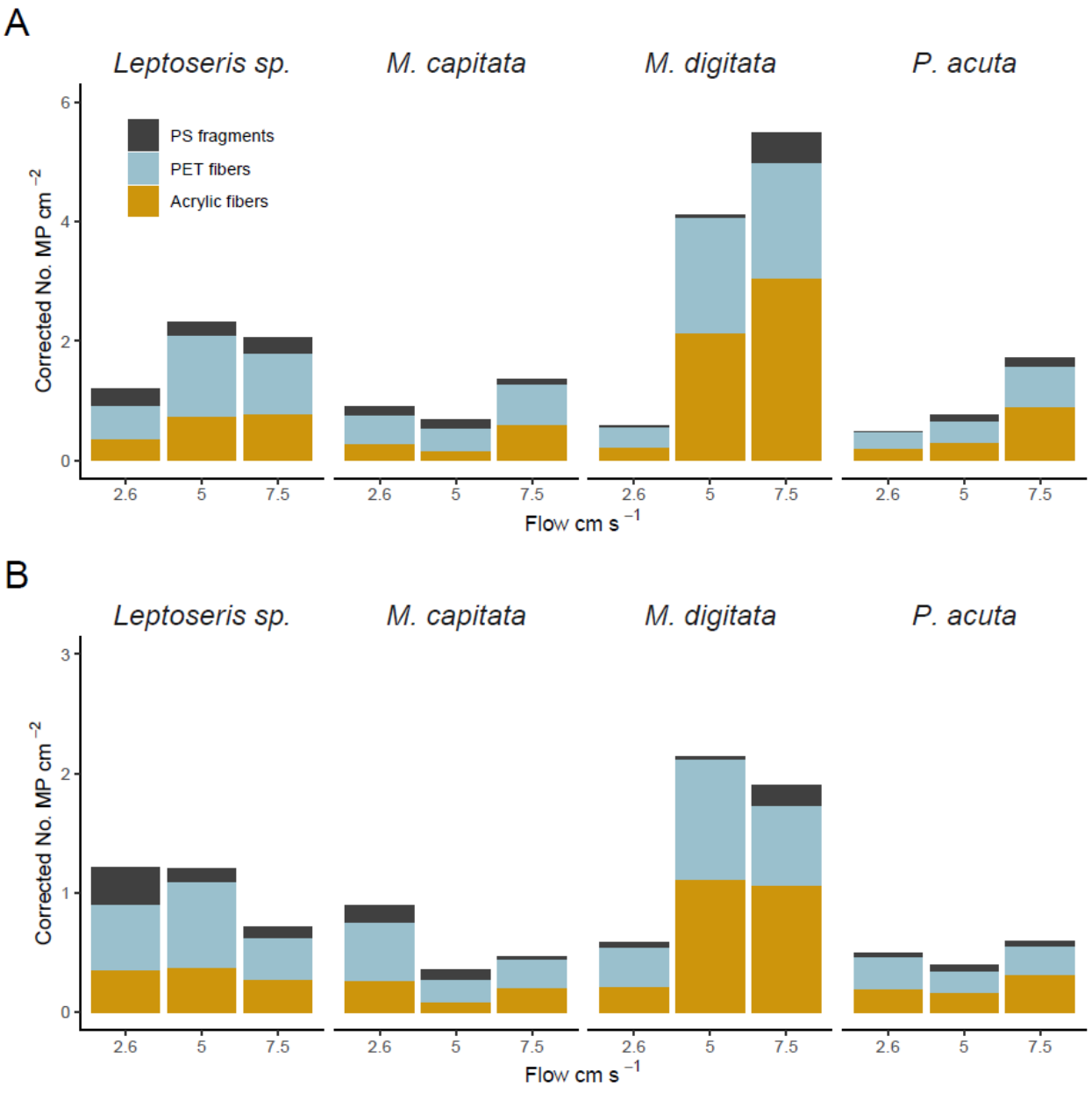

Figure 3.5 Mean corrected microplastics adhesion rates for each coral species under different flow velocities. A = corrected for different concentrations of each microplastics type. B = corrected for different concentrations of each microplastics type and particle flux under different flow velocities. PS = polystyrene, PET = polyester.

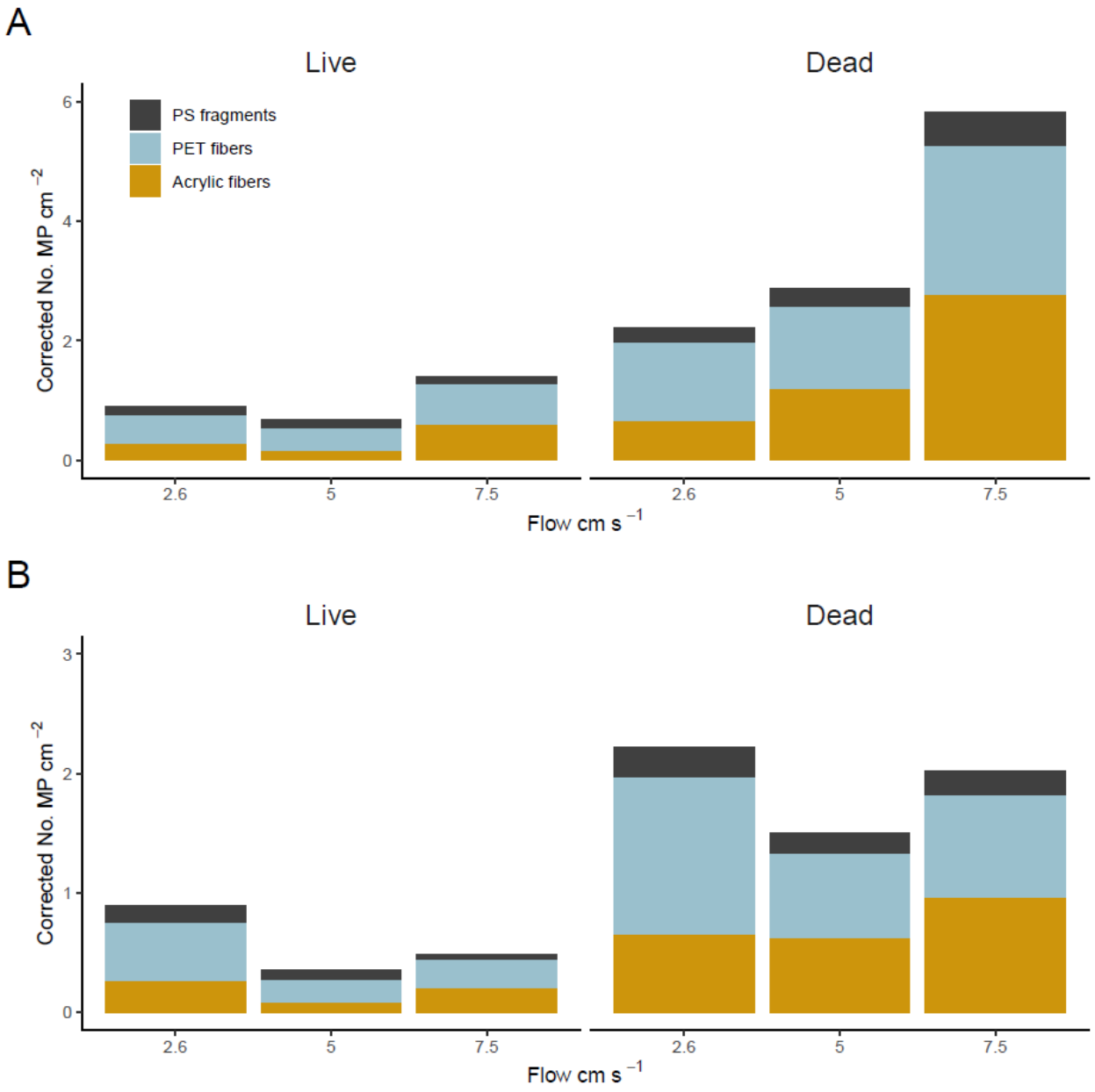

Figure 3.6 Mean corrected microplastics adhesion rates for Montipora capitata under different flow velocities. A = corrected for different concentrations of each microplastics type. B = corrected for different concentrations of each microplastics type and particle flux under different flow velocities. PS = polystyrene, PET = polyester.

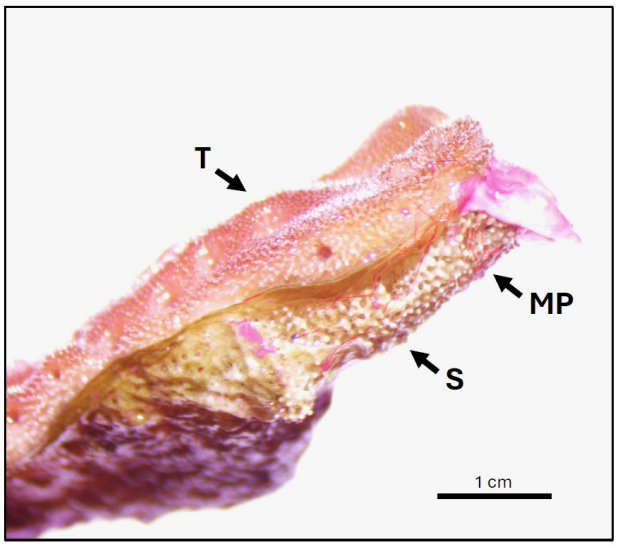

Figure 3.7 Red acrylic fibers (MP) observed at the margin of living tissue (T) and exposed skeleton (S) on *Montipora capitata*.

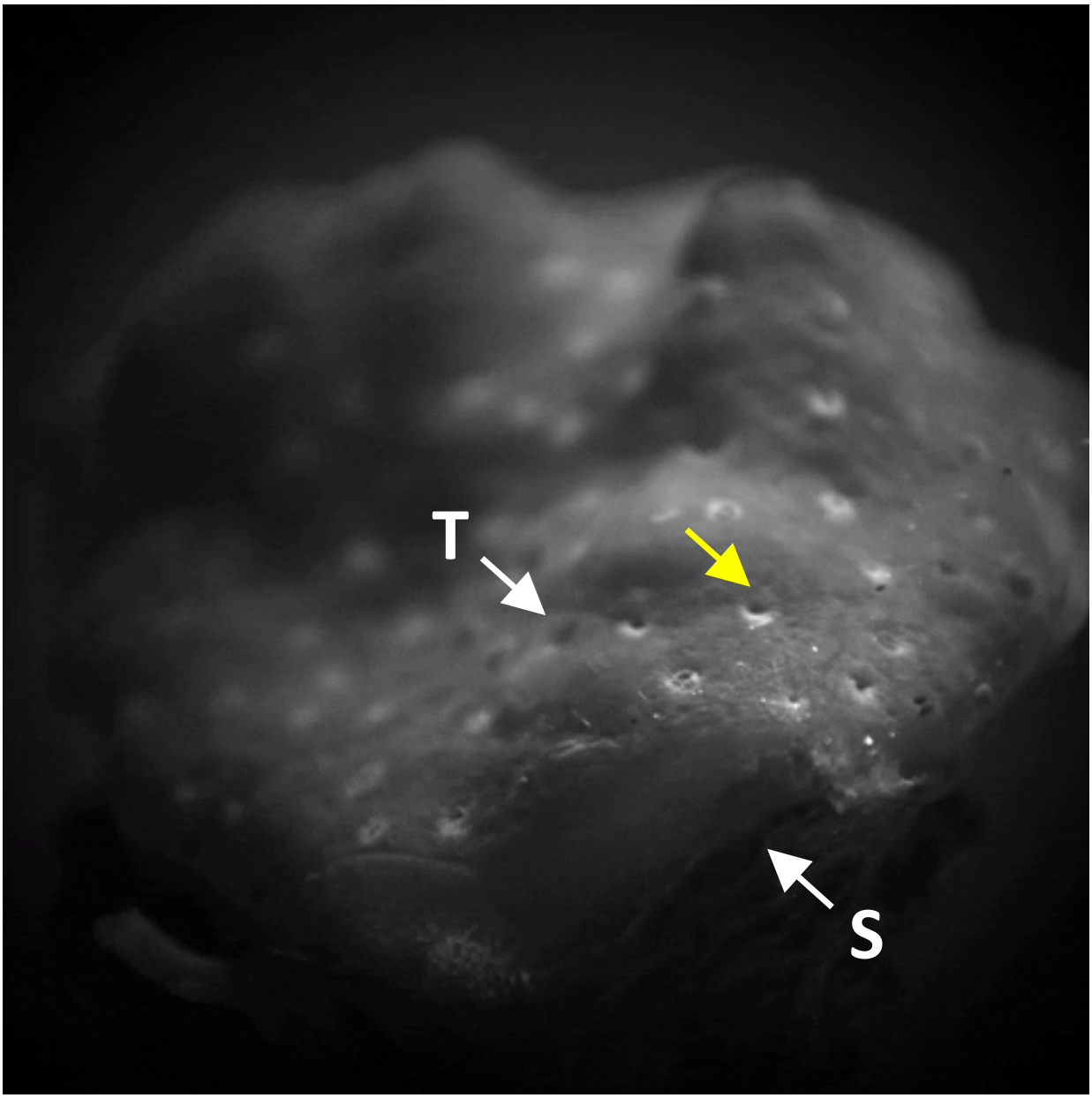

Figure 3.8 Mucus strand (yellow arrow) with microplastics embedded in it on the margin of living tissue (T) and exposed skeleton (S) of *Montipora capitata*.

3.8 References

Allen, A. S., Seymour, A. C., and Rittschof, D. (2017). Chemoreception drives plastic consumption in a hard coral. *Mar. Pollut. Bull.* 124, 198–205. doi: 10.1016/j.marpolbul.2017.07.030

Anthony, K. R. N. (1999). Coral suspension feeding on fine particulate matter. *J. Exp. Mar. Biol. Ecol.* 232, 85–106. doi: 10.1016/S0022-0981(98)00099-9

Arossa, S., Martin, C., Rossbach, S., and Duarte, C. M. (2019). Microplastic removal by Red Sea giant clam (*Tridacna maxima*). *Environ. Pollut.* 252, 1257–1266. doi: 10.1016/j.envpol.2019.05.149

Auta, H. S., Emenike, C. U., and Fauziah, S. H. (2017). Distribution and importance of microplastics in the marine environment: A review of the sources, fate, effects, and potential solutions. *Environ. Int.* 102, 165–176. doi: 10.1016/j.envint.2017.02.013

Axworthy, J. B., and Padilla-Gamiño, J. L. (2019). Microplastics ingestion and heterotrophy in thermally stressed corals. *Sci. Rep.* 9, 18193. doi: 10.1038/s41598-019-54698-7

Babcock, R. C., Baird, A., Piromvaragorn, S., Thompson, D. P., and Willis, B. L. (2003). Identification of scleractinian coral recruits from Indo-Pacific reefs. *Zool. Stud.* 42, 211–226.

Backstrom, C. H., Padilla-Gamiño, J. L., Spalding, H. L., Roth, M. S., Smith, C. M., Gates, R. D., et al. (2024). Mesophotic corals in Hawai‘i maintain autotrophy to survive low-light conditions. *Proc. R. Soc. B Biol. Sci.* 291, 20231534. doi: 10.1098/rspb.2023.1534

Bejarano, S., Diemel, V., Feuring, A., Ghilardi, M., and Harder, T. (2022). No short-term effect of sinking microplastics on heterotrophy or sediment clearing in the tropical coral *Stylophora pistillata*. *Sci. Rep.* 12, 1468. doi: 10.1038/s41598-022-05420-7

Borrelle, S. B., Ringma, J., Law, K. L., Monnahan, C. C., Lebreton, L., McGivern, A., et al. (2020). Predicted growth in plastic waste exceeds efforts to mitigate plastic pollution. *Science* 369, 1515–1518. doi: 10.1126/science.aba3656

Chappell, J. (1980). Coral morphology, diversity and reef growth. *Nature* 286, 249–252. doi: 10.1038/286249a0

Chapron, L., Peru, E., Engler, A., Ghiglione, J. F., Meistertzheim, A. L., Pruski, A. M., et al. (2018). Macro- and microplastics affect cold-water corals growth, feeding and behaviour. *Sci. Rep.* 8, 15299. doi: 10.1038/s41598-018-33683-6

Corona, E., Martin, C., Marasco, R., and Duarte, C. M. (2020). Passive and Active Removal of Marine Microplastics by a Mushroom Coral (*Danafungia scruposa*). *Front. Mar. Sci.* 7, 128. doi: 10.3389/fmars.2020.00128

Ding, J., Jiang, F., Li, J., Wang, Z., Sun, C., Wang, Z., et al. (2019). Microplastics in the Coral Reef Systems from Xisha Islands of South China Sea. *Environ. Sci. Technol.* 53, 8036–8046. doi: 10.1021/acs.est.9b01452

Espinosa-Gayosso, A., Ghisalberti, M., Shimeta, J., and Ivey, G. N. (2021). On predicting particle capture rates in aquatic ecosystems. *PLoS ONE* 16, e0261400. doi: 10.1371/journal.pone.0261400

Frossard, J., and Renaud, O. (2022). permuco: Permutation Tests for Regression, (Repeated Measures) ANOVA/ANCOVA and Comparison of Signals. Available at: https://cran.r-project.org/web/packages/permuco/index.html.

Gewert, B., M. Plassmann, M., and MacLeod, M. (2015). Pathways for degradation of plastic polymers floating in the marine environment. *Environ. Sci. Process. Impacts* 17, 1513–1521. doi: 10.1039/C5EM00207A

Hall, N. M., Berry, K. L. E., Rintoul, L., and Hoogenboom, M. O. (2015). Microplastic ingestion by scleractinian corals. *Mar. Biol.* 162, 725–732. doi: 10.1007/s00227-015-2619-7

Hankins, C., Duffy, A., and Drisco, K. (2018). Scleractinian coral microplastic ingestion: Potential calcification effects, size limits, and retention. *Mar. Pollut. Bull.* 135, 587–593. doi: 10.1016/j.marpolbul.2018.07.067

Hankins, C., Moso, E., and Lasseigne, D. (2021). Microplastics impair growth in two Atlantic scleractinian coral species, *Pseudodiploria clivosa* and *Acropora cervicornis*. *Environ. Pollut.* 275, 116649. doi: 10.1016/j.envpol.2021.116649

Hankins, C., Raimondo, S., and Lasseigne, D. (2022). Microplastic ingestion by coral as a function of the interaction between calyx and microplastic size. *Sci. Total Environ.* 810, 152333. doi: 10.1016/j.scitotenv.2021.152333

Helmuth, B., and Sebens, K. (1993). The influence of colony morphology and orientation to flow on particle capture by the scleractinian coral *Agaricia agaricites* (Linnaeus). *J. Exp. Mar. Biol. Ecol.* 165, 251–278. doi: 10.1016/0022-0981(93)90109-2

Hierl, F., Wu, H. C., and Westphal, H. (2021). Scleractinian corals incorporate microplastic particles: identification from a laboratory study. *Environ. Sci. Pollut. Res.* 28, 37882–37893. doi: 10.1007/s11356-021-13240-x

Huang, W., Chen, M., Song, B., Deng, J., Shen, M., Chen, Q., et al. (2021). Microplastics in the coral reefs and their potential impacts on corals: A mini-review. *Sci. Total Environ.* 762, 143112. doi: 10.1016/j.scitotenv.2020.143112

Jiang, S., Zhang, Y., Feng, L., He, L., Zhou, C., Hong, P., et al. (2021). Comparison of Short- and Long-Term Toxicity of Microplastics with Different Chemical Constituents on Button Polyps. (*Protopalythoa sp.*). *ACS Earth Space Chem.* 5, 12–22. doi: 10.1021/acsearthspacechem.0c00213

Johnson, A. (2021). Effects of Environmental Aging on the Acute Toxicity and Chemical Composition of Various Microplastic Leachates. *WWU Grad. Sch. Collect.* Available at: https://cedar.wwu.edu/wwuet/1064

Johnson, A. S., and Sebens, K. P. (1993). Consequences of a flattened morphology: effects of flow on feeding rates of the scleractinian coral *Meandrina meandrites*. *Mar. Ecol. Prog. Ser.* 99, 99–114.

Jokiel, P. L. (1991). Jokiel's illustrated scientific guide to Kane'ohe Bay, O'ahu. doi: 10.13140/2.1.3051.9360

Kane, I. A., and Clare, M. A. (2019). Dispersion, Accumulation, and the Ultimate Fate of Microplastics in Deep-Marine Environments: A Review and Future Directions. *Front. Earth Sci.* 7. doi: 10.3389/feart.2019.00080

Koehl, M. A. R. (1977). Water flow and the morphology of zooanthid colonies. *Proc. Third Int. Coral Reef Symp.*, 437–444.

Krishnakumar, S., Anbalagan, S., Hussain, S. M., Bharani, R., Godson, P. S., and Srinivasalu, S. (2021). Coral annual growth band impregnated microplastics (Porites sp.): a first investigation report. *Wetl. Ecol. Manag.* 29, 677–687. doi: 10.1007/s11273-021-09786-9

Labarbera, M. (1984). Feeding Currents and Particle Capture Mechanisms in Suspension Feeding Animals. *Am. Zool.* 24, 71–84. doi: 10.1093/icb/24.1.71

Lei, X., Cheng, H., Luo, Y., Zhang, Y., Jiang, L., Sun, Y., et al. (2021). Abundance and Characteristics of Microplastics in Seawater and Corals From Reef Region of Sanya Bay, China. *Front. Mar. Sci.* 8. doi: 10.3389/fmars.2021.728745

Lewis, J. B., and Price, W. S. (1975). Feeding mechanisms and feeding strategies of Atlantic reef corals. *J. Zool.* 176, 527–544. doi: 10.1111/j.1469-7998.1975.tb03219.x

Li, L., Li, M., Deng, H., Cai, L., Cai, H., Yan, B., et al. (2018). A straightforward method for measuring the range of apparent density of microplastics. *Sci. Total Environ.* 639, 367–373. doi: 10.1016/j.scitotenv.2018.05.166

Liao, B., Wang, J., Xiao, B., Yang, X., Xie, Z., Li, D., et al. (2021). Effects of acute microplastic exposure on physiological parameters in *Tubastrea aurea* corals. *Mar. Pollut. Bull.* 165, 112173. doi: 10.1016/j.marpolbul.2021.112173

Lim, Y. C., Chen, C.-W., Cheng, Y.-R., Chen, C.-F., and Dong, C.-D. (2022). Impacts of microplastics on scleractinian corals nearshore Liuqiu Island southwestern Taiwan. *Environ. Pollut.* 306, 119371. doi: 10.1016/j.envpol.2022.119371

Loya, Y., Sakai, K., Yamazato, K., Nakano, Y., Sambali, H., and van Woesik, R. (2001). Coral bleaching: the winners and the losers. *Ecol. Lett.* 4, 122–131. doi: 10.1046/j.1461-0248.2001.00203.x

Martin, C., Corona, E., Mahadik, G. A., and Duarte, C. M. (2019). Adhesion to coral surface as a potential sink for marine microplastics. *Environ. Pollut.* 255, 113281. doi: 10.1016/j.envpol.2019.113281

McFadden, C. S. (1986). Colony fission increases particle capture rates of a soft coral: Advantages of being a small colony. *J. Exp. Mar. Biol. Ecol.* 103, 1–20. doi: 10.1016/0022-0981(86)90129-2

Mendrik, F. M., Henry, T. B., Burdett, H., Hackney, C. R., Waller, C., Parsons, D. R., et al. (2021). Species-specific impact of microplastics on coral physiology. *Environ. Pollut.* 269, 116238. doi: 10.1016/j.envpol.2020.116238

Mizerek, T. L., Baird, A. H., and Madin, J. S. (2018). Species traits as indicators of coral bleaching. *Coral Reefs* 37, 791–800. doi: 10.1007/s00338-018-1702-1

Moberg, F., and Folke, C. (1999). Ecological goods and services of coral reef ecosystems. *Ecol. Econ.* 29, 215–233. doi: 10.1016/S0921-8009(99)00009-9

Mouchi, V., Chapron, L., Peru, E., Pruski, A. M., Meistertzheim, A.-L., Vétion, G., et al. (2019). Long-term aquaria study suggests species-specific responses of two cold-water corals to macro-and microplastics exposure. *Environ. Pollut.* 253, 322–329. doi: 10.1016/j.envpol.2019.07.024

Oldenburg, K. S., Urban-Rich, J., Castillo, K. D., and Baumann, J. H. (2021). Microfiber abundance associated with coral tissue varies geographically on the Belize Mesoamerican Barrier Reef System. *Mar. Pollut. Bull.* 163, 111938. doi: 10.1016/j.marpolbul.2020.111938

Orejas, C., Gori, A., Rad-Menéndez, C., Last, K. S., Davies, A. J., Beveridge, C. M., et al. (2016). The effect of flow speed and food size on the capture efficiency and feeding behaviour of the cold-water coral *Lophelia pertusa*. *J. Exp. Mar. Biol. Ecol.* 481, 34–40. doi: 10.1016/j.jembe.2016.04.002

Padilla-Gamiño, J. L., Hédouin, L., Waller, R. G., Smith, D., Truong, W., and Gates, R. D. (2014). Sedimentation and the Reproductive Biology of the Hawaiian Reef-Building Coral *Montipora capitata*. *Biol. Bull.* 226, 8–18. doi: 10.1086/BBLv226n1p8

Palardy, J., Grottoli, A., and Matthews, K. (2005). Effects of upwelling, depth, morphology and polyp size on feeding in three species of Panamanian corals. *Mar. Ecol. Prog. Ser.* 300, 79–89. doi: 10.3354/meps300079

Patterson, M. R. (1991). The Effects of Flow on Polyp-Level Prey Capture in an Octocoral, *Alcyonium siderium*. *Biol. Bull.* 180, 93–102. doi: 10.2307/1542432

Peeken, I., Primpke, S., Beyer, B., Gütermann, J., Katlein, C., Krumpen, T., et al. (2018). Arctic sea ice is an important temporal sink and means of transport for microplastic. *Nat. Commun.* 9, 1505. doi: 10.1038/s41467-018-03825-5

Piniak, G. (2002). Effects of symbiotic status, flow speed, and prey type on prey capture by the facultatively symbiotic temperate coral *Oculina arbuscula*. *Mar. Biol.* 141, 449–455. doi: 10.1007/s00227-002-0825-6

Purser, A., Larsson, A. I., Thomsen, L., and van Oevelen, D. (2010). The influence of flow velocity and food concentration on *Lophelia pertusa* (Scleractinia) zooplankton capture rates. *J. Exp. Mar. Biol. Ecol.* 395, 55–62. doi: 10.1016/j.jembe.2010.08.013

Rades, M., Schubert, P., Wilke, T., and Reichert, J. (2022). Reef-Building Corals Do Not Develop Adaptive Mechanisms to Better Cope With Microplastics. *Front. Mar. Sci.* 9. doi: 10.3389/fmars.2022.863187

Raguso, C., Saliu, F., Lasagni, M., Galli, P., Clemenza, M., and Montano, S. (2022). First detection of microplastics in reef-building corals from a Maldivian atoll. *Mar. Pollut. Bull.* 180, 113773. doi: 10.1016/j.marpolbul.2022.113773

Reichert, J., Arnold, A. L., Hammer, N., Miller, I. B., Rades, M., Schubert, P., et al. (2022). Reef-building corals act as long-term sink for microplastic. *Glob. Change Biol.* 28, 33–45. doi: 10.1111/gcb.15920

Reichert, J., Arnold, A. L., Hoogenboom, M. O., Schubert, P., and Wilke, T. (2019). Impacts of microplastics on growth and health of hermatypic corals are species-specific. *Environ. Pollut.* 254, 113074. doi: 10.1016/j.envpol.2019.113074

Reichert, J., Backes, A. R., Schubert, P., and Wilke, T. (2017). The power of 3D fractal dimensions for comparative shape and structural complexity analyses of irregularly shaped organisms. *Methods Ecol. Evol.* 8, 1650–1658. doi: 10.1111/2041-210X.12829

Reichert, J., Schellenberg, J., Schubert, P., and Wilke, T. (2016). 3D scanning as a highly precise, reproducible, and minimally invasive method for surface area and volume measurements of scleractinian corals. *Limnol. Oceanogr. Methods* 14, 518–526. doi: 10.1002/lom3.10109

Reichert, J., Schellenberg, J., Schubert, P., and Wilke, T. (2018). Responses of reef building corals to microplastic exposure. *Environ. Pollut.* 237, 955–960. doi: 10.1016/j.envpol.2017.11.006

Rotjan, R. D., Sharp, K. H., Gauthier, A. E., Yelton, R., Lopez, E. M. B., Carilli, J., et al. (2019). Patterns, dynamics and consequences of microplastic ingestion by the temperate coral, *Astrangia poculata*. *Proc. R. Soc. B Biol. Sci.* 286, 20190726. doi: 10.1098/rspb.2019.0726

Rubenstein, D. I., and Koehl, M. a. R. (1977). The Mechanisms of Filter Feeding: Some Theoretical Considerations. *Am. Nat.* 111, 981–994. doi: 10.1086/283227

Sabdono, A., Ayuningrum, D., and Sabdaningsih, A. (2022). First Evidence of Microplastics Presence in Corals of Jepara Coastal Waters, Java Sea: A Comparison Among Habitats

Receiving Different Degrees of Sedimentations. *Pol. J. Environ. Stud.* 31, 825–832. doi: 10.15244/pjoes/139376

Schlichter, D. (1991). A perforated gastrovascular cavity in the symbiotic deep-water coral *Leptoseris fragilis*: A new strategy to optimize heterotrophic nutrition. *Helgoländer Meeresunters.* 45, 423–443. doi: 10.1007/BF02367177

Sealifebase (n.d.). *Montipora digitata*. Available at: https://www.sealifebase.ca/summary/Montipora-digitata.html (Accessed March 7, 2024).

Sebens, K. P., Grace, S. P., Helmuth, B., Maney Jr., E. J., and Miles, J. S. (1998). Water flow and prey capture by three scleractinian corals, *Madracis mirabilis*, *Montastrea cavernosa* and *Porites porites*, in a field enclosure. *Mar. Biol.* 131, 347–360. doi: 10.1007/s002270050328

Sebens, K. P., and Johnson, A. S. (1991). Effects of water movement on prey capture and distribution of reef corals. *Hydrobiologia* 226, 91–101. doi: 10.1007/BF00006810

Sebens, K. P., Witting, J., and Helmuth, B. (1997). Effects of water flow and branch spacing on particle capture by the reef coral *Madracis mirabilis* (Duchassaing and Michelotti). *J. Exp. Mar. Biol. Ecol.* 211, 1–28. doi: 10.1016/S0022-0981(96)02636-6

Shimeta, J., and Jumars, P. A. (1991). PHYSICAL MECHANISMS AND RATES OF PARTICLE CAPTURE BY SUSPENSION- FEEDERS. *Oceanogr. Mar. Biol. Annu. Rev.* 29, 191–257.

Soares, M. O., Rizzo, L., Ximenes Neto, A. R., Barros, Y., Martinelli Filho, J. E., Giarrizzo, T., et al. (2023). Do coral reefs act as sinks for microplastics? *Environ. Pollut.* 337, 122509. doi: 10.1016/j.envpol.2023.122509

Stafford-Smith, M., and Ormond, R. (1992). Sediment-rejection mechanisms of 42 species of Australian scleractinian corals. *Mar. Freshw. Res.* 43, 683. doi: 10.1071/MF9920683

Strathmann, R. R. (1971). The feeding behavior of planktotrophic echinoderm larvae: Mechanisms, regulation, and rates of suspension feeding. *J. Exp. Mar. Biol. Ecol.* 6, 109–160. doi: 10.1016/0022-0981(71)90054-2

Tang, J., Wu, Z., Wan, L., Cai, W., Chen, S., Wang, X., et al. (2021). Differential enrichment and physiological impacts of ingested microplastics in scleractinian corals in situ. *J. Hazard. Mater.* 404, 124205. doi: 10.1016/j.jhazmat.2020.124205

van Sebille, E., Wilcox, C., Lebreton, L., Maximenko, N., Hardesty, B. D., van Franeker, J. A., et al. (2015). A global inventory of small floating plastic debris. *Environ. Res. Lett.* 10, 124006. doi: 10.1088/1748-9326/10/12/124006

Zawada, K. J. A., Dornelas, M., and Madin, J. S. (2019a). Quantifying coral morphology. *Coral Reefs* 38, 1281–1292. doi: 10.1007/s00338-019-01842-4

Zawada, K. J. A., Madin, J. S., Baird, A. H., Bridge, T. C. L., and Dornelas, M. (2019b). Morphological traits can track coral reef responses to the Anthropocene. *Funct. Ecol.* 33, 962–975. doi: 10.1111/1365-2435.13358

Zhou, Z., Wan, L., Cai, W., Tang, J., Wu, Z., and Zhang, K. (2022). Species-specific microplastic enrichment characteristics of scleractinian corals from reef environment: Insights from an in-situ study at the Xisha Islands. *Sci. Total Environ.* 815, 152845. doi: 10.1016/j.scitotenv.2021.152845

3.9 Supplementary Materials

3D scanning

3D meshes of the coral fragments were obtained using the Artec Spider 3D scanner and Artec Studio 13 software, similar to the methods of Reichert et al. (2016). Coral fragments still attached to ceramic base were attached to modeling clay and placed in the center of a turntable. Each fragment was scanned on all sides by rotating the turntable manually and holding the scanner at a 45-degree angle to the fragment. For some larger fragments and ones with complex morphologies, multiple scans (up to three) were recorded from different angles. Individual frames within scans that had an error value above 0.3 were discarded. “Crop surroundings” was used on each scan to remove auxiliary surfaces and random noise. If multiple scans were taken, the “align” function was used to assemble them into the same position. “Global registration” was performed next to optimize the meshes for further processing. To remove outliers, “eliminate noise” was used, and then the scans were fused into a single mesh using the “smooth fusion” function. Visible abnormalities were removed using “erase flaws,” and the resulting meshes were reduced using “simplify mesh.” Finally, texture was applied to the meshes to show their surface color and textures, and the meshes were exported as .obj files.

Morphology metrics

The surface area and volume of the whole coral fragments, as well as the surface area of the up and downstream sides, were obtained from the 3D mesh .obj files using the "compute geometric measures" function in Meshlab (ver. 2022.02). The up and downstream sides of the meshes were obtained differently depending on species. For *Leptoseris sp*. and *M. capitata*, whose encrusting and plating morphologies result in mostly upward facing polyps, the mesh for each fragment was evenly divided into front and back halves using the "plane cut" tool in Meshmixer (vers. 3.5.474), and then each half was exported separately as .obj files. For *M. digitata* and *P. acuta*, whose polyps are orientated laterally, the meshes were divided into up and downstream facing sections by highlighting only the upstream side, then adjusting using the "select more" and "select less" functions, then making manual selections of individual polygons to make the margins even, using Blender (ver. 3.50). Each half was then exported separately as a .obj file.

Morphological traits, including two metrics for volume compactness: sphericity and convexity, and one metric for surface complexity: packing, were calculated based on the equations in Zawada et al. (2019b). Another metric for surface complexity, fractal dimension, was calculated using the Bouligand–Minkowski 3D Toolbox developed by (Reichert et al., 2017; https://www.facom.ufu.br/~backes/mink3d.html). Convex hulls of 3D models were produced using the "convex hull" function in MeshLab (ver. 2022.02). Surface area and volume measurements were determined using the "compute geometric measures" function in MeshLab.

Sphericity: The ratio of the surface area of a sphere with the same volume as the object (O_{vol}) and the surface area of the object (O_{sa}).

$$S = \frac{\pi^{1/3}(6O_{vol})^{2/3}}{O_{sa}}$$

Convexity: The ratio of the volume of the object (O_{vol}) and the volume of the convex hull around the object (C_{vol}).

$$C = \frac{O_{vol}}{C_{vol}}$$

Packing: The ratio of the surface area of the object (O_{sa}) and the surface area of the convex hull around the object (C_{sa}).

$$P = \frac{O_{sa}}{C_{sa}}$$

Fractal dimension: The slope of the ratio of the influence volume (V(r)) and the dilation radius (r). Where r = 8 because it resulted in the greatest differentiation in D among corals (Reichert et al., 2017).

$$D = 3 - lim_{r \to 0} \frac{\log(V(r))}{\log(r)}$$

Table S3.1 Summary statistics of morphometric measurements. S = sphericity; P = Packing; C = convexity; FD = fractal dimension.

	Median S	*Mean (±sd) S*	*Median P*	*Mean (±sd) P*	*Median C*	*Mean (±sd) C*	*Median FD*	*Mean (±sd) FD*
Leptoseris sp.	0.60	0.60±0.04	0.98	0.94±0.11	0.76	0.75±0.05	1.98	1.98±0.02
M. capitata	0.50	0.51±0.07	0.93	0.89±0.17	0.46	0.46±0.11	2.05	2.05±0.04
M. digitata	0.43	0.44±0.09	0.59	0.63±0.19	0.20	0.25±0.31	1.94	1.94±0.06
P.damicornis	0.31	0.32±0.05	0.92	0.97±0.20	0.20	0.20±0.04	1.98	1.98±0.06

Table S3.2 Pearson's correlation values for comparisons between morphological traits and microplastics ingestion and adhesions corrected for flow.

	Packing	*Sphericity*	*Convexity*	*Fractal dimension*	*Total ingestion*	*Total adhesion*
Packing		0.119	0.449***	0.391***	-0.123	-0.312**
Sphericity	0.119		0.890***	-0.071	-0.174	-0.007
Convexity	0.449***	0.890***		0.052	-0.186	-0.125
Fractal dimension	0.391***	-0.071	0.052		-0.114	-0.233*
Total ingestion	-0.123	-0.174	-0.186	-0.114		0.175
Total adhesion	-0.312**	-0.007	-0.125	-0.233*	0.175	

Computed correlation used pearson-method with listwise-deletion.

Table S3.3 Permutated ANOVA model summary statistics for microplastic (MP) ingestion rates corrected for different concentrations of each microplastic type.

	SS	*df*	*F*	*parametric P(>F)*	*resampled P(>F)*
Species	2.5403	3	5.9254	0.0006	0.0001
Flow	0.5941	2	2.0786	0.1261	0.1268
MP_type	4.4008	2	15.3981	0.0000	0.0001
Side	0.0669	1	0.4684	0.4940	0.5106
Species:Flow	1.4662	6	1.7100	0.1164	0.0963
Species:MP_type	5.5414	6	6.4630	0.0000	0.0001
Flow:MP_type	0.9046	4	1.5825	0.1775	0.1625
Species:Flow:MP_type	2.7787	12	1.6204	0.0820	0.0587
Residuals	77.0239	539			

Table S3.4 Permutated ANOVA model summary statistics for microplastic (MP) ingestion rates corrected for different concentrations of each microplastic type and flow velocity.

	SS	*df*	*F*	*parametric P(>F)*	*resampled P(>F)*
Species	0.7753	3	7.1721	0.0001	0.0001
Flow	0.0531	2	0.7373	0.4789	0.5048
MP_type	1.1391	2	15.8074	0.0000	0.0001
Side	0.0230	1	0.6387	0.4245	0.4536
Species:Flow	0.3001	6	1.3880	0.2173	0.2053
Species:MP_type	1.6506	6	7.6352	0.0000	0.0001
Flow:MP_type	0.1142	4	0.7922	0.5305	0.5639
Species:Flow:MP_type	0.5666	12	1.3104	0.2082	0.1839
Residuals	19.4209	539			

Table S3.5 Permutated ANOVA model summary statistics for microplastic (MP) adhesion rates corrected for different concentrations of each microplastic type.

	SS	*df*	*F*	*parametric P(>F)*	*resampled P(>F)*
Species	15.5778	3	22.6872	0.0000	0.0001
Flow	9.3967	2	20.5277	0.0000	0.0001
MP.type	12.9047	2	28.1912	0.0000	0.0001
Side	4.1089	1	17.9523	0.0000	0.0001
Species:Flow	9.9489	6	7.2446	0.0000	0.0001
Species:MP.type	8.0791	6	5.8831	0.0000	0.0001
Flow:MP.type	4.1541	4	4.5375	0.0013	0.0011
Species:Flow:MP.type	4.4694	12	1.6273	0.0802	0.0806
Residuals	123.3654	539			

Table S3.6 Permutated ANOVA model summary statistics for microplastic (MP) adhesion rates corrected for different concentrations of each microplastic type and flow velocity.

	SS	*df*	*F*	*parametric* *P(>F)*	*resampled* *P(>F)*
Species	2.8238	3	17.3713	0.0000	0.0001
Flow	0.1348	2	1.2441	0.2890	0.2849
MP.type	3.0913	2	28.5252	0.0000	0.0001
Side	0.9488	1	17.5101	0.0000	0.0001
Species:Flow	2.1869	6	6.7266	0.0000	0.0001
Species:MP.type	1.6052	6	4.9374	0.0001	0.0002
Flow:MP.type	0.4935	4	2.2769	0.0599	0.0599
Species:Flow:MP.type	0.9399	12	1.4455	0.1411	0.1424
Residuals	29.2063	539			

Table S3.7 Permutated ANOVA model summary statistics for microplastic (MP) adhesion rates on *Montipora capitata*, corrected for different concentrations of each microplastic type.

	SS	*df*	*F*	*parametric* *P(>F)*	*resampled* *P(>F)*
Flow	6.7812	2	12.5881	0.0000	0.0001
Condition	14.0694	1	52.2352	0.0000	0.0001
MP.type	9.5687	2	17.7628	0.0000	0.0001
Flow:Condition	3.4133	2	6.3362	0.0020	0.0016
Flow:MP.type	2.6706	4	2.4788	0.0444	0.0418
Condition:MP.type	3.6631	2	6.8000	0.0013	0.0013
Flow:Condition:MP.type	1.0798	4	1.0022	0.4068	0.4025
Residuals	72.7238	270			

Table S3.8 Permutated ANOVA model summary statistics for microplastic (MP) adhesion rates on *Montipora capitata*, corrected for different concentrations of each microplastic type and flow velocity.

	SS	*df*	*F*	*parametric* *P(>F)*	*resampled* *P(>F)*
Flow	0.5362	2	3.6056	0.0285	0.0243
Condition	3.5656	1	47.9490	0.0000	0.0001
MP.type	2.8932	2	19.4533	0.0000	0.0001
Flow:Condition	0.0506	2	0.3403	0.7119	0.7187
Flow:MP.type	0.6314	4	2.1228	0.0783	0.0725
Condition:MP.type	0.9827	2	6.6073	0.0016	0.0015
Flow:Condition:MP.type	0.1882	4	0.6328	0.6395	0.6448
Residuals	20.0776	270			

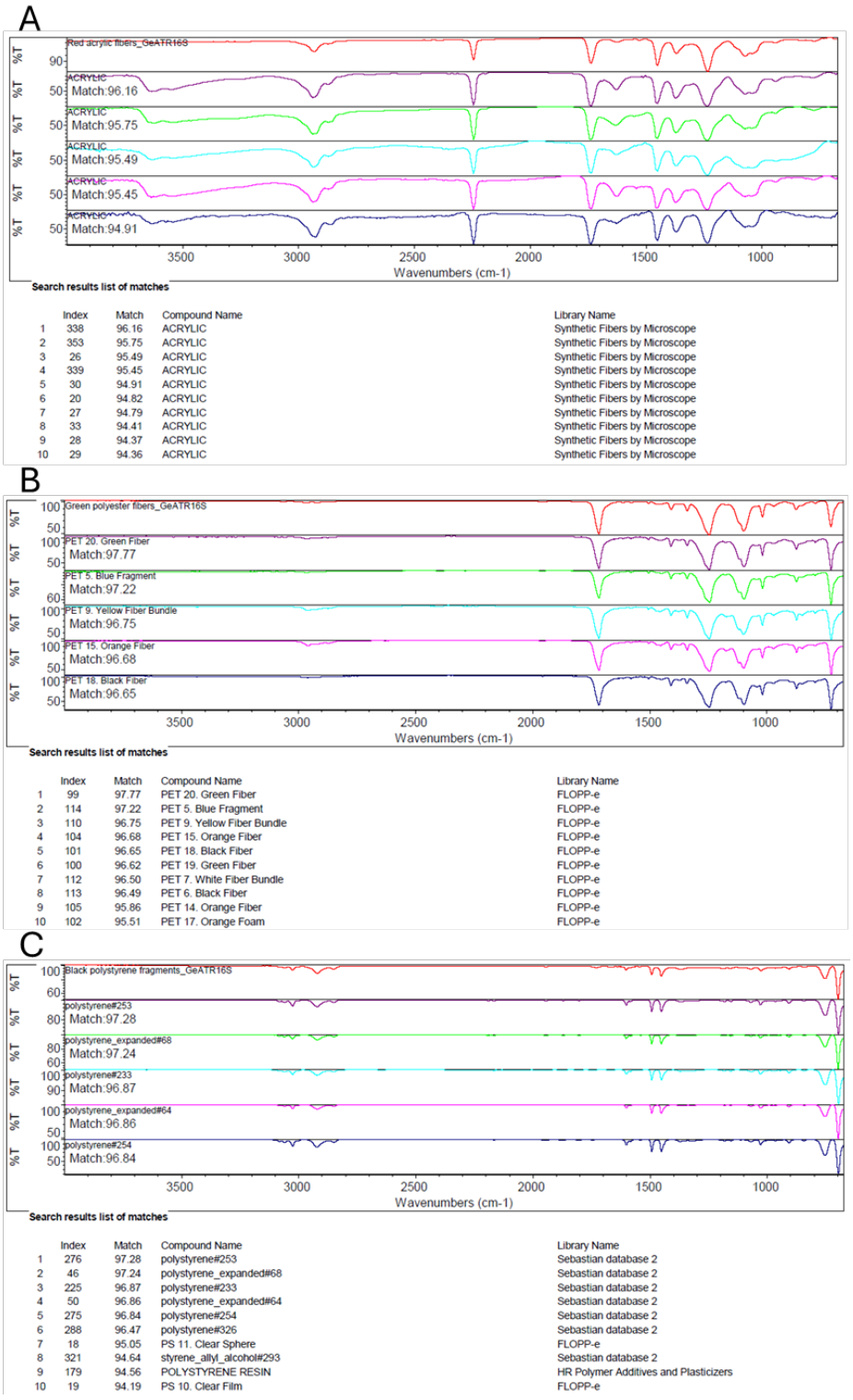

Figure S3.1 FTIR spectra of experimental microplastics and the top 10 library matches: A = acrylic fibers, B = polyester (PET) fibers, C = polystyrene fragments.

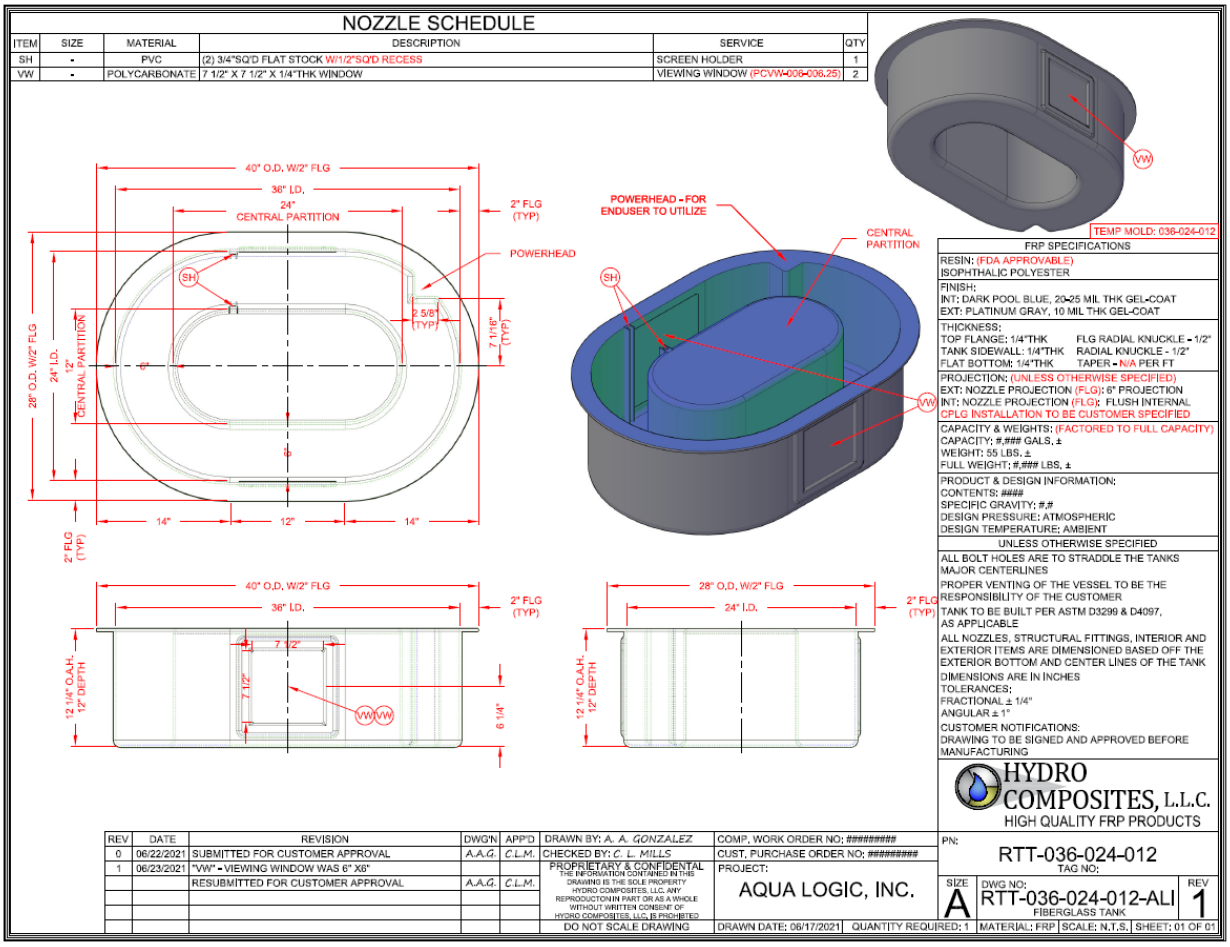

Figure S3.2 Schematics of the custom experimental flume system.

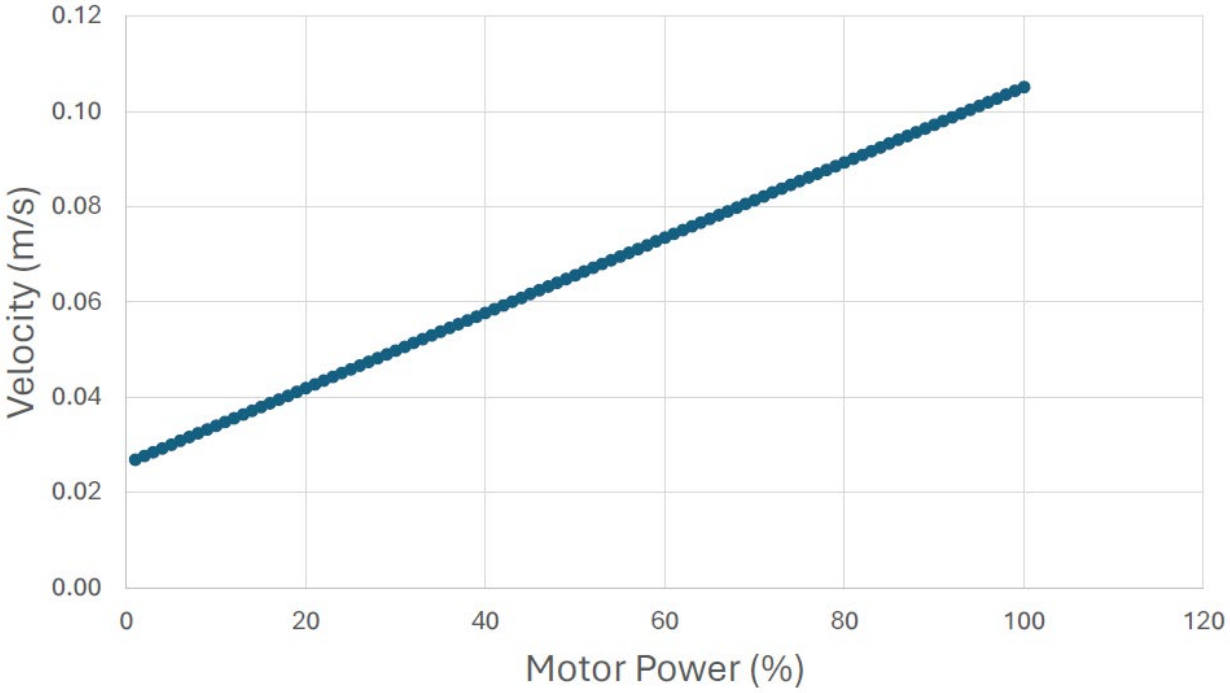

Figure S3.3 Calibration curve produced using particle tracking velocimetry to determine the water velocity corresponding to the pump output settings.

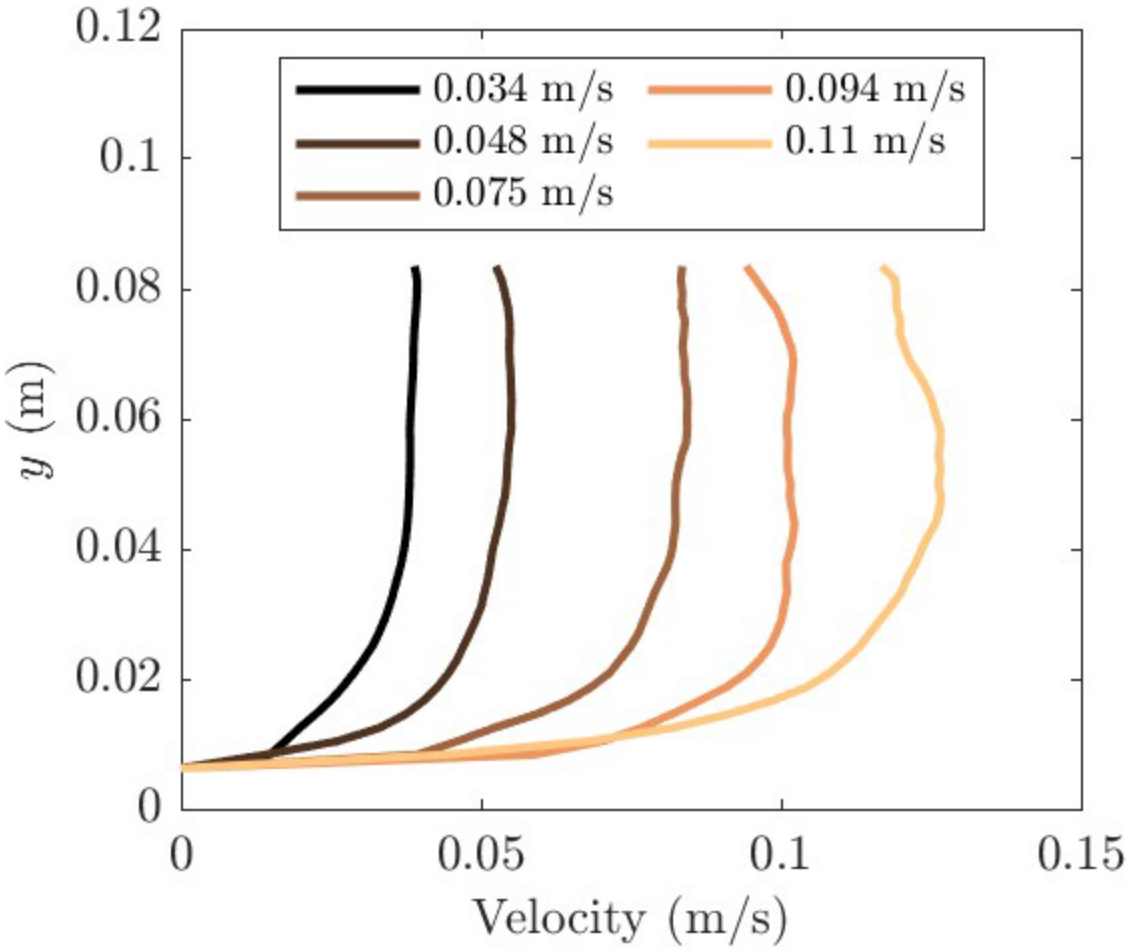

Figure S3.4 Velocity profiles measured using particle tracking velocimetry and their corresponding depth-averaged velocities (in legend box) of the pump settings we tested (1% = 0.034 m/s, 25% = 0.048 m/s, 50% = 0.075 m/s, 75% = 0.094 m/s and 100% = 0.11 m/s).

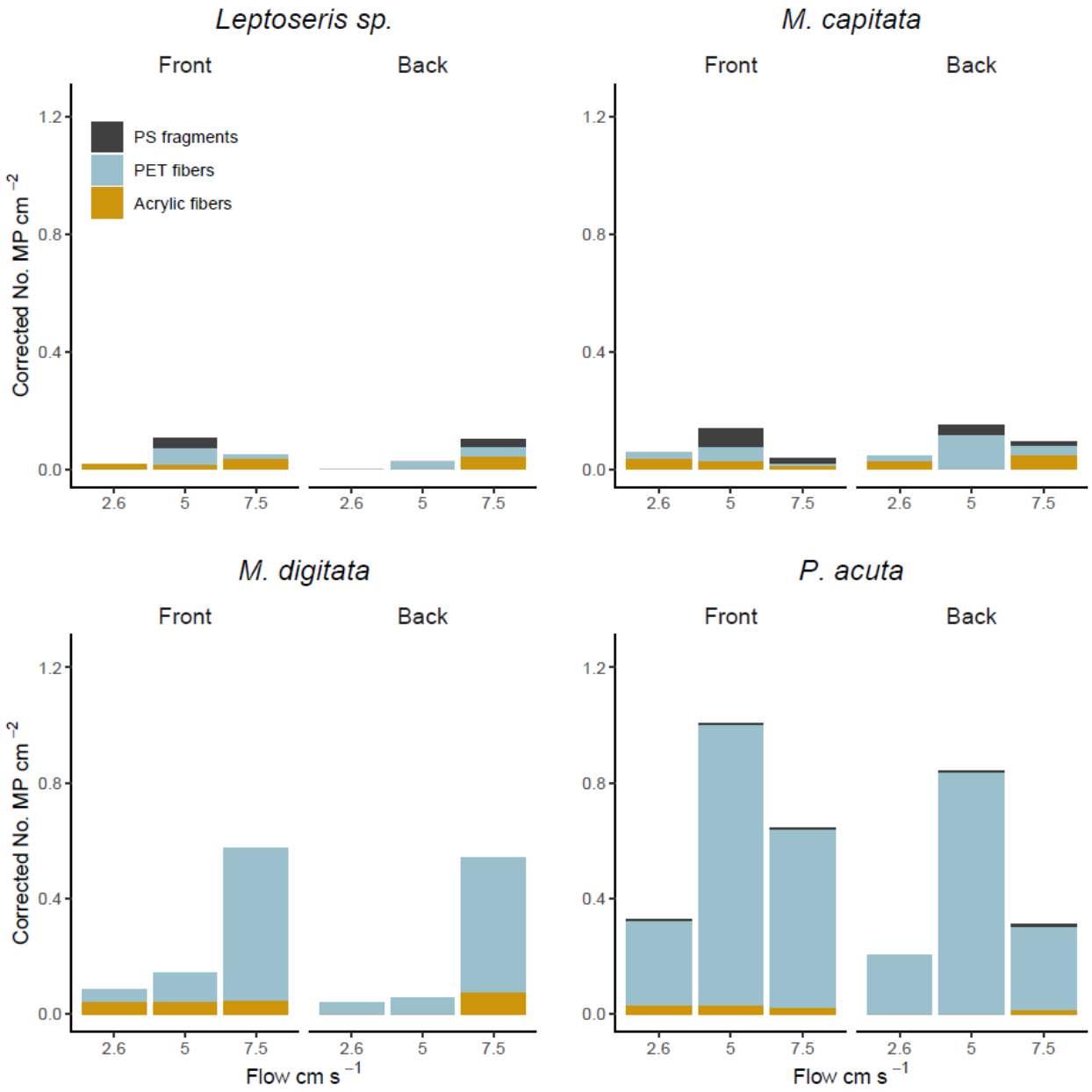

Figure S3.5 Mean corrected microplastics ingestion rates for each coral species under different flow velocities on the up- (front) and down- (back) stream sides of corals. Data are corrected for different concentrations of each microplastics type. PS = polystyrene, PET = polyester.

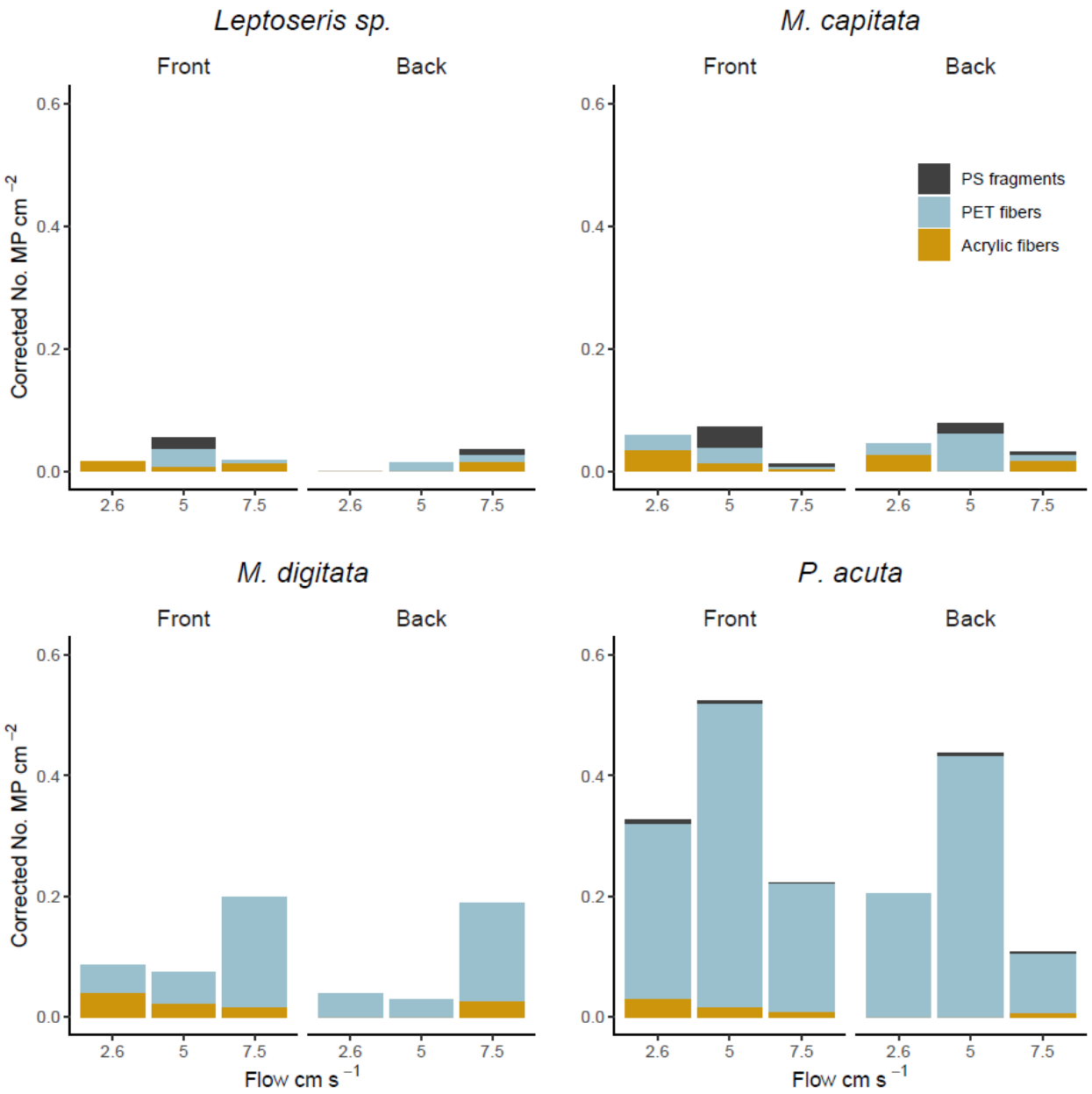

Figure S3.6 Mean corrected microplastics ingestion rates for each coral species under different flow velocities on the up- (front) and down- (back) stream sides of corals. Data are corrected for different concentrations of each microplastics type and for flow velocities. PS = polystyrene, PET = polyester.

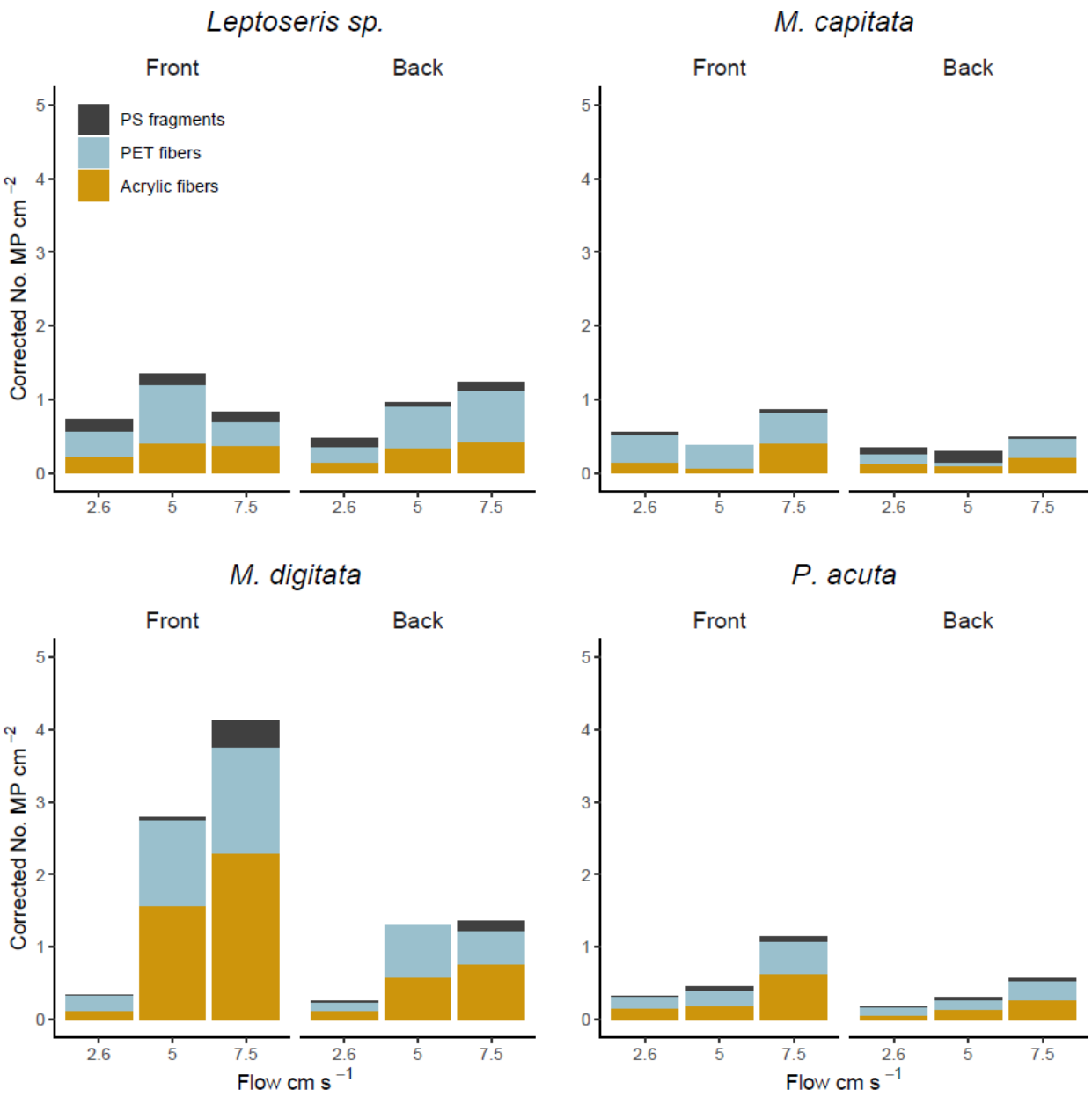

Figure S3.7 Mean corrected microplastics adhesion rates for each coral species under different flow velocities on the up- (front) and down- (back) stream sides of corals. Data are corrected for different concentrations of each microplastics type. PS = polystyrene, PET = polyester.

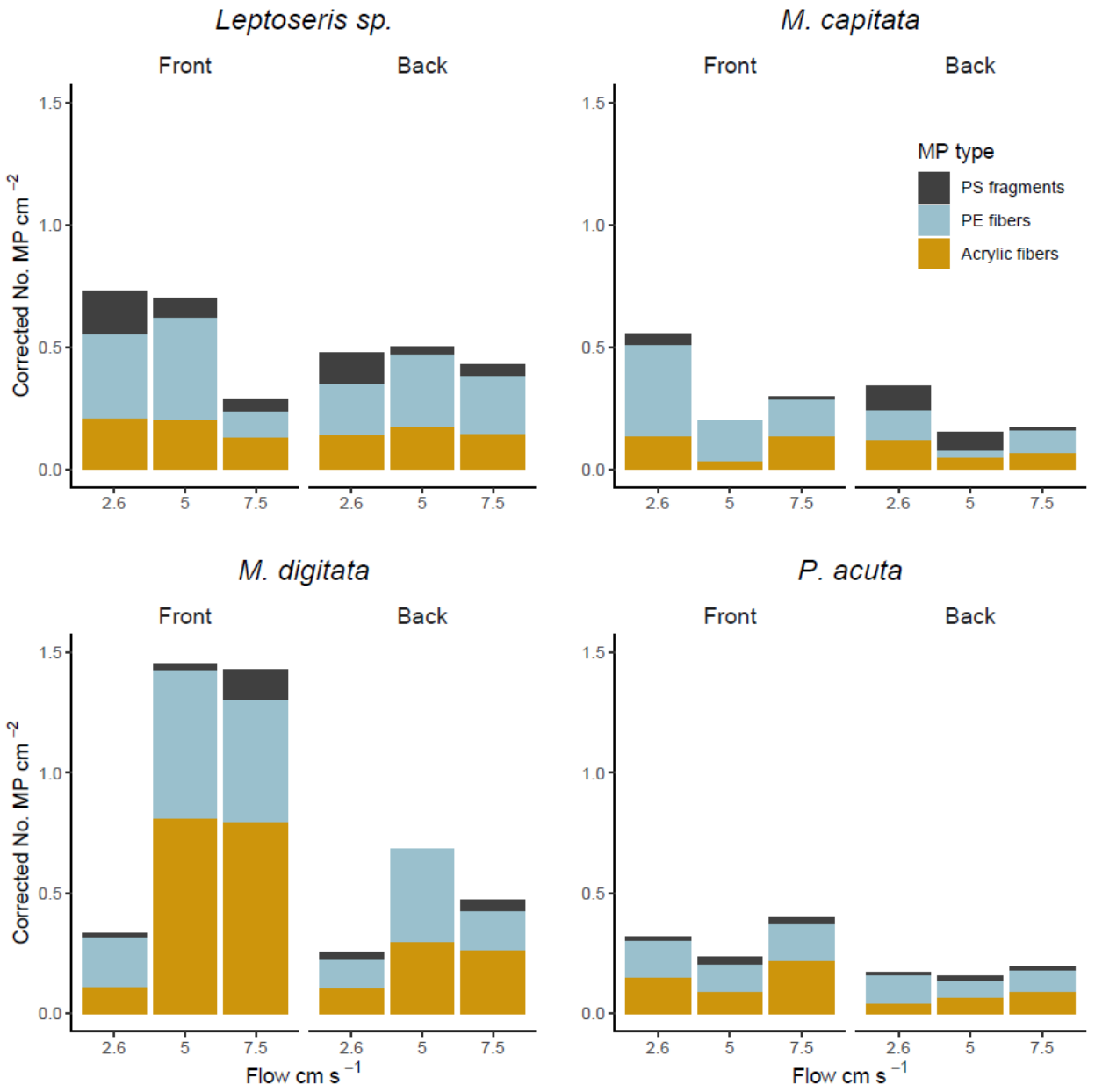

Figure S3.8 Mean corrected microplastics adhesion rates for each coral species under different flow velocities on the up- (front) and down- (back) stream sides of corals. Data are corrected for different concentrations of each microplastics type and for flow velocities. PS = polystyrene, PET = polyester.

Chapter 4. LOW INCIDENCE OF MICROPLASTICS CONTAMINANTS IN CORAL REEFS OF KĀNEʻOHE BAY, HAWAIʻI, USA

Publication history: This study was coauthored by Katherine Lasdin, and Jacqueline L. Padilla-Gamiño. At the time this dissertation was published, this chapter was not in review with a journal.

4.1 ABSTRACT

Microplastic pollution is increasing in marine environments and may cause additional stress for coral reefs already under immense pressure from global change. This study investigated microplastic and other micro-debris pollution in sediment, seawater, sea cucumbers, and corals from fringing and patch reefs in Kāneʻohe Bay, Oahu, Hawaiʻi, USA. Microplastic pollution in Kāneʻohe Bay was low compared to other tropical coral reefs. Microplastics were detected in sediments (29%), sea cucumbers (9%), and coral (0 – 2%) samples but were not quantifiable. Seawater had quantifiable microplastic (< 0.5 mm) and macro-plastic (> 0.5 mm) contamination, with mean concentrations ranging from 0.0061 – 0.081 particles m^{-3}. Most particles detected in seawater samples were larger, floating plastic debris consisting mostly of polyethylene, polypropylene fragments, and fibers. Across the other matrices, most detected particles were polyester, polypropylene, and cotton fibers. These results provide baseline data for this important coral reef ecosystem, and further monitoring is recommended to understand the seasonal and long-term trends in microplastic pollution and its potential future impacts. However, compared to the more significant impacts of climate change, plastic pollution is a minor stressor for coral reefs.

4.2 INTRODUCTION

Plastic pollution is wide-ranging and increasing rapidly, yet there is still much we do not know about the fate of plastics in marine environments. Millions of tons of plastic waste enter the oceans each year (Jambeck et al., 2015; Borrelle et al., 2020; Meijer et al., 2021), but unless countries drastically increase efforts to manage plastic waste, plastic emissions are predicted to increase substantially in the coming years (Borrelle et al., 2020). Microplastics, synthetic polymers < 5 mm, are a consequence of plastic pollution (Barnes et al., 2009). They can enter the oceans as micro-sized particles (primary microplastics) or result from the breakdown of larger plastic debris (secondary microplastics) due to physical processes such as UV radiation and abrasion (Cole et al., 2011). Microplastic pollution has been documented in nearly every corner of the planet, from polar regions and sea ice to the tropics and coral reefs (Hall et al., 2015; Peeken et al., 2018). They are thought to accumulate on the sea surface, in seafloor and coastal sediments, in biogenic marine structures, and organisms (Woodall et al., 2014; Kane and Clare, 2019; Lebreton et al., 2019; Reichert et al., 2022; Soares et al., 2023). However, we still lack a comprehensive understanding of the fate of these persistent pollutants. Thus, monitoring these pollutants to better understand their fate in different ecosystems and their potential impacts on life on our planet is critical.

Coral reefs are essential ecosystems that support the livelihoods of millions of people, protect coastlines from erosion, and harbor incredible amounts of biodiversity (Moberg and Folke, 1999). Microplastics have been detected in coral reef environments, as well as in organisms living within these reefs, including corals themselves (Hall et al., 2015; Ding et al., 2019; Lei et al., 2021; Tang et al., 2021; Lim et al., 2022; Zhou et al., 2022). Chemical cues may drive microplastics ingestion by corals (Allen et al., 2017), or corals may inadvertently ingest them

while feeding on zooplankton from the water (Axworthy and Padilla-Gamiño, 2019). Lab studies have demonstrated that exposure to microplastics can have deleterious effects on corals, including reduced growth and prey capture, impaired photosynthesis, compromised immunity, tissue necrosis, and bleaching (Chapron et al., 2018; Reichert et al., 2018, 2019; Tang et al., 2018; Lanctôt et al., 2020; Hankins et al., 2021; Liao et al., 2021; Mendrik et al., 2021). Moreover, corals and coral reefs can serve as long-term sinks for microplastics when they are incorporated into coral skeletons and other reef structures (Hierl et al., 2021; Reichert et al., 2022; Soares et al., 2023). In addition to microplastics, other micro-debris, such as semi-synthetic, e.g., rayon, and other anthropogenically altered, e.g., dyed cotton, micro-fibers may impact corals and other marine life (Kroon et al., 2018; Reichert et al., 2024). Improving the management of microplastic and other micro-debris, as well as gaining a deeper understanding of their ecological impacts, requires establishing robust baseline data and implementing consistent monitoring efforts.

Kāneʻohe Bay, Ohau, Hawaiʻi, supports a tropical coral reef ecosystem consisting of fringing reefs that line the shore and patch reefs distributed throughout the bay. The reefs are dominated by two coral species, rice coral, *Montipora capitata,* and finger coral, *Porites compressa*. Together, these two species comprise over 80% of the coral assemblage in the bay (Jokiel, 1991). Past research has shown that *M. capitata* is reluctant to ingest microplastics *ex situ* (Axworthy and Padilla-Gamiño, 2019), but it is not known whether this species or *P. compressa*, ingest them in the wild. Kāneʻohe Bay is also home to the hot dog sea cucumber, *Holothuria edulis*, which feeds on detritus in the sediment, potentially making it a good indicator of microplastic and other micro-debris pollution (Plee and Pomory, 2020; Coc et al., 2021). To our knowledge, microplastic pollution has not been assessed in Kāneʻohe Bay coral reefs despite the Hawaiian

islands being a hotspot for plastic debris accumulation (Brignac et al., 2019). An assessment of microplastic contamination in Kāneʻohe Bay could establish an initial baseline and provide valuable insights into the distribution of microplastics within the reefs, identifying areas where they are most abundant.

Microplastic pollution varies considerably in tropical systems, with some reefs being heavily polluted and others being low to moderately polluted (Huang et al., 2021). Few studies, however, have conducted simultaneous sampling of environmental and biological samples (Ding et al., 2019; Lei et al., 2021; Tang et al., 2021; Lim et al., 2022; Zhou et al., 2022), which could provide a comprehensive understanding spatial extent of these contaminants and their risk to reef organisms. The goal of this study was to investigate microplastic contamination in Kāneʻohe Bay. Specifically, we aimed to determine the abundance of microplastics and other micro-debris in sediments, seawater, sea cucumbers, and corals from the bay. We hypothesized that fringing reefs, being closer to shore and sources of terrestrial runoff, are more contaminated with microplastics than patch reefs. We also hypothesized that microplastic contamination in corals correlates to seawater microplastic contamination since corals feed from the water column and that microplastic contamination in sea cucumbers correlates to sediment microplastic contamination because *H. edulis* feeds in the sediment.

4.3 Materials and Methods

4.3.1 *Sample collection*

Environmental and biological samples were collected from two fringing reefs (K4 and K5) and two patch reefs (HIMB and P29) in Kāneʻohe Bay, Oahu, Hawaii, in the summer of 2018 (Fig. 4.1). Environmental samples included surface water and sediment. Biological samples included

sea cucumbers, *Holothuria edulis* and corals, *Montipora capitata,* and *Porites compressa* (DAR Special Activities Permit No. 2019–21; Table 4.1).

Sediments were collected on SCUBA from each reef between coral patches or at the bottom of the reef slope from depths between 2 – 8 m. Sediment was sampled from the top 10 cm of the seafloor using a stainless-steel spoon to fill a 0.47 L glass jar. Later, 200 g of wet sediment from each sample was double wrapped in pre-cleaned and weighed aluminum foil and dried overnight at 60 °C in a drying oven at the Hawai‘i Institute of Marine Biology (HIMB). The samples, still wrapped in aluminum foil, were stored and shipped in plastic freezer bags to the University of Washington.

Surface water samples were collected using a manta net with an opening of 0.069 m^2 and a mesh size of 330 µm. At each reef, five ~500 m tows were performed from the windward side of the vessel within 5 m of the reef crest above the reef slope. Distance was measured with a mechanical flowmeter (General Oceanics, USA) attached to the manta net which was used to calculate the total volume of water filtered. At the end of each tow, the contents of the net were rinsed into the cod-end by pumping seawater along the outside of the net, then transferred to a pre-cleaned glass collection jar with equal amounts of seawater and 10% formalin. Later, the samples were poured through a 250 µm stainless steel sieve and rinsed into a 200 ml plastic collection jar using Milli-Q water. An equal amount of 10% formalin was added again to preserve the samples.

Organisms were collected at each reef on SCUBA. Coral fragments (~7 cm) from each site were collected using stainless steel toenail clippers (Revlon, USA) and placed in communal plastic freezer bags. Sea cucumbers were collected by hand and placed in plastic freezer bags. Upon

surfacing, organisms were rinsed with copious amounts of filtered seawater (0.45 µm) to remove mucous and any adhered microplastics, then wrapped in pre-cleaned aluminum foil and frozen on ice. They were later stored at -80 °C at HIMB until they were shipped to the University of Washington, where they were stored at -20 ºC until they were processed for microplastics.

4.3.2 *Sample processing*

Dried sediments were placed in a glass beaker and ground with a stainless-steel pestle. Large chunks of rubble were removed, and the samples were weighed to obtain dry weight. Density separations were performed by filling the beakers with 200 ml saturated sodium chloride (NaCl) solution and then stirring the solution vigorously for one minute with a metal spatula. The samples were allowed to settle for at least 24 h before they were decanted into clean glass jars. The process was repeated three times per sample, pooling the decanted solutions into single glass jars. The resulting solutions were vacuum filtered onto 5 µm polycarbonate filters, which were transferred into glass petri dishes and then wrapped in aluminum foil until they were analyzed for particles.

Preserved seawater samples were poured over a 250 µm stainless steel sieve and rinsed with filtered DI water to wash away the formalin. The contents on the sieve were visually inspected for micro- and macro debris, which were removed and stored in glass petri dishes for later analyses. The remaining contents on the sieve were backwashed into glass beakers. To digest biological material, 200 ml of 20% potassium hydroxide (KOH) was added to the beakers, then they were covered with aluminum foil and placed in an incubator at 50 ºC for five days. The beakers were swirled every 1 – 2 days to aid the digestion reaction. The contents of the beaker

were vacuum filtered onto 5 µm polycarbonate filters, placed in glass petri dishes, then wrapped in aluminum foil until later analyses.

Sea cucumber samples were defrosted, then weighed, and measured lengthwise. The digestive tracts were dissected from the body cavities, laid on clean aluminum foil, and measured lengthwise. The digestive tract tissues were digested in glass beakers with 100 ml 20% KOH solution at 50 ºC for 3 – 4 days. The KOH solution was decanted into a clean glass jar, then vacuum filtered onto a 5 µm polycarbonate filter and stored as described above until further analysis. The sediments that remained following tissue digestion underwent density separation by adding 200 ml of saturated NaCl to the same beaker, stirring the solution vigorously for one minute, and then allowing it to settle for at least 24 hours. The NaCl solution was decanted into a clean glass jar. Density separation was performed three times for each sample, and the decanted solution was pooled together in the same jar before undergoing vacuum filtration onto a 5 µm polycarbonate filter and stored as described above.

Coral fragments were thawed and rinsed heavily with filtered DI water before being placed into glass beakers for tissue digestion. 200 ml of 20% KOH solution were added to the beakers, which were then placed in an incubator for 5 days at 50 ºC. Following this step, coral skeletons were rinsed with filtered DI water into the same beaker to remove the remaining tissue. The digested tissue solutions were vacuum filtered and stored until further analysis as described previously.

Surface areas of the coral skeletons were obtained using 3D-scanning (Reichert et al., 2016). In brief, coral skeletons were mounted on modeling clay placed on a turntable and rotated while scanning (Artec Spider) all sides at a 45 º angle. The models were processed using Artec Studio

(ver. 13). Individual frames with scans with an error value above 0.3 were discarded. “Crop surroundings” was used on each scan to remove auxiliary surfaces and random noise. “Global registration” was performed next to optimize meshes for further processing. To remove outliers, “eliminate noise” was used, and then the scans were fused into a single mesh using the “smooth fusion” function. Visible abnormalities were removed using “erase flaws,” and the resulting meshes were reduced using “simplify mesh.” Finally, the texture was applied to the meshes to show their surface color and textures, and the meshes were exported as .obj files. The meshes were imported into Meshlab (ver. 3.5.474) to obtain surface area measurements using the “compute geometric measures” function.

Coral skeletons were rinsed with filtered DI water to remove potential micro-debris contamination and then placed into glass beakers for skeleton dissolution. Skeletons were dissolved by adding ~250 ml of 10% hydrochloric acid (HCl) solution and allowing the reaction to occur overnight. If not fully dissolved by the next day, an additional 50 ml aliquots of HCl were added as needed until no skeletal material remained. The resulting solution was vacuum-filtered and stored as described above.

4.3.3 *Particle analysis*

Filters were visually inspected under a microscope (10 – 40X magnification) for suspected microplastics and other anthropogenic micro-debris. All particles that did not appear to have a cellular structure, did not crumble when probed, and did not make a scraping sound when prodded were analyzed. Photographs were taken of each particle, and their length, color, and type (morphology) were recorded. For length measurements, the longest dimension of each particle was recorded, i.e., length of fibers or ferret diameter of fragments. Particles were divided

into size classes of 0 – 500, 501 – 1000, 1001 – 2000, 2001 – 3000, 3001 – 4000, 4001 – 5000, and > 5000 µm. Color observations included primary and secondary colors, black, brown, clear, and white. Particle types included fibers, fiber bundles, films, fragments, and beads. The particles were rinsed in filtered 70% ethanol and transferred to gold-plated slides for micro-Fourier transformed infrared (µ-FTIR) analysis.

Particles were identified using a Nicolet iN10 µ-FTIR (Thermo Fisher Scientific), equipped with a liquid nitrogen cooled, mercury cadmium telluride array detector. Scans were taken with an aperture of 150 µm x 150 µm in attenuated total reflectance (ATR) mode using a germanium crystal, with a resolution of 8 cm^{-1}, using Omnic Picta software (ver. 1.8.240). Spectra were detected in the spectral range of 650 – 4000 cm^{-1}. Up to three attempts were made to identify particles: attempt 1) included 16 added scans and ATR pressure of 15, attempt 2) included 64 added scans and ATR pressure of 15, attempt 3) included 64 added scans and ATR pressure of 2. Spectra were compared with an in-house compilation of spectral libraries (Supplementary Spectral libraries). Particles were considered identified if the best spectral match score was ≥ 70. Representative FTIR spectra and images of particles detected in this study are presented in Figure 4.2.

Particle identifications were used to classify particles into four groups based on their origin: plastic, anthropogenic, natural, and unknown. Plastic refers to synthetic polymers, such as polypropylene or polyester. Anthropogenic refers to cellulosic materials, including cellophane, cellulose, and rayon, and includes dyed (i.e., black or blue) cotton. The anthropogenic category was used because the spectral similarity of these materials makes it difficult to distinctly identify them and because, although cellulosic materials originate from natural compounds (i.e.,

cellulose), the resulting products are not natural, *sensu stricto*, and may contain anthropogenic chemicals that could have ecological implications. Natural particles refer to non-dyed (i.e., white or clear) cotton and wool, fur, wood, etc. Unknown particles refer to particles that did not meet the spectral match threshold of 70 or were lost during µ-FTIR analysis.

4.3.4 *Quality assurance/quality control*

Multiple steps were taken to reduce microplastic and other micro-debris contamination. Materials and equipment used for field work were rinsed with filtered DI water or filtered seawater before and in between each use. In the lab, all personnel were encouraged to wear clothing made of non-plastic material (i.e., cotton and wool) and were required to use a lint roller and wear 100% cotton lab coats. Two HEPA filters were run simultaneously while working in the lab. Lab benches and equipment were cleaned with filtered 70% ethanol each day work was performed. Lab work was performed efficiently to reduce the time for contamination to occur. Procedures that did not involve harmful chemicals were performed in a laminar flow hood. All reagents and water were filtered to 1.2 µm. The use of plastic labware and field equipment was avoided whenever possible. All glassware used in the lab was baked in a muffle furnace at 500 ºC for four hours before first use and was washed, then rinsed 3x with filtered DI water then rinsed again with filtered 70% ethanol between each use. Airborne controls and procedural blanks were used for lab procedures to account for contamination. Procedural blanks were not used in the field (discussed later).

4.3.5 *Limit of detection/limit of quantification*

Samples were processed in batches of four. For each batch, one airborne control and one procedural blank were used. Airborne controls consisted of 90 mm glass fiber filters stamped

with a grid and placed in a glass petri dish. The petri dish was uncovered whenever samples were exposed to the environment to account for particles that fell out of the air. Procedural blanks were empty vessels treated the same way as the field-collected samples to account for contamination from lab equipment and reagents. Particles on the airborne control and blank filters were analyzed as described above and used to calculate the limits of detection (LOD) and limits of quantification (LOQ) (Dawson et al., 2023). Particle data from one procedural blank, used for a batch of sediment, was omitted from analyses because it contained an unusually high number of particles (> 50) that were mostly cellulosic, which we suspect came from using a Kimwipe when cleaning the petri dish. To calculate LOD and LOQ, particle counts from the airborne controls and blanks were summed for each batch, and then the mean and standard deviation of the particle count for each matrix (i.e., sediment, seawater, sea cucumbers, and coral) and particle origin (i.e., plastic, anthropogenic, natural, unknown), were determined. LOQ for each matrix and particle origin was the mean respective particle count plus three times the standard deviation. LOQ for each matrix and particle origin was the mean plus ten times the standard deviation. The number of samples that had particle counts above LOD and LOQ were reported and samples that had particle counts above LOQ were analyzed further to determine differences between collection sites.

4.3.6 *Data analysis*

All data analyses were performed using R Studio (ver. 2023.12.1). Natural particles were not included in the analyses. For samples with particle counts above LOQ, the LOQ was subtracted from the particle count, and the resulting values were normalized to matrix-specific parameters as follows: sediment dry weight (particles kg^{-1}), seawater volume (particles m^{-3}), sea cucumber body length (particles cm^{-1}), coral surface area (particles cm^{-2}). Samples with particle counts

below LOQ were converted to zero. Since none of the data were normally distributed, Kruskal-Wallis tests were used to test for differences in particle concentrations between sites for each particle origin class within each matrix. Differences were considered significant when $P < 0.05$. Particle characteristics (identification, type, size, and color) are reported for samples with particle counts above LOD. Pearson's correlation was used to test the relationships between the concentration of microplastics between seawater and corals and between sediment and sea cucumbers at different sites.

4.4 RESULTS

Across all matrices, we extracted a total of 1474 particles. All suspected microplastic particles were analyzed via μ-FTIR spectroscopy. Of those, 15% were plastic (n = 224), 55% were of anthropogenic origin (n = 814), 5% were natural materials (n = 80), and 24% were not identified (n = 356). Over 88% of particles were fibers (n = 1309) or fiber bundles (n = 2), 8% were fragments (n = 118), 2.7% were films (n = 41), and the remaining particles were beads (n = 2) and foams (n = 2).

4.4.1 *Sediment*

Microplastic particles were detected in 29% of sediment samples across all sites (Table 4.2, Fig. 4.3). No sediment samples had microplastic counts above LOQ. Polypropylene was the most abundant polymer type in sediments, followed by polyester, olefin, polyethylene, acrylic, neoprene, and vinyl ester. The most common particle type was fibers, followed by fragments and one bead. Most microplastic particles were blue, and the rest were clear, black, white, green, and red. The majority of microplastic particles were less than 500 μm (Figure 4.4).

One sediment sample from site HIMB contained anthropogenic particles above the LOD (Table 4.2, Fig. 4.3). No sediment samples had anthropogenic particle counts above LOQ. The most abundant material type was cotton, followed by cellophane and cellulose. All detected anthropogenic particles in the sample were fibers. Blue was the most common fiber color, followed by black and red. The most abundant size class of anthropogenic particles in the sample was 1000 – 2000 μm (Figure 4.5). Particles of unknown origin were detected in 25% of sediment samples (Table 4.2, Fig. 4.3).

4.4.2 *Seawater*

Microplastic particles were detected in 90% of surface seawater samples across all sites (Table 4.2, Fig. 4.3). Fringing reefs, K4 and K5, had microplastic particle concentrations of 0.081 ± 0.017 (mean ± 1 SE particles m^{-3}) and 0.030 ± 0.017, respectively. Patch reefs, P29 and HIMB, had microplastic particle concentrations of 0.050 ± 0.050 and 0.024 ± 0.012, respectively (Fig. 4.6). The most abundant polymer type was polyethylene, followed by polypropylene, polyester, neoprene, olefin, polyamide, and acrylonitrile butadiene styrene. The most abundant microplastic type was fragments, followed by films and fibers. Blue was the most common plastic particle color, followed by black, clear, white, green, orange, red, and yellow. Most microplastic particles in seawater were between 500 – 2000 μm (Fig. 4.4). There was no difference in microplastic concentration between sites (Kruskal-Wallis, chi-squared = 5.63, df = 3, p-value = 0.13). An observation worth noting is that the plastic fibers observed in the seawater samples were generally larger and more weathered than fibers observed in other samples.

No particles of anthropogenic origin were detected in seawater samples. Four particles of unknown origin were detected in seawater samples. One seawater sample had unknown particles above LOQ (Table 4.2, Fig. 4.3).

Seawater was the only matrix in which macro-sized particles (> 5000 μm) were detected. Macro-plastic particles were detected in 50% of surface seawater samples across all sites. Fringing reefs, K4 and K5, had macro-plastic particle concentrations of 0.011 ± 0.0069 (mean ± 1 SE particles m^{-3}) and 0.032 ± 0.014, respectively. Patch reefs, P29 and HIMB, had macro-plastic particle concentrations of 0.0061 ± 0.0061 and 0.077 ± 0.029, respectively (Fig. 4.6). The most abundant polymer type was polyethylene, followed by polypropylene, acrylonitrile butadiene styrene, polyamide, and polystyrene. The most abundant type was fibers, followed by films, foams, and a fragment. Blue was the most common macro-plastic particle color, followed by black, clear, green, brown, orange, purple, red, and white. There was no difference in macro-plastic concentration between sites (Kruskal-Wallis chi-squared = 6.83, df = 3, p-value = 0.077).

No macro-sized particles of anthropogenic or unknown origin were detected in seawater samples (Table 4.2, Fig. 4.3).

4.4.3 *Sea cucumber*

Microplastic particles were detected in 9% of *H. edulis* samples across all sites. No *H. edulis* samples contained microplastics above LOQ (Table 4.2, Fig. 4.3). The most abundant polymer type was polyester, followed by polypropylene, olefin, and polyamide. All detected microplastics in *H. edulis* were fibers. Black was the most common plastic particle color, followed by blue and orange. Most microplastic particles in *H. edulis* were less than 500 μm (Fig. 4.4).

Anthropogenic particles were detected in 7% of *H. edulis* samples. No *H. edulis* samples contained anthropogenic particles above LOQ (Table 4.2, Fig. 4.3). The most abundant material type was cotton, followed by cellophane, cellulose, and rayon. All detected anthropogenic particles in *H. edulis* were fibers. Black was the most common fiber color, followed by blue, red, and clear. The most abundant size class of anthropogenic particles in *H. edulis* was 0 – 500 µm (Fig. 4.5). Particles of unknown origin were detected in 7% of *H. edulis* samples.

4.4.4 *Coral*

Microplastic particles were detected in 1 (2%) *M. capitata* sample from site K4 (Table 4.2, Fig. 4.3). Of the microplastics recovered from that sample, three were purple and black polyester fibers, and one was a red acrylic fiber, all between 1000 – 3000 µm (Fig. 4.4). No *M. capitata* samples had microplastics above LOQ (Table 4.2, Fig. 4.3).

Anthropogenic particles were detected in two *M. capitata* samples (Table 4.2, Fig. 4.3), one from site K4 and one from site P29. No *M. capitata* samples had anthropogenic particles above LOQ (Table 4.2, Fig. 4.3). The most abundant material type was cotton, followed by cellophane, rayon, and cellulose. All detected anthropogenic particles in *M. capitata* were fibers. Black was the most common fiber color, followed by blue, red, clear, and orange. The most abundant size class of anthropogenic particles in *M. capitata* was 1000 – 2000 µm (Fig. 4.5).

No microplastics or anthropogenic particles were detected in *P. compressa* (Table 4.2, Fig. 4.3).

Particles of unknown origin were detected in two *M. capitata* samples and in one *P. compressa* sample (Table 4.2, Fig. 4.3).

4.4.5 *Correlation tests*

Correlation tests between corals and seawater or sea cucumbers and sediment could not be performed because no coral or sea cucumber samples had quantifiable particle concentrations.

4.5 DISCUSSION

Here we present, to the best of our knowledge, the first assessment of microplastic, and other micro-debris, pollution in the coral reef ecosystem in Kāneʻohe Bay, Oahu, Hawaiʻi. Overall, there was very low microplastic contamination in the matrices studied, with seawater having the only quantifiable microplastic contamination. Given these low contamination levels, we could not support our hypotheses that fringing reefs in the bay are more contaminated than patch reefs or that microplastic contamination in corals and sea cucumbers correlates to microplastic concentrations in seawater and sediment, respectively. Our data, based on a comprehensive sampling regime that covered a range of matrices known to be contaminated with microplastics, suggests that microplastic pollution is likely not a serious threat to Kāneʻohe Bay's coral reefs.

4.5.1 *Microplastics in environmental samples*

Surface seawater had the highest detected levels of microplastics (0.049 – 0.11 particles m^{-3}) in our study compared to the sub-surface matrices. Compared to studies that used similar collection methods (i.e., surface water plankton trawl and mesh size: 80 – 333 µm, and FTIR or Raman spectroscopy), the sea surface microplastic concentrations detected in Kāneʻohe Bay were on the same order of magnitude as the Maldives (0.02 – 0.65 particles m^{-3}; Saliu et al., 2018, 2019), the South China sea (0.148 to 0.842 particles m^{-3}; Wang et al., 2019), Nansha Reef, China (0.056 particles m^{-3}; Tan et al., 2020), and Sri Lanka (0.28 – 0.52 particles $m^{-3;}$ Sevwandi Dharmadasa et al., 2021). Conversely, sea surface microplastic concentration in Kāneʻohe Bay was much

lower than in the Gulf of Mannar, India (6000 – 126000 particles m^{-3}; Patterson et al., 2020, 2022), and Rameswaram Island, India (24000 – 96000 particles m^{-3}; Jeyasanta et al., 2020). Differences in sampling methods make it difficult to compare our data to other studies, highlighting the need for harmonization between studies. However, many recent studies employ bulk sampling to obtain seawater samples (Huang et al., 2021). Unlike plankton tows, which are limited by mesh size, bulk sampling methods can capture smaller particles than plankton nets. The trade-off is that plankton nets allow more efficient sampling of greater water volumes. Thus, our sampling technique likely underestimated the amount of smaller-sized microplastics and other micro-debris, but we can more confidently infer particle concentration over a larger spatial scale.

Microplastic contamination levels in the sediments, sea cucumbers, and corals from Kāneʻohe Bay were considerably lower compared to those found in surface water. This indicates that a significant portion of the plastic debris polluting the bay consists of positively buoyant, floating particles. Floating plastics may sink over time when they degrade into smaller particles and become fouled (Chubarenko et al., 2016), which in turn could enter the sediment or be ingested by biota. However, it is likely that much of the floating plastic debris will end up on the shorelines of the islands. Driven by large-scale circulation patterns and climatic variations, a substantial amount of floating marine debris that enters the North Pacific Ocean makes its way onto Hawaiʻi's coastlines (Howell et al., 2012; Ribic et al., 2012; Brignac et al., 2019). Coastlines on the windward side of the islands, such as Kāneʻohe Bay, are more heavily impacted as onshore winds help carry debris to the shore (Brignac et al., 2019). In alignment with the findings of Brignac et al. (2019), the dominant plastics detected in sea surface waters in this study were polyethylene and polypropylene, which have low densities, making them

resistant to sinking. Thus, a potential explanation for the relatively low detection of microplastics in subsurface samples could be that floating plastic debris entering Kāneʻohe Bay via ocean currents and wind-driven processes are rapidly transported to the shore before becoming negatively buoyant and sinking to the reefs.

Other potential reasons for the low abundance of microplastics detected in subsurface samples could be associated with the characteristics of sediment and our extraction method. The upper layer of sediment in the reef slopes of Kāneʻohe Bay is fine silt, which is very soft and loose. This could result in particles sinking deeper into the sediment beyond the depth of our sampling, which was limited to the top 10 cm. Therefore, we may not have sampled deep enough to find many particles. This could also explain why we detected only a few microplastics in sea cucumbers, which feed on detritus in the upper sediment layers. Additionally, we may not have detected much microplastic contamination in sediments and sea cucumbers due to the density separation method used. Saturated NaCl has a density of approximately 1.2 mg ml^{-1}, limiting its ability to float certain denser types of plastic, such as polyester and polystyrene. Other solutions with higher densities are more efficient at separating more types of plastic, such as zinc bromide or sodium iodide (Quinn et al., 2017), but these chemicals are not as cost-effective or environmentally friendly as NaCl. We acknowledge that by using the methods employed in this study, we might not have detected particles with higher densities, which have been detected in Hawaiian seafloor habitats (Brignac et al., 2019).

Compared to other studies, very little microplastic contamination was detected in Kāneʻohe Bay corals (see review by Huang et al., 2021). For example, microplastic contamination in corals from atolls of Xisha Islands, China, ranged from 0.9 – 2.5 particles cm^{-2} (Zhou et al., 2022), and

corals from Hainan Island, China, had microplastic levels of nearly 5 particles cm^{-2} (Tang et al., 2021). Since we rinsed coral fragments to remove potential contaminants before processing, we were only able to detect microplastics that were ingested by the corals or microplastics that had been incorporated internally by corals prior to sampling. For *M. captiata*, this was not surprising since our past research has indicated that it does not readily ingest microplastics (Axworthy and Padilla-Gamiño, 2019). Given that, and the fact that we used the identical extraction method for *P. compressa*, it is reasonable to conclude that neither of these species ingest many microplastics. However, adhesion to surface tissue appears to be a more important mechanism for coral-microplastic interactions. Microplastic adhesion rates may be 40 times higher than ingestion rates for some corals (Martin et al., 2019; Corona et al., 2020), or 3 – 4 fold higher for others, such as *M capitata* (Axworthy et al., *in prep*). The adhesion of microplastics to coral surfaces can lead to tissue necrosis, bleaching, and overgrowth, ultimately leading to their deposition into the skeleton (Reichert et al., 2018; Hierl et al., 2021). However, corals may be able to remove adhered microplastics using the same mechanisms for removing sediments (Stafford-Smith and Ormond, 1992; Martin et al., 2019; Bejarano et al., 2022; Axworthy et al., *in prep*). Sampling protocols that differentiate ingested and adhered microplastics from corals should be considered for future studies.

4.5.2 *Method justifications and limitations*

Recently, there has been a call for more transparency when reporting the use of experimental controls in environmental microplastic studies (Dawson et al., 2023; Lao and Wong, 2023; Munno et al., 2023). We chose to use the LOD/LOQ method suggested in Dawson et al. (2023) because it was reported to differentiate microplastic contamination between samples and controls with over 95% accuracy. The method was easy to employ; however, the detection and

quantification limits (LOD and LOQ) depended on the standard deviation of particles in control samples. Given the variability in particle numbers on control filters, this likely increased our detection limit, potentially explaining the lower contamination levels observed compared to other studies. Interestingly, LODs and LOQs for anthropogenic particles (dyed cotton, cellulose, cellophane, and rayon) were considerably higher than the ones for plastic and unknown particles. These anthropogenic particles were almost entirely small fibers, indicating fibers shed from clothing (Carney Almroth et al., 2018). While we made a great effort to reduce contamination in the lab, there was still considerable and variable contamination. Given this uncertainty in contamination levels, the use of stringent LOD/LOQ methods for accounting for our control data was warranted, and we encourage other labs to follow the same method.

In hindsight, our LOD and LOQ might have been higher if we had used procedural blanks in the field, which we acknowledge we overlooked. However, we are confident that there was little chance for contamination during most aspects of field collections. Upon surfacing, the organisms collected underwater were immediately rinsed with filtered (1.2 μm) seawater for contamination and concealed in pre-cleaned foil, then they were rinsed again before processing in the lab. Sediment collected underwater was immediately stored in closed glass mason jars. A potential source of contamination in those samples could have come from the rubber gaskets in the lids, but we did not detect rubber in any samples. Seawater samples could have been contaminated by formalin or when the collection jars were open to the air. However, contamination would have likely consisted of small particles or fibers while the plastics we observed in seawater samples tended to be larger, mostly macroscopic sized particles.

4.5.3 *Implications*

Sub-surface habitats in Kāneʻohe Bay show minor contamination with microplastics, to the extent that microplastics were detected but not quantifiable. This may sound reassuring for the corals and other organisms that live there, but it should be noted that our sampling occurred over one summer, and as such, our data represents just one point in time. While it rains on most days in the Hawaiian Islands, the most rainfall occurs during the rainy season from November to March. During the rainy season, it is possible that more microplastics are transported to the bay via river discharge and other sources of runoff (Lebreton et al., 2017). Seasonal fluctuations in microplastic contamination in coastal waters have been documented in other places, with increases typically associated with monsoon seasons (James et al., 2021; Jong et al., 2022; Nakano et al., 2024). Moreover, storm surge and wind could result in resuspension of microplastics from the seabed sediments (Zhang, 2017). Consistent monitoring over multiple seasons should be implemented to better understand temporal trends in microplastic pollution in Kāneʻohe Bay. The results of this study can serve as critical baseline data for future studies.

The results of this study indicate that surface waters of Kāneʻohe Bay were more polluted by microplastics than the subsurface environments. Based on the season when we collected samples and the geography of the study area, it is most likely that the observed plastic pollution entered the bay from the North Pacific Ocean, likely originating from so-called “garbage patches” (Brignac et al., 2019). The most likely fate for these floating plastic debris is the bay’s shorelines, where they can accumulate. This could have implications for coastal organisms, where microplastic debris could alter the composition of shoreline sediments, and for tourism, where plastic debris could render the waterfront less attractive for tourists. Hawaiʻi has multiple programs that address marine debris, both governmental (Hawaii Department of Land and

Natural Resources, n.d.; Hawaii Sea Grant, n.d.; NOAA Marine Debris Program, n.d.) and non-governmental (Hawai‘i Wildlife Fund, n.d.; Ocean Defenders Alliance, n.d.; Sustainable Coastlines Hawai‘i, n.d., etc.). These programs will be critical for managing shoreline plastic pollution. However, it is essential to implement global efforts to reduce plastic waste in the North Pacific Ocean and worldwide. This approach ensures that states are not solely responsible for cleaning up waste that they did not generate.

Coral reefs are under increasing pressure from a suite of stressors, but is all the attention given to microplastics pollution on reefs warranted? Reef-building corals are the keystone sentinels of tropical reefs, and laboratory experiments have demonstrated a range of negative physiological effects in corals exposed to microplastics (Chapron et al., 2018; Reichert et al., 2018, 2019; Tang et al., 2018; Lanctôt et al., 2020; Hankins et al., 2021; Liao et al., 2021; Mendrik et al., 2021). However, many studies acknowledge that microplastic treatment concentrations in experiments exceed what corals experience in the field or use particle types (e.g., microspheres) that are not commonly observed on reefs (Hankins et al., 2018, 2021; Tang et al., 2018; Axworthy and Padilla-Gamiño, 2019; Rotjan et al., 2019; Lanctôt et al., 2020; Liao et al., 2021; Chen et al., 2022; Montalbetti et al., 2022; Bove et al., 2023). Some studies have attempted to investigate the effects of environmentally relevant microplastic treatments on corals (Berry et al., 2019; Mendrik et al., 2021; Bejarano et al., 2022; Boodraj and Glassom, 2022; Plafcan and Stallings, 2022; Reichert et al., 2022), and those studies often conclude that there are minimal or uncertain effects on certain corals (Berry et al., 2019; Bejarano et al., 2022; Boodraj and Glassom, 2022; Plafcan and Stallings, 2022). Moreover, there is little evidence that corals in the field are suffering significantly from microplastics (Tang et al., 2021; Lim et al., 2022; Zhou et al., 2023). The effects of climate change, most notably coral bleaching and mortality due to rising

temperatures, are impacting corals at enormous and rapid scales (Hoegh-Guldberg, 1999; Hughes et al., 2018; Eakin et al., 2019). Localized issues, such as nutrification, disease, overfishing, and even macro-plastic pollution could also contribute to substantial coral declines (Roberts, 1995; Green and Bruckner, 2000; D'Angelo and Wiedenmann, 2014; Lamb et al., 2018). Reducing plastic pollution (macro and micro) can alleviate additional stress on already vulnerable organisms, potentially avoiding additive or synergistic effects that can worsen their condition. Given the undeniable trend of increasing plastic pollution, proactive measures to curb its impact are crucial for the long-term health of marine ecosystems, like coral reefs. We recommend ongoing monitoring of plastic pollution in reefs and efforts to deepen our understanding of its implications. However, without decisive action to reduce global emissions, mitigate the effects of climate change, and address imminent local stressors in tropical systems, we risk losing our corals before fully understanding the extent of plastic pollution in them.

4.5.4 *Conclusion*

In the summer of 2018, microplastic contamination in Kāneʻohe Bay was relatively low compared to other tropical coral reefs, providing valuable baseline data regarding these persistent pollutants. Most plastic pollution was concentrated in surface waters, consisting of floating plastic debris that will likely end up on the bay's shorelines rather than in the reefs below the water's surface. Further monitoring and laboratory testing are recommended to better understand seasonal and long-term trends in microplastic pollution and the potential future impacts of microplastic pollution in Kāneʻohe Bay. However, microplastics are likely a relatively minor form of stress to coral reefs compared to climate change's more significant impacts.

4.6 ACKNOWLEDGEMENTS

We offer our warmest gratitude to the Gates Coral Lab for hosting and supporting us during this experiment at the Hawai‘i Institute of Marine Biology. We thank Tanya Brown, Brenner Wakayama, Gavin Kreitman, Melissa Jaffe, and Sean Frangos for help with fieldwork. We are grateful to Julie Masura and Kathy Newell for loaning us a manta net. We thank Romina Centurion, Alessia Mei Simmens, and Malcolm Munsil for helping extract microplastics in the lab. We thank Katie Anderson and Michael Holland from the Burke Museum for their assistance with 3D scanning. This work was supported by the National Science Foundation CAREER program (NSF CAREER, BIO-OCE, 2044840) and the Sloan Foundation Fellowship awarded to JPG, and the National Science Foundation Graduate Research Fellowship Program (DGE1762114) awarded to JBA.

4.7 TABLES AND FIGURES

Table 4.1 Field site coordinates and sample size for each matrix.

Site	Latitude	Longitude	Sediment	Seawater	*H. edulis*	*M. capitata*	*P.compressa*
K4	21.26682	-157.48356	7	5	9	11	12
K5	21.27886	-157.49991	7	5	12	13	11
P29	21.28241	-157.49145	7	5	13	10	10
HIMB	21.26273	-157.47424	7	5	10	10	10

Table 4.2 Limit of detection (LOD) and limit of quantification (LOQ) and the number of samples with particle counts above them for each matrix and each particle origin. Particles were pooled from airborne controls and procedural blanks. The LOD is equal to the mean number of particles plus three times the standard deviation. The LOQ is equal to the mean number of particles plus ten times the standard deviation (Dawson et al., 2023).

Matrix	Origin	LOD (# particles)	LOQ (# particles)	# samples above LOD	# samples above LOQ
Sediment	Plastic	4.58	13.19	8	0
n = 28	Anthropogenic	25.47	69.00	1	0
	Unknown	8.22	22.90	7	0
Seawater	Plastic	0.39	1.17	18	12
n = 20	Anthropogenic	3.11	8.51	0	0
	Unknown	3.06	8.46	4	1
Holothuria edulis	Plastic	1.60	4.89	4	0
n = 44	Anthropogenic	13.23	35.74	3	0
	Unknown	4.93	14.15	3	0
Montipora capitata	Plastic	3.01	9.06	1	0
n = 44	Anthropogenic	17.34	44.66	2	0
	Unknown	4.74	13.90	2	0
Porites compressa	Plastic	3.01	9.06	0	0
n = 43	Anthropogenic	17.34	44.66	0	0
	Unknown	4.74	13.90	1	0

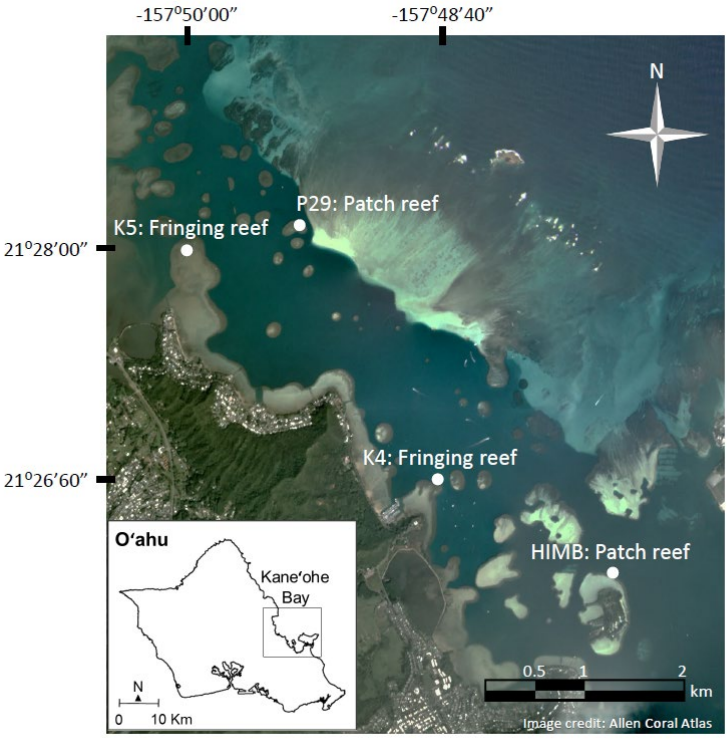

Figure 4.1 Map of Kāne'ohe Bay Bay and sample collection sites.

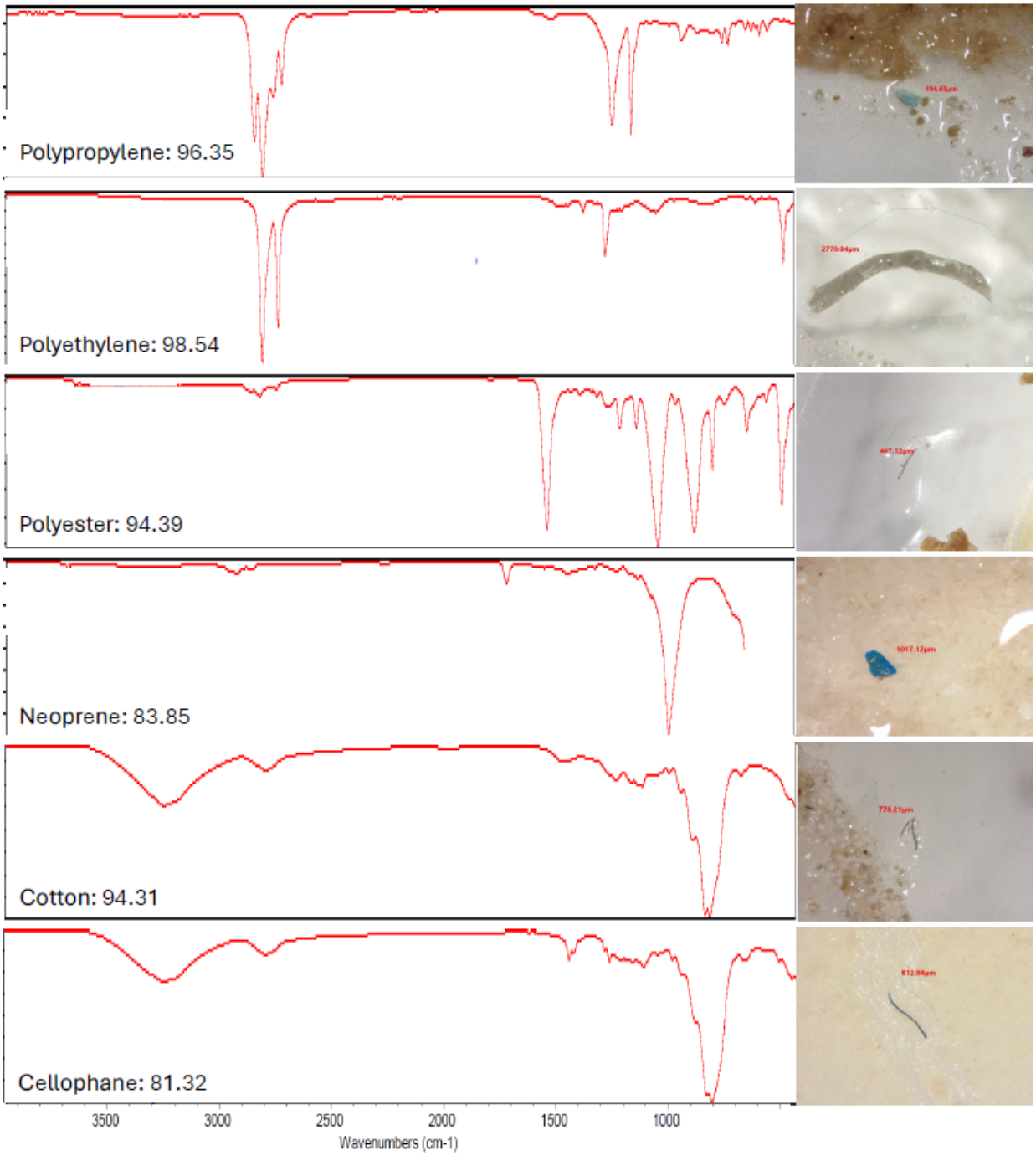

Figure 4.2 FTIR spectra, match scores, and microscope images of particles representative of the most abundant polymers and anthropogenic materials detected in this study. Note the spectral similarity between cotton and cellophane, making it difficult to identify each material.

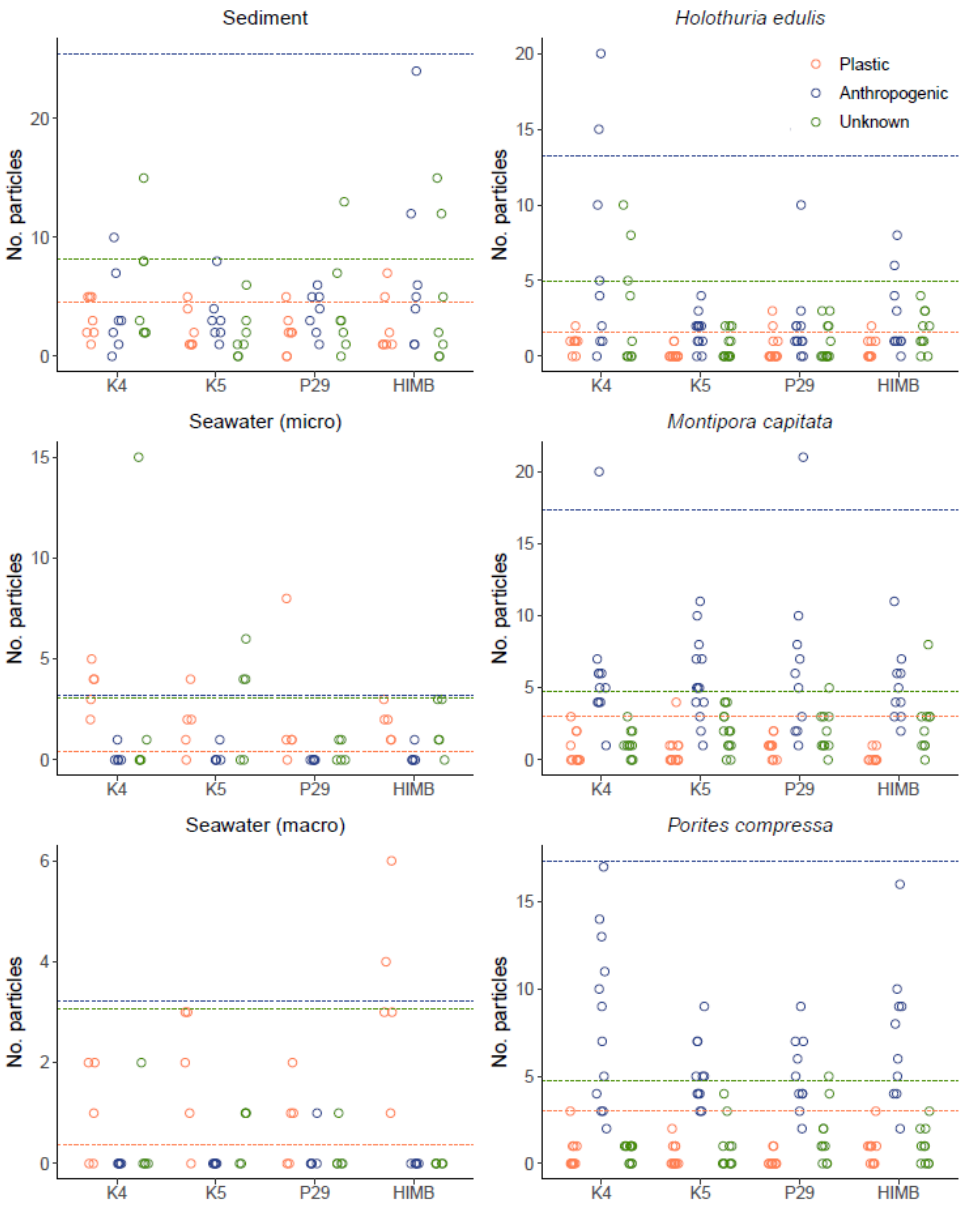

Figure 4.3 Number of particles per sample by site for each matrix from samples collected from Kaneohe Bay, Oahu, Hawaii, and the limits of detection (dotted lines). Particle origins (plastic, anthropogenic, and unknown) were determined by µ-FTIR spectroscopy. Plastic particles include synthetic polymers. Anthropogenic particles include cotton, rayon, cellulose, and cellophane, which are derived from natural materials but have been modified anthropogenically. Unknown particles did not meet the criteria for a good spectral match (≥ 70) or were lost during analysis. Dotted lines represent respective limits of detection.

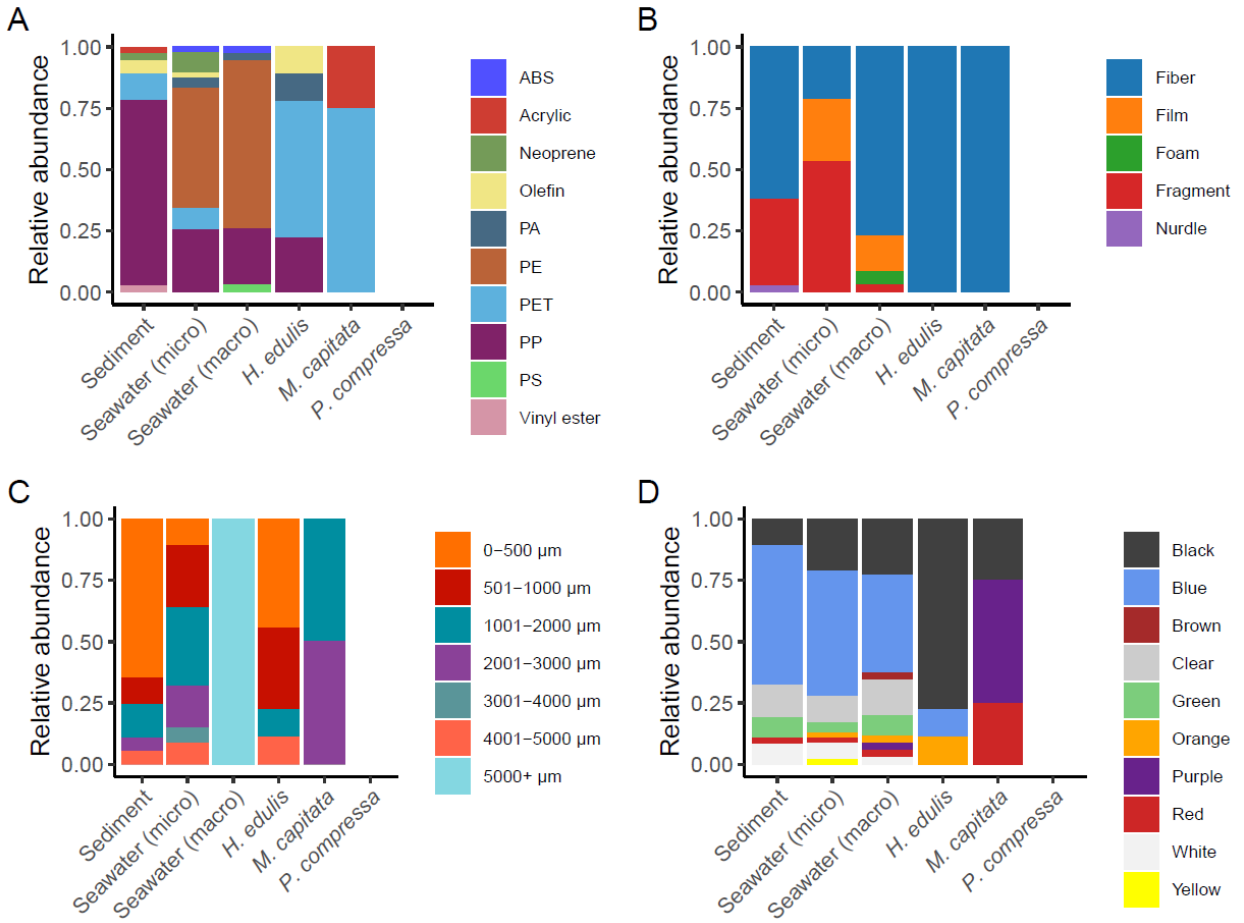

Figure 4.4 Characteristics of plastic particles detected in different matrices. A) plastic polymer identified by µ-FTIR, B) particle type, C) particle size (maximum dimension), and D) particle color.

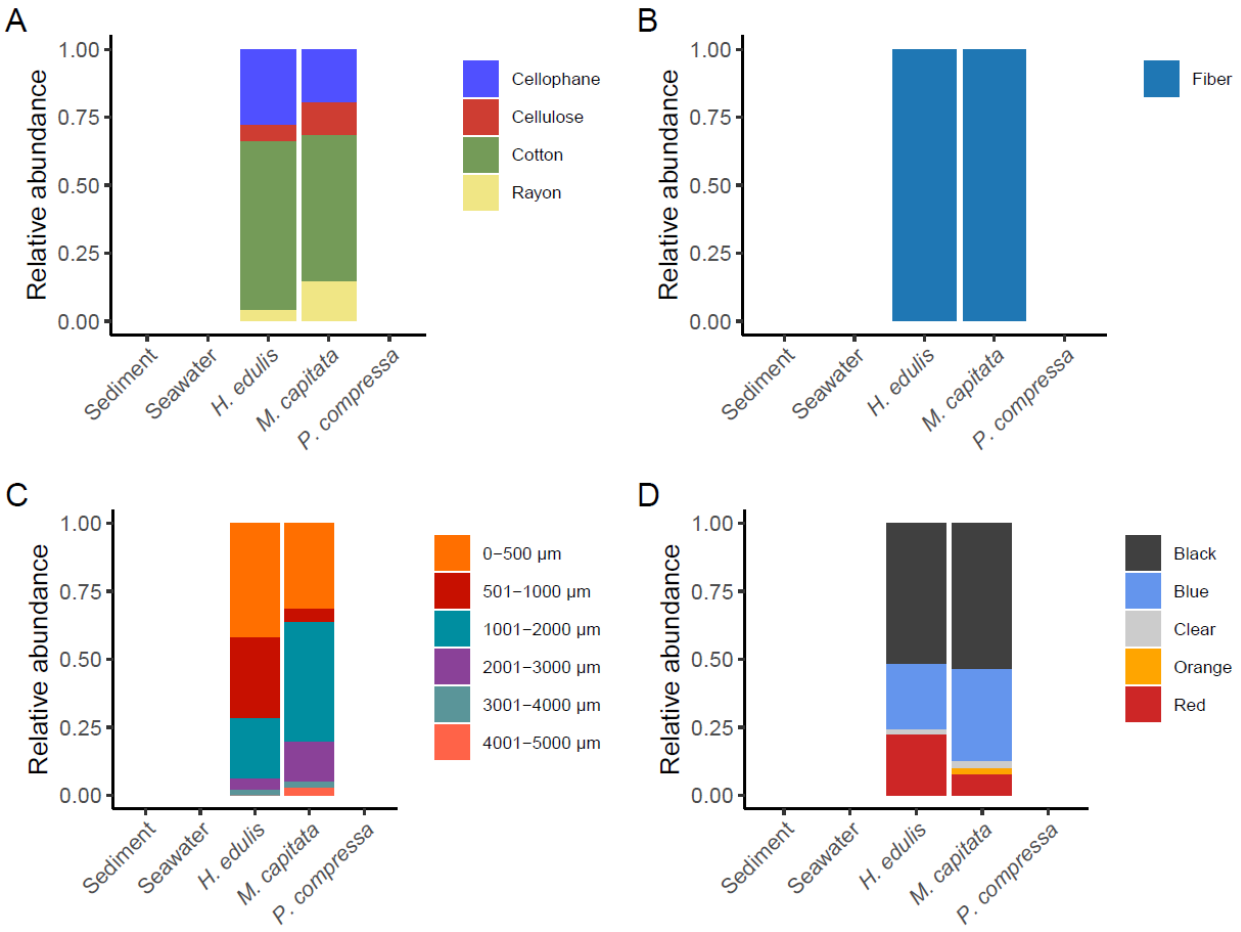

Figure 4.5 Characteristics of anthropogenic particles detected in different matrices. A) material identified by µ-FTIR, B) particle type, C) particle size (maximum dimension), and D) particle color.

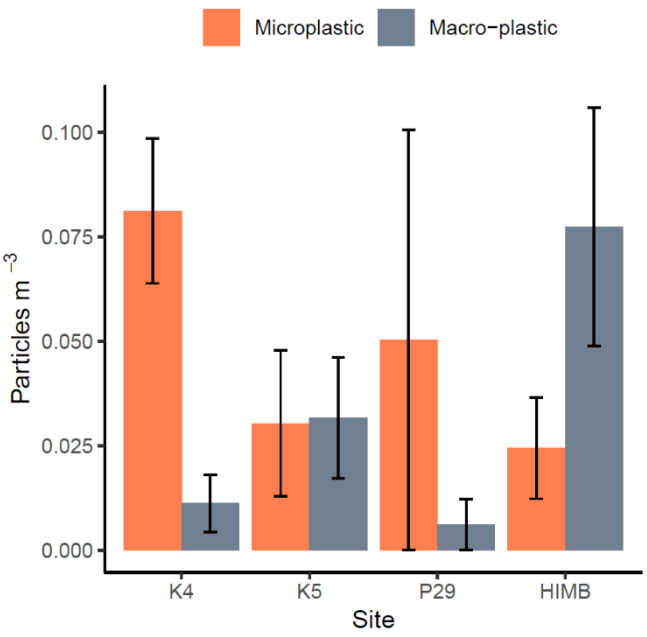

Figure 4.6 Mean microplastic and macro-plastic concentration in seawater by collection site. The data represent quantifiable particle concentrations in samples with particle counts above the limit of quantification based on control data. Microplastics were not quantifiable for sediment, sea cucumbers, or corals. Error bars represent one standard error.

4.8 REFERENCES

Allen, A. S., Seymour, A. C., and Rittschof, D. (2017). Chemoreception drives plastic consumption in a hard coral. *Mar. Pollut. Bull.* 124, 198–205. doi: 10.1016/j.marpolbul.2017.07.030

Axworthy, J. B., and Padilla-Gamiño, J. L. (2019). Microplastics ingestion and heterotrophy in thermally stressed corals. *Sci. Rep.* 9, 18193. doi: 10.1038/s41598-019-54698-7

Axworthy, J. B., Wang, S., Sofield, R. M., DiBenedetto, M., and Padilla-Gamiño, J. L. (in prep). Microplastics ingestion and adhesion by reef-building corals under different flow velocities.

Barnes, D. K. A., Galgani, F., Thompson, R. C., and Barlaz, M. (2009). Accumulation and fragmentation of plastic debris in global environments. *Philosophical Transactions of the R. Soc. B Biol. Sci.* 364, 1985–1998. doi: 10.1098/rstb.2008.0205

Bejarano, S., Diemel, V., Feuring, A., Ghilardi, M., and Harder, T. (2022). No short-term effect of sinking microplastics on heterotrophy or sediment clearing in the tropical coral *Stylophora pistillata*. *Sci Rep* 12, 1468. doi: 10.1038/s41598-022-05420-7

Berry, K. L. E., Epstein, H. E., Lewis, P. J., Hall, N. M., and Negri, A. P. (2019). Microplastic Contamination Has Limited Effects on Coral Fertilisation and Larvae. *Diversity* 11, 228. doi: 10.3390/d11120228

Boodraj, P., and Glassom, D. (2022). Experimental exposure to microplastics does not affect the physiology of healthy or moderately bleached *Anomastraea irregularis* and *Pocillopora verrucosa* corals. *Mar. Biol.* 169, 48. doi: 10.1007/s00227-022-04038-7

Borrelle, S. B., Ringma, J., Law, K. L., Monnahan, C. C., Lebreton, L., McGivern, A., et al. (2020). Predicted growth in plastic waste exceeds efforts to mitigate plastic pollution. *Science* 369, 1515–1518. doi: 10.1126/science.aba3656

Bove, C. B., Greene, K., Sugierski, S., Kriefall, N. G., Huzar, A. K., Hughes, A. M., et al. (2023). Exposure to global change and microplastics elicits an immune response in an endangered coral. *Front. Mar. Sci.* 9. doi: 10.3389/fmars.2022.1037130

Brignac, K. C., Jung, M. R., King, C., Royer, S.-J., Blickley, L., Lamson, M. R., et al. (2019). Marine Debris Polymers on Main Hawaiian Island Beaches, Sea Surface, and Seafloor. *Environ. Sci. Technol.* 53, 12218–12226. doi: 10.1021/acs.est.9b03561

Carney Almroth, B. M., Åström, L., Roslund, S., Petersson, H., Johansson, M., and Persson, N.-K. (2018). Quantifying shedding of synthetic fibers from textiles; a source of microplastics released into the environment. *Environ. Sci. Pollut. Res.* 25, 1191–1199. doi: 10.1007/s11356-017-0528-7

Chapron, L., Peru, E., Engler, A., Ghiglione, J. F., Meistertzheim, A. L., Pruski, A. M., et al. (2018). Macro- and microplastics affect cold-water corals growth, feeding and behaviour. *Sci. Rep.* 8, 15299. doi: 10.1038/s41598-018-33683-6

Chen, Y.-T., Ding, D.-S., Lim, Y. C., Singhania, R. R., Hsieh, S., Chen, C.-W., et al. (2022). Impact of polyethylene microplastics on coral *Goniopora columna* causing oxidative stress and histopathology damages. *Sci. Total Environ.* 828, 154234. doi: 10.1016/j.scitotenv.2022.154234

Chubarenko, I., Bagaev, A., Zobkov, M., and Esiukova, E. (2016). On some physical and dynamical properties of microplastic particles in marine environment. *Mar. Pollut. Bull.* 108, 105–112. doi: 10.1016/j.marpolbul.2016.04.048

Coc, C., Rogers, A., Barrientos, E., and Sanchez, H. (2021). Micro and Macroplastics Analysis in the Digestive Tract of a Sea Cucumber (Holothuriidae, *Holothuria floridana*) of the Placencia Lagoon, Belize. *cjos* 51, 166–174. doi: 10.18475/cjos.v51i2.a2

Cole, M., Lindeque, P., Halsband, C., and Galloway, T. S. (2011). Microplastics as contaminants in the marine environment: A review. *Mar. Pollut. Bull.* 62, 2588–2597. doi: 10.1016/j.marpolbul.2011.09.025

Corona, E., Martin, C., Marasco, R., and Duarte, C. M. (2020). Passive and Active Removal of Marine Microplastics by a Mushroom Coral (*Danafungia scruposa*). *Front. Mar. Sci.* 7, 128. doi: 10.3389/fmars.2020.00128

D'Angelo, C., and Wiedenmann, J. (2014). Impacts of nutrient enrichment on coral reefs: new perspectives and implications for coastal management and reef survival. *Curr. Opin. Environ. Sust.* 7, 82–93. doi: 10.1016/j.cosust.2013.11.029

Dawson, A. L., Santana, M. F. M., Nelis, J. L. D., and Motti, C. A. (2023). Taking control of microplastics data: A comparison of control and blank data correction methods. *J. Hazard. Mat.* 443, 130218. doi: 10.1016/j.jhazmat.2022.130218

Ding, J., Jiang, F., Li, J., Wang, Z., Sun, C., Wang, Z., et al. (2019). Microplastics in the Coral Reef Systems from Xisha Islands of South China Sea. *Environ. Sci. Technol.* 53, 8036–8046. doi: 10.1021/acs.est.9b01452

Eakin, C. M., Sweatman, H. P. A., and Brainard, R. E. (2019). The 2014–2017 global-scale coral bleaching event: insights and impacts. *Coral Reefs* 38, 539–545. doi: 10.1007/s00338-019-01844-2

Green, E. P., and Bruckner, A. W. (2000). The significance of coral disease epizootiology for coral reef conservation. *Biol. Conserv.* 96, 347–361. doi: 10.1016/S0006-3207(00)00073-2

Hall, N. M., Berry, K. L. E., Rintoul, L., and Hoogenboom, M. O. (2015). Microplastic ingestion by scleractinian corals. *Mar. Biol.* 162, 725–732. doi: 10.1007/s00227-015-2619-7

Hankins, C., Duffy, A., and Drisco, K. (2018). Scleractinian coral microplastic ingestion: Potential calcification effects, size limits, and retention. *Mar. Pollut. Bull.* 135, 587–593. doi: 10.1016/j.marpolbul.2018.07.067

Hankins, C., Moso, E., and Lasseigne, D. (2021). Microplastics impair growth in two Atlantic scleractinian coral species, *Pseudodiploria clivosa* and *Acropora cervicornis*. *Environ. Pollut.* 275, 116649. doi: 10.1016/j.envpol.2021.116649

Hawaii Department of Land and Natural Resources (n.d.). Marine Debris. Available at: https://dlnr.hawaii.gov/dobor/marine-debris/ (Accessed April 16, 2024).

Hawaii Sea Grant (n.d.). Marine Debris – Hawaii Sea Grant. Available at: https://seagrant.soest.hawaii.edu/marine-debris/ (Accessed May 31, 2024).

Hawaii Wildlife Fund (n.d.). Marine Debris Removal Project. *Hawaii Wildlife Fund*. Available at: https://www.wildhawaii.org/our-work/conservation/marine-debris-removal/ (Accessed April 16, 2024).

Hierl, F., Wu, H. C., and Westphal, H. (2021). Scleractinian corals incorporate microplastic particles: identification from a laboratory study. *Environ. Sci. Pollut. Res.* 28, 37882–37893. doi: 10.1007/s11356-021-13240-x

Hoegh-Guldberg, O. (1999). Climate change, coral bleaching and the future of the world's coral reefs. *Mar. Freshw. Res.* 50, 839–866. doi: 10.1071/mf99078

Howell, E. A., Bograd, S. J., Morishige, C., Seki, M. P., and Polovina, J. J. (2012). On North Pacific circulation and associated marine debris concentration. *Mar. Pollut. Bull.* 65, 16–22. doi: 10.1016/j.marpolbul.2011.04.034

Huang, W., Chen, M., Song, B., Deng, J., Shen, M., Chen, Q., et al. (2021). Microplastics in the coral reefs and their potential impacts on corals: A mini-review. *Sci. Total Environ.* 762, 143112. doi: 10.1016/j.scitotenv.2020.143112

Hughes, T. P., Kerry, J. T., and Simpson, T. (2018). Large-scale bleaching of corals on the Great Barrier Reef. *Ecology* 99, 501–501. doi: 10.1002/ecy.2092

Jambeck, J. R., Geyer, R., Wilcox, C., Siegler, T. R., Perryman, M., Andrady, A., et al. (2015). Plastic waste inputs from land into the ocean. *Science* 347, 768–771. doi: 10.1126/science.1260352

James, K., Vasant, K., S.m., S. B., Padua, S., Jeyabaskaran, R., Thirumalaiselvan, S., et al. (2021). Seasonal variability in the distribution of microplastics in the coastal ecosystems and in some commercially important fishes of the Gulf of Mannar and Palk Bay, Southeast coast of India. *Reg. Stud. Mar. Sci.* 41, 101558. doi: 10.1016/j.rsma.2020.101558

Jeyasanta, K. I., Patterson, J., Grimsditch, G., and Edward, J. K. P. (2020). Occurrence and characteristics of microplastics in the coral reef, sea grass and near shore habitats of Rameswaram Island, India. *Mar. Pollut. Bull.* 160, 111674. doi: 10.1016/j.marpolbul.2020.111674

Jokiel, P. L. (1991). Jokiel's illustrated scientific guide to Kane'ohe Bay, O'ahu. doi: 10.13140/2.1.3051.9360

Jong, M.-C., Tong, X., Li, J., Xu, Z., Chng, S. H. Q., He, Y., et al. (2022). Microplastics in equatorial coasts: Pollution hotspots and spatiotemporal variations associated with tropical monsoons. *J. Hazard. Mat.* 424, 127626. doi: 10.1016/j.jhazmat.2021.127626

Kane, I. A., and Clare, M. A. (2019). Dispersion, Accumulation, and the Ultimate Fate of Microplastics in Deep-Marine Environments: A Review and Future Directions. *Front. Earth Sci.* 7. doi: 10.3389/feart.2019.00080

Kroon, F. J., Motti, C. E., Jensen, L. H., and Berry, K. L. E. (2018). Classification of marine microdebris: A review and case study on fish from the Great Barrier Reef, Australia. *Sci. Rep.* 8, 16422. doi: 10.1038/s41598-018-34590-6

Lamb, J. B., Willis, B. L., Fiorenza, E. A., Couch, C. S., Howard, R., Rader, D. N., et al. (2018). Plastic waste associated with disease on coral reefs. *Science* 359, 460–462. doi: 10.1126/science.aar3320

Lanctôt, C. M., Bednarz, V. N., Melvin, S., Jacob, H., Oberhaensli, F., Swarzenski, P. W., et al. (2020). Physiological stress response of the scleractinian coral *Stylophora pistillata* exposed to polyethylene microplastics. *Environ. Pollut.* 263, 114559. doi: 10.1016/j.envpol.2020.114559

Lao, W., and Wong, C. S. (2023). How to establish detection limits for environmental microplastics analysis. *Chemosphere* 327, 138456. doi: 10.1016/j.chemosphere.2023.138456

Lebreton, L. C. M., van der Zwet, J., Damsteeg, J.-W., Slat, B., Andrady, A., and Reisser, J. (2017). River plastic emissions to the world's oceans. *Nat. Commun.* 8, 15611. doi: 10.1038/ncomms15611

Lebreton, L., Egger, M., and Slat, B. (2019). A global mass budget for positively buoyant macroplastic debris in the ocean. *Sci. Rep.* 9, 12922. doi: 10.1038/s41598-019-49413-5

Lei, X., Cheng, H., Luo, Y., Zhang, Y., Jiang, L., Sun, Y., et al. (2021). Abundance and Characteristics of Microplastics in Seawater and Corals From Reef Region of Sanya Bay, China. *Front. Mar. Sci.* 8. doi: 10.3389/fmars.2021.728745

Liao, B., Wang, J., Xiao, B., Yang, X., Xie, Z., Li, D., et al. (2021). Effects of acute microplastic exposure on physiological parameters in *Tubastrea aurea* corals. *Mar. Pollut. Bull.* 165, 112173. doi: 10.1016/j.marpolbul.2021.112173

Lim, Y. C., Chen, C.-W., Cheng, Y.-R., Chen, C.-F., and Dong, C.-D. (2022). Impacts of microplastics on scleractinian corals nearshore Liuqiu Island southwestern Taiwan. *Environ. Pollut.* 306, 119371. doi: 10.1016/j.envpol.2022.119371

Martin, C., Corona, E., Mahadik, G. A., and Duarte, C. M. (2019). Adhesion to coral surface as a potential sink for marine microplastics. *Environ. Pollut.* 255, 113281. doi: 10.1016/j.envpol.2019.113281

Meijer, L. J. J., van Emmerik, T., van der Ent, R., Schmidt, C., and Lebreton, L. (2021). More than 1000 rivers account for 80% of global riverine plastic emissions into the ocean. *Sci. Adv.* 7, eaaz5803. doi: 10.1126/sciadv.aaz5803

Mendrik, F. M., Henry, T. B., Burdett, H., Hackney, C. R., Waller, C., Parsons, D. R., et al. (2021). Species-specific impact of microplastics on coral physiology. *Environ. Pollut.* 269, 116238. doi: 10.1016/j.envpol.2020.116238

Moberg, F., and Folke, C. (1999). Ecological goods and services of coral reef ecosystems. *Ecol. Econ.* 29, 215–233. doi: 10.1016/S0921-8009(99)00009-9

Montalbetti, E., Isa, V., Vencato, S., Louis, Y., Montano, S., Lavorano, S., et al. (2022). Short-term microplastic exposure triggers cellular damage through oxidative stress in the soft coral *Coelogorgia palmosa*. *Mar. Biol. Res.* 18, 495–508. doi: 10.1080/17451000.2022.2137199

Munno, K., Lusher, A. L., Minor, E. C., Gray, A., Ho, K., Hankett, J., et al. (2023). Patterns of microparticles in blank samples: A study to inform best practices for microplastic analysis. *Chemosphere* 333, 138883. doi: 10.1016/j.chemosphere.2023.138883

Nakano, H., Alfonso, M. B., Jandang, S., Phinchan, N., Chavanich, S., Viyakarn, V., et al. (2024). Influence of monsoon seasonality and tidal cycle on microplastics presence and distribution in the Upper Gulf of Thailand. *Sci. Total Environ.* 920, 170787. doi: 10.1016/j.scitotenv.2024.170787

NOAA Marine Debris Program (n.d.). Enhancing Marine Debris Prevention and Removal Across O‘ahu Coastlines | Marine Debris Program. Available at: https://marinedebris.noaa.gov/prevention/enhancing-marine-debris-prevention-and-removal-across-o-ahu-coastlines (Accessed April 16, 2024).

Ocean Defenders Alliance (n.d.). Hawai’i. *Ocean Defenders Alliance*. Available at: https://www.oceandefenders.org/what-we-do/hawaii.html (Accessed April 16, 2024).

Patterson, J., Jeyasanta, K. I., Laju, R. L., Booth, A. M., Sathish, N., and Edward, J. K. P. (2022). Microplastic in the coral reef environments of the Gulf of Mannar, India - Characteristics, distributions, sources and ecological risks. *Environ. Pollut.* 298, 118848. doi: 10.1016/j.envpol.2022.118848

Patterson, J., Jeyasanta, K. I., Sathish, N., Edward, J. K. P., and Booth, A. M. (2020). Microplastic and heavy metal distributions in an Indian coral reef ecosystem. *Sci. Total Environ.* 744, 140706. doi: 10.1016/j.scitotenv.2020.140706

Peeken, I., Primpke, S., Beyer, B., Gütermann, J., Katlein, C., Krumpen, T., et al. (2018). Arctic sea ice is an important temporal sink and means of transport for microplastic. *Nat. Commun.* 9, 1505. doi: 10.1038/s41467-018-03825-5

Plafcan, M. M., and Stallings, C. D. (2022). Microplastics do not affect bleaching of *Acropora cervicornis* at ambient or elevated temperatures. *PeerJ* 10, e13578. doi: 10.7717/peerj.13578

Plee, T. A., and Pomory, C. M. (2020). Microplastics in sandy environments in the Florida Keys and the panhandle of Florida, and the ingestion by sea cucumbers (Echinodermata: Holothuroidea) and sand dollars (Echinodermata: Echinoidea). *Mar. Pollut. Bull.* 158, 111437. doi: 10.1016/j.marpolbul.2020.111437

Quinn, B., Murphy, F., and Ewins, C. (2017). Validation of density separation for the rapid recovery of microplastics from sediment. *Anal. Methods* 9, 1491–1498. doi: 10.1039/C6AY02542K

Reichert, J., Arnold, A. L., Hammer, N., Miller, I. B., Rades, M., Schubert, P., et al. (2022). Reef-building corals act as long-term sink for microplastic. *Glob. Change Biol.* 28, 33–45. doi: 10.1111/gcb.15920

Reichert, J., Arnold, A. L., Hoogenboom, M. O., Schubert, P., and Wilke, T. (2019). Impacts of microplastics on growth and health of hermatypic corals are species-specific. *Environ. Pollut.* 254, 113074. doi: 10.1016/j.envpol.2019.113074

Reichert, J., Schellenberg, J., Schubert, P., and Wilke, T. (2016). 3D scanning as a highly precise, reproducible, and minimally invasive method for surface area and volume measurements of scleractinian corals. *Limnol. Oceanogr. Methods* 14, 518–526. doi: 10.1002/lom3.10109

Reichert, J., Schellenberg, J., Schubert, P., and Wilke, T. (2018). Responses of reef building corals to microplastic exposure. *Environ. Pollut.* 237, 955–960. doi: 10.1016/j.envpol.2017.11.006

Reichert, J., Tirpitz, V., Plaza, K., Wörner, E., Bösser, L., Kühn, S., et al. (2024). Common types of microdebris affect the physiology of reef-building corals. *Sci. Total Environ.* 912, 169276. doi: 10.1016/j.scitotenv.2023.169276

Ribic, C. A., Sheavly, S. B., Rugg, D. J., and Erdmann, E. S. (2012). Trends in marine debris along the U.S. Pacific Coast and Hawai'i 1998–2007. *Mar. Pollut. Bull.* 64, 994–1004. doi: 10.1016/j.marpolbul.2012.02.008

Roberts, C. M. (1995). Effects of Fishing on the Ecosystem Structure of Coral Reefs. *Conserv. Biol.* 9, 988–995. doi: 10.1046/j.1523-1739.1995.9051332.x-i1

Rotjan, R. D., Sharp, K. H., Gauthier, A. E., Yelton, R., Lopez, E. M. B., Carilli, J., et al. (2019). Patterns, dynamics and consequences of microplastic ingestion by the temperate coral, *Astrangia poculata*. *Proc. R. Soc. B.* 286, 20190726. doi: 10.1098/rspb.2019.0726

Saliu, F., Montano, S., Garavaglia, M. G., Lasagni, M., Seveso, D., and Galli, P. (2018). Microplastic and charred microplastic in the Faafu Atoll, Maldives. *Mar. Pollut. Bull.* 136, 464–471. doi: 10.1016/j.marpolbul.2018.09.023

Saliu, F., Montano, S., Leoni, B., Lasagni, M., and Galli, P. (2019). Microplastics as a threat to coral reef environments: Detection of phthalate esters in neuston and scleractinian corals from the Faafu Atoll, Maldives. *Mar. Pollut. Bull.* 142, 234–241. doi: 10.1016/j.marpolbul.2019.03.043

Sevwandi Dharmadasa, W. L. S., Andrady, A. L., Kumara, P. B. T. P., Maes, T., and Gangabadage, C. S. (2021). Microplastic pollution in Marine Protected Areas of Southern Sri Lanka. *Mar. Pollut. Bull.* 168, 112462. doi: 10.1016/j.marpolbul.2021.112462

Soares, M. O., Rizzo, L., Ximenes Neto, A. R., Barros, Y., Martinelli Filho, J. E., Giarrizzo, T., et al. (2023). Do coral reefs act as sinks for microplastics? *Environ. Pollut.* 337, 122509. doi: 10.1016/j.envpol.2023.122509

Stafford-Smith, M., and Ormond, R. (1992). Sediment-rejection mechanisms of 42 species of Australian scleractinian corals. *Mar. Freshwater Res.* 43, 683. doi: 10.1071/MF9920683

Sustainable Coastlines Hawaii (n.d.). Sustainable Coastlines. Available at: https://www.sustainablecoastlineshawaii.org/ (Accessed April 16, 2024).

Tan, F., Yang, H., Xu, X., Fang, Z., Xu, H., Shi, Q., et al. (2020). Microplastic pollution around remote uninhabited coral reefs of Nansha Islands, South China Sea. *Sci. Total Environ.* 725, 138383. doi: 10.1016/j.scitotenv.2020.138383

Tang, J., Ni, X., Zhou, Z., Wang, L., and Lin, S. (2018). Acute microplastic exposure raises stress response and suppresses detoxification and immune capacities in the scleractinian coral *Pocillopora damicornis*. *Environ. Pollut.* 243, 66–74. doi: 10.1016/j.envpol.2018.08.045

Tang, J., Wu, Z., Wan, L., Cai, W., Chen, S., Wang, X., et al. (2021). Differential enrichment and physiological impacts of ingested microplastics in scleractinian corals in situ. *J. Hazard. Mat.* 404, 124205. doi: 10.1016/j.jhazmat.2020.124205

Wang, T., Zou, X., Li, B., Yao, Y., Zang, Z., Li, Y., et al. (2019). Preliminary study of the source apportionment and diversity of microplastics: Taking floating microplastics in the South China Sea as an example. *Environ. Pollut.* 245, 965–974. doi: 10.1016/j.envpol.2018.10.110

Woodall, L. C., Sanchez-Vidal, A., Canals, M., Paterson, G. L. J., Coppock, R., Sleight, V., et al. (2014). The deep sea is a major sink for microplastic debris. *R. Soc. Open Sci.* 1, 140317. doi: 10.1098/rsos.140317

Zhang, H. (2017). Transport of microplastics in coastal seas. *Estuar. Coast. Shelf S.* 199, 74–86. doi: 10.1016/j.ecss.2017.09.032

Zhou, Z., Tang, J., Cao, X., Wu, C., Cai, W., and Lin, S. (2023). High Heterotrophic Plasticity of Massive Coral *Porites pukoensis* Contributes to Its Tolerance to Bioaccumulated Microplastics. *Environ. Sci. Technol.* 57, 3391–3401. doi: 10.1021/acs.est.2c08188

Zhou, Z., Wan, L., Cai, W., Tang, J., Wu, Z., and Zhang, K. (2022). Species-specific microplastic enrichment characteristics of scleractinian corals from reef environment: Insights from an in-situ study at the Xisha Islands. *Sci. Total Environ.* 815, 152845. doi: 10.1016/j.scitotenv.2021.152845

4.9 SUPPLEMENTARY MATERIALS

Spectral Libraries

Aldrich condensed phase sample library
Aldrich vapor phase sample library
Cross sections wizard
Demo 1
FLOPP
FLOPP-e
Georgia state crime sample library
HR Aldrich alcohols and phenols
HR Aldrich aldehydes and ketones
HR Aldrich dyes, indicators, nitro and azo compounds
HR Aldrich esters, lactones, and anhydrides
HR Aldrich hydrocarbons
HR Aldrich organometallic, inorganic, silanes, boranes, and deuterated compounds
HR Aldrich phosphorous and sulfur compounds
HR Aldrich solvents
HR Hummel polymer and additives
HR Nicolet sampler library
HR polymer additives and plasticizers
HR spectra IR demo
HR spectra Raman demo
Hummel polymer sample library
Organics by Raman sample library
OTC pharmaceuticals microscope
Polymer kit 1.0 – HPU
Polymer laminate films
Random mixture demo library
Sebastian database 2
Sigma biological sample library
Synthetic fibers by microscope
User example library
Wizard library

CONCLUSION

In this dissertation, I investigated how climate change and microplastic pollution impact and interact with reef-building corals to better understand how coral reefs are being shaped by our changing world. The effects of climate change are already devastating coral reefs, and current projections are dire for corals if we do not reduce greenhouse gas emissions (Hoegh-Guldberg, 1999; Hughes et al., 2017). Coral bleaching is a major consequence of rising ocean temperatures that results in energetic and nutritional deficits in corals (Hoegh-Guldberg and Smith, 1989; Iglesias-Prieto et al., 1992). A coral's resilience to bleaching may be determined by how and if they are able to obtain energy and nutrients during this crucial time (Loya et al., 2001; Grottoli et al., 2006). However, other stressors, such as microplastic pollution, could add to this nutritional deficit when corals interact with them (Hall et al., 2015; Hankins et al., 2018; Reichert et al., 2018). My dissertation addresses these aspects of coral conservation using various field and laboratory methods to examine changes in nutritional pathways in bleached corals and how bleaching stress and other factors affect coral and microplastic interactions. It then concludes with a field survey in a Hawaiian coral reef to assess the levels of microplastics present and evaluate the associated risk levels of this additional form of stress.

My first chapter used proteomics to uncover ways bleached coral tissue and skeleton respond metabolically to bleaching stress in *Montipora capitata*. The results revealed different mechanisms by which coral tissue and skeletal compartments utilize energy and obtain nutrients during this critical period. This suggests unique strategies for these compartments to efficiently maintain their specific functions while undergoing bleaching. Further research could investigate if the observed compartment-specific responses are linked to compartment-specific functions.

For example, I observed increased proteins involved in the glyoxylate cycle in bleached coral tissue; could this pathway be linked to reproduction or heterotrophic feeding? In the bleached skeleton, I observed increased proteins involved in the pentose phosphate pathway (PPP); could the PPP be linked to skeleton formation? Moreover, given that the studied species is relatively resilient to bleaching compared to other species (Grottoli et al., 2006; Cox, 2007; Ritson-Williams and Gates, 2020), the proteins and cellular processes I observed could potentially be indicators of bleaching resilience and could be used as biomarkers that could be searched for in other corals to determine which species will be able to persist future bleaching events and would thus be great candidates to use in coral restoration.

In my second and third chapters, I shifted focus to microplastic pollution and investigated the factors influencing coral-microplastic interactions. This included examining the role of bleaching stress, water flow, and different types of microplastics and coral species on microplastic interactions (e.g., ingestion and adhesion). The goal of these studies was to provide insights for conservation initiatives, particularly in identifying which coral species are more or less susceptible to different types of microplastics under varying environmental conditions. My results align well with other coral and microplastic studies (Reichert et al., 2018, 2019; Mendrik et al., 2021; Reichert et al., 2024a) where species-specific differences play one of the biggest roles in coral and microplastic interactions. One of the biggest species-specific differences affecting microplastic ingestion appears to be their rate of heterotrophy (Reichert et al., 2024a), while for adhesion, one of the biggest factors appears to be how efficient corals are at removing microplastics using sediment rejection mechanisms such as mucus (Martin et al., 2019; Hierl et al., 2021; Bejarano et al., 2022). This information is valuable because it can guide conservation work in selecting corals that are less likely to interact with microplastics for restoration projects.

However, we still lack data on the feeding rates and sediment rejection efficiencies of many coral species. Thus, future studies on microplastic interactions in corals should encompass a wider range of species, focusing on these processes. Additionally, it is essential to continue exploring other factors that can affect coral feeding rates or mucus dynamics, such as heterotrophic plasticity (Grottoli et al., 2006) and water flow (Sebens et al., 1997, 1998). Some aspects of my dissertation work could not fully elucidate their influence, and interactions with these factors also seem to be species-specific. Continued investigation into these factors will contribute to a more comprehensive understanding of coral-microplastic interactions.

In the third chapter of my dissertation, I found that fibers were the type of microplastic that interacted with corals the most, suggesting that they pose the largest threat to corals. This finding is critical because it can guide the prioritization of pollution mitigation efforts, indicating a need to minimize the release of fibers into the oceans. Microplastic fibers are thought to come largely from clothing and textiles and could be reduced by using more natural fibers in materials and by filtering domestic wastewater from washing machines (Periyasamy and Tehrani-Bagha, 2022). However, very few studies have tested the effects of microplastic fibers in corals and other organisms (Mendrik et al., 2021; Reichert et al., 2024b), which is probably due to difficulties using them in experiments because they tend to behave differently than microplastic fragments and spheres. Future studies should work to improve our ability to use microfibers in experimental systems.

In chapter four of this dissertation, I report that microplastic pollution in a Hawaiian reef was low and that corals and other marine life in the bay are probably not at great risk of microplastics. In fact, microplastic contamination in corals was far below the levels used

experimentally to elicit negative effects in corals (Huang et al., 2021). However, had sampling occurred during the rainy season, microplastics would likely have been detected more frequently and at higher levels (James et al., 2021; Jong et al., 2022). Microplastic contamination in coral reefs varies considerably (Huang et al., 2021), but not many studies conduct sampling regimes that encompass potential seasonal trends. Thus, I advocate for ongoing and regular monitoring of microplastics in coral reefs, including those in Kaneohe Bay. Moreover, while the immediate risk of microplastics to the reef organisms in Kaneohe Bay seems low, we still lack an understanding of the potential community-scale effects of these pollutants. Microplastics in seawater could indirectly affect coral reef communities by interacting with the spawn of corals and other organisms. For example, chemicals such as endocrine disruptors could leach from sea surface microplastics and disrupt fertilization or embryo development in broadcast spawners, which in turn could have cascading ecosystem level effects. Microplastics in sediments could act in a similar way but have unseen effects on infaunal benthic communities, which could affect nutrient cycling in reefs. Microplastics that adhere to non-living reef structures could impact reef accretion and dissolution processes. Thus, even though this chapter reports some good news for a coral reef, there is still much we do not understand about how microplastics stand to impact them, and we must continue to study their distribution and impacts to be able to guide conservation efforts. There is still much to learn about the interactions between microplastics and other stressors, which should be prioritized in future work.

The work presented in this dissertation has increased our understanding of how climate change and microplastic pollution will shape the future of coral reefs. It highlights how corals are adapted to cope with global change, how they interact with stressors, and, to some degree, their levels of risk. In addition, it establishes a foundation for future work essential to understanding

the trajectory of coral reefs in an uncertain future. Most importantly, it has inspired me to continue trying to understand and conserve these incredibly amazing and important ecosystems.

References

Bejarano, S., Diemel, V., Feuring, A., Ghilardi, M., and Harder, T. (2022). No short-term effect of sinking microplastics on heterotrophy or sediment clearing in the tropical coral *Stylophora pistillata*. *Sci. Rep.* 12, 1468. doi: 10.1038/s41598-022-05420-7

Cox, E. F. (2007). Continuation of sexual reproduction in *Montipora capitata* following bleaching. *Coral Reefs* 26, 721–724. doi: 10.1007/s00338-007-0251-9

Grottoli, A. G., Rodrigues, L. J., and Palardy, J. E. (2006). Heterotrophic plasticity and resilience in bleached corals. *Nature* 440, 1186–1189. doi: 10.1038/nature04565

Hall, N. M., Berry, K. L. E., Rintoul, L., and Hoogenboom, M. O. (2015). Microplastic ingestion by scleractinian corals. *Mar. Biol.* 162, 725–732. doi: 10.1007/s00227-015-2619-7

Hankins, C., Duffy, A., and Drisco, K. (2018). Scleractinian coral microplastic ingestion: Potential calcification effects, size limits, and retention. *Mar. Pollut. Bull.* 135, 587–593. doi: 10.1016/j.marpolbul.2018.07.067

Hierl, F., Wu, H. C., and Westphal, H. (2021). Scleractinian corals incorporate microplastic particles: identification from a laboratory study. *Environ. Sci. Pollut. Res.* 28, 37882–37893. doi: 10.1007/s11356-021-13240-x

Hoegh-Guldberg, O. (1999). Climate change, coral bleaching and the future of the world's coral reefs. *Mar. Freshw. Res.* 50, 839–866. doi: 10.1071/mf99078

Hoegh-Guldberg, O., and Smith, G. J. (1989). The effect of sudden changes in temperature, light and salinity on the population density and export of zooxanthellae from the reef corals *Stylophora pistillata* Esper and *Seriatopora* hystrix Dana. *J. Exp. Mar. Biol. Ecol.* 129, 279–303. doi: 10.1016/0022-0981(89)90109-3

Huang, W., Chen, M., Song, B., Deng, J., Shen, M., Chen, Q., et al. (2021). Microplastics in the coral reefs and their potential impacts on corals: A mini-review. *Sci. Total Environ.* 762, 143112. doi: 10.1016/j.scitotenv.2020.143112

Hughes, T. P., Kerry, J. T., Álvarez-Noriega, M., Álvarez-Romero, J. G., Anderson, K. D., Baird, A. H., et al. (2017). Global warming and recurrent mass bleaching of corals. *Nature* 543, 373–377. doi: 10.1038/nature21707

Iglesias-Prieto, R., Matta, J. L., Robins, W. A., and Trench, R. K. (1992). Photosynthetic response to elevated temperature in the symbiotic dinoflagellate *Symbiodinium microadriaticum* in culture. *Proc. Nat. Acad. Sci.* 89, 10302–10305. doi: 10.1073/pnas.89.21.10302

James, K., Vasant, K., S.m., S. B., Padua, S., Jeyabaskaran, R., Thirumalaiselvan, S., et al. (2021). Seasonal variability in the distribution of microplastics in the coastal ecosystems and in some commercially important fishes of the Gulf of Mannar and Palk Bay, Southeast coast of India. *Reg. Stud. Mar. Sci.* 41, 101558. doi: 10.1016/j.rsma.2020.101558

Jong, M.-C., Tong, X., Li, J., Xu, Z., Chng, S. H. Q., He, Y., et al. (2022). Microplastics in equatorial coasts: Pollution hotspots and spatiotemporal variations associated with tropical monsoons. *Jour. Hazard. Mat.* 424, 127626. doi: 10.1016/j.jhazmat.2021.127626

Loya, Y., Sakai, K., Yamazato, K., Nakano, Y., Sambali, H., and van Woesik, R. (2001). Coral bleaching: the winners and the losers. *Ecol. Lett.* 4, 122–131. doi: 10.1046/j.1461-0248.2001.00203.x

Martin, C., Corona, E., Mahadik, G. A., and Duarte, C. M. (2019). Adhesion to coral surface as a potential sink for marine microplastics. *Environ. Pollut.* 255, 113281. doi: 10.1016/j.envpol.2019.113281

Mendrik, F. M., Henry, T. B., Burdett, H., Hackney, C. R., Waller, C., Parsons, D. R., et al. (2021). Species-specific impact of microplastics on coral physiology. *Environ. Pollut.* 269, 116238. doi: 10.1016/j.envpol.2020.116238

Periyasamy, A. P., and Tehrani-Bagha, A. (2022). A review on microplastic emission from textile materials and its reduction techniques. *Polym. Degrad. Stab.* 199, 109901. doi: 10.1016/j.polymdegradstab.2022.109901

Reichert, J., Arnold, A. L., Hoogenboom, M. O., Schubert, P., and Wilke, T. (2019). Impacts of microplastics on growth and health of hermatypic corals are species-specific. *Environ. Pollut.* 254, 113074. doi: 10.1016/j.envpol.2019.113074

Reichert, J., Schellenberg, J., Schubert, P., and Wilke, T. (2018). Responses of reef building corals to microplastic exposure. *Environ. Pollut.* 237, 955–960. doi: 10.1016/j.envpol.2017.11.006

Reichert, J., Tirpitz, V., Oponczewski, M., Lin, C., Franke, N., Ziegler, M., et al. (2024a). Feeding responses of reef-building corals provide species- and concentration-dependent risk assessment of microplastic. *Sci. Total Environ.* 913, 169485. doi: 10.1016/j.scitotenv.2023.169485

Reichert, J., Tirpitz, V., Plaza, K., Wörner, E., Bösser, L., Kühn, S., et al. (2024b). Common types of microdebris affect the physiology of reef-building corals. *Sci. Total Environ.* 912, 169276. doi: 10.1016/j.scitotenv.2023.169276

Ritson-Williams, R., and Gates, R. D. (2020). Coral community resilience to successive years of bleaching in Kāneʻohe Bay, Hawaiʻi. *Coral Reefs* 39, 757–769. doi: 10.1007/s00338-020-01944-4

Sebens, K. P., Grace, S. P., Helmuth, B., Maney Jr., E. J., and Miles, J. S. (1998). Water flow and prey capture by three scleractinian corals, *Madracis mirabilis*, *Montastrea cavernosa* and *Porites porites*, in a field enclosure. *Mar. Biol.* 131, 347–360. doi: 10.1007/s002270050328

Sebens, K. P., Witting, J., and Helmuth, B. (1997). Effects of water flow and branch spacing on particle capture by the reef coral *Madracis mirabilis* (Duchassaing and Michelotti). *J. Exp. Mar. Biol. Ecol.* 211, 1–28. doi: 10.1016/S0022-0981(96)02636-6

VITA

Jeremy Axworthy will receive a PhD in Fishery Sciences, but he really studies marine biology. Before studying to be a scientist, Jeremy worked as a diving instructor all over SE Asia for several years. In 2011, he moved to Seattle, got his associate degree as Seattle Central College, his BS in SAFS, followed by his PhD in Dr. Jacqueline Padilla's ecophysiology lab. His research focuses on the effects and interactions of climate change and pollution, such as microplastics, on corals and coral reefs. He hopes to return to SE Asia to teach and conduct research on coral reefs. When he's not studying, Jeremy maintains a collection of tropical pitcher plants and other carnivorous plants and entertains his 4-year-old son.